PERFORMANCE EVALUATION OF CEMENT AND EMULSIFIED ASPHALT TREATED BASES

Submitted in partial fulfillment of the requirements

for the award of the degree of

DOCTOR OF PHILOSOPHY

in

CIVIL ENGINEERING

by

SARELLA CHAKRAVARTHI
717112

TRANSPORTATION DIVISION
DEPARTMENT OF CIVIL ENGINEERING
NATIONAL INSTITUTE OF TECHNOLOGY
WARANGAL-506004 (TS) INDIA
MAY 2022

PERFORMANCE EVALUATION OF CEMENT AND EMULSIFIED ASPHALT TREATED BASES

Submitted in partial fulfillment of the requirements

for the award of the degree of

Doctor of Philosophy

by

SARELLA CHAKRAVARTHI

717112

Supervisor

Dr. S. SHANKAR

TRANSPORTATION DIVISION
DEPARTMENT OF CIVIL ENGINEERING
NATIONAL INSTITUTE OF TECHNOLOGY, WARANGAL
MAY 2022

NATIONAL INSTITUTE OF TECHNOLOGY, WARANGAL

CERTIFICATE

This is to certify that the thesis entitled **"Performance Evaluation of Cement and Emulsified Asphalt Treated Bases"** being submitted by **Mr. SARELLA CHAKRAVARTHI** for the award of the degree of **DOCTOR OF PHILOSOPHY** to the Department of **Civil Engineering** of **NATIONAL INSTITUTE OF TECHNOLOGY, WARANGAL** is a record of bonafide research work carried out by him under my supervision and it has not been submitted elsewhere for the award of any degree.

Dr. S. SHANKAR
Thesis Supervisor
Assistant Professor
Department of Civil Engineering
National Institute of Technology, Warangal
Telangana, India

APPROVAL SHEET

This Thesis entitled **"Performance Evaluation of Cement and Emulsified Asphalt Treated Bases"** by **Mr. SARELLA CHAKRAVARTHI** is approved for the degree of Doctor of Philosophy.

Examiners

_____

_____

_____

Supervisor

_____

Chairman

_____

Date: _____

DECLARATION

This is to certify that the work presented in the thesis entitled **"Performance Evaluation of Cement and Emulsified Asphalt Treated Bases"** is a bonafide work done by me under the supervision of **Dr. S. Shankar**, Assistant Professor, Department of Civil Engineering, NIT, Warangal, Telangana, India and was not submitted elsewhere for the award of any degree. I declare that this written submission represents my ideas in my own words. I have adequately cited and referenced the original sources where others' ideas or words have been included. I also declare that I have adhered to all principles of academic honesty and integrity and have not misrepresented or fabricated, or falsified any idea /data/ fact/source in my submission. I understand that any violation of the above will be cause for disciplinary action by the institute and can also evoke penal action from the sources which have thus not been properly cited or from whom proper permission has not been taken when needed.

_____

SARELLA CHAKRAVARTHI

Roll No. (717112)

Date:

Dedicated to

My

PARENTS, TEACHERS and GOD

ACKNOWLEDGEMENTS

I express my deep sense of gratitude and acknowledgment to **Dr. S. Shankar,** Assistant Professor, Department of Civil Engineering, Transportation Division, National Institute of Technology, Warangal, under whose guidance this research work was carried out. It was a pleasant experience to work with him for his continuous guidance and giving valuable suggestions encouragement regarding research matters and has helped me a lot. I consider it a privilege to have worked with him.

I am highly indebted to my Doctoral Committee Member and Chairman **Prof. C. S. R. K. Prasad**, Professor, Department of Civil Engineering, Doctoral Committee Members **Dr. Venkaiah Chowdary**, Associate Professor, Head of Transportation Division, Department of Civil Engineering, **Prof. G. Rajesh Kumar**, Professor, Department of Civil Engineering, **Prof. A. Sarat Babu**, Professor, Department of Chemical Engineering, National Institute of Technology, Warangal for their assistance, encouragement, inspiration and continuous monitoring of my work during this research work.

I wish to take this opportunity to express my sincere thanks to **Dr. Vishnu. R,** Assistant Professor, Transportation Division, Department of Civil Engineering, National Institute of Technology, Warangal for his valuable suggestions during the work, **Dr. K. V. R. Ravi Shankar,** Assistant Professor, Transportation Division, Department of Civil Engineering, National Institute of Technology, Warangal, **Dr. Arpan Mehar**, Assistant Professor, Transportation Division, Department of Civil Engineering, National Institute of Technology, Warangal, **Dr. B. Raghuram Kadali,** Assistant Professor, Transportation Division, Department of Civil Engineering, National Institute of Technology, Warangal, for their valuable suggestions and encouragement throughout my research work.

I express my sincere acknowledgment for funding this research study by the Ministry of Human Resource and Development, Government of India. I am deeply grateful to **Dr. P. Rathish Kumar,** Professor and Head, Department of Civil Engineering, for his valuable comments and immense support during this research work. I am grateful to **Prof. N.V. Ramana Rao,** Director, National Institute of Technology, Warangal, for extending every possible help during the study.

I wish to place on record heartfelt gratitude and indebtedness to **the Department of Science and Technology (DST), Government of India, for sponsoring this prestigious research project at the National Institute of Technology Warangal** Telangana, India.

I am thankful to **Mr. Nagraj Vittal, Director, Spranktronics**, Bengaluru, for his clarifications and valuable suggestions regarding Fatigue Testing.

I extend my sincere acknowledgment to former **M.Tech students Boyina Anusha, Seelam Jaeson Hemanth, Arun Kumar Singh, Devendra Vara Prasad, Mahammad Sameer, Satyaveer Rajawat, Galipelli Raj Kumar and Martha Daniel** for their help in Research work. I have been lucky to get so many beautiful friends in the Department of Civil Engineering: **Gummadi Chiranjeevi, Lalam Govinda, G. Shravan Kumar, J. Jithender, Prasanth Sekhar Lokku, K. Mahaboob Peera, T. Arjun Kumar, K. Srikanth, Dr. D. Harinder, K. Ramesh Babu and Dharma Teja**. The dreary periods during the research were enlivened up by the lighter moments we shared.

I want to thank **Mr. MD. Abdul Gaffar and Mr. K. Ramesh**, laboratory staff of Transportation Division. I am grateful to all the Research Scholars of the Transportation Division, Department of Civil Engineering, and NITW for their constant encouragement and timely help.

I express my deepest gratitude to my parents, **Sekhar** and **Rani**, Grand Father **Satyam** (late) and my wife, **Dr. Y. Megha Spandana,** for their love, support, and encouragement, without which this work would not have been possible. I would like to thank my friends, Thota Abhishek, Mutyala Ravi Kumar, Bollepally Venkateswarlu, Chittala Abhilash, Barre Priyanka, for their timely support and help. I would like to thank many others whose names would be too numerous to mention here for their assistance, suggestions, friendship, and insightful discussions. Finally, I thank everyone who contributed either directly or indirectly to successfully completing this work.

SARELLA CHAKRAVARTHI

TABLE OF CONTENTS

Page No.

CERTIFICATE **iii**

APPROVAL SHEET **iv**

DECLARATION **v**

DEDICATION **vi**

ACKNOWLEDGEMENTS **vii**

TABLE OF CONTENTS **ix**

LIST OF FIGURES **xiii**

LIST OF TABLES **xvii**

LIST OF ABBREVIATIONS **xviii**

ABSTRACT **xxii**

CHAPTER 1 INTRODUCTION

1.1 General 1
1.2 Pavement types and their functions 2
1.2.1 Flexible Pavements 2
1.2.2 Rigid Pavements 3
1.2.3 Composite Pavements 4
1.3 Use of Recycled Concrete Aggregate and Reclaimed Asphalt Pavement in Pavements 5
1.4 Demand of Aggregates around the World 6
1.5 Need for the Study 7
1.6 Objectives of the study 9
1.7 Organization of the Thesis 9

CHAPTER 2 LITERATURE REVIEW

2.1 General 11
2.2 Cement Treated Bases 11
2.2.1 History of Cement Treated Bases 11
2.2.2 Mechanism of Cement Treated Bases 12
2.2.3 Compaction Characteristics of Cement Treated Bases 13
2.2.4 Unconfined Compressive Strength (UCS) of CTB 14
2.2.4.1 Variation of UCS with Cement 16
2.2.4.2 Variation of UCS with recycled aggregate content 18
2.2.4.3 Variation of UCS with curing period 20

2.2.4.4 Variation of UCS with fines content 20
2.2.5 Flexural Strength Properties of Cement Treated Recycled Bases 21
2.2.6 Indirect Tensile Strength Properties of Cement Treated Recycled Bases 22
2.2.7 Modulus Characteristics of Cement Treated Recycled Bases 24
2.2.7.1 Resilient Modulus (M_R) 24
2.2.7.2 Resilient Modulus of Untreated Recycled Bases 24
2.2.7.3 Resilient Modulus of Treated Recycled Bases 25
2.2.7.4 Influence of Elastic Modulus and Secant Modulus on Cement Treated Recycled Bases 26
2.2.7.5 Effect of Shear Modulus on Cement Treated Recycled Bases 27
2.2.8 Permanent Deformation Characteristics of CTB 27
2.2.9 Durability, Hydraulic Conductivity, Shrinkage and Thermal Expansion Characteristics 28
2.2.10 Field Evaluation and Fatigue Characteristics of CTB 30

2.3 Emulsified Asphalt Treated Bases 32

2.3.1 Different Stages of Setting of Emulsified Asphalts 32
2.3.2 Constituents of Emulsified Asphalt Treated Bases 33
2.3.3 Role of Additives in EATB 33
2.3.4 Mix design of EATB 35
2.3.5 Mix Design Parameters 35
2.3.6 General Code of Practices for the Mix Design of EATB 36
2.3.7 Initial Emulsified Asphalt Content and Total Fluid Contents 36
2.3.8 Cement Water Emulsion Interactions of EATB 38
2.3.9 Criteria Selected for Fixing Optimum Emulsified Asphalt Content 39
2.3.10 Mixing, Compaction and Curing of EATB 41
2.3.11 EATB with Recycled Aggregates Other than RAP 43
2.3.12 Performance Characteristics of EATB 44
2.3.12.1 Indirect Tensile Strength of EATB 44
2.3.12.2 Tensile Strength Ratio 44
2.3.12.3 Rutting Behaviour of EATB 45
2.3.12.4 Indirect Tensile Stiffness Modulus and Resilient Modulus 45
2.3.12.5 Marshall Stability and Percentage of Air Voids in EATB 46
2.3.12.6 Field Evaluation of EATB 46
2.3.12.7 Fatigue Characteristics off EATB 47

2.4 Summary of Literature Review 49
2.5 Gaps in the Literature Review 51
2.6 Scope of the present Work 51

CHAPTER 3 RESEARCH METHODOLOGY 53

3.1 General 53
3.2 Materials and Testing 56
3.2.1 Aggregates 56
3.2.2 Cement 57

3.2.3 Cationic Slow Setting Asphalt Emulsion 58
3.3 Mix Design of CTB 58
3.4 Mix Design of EATB 58
3.5 Laboratory Performance Tests 60
3.5.1 Unconfined Compressive Strength 60
3.5.2 Indirect Tensile Strength 61
3.5.3 Tensile Strength Ratio 61
3.5.4 Density and Moisture loss of EATB 62
3.5.5 Resilient Modulus 62
3.5.6 Dynamic Creep Rutting Test on EATB 63
3.5.7 Indirect Tensile Fatigue Testing 64
3.6 Summary 66

CHAPTER 4 LABORATORY INVESTIGATION OF CTB 67

4.1 General 67
4.2 Engineering Properties of the Aggregates 67
4.2.1 Aggregates 67
4.3 Properties of Cement 69
4.3.1 Gradation of RAP and RCA 70
4.4 Design of Cement Treated Bases 70
4.5 Performance Evaluation of CTB 71
4.5.1 Unconfined Compressive Strength of CTB 71
4.5.2 Indirect Tensile Strength Properties of CTB 74
4.5.3 Resilient Modulus Characteristics of CTB 79
4.5.4 Fatigue Evaluation of CTB 82
4.6 Summary 87

CHAPTER 5 LABORATORY PERFORMANCE EVALUATION OF EATB 89

5.1 General 89
5.2 Properties of Emulsified Asphalt 89
5.3 Gradation and Blending of RAP and RCA with Virgin Aggregates 89
5.4 Mix Design of EATB 90
5.5 Density and Water Loss Variation in EATB 96
5.6 Tensile Strength Ratio of EATB 99
5.7 Dynamic Creep Rutting Characteristics of EATB 100
5.8 Resilient Modulus Characteristics of EATB 106
5.9 Fatigue Characteristics of EATB 108
5.10 Summary 112

CHAPTER 6 PAVEMENT ANALYSIS AND DESIGN 113

6.1 General 114
6.2 Pavement Analysis 114
6.3 Pavement Analysis of EATB 117
6.4 Summary 119

CHAPTER 7 CONCLUSIONS AND SCOPE FOR FUTURE STUDY **120**

7.1 General 120
7.2 Conclusions of Cement Treated Bases 120
7.3 Conclusions of Emulsified Asphalt Treated Bases 120
7.4 Recommendations 122
7.5 Scope for Future Study 122

REFERENCES **123**

APPENDIX A **138**

APPENDIX B **139**

APPENDIX C **141**

APPENDIX D **143**

APPENDIX E **144**

LIST OF PUBLICATIONS **145**

BIODATA **146**

LIST OF FIGURES

Figure No.	Title	Page No.
1.1	Typical Cross-Section of a Flexible Pavement	3
1.2	Typical Cross-Section of a Rigid Pavement	4
1.3	Energy consumption and GHG emissions for different Bases	5
1.4	Statistics of C&D in different countries	6
1.5	Composition of C & D waste in India	7
1.6	Total length of road construction in India during financial years	8
2.1	Stress distribution in pavements with conventional bass and CTB	12
2.2	Typical OMC and MDD for different aggregates at constant cement content	14
2.3	Variation of UCS with cement content and its by-products	17
2.4	Variation of UCS with RAP content	18
2.5	Variation of UCS with RCA content	19
2.6	Variation of ITS with Cement and recycled aggregate content	23
2.7	Effectiveness of different additives in terms of performance parameters	34
2.8	Different Compaction techniques adopted for laboratory evaluation of EATB	41
2.9	Curing techniques adopted for EATB around the world	42
3.1	Adopted Research Approach	53
3.2	Parameters that are used in the CTB studies	54
3.3	Percentage of studies adopted different Recycled aggregates in CTB	54
3.4	Parameters that are used in the EATB studies	55
3.5	Percentage of studies adopted different Recycled aggregates in EATB	55
3.6	Location of the RAP material collected	56
3.7	Steps involved in the mix design of EATB	59
3.8	Testing of samples for UCS	61
3.9	Conditioning of samples under water	62
3.10	Typical data acquisition and setup of fatigue testing machine	63
3.11	Dynamic creep rutting test apparatus	64
3.12	Fatigue testing machine with necessary components	65
4.1	(a) First stage manual crushing of RCA in the range of 50-100 mm size, (b) Screening and crushing of RCA into the size range of 30-40 mm, (c) Final Crushing using Jaw crusher in two stages, (d) Final product of RCA after processing	67
4.2	Variation of physical properties with RCA content in the blends	68
4.3	Gradation charts for CTB	70
4.4	A typical Unconfined Compressive Strength testing	72

4.5	Unconfined Compressive Strength at 7 days of curing period	72
4.6	Unconfined Compressive Strengths at varying cement percentages	73
4.7	Unconfined Compressive Strengths of RAP-VA blends at various curing periods	74
4.8	Unconfined Compressive Strengths of RCA-VA blends at various curing periods	74
4.9	Typical testing for Indirect Tensile Strength	75
4.10	Indirect Tensile Strength at 7 days of curing period	75
4.11	Indirect Tensile Strengths at varying cement percentages	76
4.12	Variation of the ITS with the curing period	77
4.13	Variation of ITS with Cement content, RCA and curing period	77
4.14	Variation of the ITS with the cement content for RAP blends	78
4.15	Variation of ITS with Cement content, RAP, and curing period	78
4.16	Typical deformation pulse diagram	79
4.17	Resilient Modulus of RAP-VA mixes at various curing periods	80
4.18	Resilient Modulus of RCA-VA mixes at various curing periods	81
4.19	Relation between Resilient Modulus and UCS for RCA blends	82
4.20	Relation between Resilient Modulus and UCS for RAP blends	82
4.21	Typical failure of 25% RAP specimen at 85% stress level	83
4.22	Fatigue life of RAP-VA mixes at 6% cement content	84
4.23	Fatigue life of RCA-VA mixes at 6% cement content	84
4.24	Fatigue life of 25RAP mix at various cement contents	85
4.25	Fatigue life of 50RAP mix at various cement contents	85
4.26	Fatigue life of 75RAP mix at various cement contents	85
4.27	Fatigue life of RAP mix at various cement contents	86
4.28	Fatigue life of RCA mix at various cement contents	86
4.29	Fatigue life of 75RCA mix at various cement contents	87
4.30	Fatigue life of 50RCA mix at various cement contents	87
4.31	Fatigue life of 25RCA mix at various cement contents	87
5.1	Gradation of EATB RAP mixes with lower and upper limits of AA-2009	90
5.2	Comparison of RCA-VA blended with lower and upper limits of AA-2009	90
5.3	ITS results of EATB for RAP-25	91
5.4	ITS results of EATB for RAP-50	92
5.5	ITS results of EATB for RAP-75	92
5.6	Variation of ITS of EATB with curing period	93

5.7	Variation of ITS with RAP content at OEAC	94
5.8	Variation of ORBC/OEBC/OTFC with RAP content	94
5.9	Failure patterns of RAP blends	95
5.10	Failure pattern of a) RCA-25 b) RCA-50	95
5.11	Dry and Wet ITS values of EATB with 25% RCA	96
5.12	Dry and Wet ITS values of EATB with 50% RCA	96
5.13	Variation of density with Emulsified Asphalt Content	97
5.14	Percentage of water loss with time for different %RAP mixes	98
5.15	The dry densities of EATB with RCA	98
5.16	Dynamics of moisture loss for (a) 25% RCA (b) 50% RCA mixes	99
5.17	Tensile strength ratio of RAP mixes	100
5.18	Tensile strength ratio of RCA mixes	100
5.19	Permanent Deformation Curves for different Percentage of RAP	101
5.20	Comparison of permanent deformation curves of different RAP blends at optimum, below optimum, and above optimum emulsified asphalt contents	102
5.21	Effect of Total Binder Content on Permanent deformation	103
5.22	Permanent deformation of RCA mixes	104
5.23	Accumulate strains for RAP mixes at 40°C	105
5.24	Accumulated strains for RCA mixes at 40°C	106
5.25	Resilient moduli of Cold mixes with RCA	106
5.26	Resilient moduli of Cold mixes with RAP	107
5.27	Resilient moduli of Cold mixes with RAP at 40°C temperature	108
5.28	Resilient moduli of Cold mixes with RCA at 40°C temperature	108
5.29	Fatigue performance of 25RAP mixes	110
5.30	Fatigue performance of 50RAP mixes	110
5.31	Fatigue performance of 75RAP mixes	110
5.32	Fatigue performance of 25RCA mixes	111
5.33	Fatigue performance of 50RCA mixes	111
5.34	Fatigue performance of RAP mixes at OEAC	112
6.1	A Pavement Section with Bituminous Layer(s), Granular Base and GSB Showing the Locations of Critical Strains	114
6.2	A Pavement Section with Bituminous Layer(s), Granular Crack Relief Layer, CTB, and CTSB Showing the Locations of Critical Strains/Stresses	114
6.3	A Pavement Section with Bituminous Layer(s), SAMI Crack Relief Layer, CTB, and CTSB Showing the Locations of Critical Strains/Stresses	115

6.4 A Pavement Section with Bituminous Layer(s), Emulsion/Foam Bitumen Stabilised RAP/Virgin Aggregate Layer and CTSB Showing the Locations of Critical Strains 115
6.5 A Pavement Section with Bituminous Layer(s), Granular Crack Relief Layer, CTB, and GSB Showing the Locations of Critical Strains/Stresses 115
6.6 A Pavement Section with Bituminous Layer(s), Granular Base (WMM) and CTSB Showing the Locations of Critical Strains 116
6.7 Thickness comparison of stabilized recycled aggregate mixes with conventional stabilized bases 117

LIST OF TABLES

Table No.	Title	Page No.
2.1	Influence of different parameters on UCS of RAP materials	15
2.2	Influence of different parameters on UCS of RCA materials	15
2.3	Summary of UCS specifications for road bases at seven days of curing period	16
2.4	Flexural strength of different recycled materials by different authors	21
2.5	Summary of ITS specifications for road bases at 7 days of curing period	22
2.6	Effect of resilient modulus on cement treated recycled bases	25
2.7	Fatigue studies on different cement treated materials	31
2.8	Permissible ITS values used in the design of EATB	35
2.9	Various design methods used for EATB	36
2.10	Equations to calculate the required emulsified asphalt content for EATB	37
2.11	Summary of research works on cement water and asphalt emulsion interactions	38
2.12	Variation of mechanical properties with different parameters	40
2.13	Fatigue characteristics of EATB highlighted by the authors	48
3.1	Physical properties of aggregates for unbound or bound base layer as per MoRTH, 2013	56
3.2	Gradation requirements of EATB	57
3.3	Gradation requirements of CTB	57
3.4	Summary of tests on Cationic slow setting asphalt emulsion	58
3.5	Experimental sample test matrix for CTB	58
3.6	Experimental sample test matrix for EATB	60
4.1	Properties of RAP, RCA and VA	69
4.2	Physical properties of cement	70
4.3	Optimum Moisture Content and Maximum Dry Density Results for RAP blends	71
4.5	Optimum Moisture Content and Maximum Dry Density Results for RCA blends	71
5.1	Properties of CSS-2	89
6.1	Calculation of critical strains for a cross section incorporating EATB	118

LIST OF ABBREVIATIONS

RAP	Reclaimed Asphalt Pavement
RCA	Recycled Concrete Aggregate
VA	Virgin Aggregate
CTB	Cement Treated Bases
EATB	Emulsified Asphalt Treated Bases
UCS	Unconfined Compressive Strength
ITS	Indirect Tensile Strength
NH	National Highway
NHAI	National Highways Authority of India
SH	State Highways
MDR	Major District Roads
VR	Village Roads
MoRTH	Ministry of Road Transport and Highways
C&D	Construction and Demolition
WMM	Wet Mix Macadam
WBM	Water Bound Macadam
CRM	Crushed Run Macadam
DLC	Dry Lean Concrete
CTSB	Cement Treated Sub-Base
PQC	Pavement Quality Concrete
CFD	Cumulative Fatigue Damage
CIPR	Cold In-Place Recycling
CBM	Cement Bound Macadam
UGM	Unbound Granular Materials
GHG	Green House Gas

HMA	Hot Mix Asphalt
IRC	Indian Roads Congress
OMC	Optimum Moisture Content
FS	Flexural Strength
CP	Curing Periods
MDD	Maximum Dry Density
RMA	Recycled Masnary Aggregate
CB	Crushed Brick
FRG	Fine Recycled Glass
RLT	Repeated Load Test
CC	Cement Content
QF	Quarry Fines
FWD	Falling Weight Deflectometer
TST	Tube Suction Test
CTE	Coefficient of Thermal Expansion
IRI	International Roughness Index
OEAC	Optimum Emulsified Asphalt Content
GGBS	Ground Granulated Blast-furnace Slag
TSR	Tensile Strength Ratio
TFC	Total Fluid Content
DGB	Dense Graded Bituminous mix
IEAC	Initial Emulsified Asphalt Content
BM	Bituminous Macadam
SDMB	Semi Dense Bituminous Macadam
ITSM	Indirect Tensile Stiffness Modulus
FS	Flexural Strength

CT	Curing Temperature
TS	Temperature Sensitivity
PWWC	Pre Wetting Water Content
VVCM	Vertical Vibration Compaction Method
MMC	Marshall Method of Compaction
EAC	Emulsified Asphalt Content
SCB	Semi-Circular Bending (SCB)
ITFT	Indirect Tensile Fatigue Testing
SEM	Scanning Electron Microscope
EDS	Energy-dispersive X-ray Spectroscopy
EMR	Electrolyte Manganese Residue
RM	Red Mud
CRT	Cathode Ray Tubes
CS	Compressive Strength
MS	Marshall Stability
HTST	High Temperature Stability Test
LTCRT	Low Temperature Cracking Resistance Test
XRM	X-Ray Micro-tomography
XRD	X-Ray Diffraction
HC	Hydraulic Conductivity
CTI	Cracking Test Index
SCB	Semi-Circular Bending
CSS	Cationic Slow Setting asphalt emulsion
OPC	Ordinary Portland Cement
TEAC	Trail Emulsified Asphalt Content
MoRD	Ministry of Rural Development

LVDT	Linear Variable Deformation Transducer
NMAS	Nominal Maximum Aggregate Size
OTFC	Optimum Total Fluid Content
ORBC	Optimum Residual Binder Content
TBC	Total Binder Content
SBS	Styrene-Butadiene-Styrene

ABSTRACT

Due to the rapid development of infrastructure, there is a depletion of natural resources of pavement materials. Aggregates are the primary raw material for pavement and building construction. The world is facing a scarcity of availability of excellent quality aggregates, which increases the cost of construction. With these shortcomings, there is a search for alternative materials. Alternative materials include recycled materials, wastes from the industries etc.

In the current study, two types of recycled materials, namely Reclaimed Asphalt Pavement (RAP) and Recycled Concrete Aggregates (RCA), are used as a base course material in the pavements stabilizing with cement and emulsified asphalt at various stabilization levels. The stabilization levels include low, medium and high (2.0%, 4.0%, 6.0%) in cement stabilization. For Emulsified Asphalt stabilization, at the lower side, at the optimum and higher side of optimum emulsified asphalt contents were considered. The recycled aggregates are replaced with Virgin Aggregates (VA) in various proportions (1:1, 1:3, 3:1) along with recycled aggregates alone and compared with VA in the case of Cement Treated Bases (CTB). Whereas five mix proportions were considered for Emulsified Asphalt Treated Bases (EATB), in which three are RAP-VA blends (25% RAP, 50% RAP and 75% RAP) and two are RCA blends (25% RCA and 50% RCA).

From the laboratory performance evaluation, the compaction characteristics, UCS, ITS, and fatigue life of CTB are significantly influenced by the RAP content in the mix. RAP and RCA bases require more than 6% cement content or 28 days of curing period to serve as pavement bases according to the Indian specifications. Self-cementing properties and Heterogeneity nature is observed in cement-treated RCA bases. The fatigue life is maximum at the 6% cement content and the 25% replacement of recycled aggregates than other combinations. In the case of EATB, RAP content emulsified asphalt content influence the bases' fatigue and permanent deformation characteristics. The residual binder content present in the mix significantly influences the rutting characteristics. The lower side of optimum emulsified asphalt content is suitable for the mixes having 50% or more RAP content. The sensitivity towards emulsified asphalt content is significantly less for EATB prepared with RCA. Treated bases reduce the overall thickness of the pavement and save the conventional aggregate materials.

Keywords: Recycling, RAP, RCA, Stabilization, Cement, Emulsified asphalt

CHAPTER 1

INTRODUCTION

1.1 General

Road transport is a critical infrastructure for the economic development of any country. In India, roads are one of the dominant modes of transport, carrying about 65% freight and 80% passenger traffic. India has the second-largest road network globally at approximately 62.16 lakh km (6.2 million km). This comprises National Highways (NHs), Expressways, State Highways (SHs), Major District Roads (MDRs) and Village Roads (VRs). The NHs and SHs have 1,36,440 km and 1,76 818 km, respectively. The other roads consist of 59,02,539 km. (Ministry of Road Transport and Highways (MoRTH) 2020-21). According to the National Highways Authority of India (NHAI), it is estimated that approximately 37 km of NHs are constructed per day during the financial year 2020-2021. Apart from NHs, many other road construction activities occur under various development schemes. This requires enormous quantities of natural resources like aggregates.

Further, the construction cost per km of four-lane NHs touches ten crores (100 million) rupees (MoRTH, 2020-21). The increase in construction costs is due to the scarcity of suitable quality aggregates and transportation costs. This problem is faced all over the world, including in developed countries. In a search for alternative materials, the recycled material in pavements has gained a lot of interest in recent years which can substitute the conventional aggregates.

Reclaimed Asphalt Pavement (RAP) and the Recycled Concrete Aggregate (RCA) are the two primarily recycled materials. RAP is a recycled material obtained from the deteriorated in-service flexible pavements and RCA is obtained from the Construction and Demolition (C&D) of old concrete pavements, buildings, dams and other concrete structures. The majority of these materials are used for landfilling and very few are used for recycling. These recycled materials can be used in bituminous and base layers. However, the utilization of recycled aggregates in surface layers is limited to 50%. But, the base layers which transfer the traffic load onto the subgrade can be replaced with recycled aggregates. Generally, the base layers are granular materials such as Wet Mix Macadam (WMM), Water Bound Macadam (WBM) or Crusher Run Macadam (CRM) made of natural aggregates. Replacing these natural aggregates with recycled materials preserves the natural resources. It also helps in the sustainable development of roads which remains a challenge worldwide. But, the recycled materials have already been in service for several years and can be deteriorated due to traffic, climate, and environmental factors. As a result, these materials cannot be used directly for construction as they do not satisfy all the

required engineering properties of conventional pavement materials. To improve the properties of the recycled materials, mechanical and chemical stabilization can be done, which improves the recycled materials' mechanical properties. The chemical stabilizers include cement, lime, emulsified asphalt, fly ash etc. However, cement and emulsified asphalt are primarily used in the recycling process and are widely available. The present study investigated the cement and emulsified asphalt stabilized recycled bases using several parameters at various stabilization levels.

1.2 Types of Pavements and their Functions

Based on the structural behavior, pavements are generally classified into three categories;

1. Flexible Pavements
2. Rigid Pavements
3. Composite Pavements

1.2.1. Flexible Pavements

Flexible pavements are those, on the whole, have low or negligible flexural strength and are somewhat flexible in their structural action under loads. The flexible pavement layers reflect the deformation of the lower layers onto the surface of the layer. Thus, if the lower layer of the pavement or soil subgrade is undulated, the flexible pavement surface also gets undulated. A typical flexible pavement consists of five components, soil subgrade, Sub base course, Base course, binder course and surface course. The surface course resists the wear and tear due to traffic, and all the bituminous layers resist fatigue and rutting. Rutting is a phenomenon where surface depression occurs due to traffic loading along the wheel path.

Similarly, a series of interconnected cracks, termed fatigue cracking, will form due to repeated application of traffic loading. The flexible pavement layers transmit the vertical or compressive stresses to the lower layers by grain transfer through the contact points in the granular structure. A well-compacted granular system consisting of strong graded aggregate (interlocked aggregate structure with or without binder materials) can transfer the compressive stresses through a wider area and thus form an excellent flexible pavement layer. Due to the ability to distribute the stresses to a larger area in the shape of a truncated cone, the stresses decrease at the lower layers. Therefore, the load spreading ability of this layer depends on the type of materials and the mix design factors. Bituminous concrete is one of the best flexible pavement layer materials. Other materials which fall under this group are all granular base and sub-base course materials like WBM, crushed aggregate, gravel, and soil aggregate surface directly under the wheel load and are equal to the contact pressure under the wheel load. A typical flexible pavement section is shown in Figure 1.1.

Therefore, the layer concept system was developed by taking full advantage of the stress distribution characteristics of the flexible pavements. According to this, the flexible pavement may be constructed in several layers. The top layer has to be the strongest as the highest compressive stresses are to be sustained by this layer and the wear and tear due to traffic. The lower layers have to take up only lesser magnitudes of stresses, and there is no direct wearing action due to traffic loads. Therefore, inferior materials with lower costs can be used in lower layers. The lowest layer is the prepared surface consisting of the local soil; itself called the subgrade.

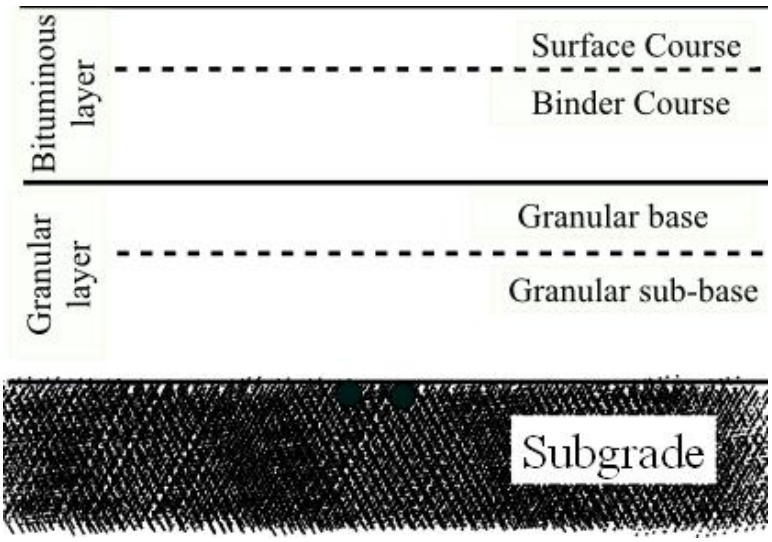

Figure 1.1 Typical Cross-Section of a Flexible Pavement

1.2.2. Rigid Pavements

Rigid pavements have higher flexural strength, modulus of elasticity, and slab-like behavior and spread the stresses to more extensive areas than flexible pavements. The rigid pavement does not reflect the lower layers' deformation on the surface. However, localized failure occurs due to inadequate support from the subgrade layer. In the earlier years, the rigid pavements were placed directly on the subgrade without providing a base or sub-base. With the increase in traffic loads and volume, mud pumping occurs, then base layers and drainage layers are used. A typical rigid pavement consists of the following components like soil subgrade, Sub-base course, drainage layer, Dry Lean Concrete (DLC) or Cement Treated Sub Base (CTSB), debonding layer and Pavement Quality Concrete (PQC) as a surface course. The debonding layer may be a Polythene sheet. The debonding layer is used in unreinforced and jointly reinforced rigid pavements. However, it is not applicable for continuously reinforced concrete pavements. Rigid pavements are used in high-stress areas like near toll gates, runways, waterlogging areas, heavy rainfall, and poor drainage conditions. Rigid pavements have slab-like behavior and have poor riding quality compared with flexible pavements. Rigid pavements are divided into 4 types:

- Jointed Plain Concrete Pavement
- Jointed Reinforced Concrete Pavement
- Continuous Reinforced Concrete Pavement
- Pre-stressed Concrete Pavement

Rigid pavements are generally subjected to different stresses, including wheel load, frictional, and temperature stresses. Rigid pavements perform well when the combined stresses falls within the allowable tensile stresses. Generally, fatigue analysis is carried out for the rigid pavements to determine the damage due to the traffic loads. It is expressed in Cumulative Fatigue Damage (CFD), the ratio of repetitions to the allowable number of repetitions. It should be less than 1 to consider the pavement is safe. A typical cross-section of the rigid pavement is shown in Figure 1.2.

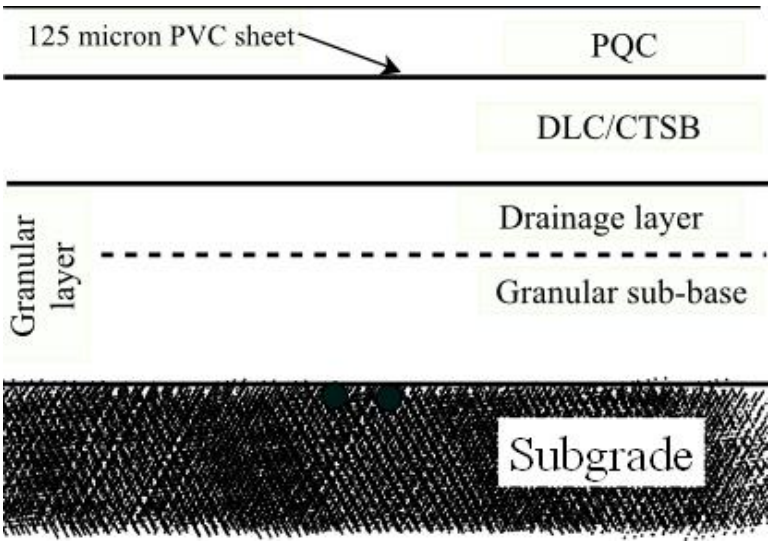

Figure 1.2 Typical Cross-Section of a Rigid Pavement

1.2.3. Composite Pavements

There are two types of composite pavements, namely semi-flexible and semi-rigid pavement. Flexible composite pavement is part of an unbound layer replaced with a cement-bound layer in a conventional flexible pavement. On the other hand, an asphalt layer is placed on a rigid pavement in rigid composite pavements. The base and sub-base courses are common layers that distribute stresses from the top layers to the subgrade safely from the different pavements. Base layers are essential because quality base materials increase the longevity of the final pavements. The outermost layer or surface course life depends on the base layer present underneath. So, due importance is given to the base layer design and construction.

1.3 Use of Recycled Concrete Aggregate and Reclaimed Asphalt Pavement in Pavements

RCA comprises aggregates and cement mortar widely used for landfills and sometimes for the construction of shoulders. RAP consists of valuable aggregates, which are covered by an asphalt coating. These materials will create a sustainable environment and decrease conventional aggregates' usage, protecting natural resources. In different percentages, RAP can be used in several pavement layers like a surface course, binder course, bases, and sub-bases. Studies recommended using RAP as granular material for shoulders, backfills, bicycle tracks, parking areas, etc. (Chesner et al.1998).

Similarly, RCA can be used as base and sub-base courses in pavement construction. Utilizing these wastes can help cleaner production with less pollution and low carbon footprints. However, the utilization of these materials is limited by several agencies due to poor engineering properties and heterogeneity and is recommended for stabilization. Cement stabilization of these recycled waste materials will improve the load-bearing capacity and makes stiffer bases (Xuan et al. 2011).

Similarly, emulsified asphalt stabilization of recycled materials improves mechanical properties, commonly known as Emulsified Asphalt Treated Bases (EATB). When the recycling takes place using emulsified asphalt or foamed asphalt, the process is termed Cold In-Place Recycling (CIPR). When CIPR is compared with cement stabilization or Cement Bound Macadam (CBM) and Unbound Granular Materials (UGM) in terms of Green House Gas (GHG) emission and energy consumption, CIPR exhibits lower GHG emissions and consumes less energy, as shown in Figure 1.3 (Chehovits & Galehouse 2010).

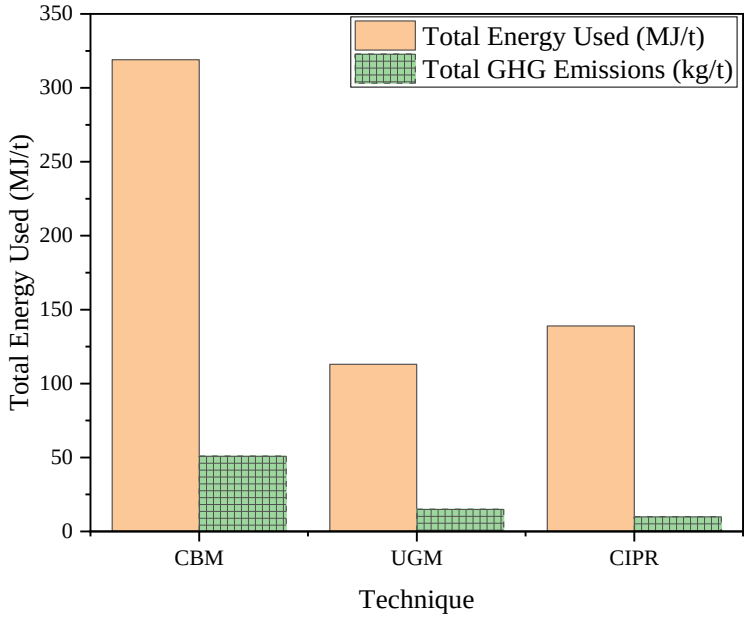

Figure 1.3 Energy consumption and GHG emissions for different Bases (Chehovits & Galehouse 2010)

1.4 Demand for Aggregates around the World

The demand for the usage of Virgin Aggregates (VA) for the present and future is increasing day by day. According to the Freedonia Group, in world road construction aggregates of 2017, 43 billion tons of non-metallic minerals are extracted for usage worldwide. The aggregates demand is more for the Asia/Pacific region worldwide (The Freedonia Group. 2012). Non-metallic minerals include limestone, manganese, mica, gypsum, coal, dolomite, phosphate, salt, granite, etc. The highest consumption is limestone, which is used to construct the roads, buildings, and railways.

A typical percentage of Construction and Demolition (C&D) waste generation of total waste and the percentage of recycling of C&D is shown in Figure 1.4 (Tam 2008). Moreover, more recycling takes place in Denmark, followed by the Netherlands. Concerning India, the second-largest country in terms of population, the total C & D waste is around 23 million tonnes generated every year, and only 5% is recycled. Out of the total C & D waste, 1.8 million tons of RCA have been generated annually (Central Pollution Control Board 2017). Jain et al. (2018) estimated the C&D waste generation using around 112 to 431 million tonnes of material flow patterns. From the C & D waste statistics, it is clear that the generation of recycled aggregates will surpass natural aggregates production in the future. This will increase the generation of C&D and utilization of natural aggregates as well. If the same trend is continued, there might be no VA to cater needs of the future generation. Nowadays, recycled aggregates are considered waste materials and dumped at the roadsides and used for land fillings. Recycling these aggregates is the only option available to preserve the natural aggregates and protect the environment. The utilization of recycled aggregates is cheaper and consumes less energy than processing the natural aggregates. The only thing is to identify recycled materials from different sources like roads, industries, buildings, etc. and conserve them effectively for pavement construction activities.

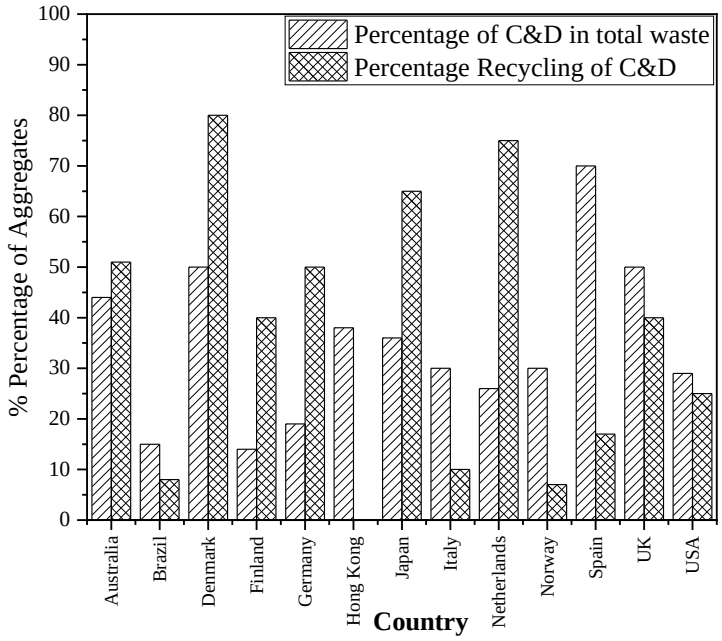

Figure 1.4 Statistics of C&D in different countries (Tam 2008).

The composition of C&D waste varies between countries based on the construction and demolition activities. A typical composition of C&D waste in India is presented in Figure 1.5 as given by Technology Information, forecasting and Assessment Council (TIFAC 2001). More than 50% of the total C&D comprises brick, masonry, and concrete waste.

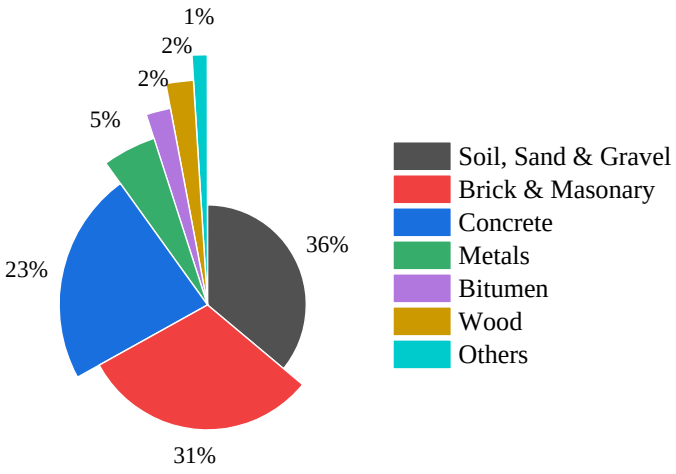

Figure 1.5 Composition of Construction and Demolition waste in India

1.5 Need for the Study

When Hot-Mix Asphalt (HMA) pavements reach the end of their usable service lives, their materials retain considerable value. In the early 1970s, road agency contractors began using Reclaimed Asphalt Pavement (RAP) in new HMA pavements. Besides possible cost savings, this use of RAP represents an environmentally positive method of recycling. Similarly, the Recycled Concrete Aggregate (RCA) is a granular material manufactured by removing,

crushing, and processing hydraulic-cement concrete pavement for reuse with a hydraulic cementing medium to produce fresh paving concrete in pavement construction.

It is evident that the total length of road construction in India is increasing year by year, as shown in Figure1.6 (MoRTH 2020-21).This requires enormous quantities of natural aggregates. Reddy et al. (2016) stated that about 5 billion tonnes of aggregates are needed for total construction activities in India by 2020; likewise, the rapid construction activities led to the non-availability of the aggregates of good quality around the world. The scarcity of natural aggregates increased the cost of road construction. So, there is a search for alternative materials like recycled aggregates from different sources like RAP and RCA, which are obtained from the rehabilitation of the deteriorated pavements and the C&D industry. At the same time, the C&D waste generation is increased at a tremendous rate and illegal dumping activities were raised. Owing to the generation of massive quantities of C&D, the major portion is utilized in road construction as a road base (Cardoso et al. 2016). Using the C&D in pavement bases allows enormous quantities of the conventional materials to be replaced, saves cost, and is a sustainable activity. But, the recycled materials in the pavement construction activities were constrained due to the variability in recycled materials.

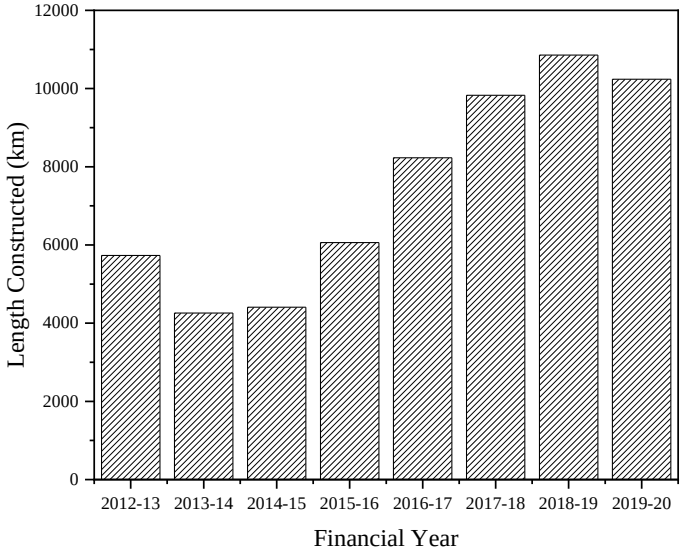

Figure 1.6 Total length of road construction in India during financial years

Considering the due importance of recycled materials, the present study aimed to utilize recycled aggregates, namely RAP and RCA, in road bases by stabilization. Although there are studies on including these recycled materials in pavement bases, considerable gaps were observed in the available literature (Taha 2003; Xuan et al. 2012; Agrela et al. 2014; Del Ray et al. 2016; Arisha et al. 2018; Marvila et al. 2020; Arshad 2020). At the same time, the Indian code of practice (IRC SP 100: 2014) throws a little light on the design of EATB and most of them are adopted from the other countries' specifications. Further, there are minimum studies

on recycled aggregates and cement content that influence the fatigue characteristics of CTB and the performance of EATB at different stabilization levels. From the anticipation of stabilizing partial to full replacement of C&D waste, the present study aimed to fulfill the above gaps where cement and emulsified asphalt are the primary stabilizers used. This study evaluates the stabilized bases for various performance characteristics like strength, stiffness, rutting, and fatigue. The focus was to figure out the response of the recycled bases with respect to the recycled aggregate portion at low, moderate and high stabilization levels.

1.6 Objectives of the Study

The following are the main objectives of the present study

1. To study the strength and Resilient modulus of Cement Treated Bases (CTB) at different stabilization levels for different recycled aggregate combinations.
2. To evaluate the fatigue characteristics of CTB at different stabilization levels for different recycled aggregate combinations.
3. To evaluate the Resilient modulus and permanent deformation characteristics of EATB at different stabilization levels and temperatures
4. To study the fatigue characteristics of EATB at different stabilization levels.
5. To Analyze and compare the design with different stabilized layers using IITPAVE software.

1.7 Organisation of the Thesis

This section presents the details of the organization of the thesis into different chapters.

Chapter 1 deals with the significance and importance of the proposed thesis work. The study's objectives and need for the study are presented in this chapter.

Chapter 2 explains various research works that are previously relevant to the present study and different design procedures involved in the stabilization of recycled aggregates. Blending and proportions of the recycled aggregates, mechanical properties, and performance characteristics of Cement treated and emulsified asphalt treated bases have been reviewed.

Chapter 3 presents a detailed description of the present research work, including the experimental program with specifications. The experimental program includes material characterization and various performance tests.

Chapter 4 presents the RAP, RCA, and VA characteristics following blending, gradation, and mix design of cement-treated bases at various cement contents. After mix design, mechanical characterization of unconfined compressive strength, indirect tensile strength, resilient modulus, and fatigue life were presented.

Chapter 5 presents the mix design of emulsified asphalt treated bases and the specifications limitations. After the mixes' performance characteristics like Indirect Tensile Strength, Tensile strength ratio, dynamic creep rutting, stiffness at different temperatures, stabilization levels and fatigue life were presented in detail.

Chapter 6 pavement analysis using IIT PAVE software incorporates Cement Treated Bases and Emulsified Asphalt Treated Bases stiffness results compared with conventional bases.

Chapter 7 presents a summary, conclusions and future scope of the study.

CHAPTER 2

LITERATURE REVIEW

2.1 General

Keeping in view of the main objective of the present research to evaluate the performance of CTB and EATB that are prepared using RAP and RCA, different aspects related to the history, mix design, characterization of the mechanical properties of the mixes around the world that includes strength, modulus and fatigue characteristics of the stabilized bases are reviewed and presented in this chapter. The primary and important literature is summarized in the following sections.

2.2 Cement Treated Bases (CTB)

Cement Treated Base is a mixture of aggregate or soil material with cement, compacted at Optimum Moisture Content (OMC) and cured for a certain period to obtain a stiffer base. Cement stabilization is mainly used to strengthen the weak subgrade, base, and sub-base course, increasing the pavement's load transfer efficiency. Different studies were carried out on stabilizing recycled materials in combination with VA. The adopted cement contents in these studies ranged from 2% to 10%, depending on the strength requirements. These stabilization levels depend on material properties, traffic conditions, strength, and durability. The performance parameters considered to study the CTB are Unconfined Compressive Strength (UCS), Flexural Strength (FS), Indirect Tensile Strength (ITS), Resilient modulus, Secant modulus, permanent deformation, fatigue, etc.

2.2.1 History of Cement Treated Bases

The CTB was first coined in 1935 (Halsted et al. 2006). The utilization of CTB enabled the use of recycled aggregates and reductions in the overall thickness of the pavements. In addition to it, the soil subbases were also used to stabilize with a lesser amount of cement than the CTB. In present days, the utilization of cement is extensively extended to the different pavement applications like white-topping, stabilizing the bases and sub-bases during the pavement constructions. Cement treated bases are different from the concrete mixtures, where lightly cemented (2-10%) than concrete mixtures (10-15%). The amount of cement is selected based on the required compressive strength for both mixes. The utilization of super-plasticizers is adopted in concretes to achieve early strength, curing, and some particular purposes. However, pre-treatment is done for recycled materials using super-plasticizers or other additives to achieve adequate strength. Also, the aggregate composition of the CTB is entirely different

from the concrete mixtures. In addition to the super-plasticizers, some air-entertaining agents for particular concrete application purposes are used.

Cement-treated bases can be evaluated using different parameters. UCS is the primary parameter adopted by more than 70% of the researchers, followed by stiffness and Resilient Modulus (M_R). The measurement of cohesion is represented in terms of UCS. Every country has its specification limits of UCS for base material. Besides, ITS is an important parameter determining the resistance towards tensile cracks. The modulus is used to characterize the materials and to design/ analysis of pavements. Durability studies include wet-dry cycles and freeze-thaw cycles that replicate the long-lasting nature of the pavement bases. This section presents all these parameters at different Curing Periods (CP) and cement contents. Some studies used recycled materials directly, and others treated them before using them. Some mixes need to be designed appropriately with suitable aggregate combinations. Likewise, a balanced mix designed electric arc furnace slag and VA can be used to alternative the conventional base and sub-bases (Autelitano and Giuliani 2016). In this way, most recycled materials are induced into the pavement base layers by cement stabilization.

2.2.2 Mechanism and Critical Locations of strains of Cement Treated Bases

Cement-treated bases are advantageous over conventional base materials. CTB has higher stiffness and distributes the loads evenly to the subgrade to larger areas. This results in a lower intensity of stresses onto the subgrade that avoids excessive deformations. The response of CTB is like a slab instead of granular materials, which is grain to grain contact. In the presence of CTB, the vertical compressive strains on top of the subgrade are comparatively lower than that of the conventional aggregate base sections.

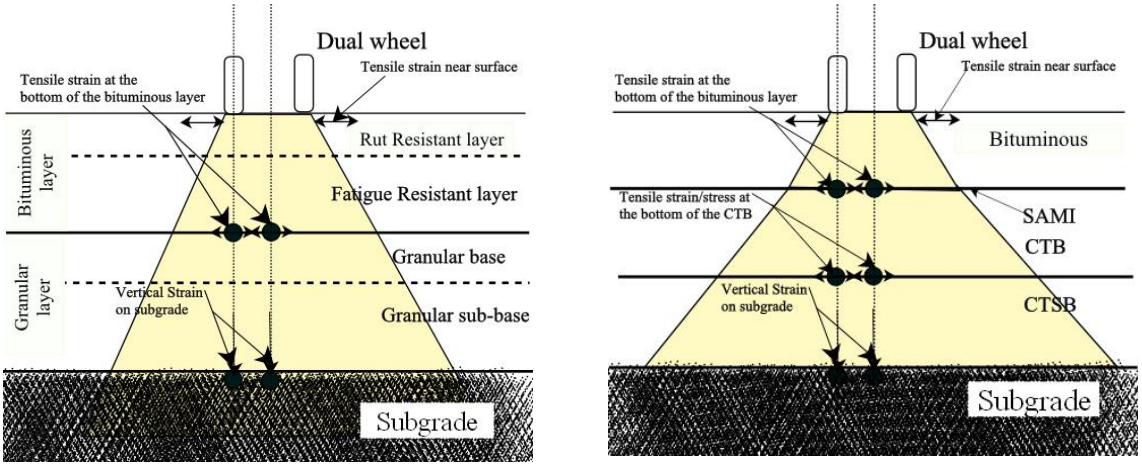

Figure 2.1 Stress distribution in pavements with conventional bases and CTB

Further, the CTB layer is impervious and durable, preventing water and soil particles from moving onto the top surface layers. A typical CTB and conventional bases comparison is made in Figure 2.1, where the intensity of stresses is more on subgrade in traditional bases. The stress

intensity is less and well distributed in the case of CTB. Further, the overall pavement thicknesses are less in CTB incorporated pavements compared with pavements with conventional bases.

2.2.3 Compaction Characteristics of Cement Treated Bases

Compaction characteristics include OMC and Maximum Dry Density (MDD) which are important in achieving the excellent compatibility of the bases. The compaction is performed using a modified proctor testing procedure according to the AASTHO T180 protocol. In this test, a mould size of 102 mm diameter and 127 mm height is used, and each layer is compacted using a 4.5 kg hammer from a free fall of 457 mm. OMC and MDD depend on the water absorption capacity of the ingredients in the mixture and their compatibility. The behaviour of the cement-treated bases is different from the normal bases as it involves different percentages of recycled aggregate contents and cement contents. Fedrigo et al. (2018) concluded that OMC and MDD are not significantly influenced by the cement content and percentage of RAP content. Xuan et al. (2012) concluded that the MDD for recycled mixes (RMA and RCA) is influenced by the compaction method and energy, where OMC increases and MDD decreases with an increase in RMA. Higher OMC is observed for RCA mixes compared with conventional aggregates because of higher water absorption of the RCA, and also coarse RCA has a higher demand for water than that of the fine RCA (Lim and Zollinger 2003). Liu et al. (2020) observed an increase in MDD and OMC with the increase in the steel slag content. A typical comparison of different recycled materials at constant cement content is shown in Figure 2.2. RAP has low OMC and high dry density, and RCA has the opposite with high OMC and lowers dry density (Taha 2003; Mohammadinia et al. 2015). The nature of more water absorption of RCA is due to the porous nature of the surrounding mortar, and the lower OMC of RAP is due to the asphalt coating that prevents the water absorption of the RAP. For cement-treated recycled bases, MDD might not replicate the compressive strength as many factors influence strength development. Lim and Zollinger (2003) revealed that two different materials, namely recycled concrete and crushed limestone with the same MDD, achieved different strengths. Typically, Leite (2007) concluded that the determination of the OMC for the C&D waste mixtures is slightly tricky due to the differences in the constituent's materials due to breakage during the compaction process. Besides, Guo et al. (2020) used a combination of VA and RCA from cement stabilized macadam at various percentages. It is observed that an increase in the OMC and MDD with the cement content observed a reduction in MDD and an increase in OMC with RCA. While the MDD of VA is significantly higher than that of the recycled aggregates, there is no particular trend observed in the case of OMC from the studies (Taha et al. 2002; Marvila et al. 2020). The lower MDD of recycled materials is due to their combination with other materials. For example,

the RAP combines aggregates and asphalt; RCA combines aggregates and mortar; Crushed Brick (CB) is a combination of brick and mortar.

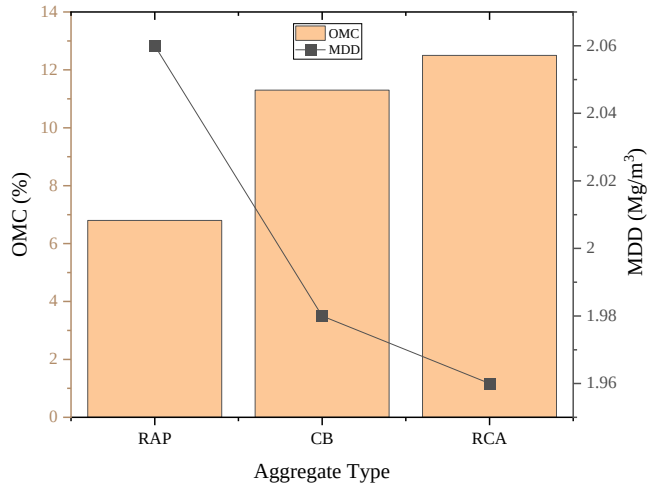

Figure 2.2 Typical OMC and MDD for different aggregates at constant cement content

Water and cement are the two critical components that impart workability and strength. It is reported that there is a decline in the strength of the base with the increase in water to cement ratio irrespective of the type of recycled material and improves the workability (Mohammadinia et al. 2015). The properties like compressive strength, density, water absorption capacity, porosity, and flexural strength were affected by increasing the water to cement ratio (Marvila et al. 2020). Hence, the water content shall be selected so that the maximum strength is achieved, and it is better to skip the construction of the treated bases in wet conditions. The water should be optimum to complete the hydration reaction, and more water leads to the voids in the mixture after the evaporation process. The recommended water to cement ratio is less than or equal to 0.5 (Mohammadinia et al. 2015). Generally, OMC is considered to counteract this problem. However, laboratory conditions might not exist in the field as free moisture exists in the aggregate before mixing due to environmental factors. All these factors and field conditions should be taken while constructing a pavement base.

2.2.4 Unconfined Compressive Strength (UCS) of Cement Treated Bases

UCS is one of the parameters used to measure bound materials' strength and cohesive nature, like chemically treated soil or aggregate specimens. Generally, the specimen size used in this test is 100 mm in diameter and 200 mm in height according to the ASTM D1632 protocol and compacted at OMC. In some studies, 100 mm diameter and 100 mm height are adopted. The prepared samples are cured at various periods and tested for compressive strength using a standard compression testing machine. This parameter primarily defines the bound bases' resilience and optimizes the stabilizer. The acceptable UCS range is approximately 300- 600 psi (2.1-4.1 MPa). Several studies were carried out on UCS of cement/Cement Kiln Dust (CKD)

stabilized recycled aggregate blends (Taha 2002; Yuan et al. 2011; Guthrie et al. 2007; Taha 2003; Hoyos et al. 2011) discussed in the following sections. Besides, some industrial waste materials like EMR and RM are used in some studies. However, pre-treatment is required for such materials to prevent leachate problems and unwanted reactions (Zhang et al. 2019). In addition, Guo et al. (2020) used additives and early strength anti-cracking materials, improving the strength within the 7 days of curing compared with normal mixtures. UCS depends on several factors like material type, gradation, stabilizer, curing period, RAP or RCA or ceramic or glass or any other recycled materials percentage, cement type, the addition of fibers, etc. Some of the factors that influence the strength of the bases are presented in Table 2.1.

Table 2.1 Influence of different parameters on UCS of RAP materials

Parameter	Yuan et al. (2011)	Guthrie et al. (2007)	Taha (2003)	Taha et al. (2002)	Suebsuk et al. (2019)
RAP content	UCS #	UCS #	-	UCS #	UCS #
Cement content/CKD	UCS *	UCS *	UCS *up to 15%	UCS *	UCS *
Curing period	-	-	UCS *	UCS *	UCS *
Asphalt content	No impact on strength	-	-	-	Have a significant effect on the strength of CTB

*-Increases, #-Decrease

Demolition waste includes CB, Fine Recycled Glass (FRG), ceramic materials, Recycled Masonry Aggregate (RMA), RAP, etc. On the other hand, several studies on RCA with different percentages of cement contents, size fractions, and other C&D waste results of UCS are summarized in Table 2.2.

Table 2.2 Influence of different parameters on UCS of RCA materials

Parameter	Faysal et al. (2016)	Mohammadinia et al. (2015)	Lim and Zolliner (2003)	Arulrajah et al. (2015)
RCA content	UCS *	-	-	RCA-FRG blends have more UCS than pure RCA.
Cement content	UCS *	UCS *	-	
Curing period	-	UCS *	UCS *	UCS *
OMC	100% RCA has high OMC	RCA has higher OMC compared with other C &D	RCA has more OMC compared than VA,	RCA has higher OMC

2.2.4.1 Variation of UCS with Cement Content/Cement Klin Dust (CKD)

UCS increases linearly with the cement content irrespective of the RAP material type, as shown in Figure 2.2 (Yuan et al. 2011; Guthrie et al. 2007; Fedrigo et al. 2019; Taha 2003; Arshad 2020). However, the UCS increases up to 15 % in CKD stabilization and starts to decline (Taha 2003). Further, a similar increase in UCS with cement content is observed for 50% RAP blended with VA (Yuan et al. 2011; Guthrie et al. 2007; Puppala et al. 2017). The strength increases with the amount of binder through pozzolanic reactions and establishes strong bonds. The gain in strength of 100% RAP is low and requires more cement to reach the desired strength than other blends. This is because of the improper bonding with less cement as the RAP material is asphalt coated and has more slip surfaces. In a study by Suebsuk et al. (2019), two materials, namely RAP and laterite soils, were stabilized using cement. The gain in strength is more when cement content is less than 10% and decreases when it exceeds 10%. The cement requirement varies from cement type, base material, depth of milling, and type of recycled material. When utilizing the cement by-products like CKD, it is necessary to determine optimum dosage; otherwise, there might be a decline in strength (Taha 2003). A typical comparison is made with the specifications mentioned in Table 2.3 with the researchers' results. There is variability in meeting the required specifications, depending on the cement content, recycled aggregate type, and aggregate content. However, most of the results achieved the requirement as a base, and the sub-base with the cement content was less than 5%. The efficiency of the cement by-products like CKD and fly ash are less than that of the cement as large amounts are required for stabilization. Further, optimization is needed for cement by-products, whereas the cement stabilized bases proportionally increased their strengths.

Table 2.3 Summary of UCS specifications for road bases at seven days of curing period

Country/ Code	UCS (MPa)			
India	LVR < 2 msa		HVR> 3 msa	
	Sub-base	Base	Sub-base	Base
	1.70	2.76	1.5-3.0	4.5-7.0
China	Secondary road		Highway	
	1.5-2.0	1.5-2.5	1.5-2.5	3.0-5.0
United Kingdom	CBM 1	CBM 2	CBM 3	CBM 4
	2.5-4.5	4.5-7.5	6.5-10.0	10.0-15.0
South Africa	C1	C2	C3	C4
	4-8	2-4	1-2	0.5-1
New Zealand	3			
Portland Cement Association	2.1-5.5			
Spain	2.5-4.5			
Australia	>3			

Brazil	>3.5
Spain	4.5-6
USA	3.5-6.9 for PCC, 5.2-6.9 for HMA
Italy	2.5-5.5

CBM 1, CBM 2, CBM 3, and CBM 4 are classified based on gradation according to Britain, and C1, C2, C3, and C4 are classified based on the South Africa specification. LVR-Low Volume Roads, HVR-High Volume Roads

Overall the strength of the RAP blended mixes increases with the cement and VA in which cement acts as a bonding material, and VA results in better interlocking between the RAP and VA. Similarly, there is an improvement in the UCS when cement is added to the RCA, irrespective of the type of material. Studies conducted on RCA stabilized with cement are shown in Figure 2.3 (Lim and Zollinger 2003; Mohammadinia et al. 2015; Faysal et al. 2016; Arulrajah et al. 2015; Behiry 2013). Figure 2.3 (d) shows the strength variation of VA, RAP, and RCA cement-treated bases. It is observed that the rate of gain in strength of RCA treated bases is more with the addition of cement content compared with RAP and VA. RAP has a significantly lower rate of strength gain with the addition of cement because of asphalt coating. In addition to the cement, the existing mortar in the RCA contributed to the higher strengths.

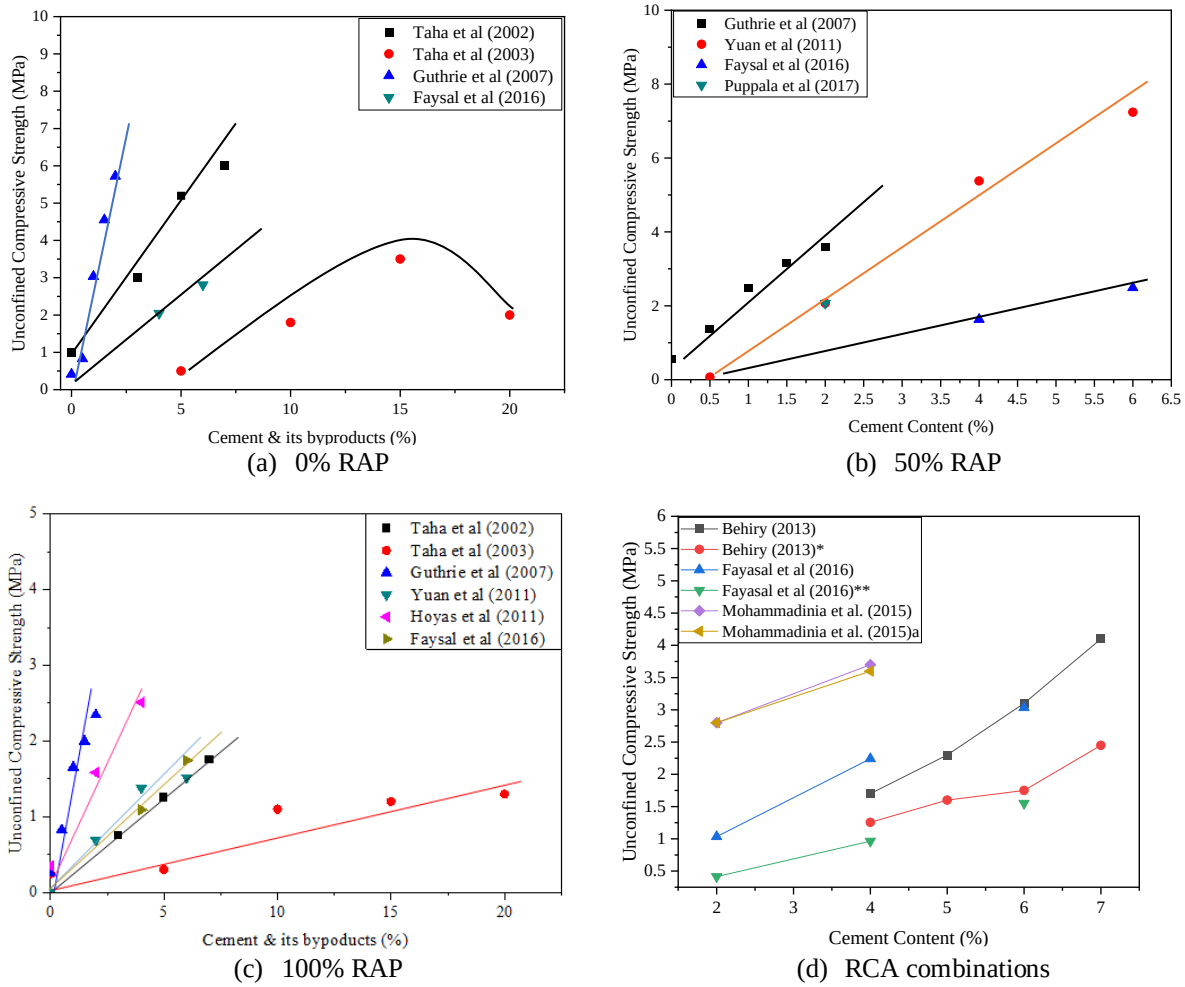

Figure 2.3 Variation of UCS with Cement content and its by-products

* VA, ** RAP, 'a' is another source

2.2.4.2 Variation of UCS with Recycled Aggregate Content

The UCS of cement-treated bases gradually decreases with the increase in the percentage of RAP independent of the stabilization levels, as shown in Figure 2.4 (Guthrie et al. 2007; Yuan et al. 2011; Fedrigo et al. 2018; Arshad 2020; Puppala et al. 2017; Arisha et al. 2018).

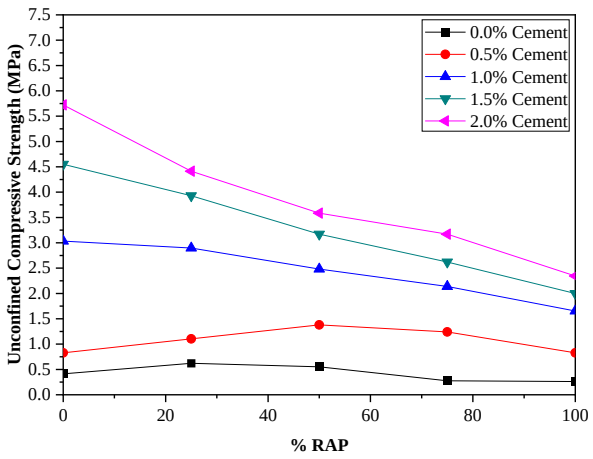

Modified and redrawn from Guthrie et al. (2007)

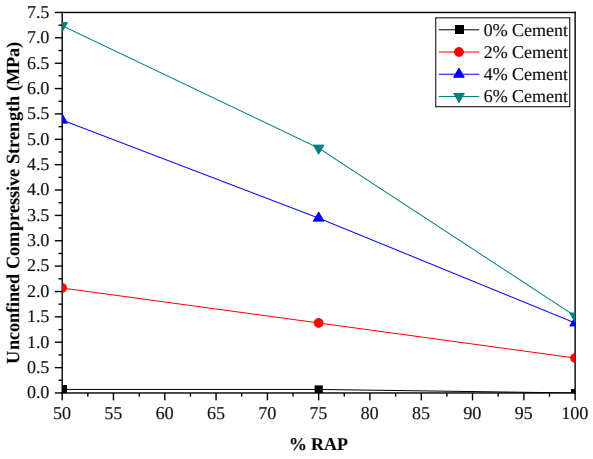

Modified and redrawn from Yuan et al. (2011)

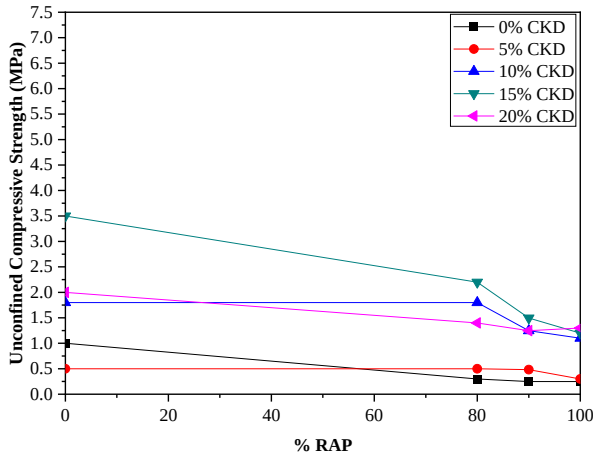

Modified and redrawn from Taha (2003)

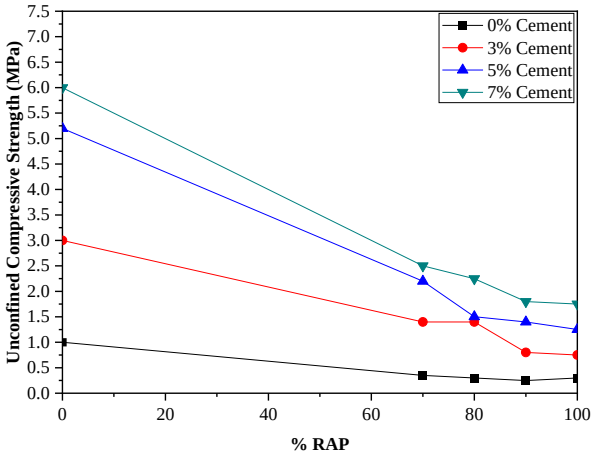

Modified and redrawn from Taha et al. (2002)

Figure 2.4 Variation of UCS with RAP content

From Figure 2.4, 100% of RAP has a low UCS value compared with VA. The UCS values for 100% RAP mixes without stabilization fall below the acceptable limits. Other blended mixes with VA or other base materials require lower cement than the 100% RAP. The decrease in strength with RAP content is due to the lowest specific gravity of RAP materials and slippery surfaces of the asphalt coating. The increase in strength with VA or base materials is due to good inter-locking nature (Subsuk et al. 2019). Apart from RAP content, cement content, curing time, and compaction effort influence the strength of the treated base (Fedrigo et al. 2018; Behiry 2013). So, these are the available options to increase the strength of the RAP mixes, including an increase in the amount of cement stabilizer or compaction effort or VA or base material proportion in the mixes. In case of scarcity of the base materials or conventional aggregates, stabilization and compaction effort are the only available alternatives.

Besides, the strength of RCA blended with other aggregates like VA, RAP, and CB in various proportions depends on the type of material replaced. Figure 2.5 shows the variation of UCS with RCA in which three different materials are used as a replacement. When RCA is replaced with VA and stabilized with 5% cement, the UCS increases with an increase in the RCA content up to 75% replacement and decreases at 100% RCA alone (Behiry 2013). Guo et al. (2020) observed a decrease in compressive strength with RCA content. The packing density also influences the strength of the RCA mixes (Yehia et al. 2015). When RCA was replaced with RAP, the UCS significantly improved with RCA content irrespective of the cement content (Faysal et al. 2016). Xuan et al. (2012) replaced CB with RCA at different cement contents (0 to 5.5%) and observed an increase in UCS with RCA content.

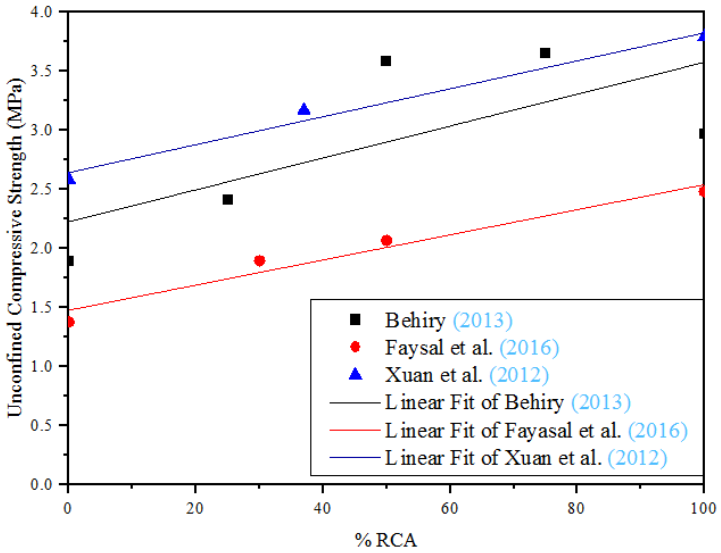

Figure 2.5 Variation of UCS with RCA content

Faysal et al. (2016) proposed a model for the strength of the unbound and cement treated RCA-RAP blended Bases as a function of RAP content at seven days of the curing period, as shown in equations 2.1 and 2.2.

For cement-treated bases,

$$f_{c7}(RAP) = f_{c7}(RCA) - 1.285(RAP\%) \tag{2.1}$$

For Unbound bases,

$$f_{c7}(RAP) = f_{c7}(RCA) - 0.098(RAP\%) \tag{2.2}$$

Experimental studies on stabilizing two recycled materials with different percentages of replacements were carried out. The replacement is successful in achieving the desired strength specified by local authorities. However, the percentage of replacement is restricted depending on the strength achieved. Some studies include RAP/RCA, RCA/FRG, RCA/RMA, or a combination of recycled materials in some percentages. Arulrajah et al. (2015) studied the

replacement of FRG with RCA at 3% of cement stabilization and found encouraging results with acceptable strength. Faysal et al. (2016) replaced RAP/RCA and concluded that 100%RAP could not be used as it required higher cement content than 6%, which is uneconomical. Xuan et al. (2012) confirmed that the RMA percentage and cement content influence the strength of the mixture and concluded that the masonry particles' failure affects the strength rather than the bonding interface. Similarly, industrial by-products like steel slag are used in the road bases, and maximum strength is achieved at 50% replacement.

2.2.4.3 Variation of UCS with Curing Period

The curing period is one of the critical factors in evaluating cement-treated bases. The authorities prefer sufficient compressive strengths at lower curing periods (less than 7days) to allow traffic early. In general, cementitious materials gradually attain strength with time. There is an increase in strength with the curing period independent of the material or cement used (Taha 2003; Arshad 2020; Arisha et al. 2018). The increase in strength is logarithmic (Hou et al. 2019). There is an increase in the UCS in RCA with the curing period independent of stabilization. This is due to the self-cementing properties of the RCA in which the size of less than 0.15 mm and 0.3 to 0.6 mm are significant for the self-cementing nature (Gabr and Cameron 2012; Poon et al. 2006). Cement-treated recycled aggregates combined with other marginal materials like RMA, ceramic material, FRG, sand, and brick also exhibited increased strength during the curing period (Xuan et al. 2012; Marvila et al. 2020; Agrela et al. 2014; Del Ray et al. 2016). The gain in strength continues to increase for 28 days in all the recycled materials, irrespective of the source.

2.2.4.4 Variation of UCS with Fines Content

The fines content in a mix plays a vital role in the strength variation. Fines content is one of the causes of shrinkage cracks when it is high in amounts, leading to insufficient interlocking and losing load transfer capacity when it is in low amounts (Adaska et al. 2004). Fines content in any blend has some ranges to achieve maximum density and strength as too many fines create a problem. The increase in the fines reduces the void ratio and increases the density of the mixture. Generally, material passing through a 0.075 mm sieve is represented as fines. From a study by Behiry (2013), the RCA blends exhibited higher strengths with increased fines. The UCS of RAP blended bases with VA increases with fines content (0.3% to 2.7%), and maximum UCS is observed at 2.7% (Yuan et al. 2011). So, there is an increase in the strength of the recycled bases with fines, irrespective of the material. However, this statement is valid up to certain limits of fines content. Lim and Zollinger (2003) concluded that the mixes show higher strength at 5% fines content than 10% fines content. This phenomenon is observed in both RCA and VA. The variation of strength may depend on material and gradation. Many specifications

adopted the fines range was less than 10% (Autelitano and Giuliani 2016; Gabr and Cameron 2012; MoRTH 2013).

2.2.5 Flexural Strength Properties of Cement Treated Recycled Bases

Flexural strength is simply resistance to bending, an essential parameter for the cement-treated bases as they experience bending during traffic movements. It can be determined using either a one-point or three-point bending test, mostly four-point bending, by applying loading at a constant rate. Table 2.4 presents the flexural strength of different recycled materials investigated by various researchers worldwide. The dimensions of the specimens are 7 x 7 x 28 cm3 or 10 x 10 x 40 cm3 are considered according to the standards. The nomenclature RCA0 represents the percentage of RCA is 0% in the mix, RAP0 represents the percentage of RAP percentage is 0% in the mix, and 90RCA/10FRG means the mix is a combination of 90% of RCA and 10% of FRG.

Table 2.4 Flexural strength of different recycled materials by different authors

Author (year)	**Mix**	**CC (%)**	**FS (MPa)**		**Specifications**
			7 days	**28 days**	
Behiry (2013)	100%VA	5.0	0.295	0.471	ASTM C-78
	25%RCA	5.0	0.281	0.452	
	50%RCA	5.0	0.272	0.428	
	75%RCA	5.0	0.265	0.41	
Khay et al. (2015)	VA	6.0	3.39		France Specifications NFP18-433
	25%RAP	6.0	2.38		
	50%RAP	6.0	2.14		
	75%RAP	6.0	1.60		
	100%RAP	6.0	1.08	NA	
Arulrajah et al. (2015)	100%RCA		1.23		Australia Standards AS2000
	90%RCA/10%FRG	3.0	1.85		
	80%RCA/20%FRG	3.0	1.66		
	70%RCA/30%FRG	3.0	1.56		
Jitsangiam et al. (2021)	100%VA	5.0	1.53	-	AS 2000
López et al. (2018)	20%RAP/80%VA	2.0/4.0		0.26/0.87	NCHRP Report-789
	50%RAP/50%VA	2.0/4.0		0.32/0.77	
	70%RAP/30%VA	2.0/4.0		0.21/0.80	
Liu et al. (2020)	30% Steel Slag	4.0	0.613		
	50% Steel Slag	4.0	1.063	NA	NA
	70% Steel Slag	4.0	0.929		

CC-Cement Content, FS-Flexural Strength

From the above Table 2.4, it is observed that the flexural strength of the recycled aggregate mixes decreases with the increase in the recycled material content (Behiry 2013; Khay et al.

2015). However, maximum flexural strength is observed at 50% replacement (Liu et al. 2020). Further, an increase in the flexural strength with the curing period, cement content, and early strength of anti-cracking additives is observed (Guo et al. 2020; López et al. 2018). The flexural strength ranges between 10-20 % of the UCS (Behiry 2013; Khay et al. 2015). Fedrigo et al. (2019) conducted a study on the cement-treated RAP and Laterite soil blends, revealing an increase in the flexural strength and modulus with the cement and RAP content. This is due to the increase in the specific surface area of the Laterite soils, which requires more cement contents for bonding. López et al. (2018) reported an increase in ductile nature with the RAP content when RAP and crushed aggregates combination is used. The results showed improved flexural strength and modulus with the cement content. Khay et al. (2015) observed a decline in the flexural strength with the RAP content. Overall, the recycled materials performed almost equal to natural aggregates in flexural strength.

2.2.6 Indirect Tensile Strength Properties of Cement-Treated Recycled Bases

Indirect Tensile Strength **(**ITS) is one of the essential properties of the cement-treated bases in which the tensile strains produced due to the traffic loads should be within limits to arrest the bottom-up cracking. In general, the tensile strains developed at the bottom of the cement-treated bases are critical, which leads to bottom-up cracking. The test specimens of size 100 mm diameter and 63 mm height or 100 mm diameter and 200 height or 150 mm height and 150 mm diameter are used. The samples are tested for ITS under loading on a diametric plane at different curing periods, different cement contents, and varying recycled aggregate percentages. Similar trends observed in the UCS are repeated in the ITS results in several research works. The ITS of the cement stabilized recycled blends decrease with the increase in recycled aggregate content and increases with the curing period and cement content (Yuan et al. 2011; Arshad 2020; Behiry 2013; Khay et al. 2015; Jitsangiam et al. 2021). The increase in strength is logarithmic (Hou et al. 2019). A typical variation of ITS with CC and recycled aggregate content is presented in Figure 2.6. Some of the specification limits of ITS for different countries are shown in Table.2.5. The ITS limitations are recommended based on the compaction type percentage of cement used. Compared with the earlier researchers' results compared with the specifications, the ITS is satisfied by all the combinations, except RAP treated bases that require more CC.

Table 2.5 Summary of ITS specifications for road bases at 7 days of curing period

Country/ Code	**Indirect Tensile Strength (MPa)**	
Italy	0.32-0.60 (Gyratory Compaction)	> 0.25 (Proctor Compaction)
South Africa	>0.25 for Cement 1.5-3%	>0.20 for Cement 3-5%

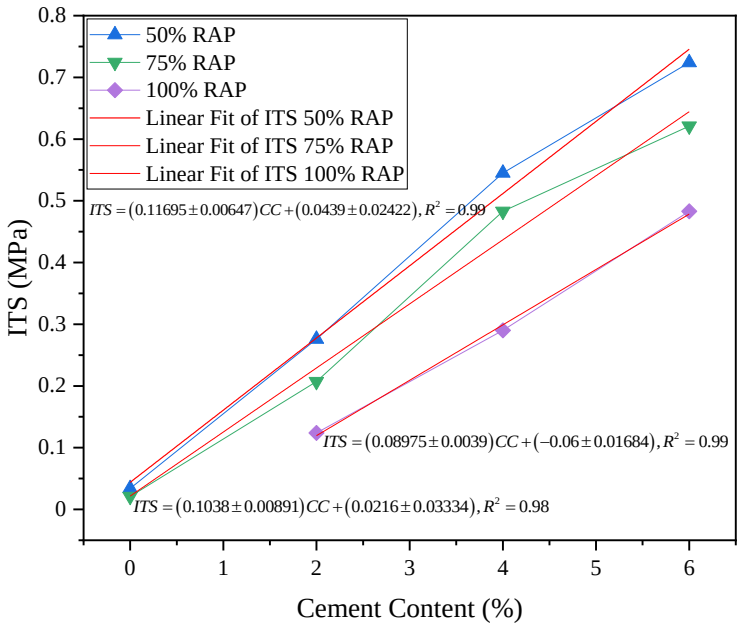

Figure 2.6 Variation of ITS with Cement and recycled aggregate content

The strength of cement-treated bases depends on several factors. The most influential factors are water-cement ratio, dry density, masonry content, and curing time. Different investigators proposed several models for ITS based on the experimental analysis, as shown in the equations below.

Xuan et al. (2012),

$$f_{it} = 0.0293 \times \left(\frac{C}{W}\right)^{1.3} \times D^7 \times e^{0.008M} \times e^{\{1.6[1-\left(\frac{28}{t}\right)^{0.2}]\}} \tag{2.3}$$

ACI Model (Xuan et al. 2012)

$$f_{it} = 0.0293 \times \left(\frac{C}{W}\right)^{1.3} \times D^7 \times e^{0.008M} \times \frac{t}{6.5 + 0.7t} \tag{2.4}$$

Log Scale Model (Xuan et al. 2012)

$$f_c = 0.0293 \times \left(\frac{C}{W}\right)^{1.3} \times D^7 \times e^{0.008M} \times \{1 + 0.87 \log \frac{t}{28}\} \tag{2.5}$$

Where,

D is dry density, C is the cement content by mass of the aggregate, W is the water content, M is RMA content, and t is the curing time.

Fedrigo et al. (2018),

$$ITS = 0.69 + 0.34CC - 0.06RC + 0.15CT + 0.16CE \tag{2.6}$$

Here,

CC is Cement Content, RC is RAP content, CT is Curing Time, and CE is a Compaction effort.

2.2.7 Modulus Characteristics of Cement-Treated Recycled Bases

Modulus is the term used to define the stiffness of the material. There are several types of moduli, depending on the application's state. Resilient Modulus (M_R), Elastic Modulus (E), shear modulus, and secant modulus are frequently used to characterize the pavement material. The most common modulus used to describe the pavement base materials is the Resilient Modulus (M_R). The other modulus is the elastic modulus which is the stress ratio to the strain within the elastic limit. The elastic modulus characterizes the materials under a static loading rate and pavement analysis. In the case of elastic modulus, the loading and unloading curves follow the same path.

Similarly, the shear modulus is the ratio of the shear stress to the shear strain. These shear strains are caused at the interface of the two layers in the pavement. Furthermore, the secant modulus is similar to the elastic modulus, which is considered in the inelastic region. Several moduli used in the pavement bases are discussed in detail in the following sections.

2.2.7.1 Resilient Modulus (M_R)

Resilient Modulus (M_R) is used to characterize the pavement materials. M_R is the ratio of deviator stress to the recoverable strain when the specimen is subjected to repeated loading. M_R is influenced by several parameters apart from deviatoric stress and confining stress, including moisture content and degree of compaction (Arulrajah et al. 2015). Generally, the Repeated Load Test (RLT) is preferred for unbound materials rather than cement stabilized materials and is performed according to the AASHTO T307 protocol. The RLT test can be used to understand the material behaviour under simulated traffic loads (Arulrajah et al. 2015). Several experimental studies carried out on treated and untreated recycled materials are presented in the following sections.

2.2.7.2 Resilient Modulus of Untreated Recycled Bases

Some researchers found that the moisture content did not have any impact on M_R, and some others declared that the M_R increases with the decrease in the moisture content than that of OMC (Arulrajah et al. 2014b; Gabr and Cameron 2012; Alam et al. 2010; Attia et al. 2010; Kim et al. 2007). The dry density positively impacts M_R (Mallick et al. 2002). On the other hand, RCA aggregates show higher M_R than VA, and RCA is sensitive to the moisture content (Haider et al. 2014; Arulrajah et al. 2012). RCA alone has a higher M_R than RCA blends with other materials (Hiader et al. 2014; Gabr and Cameron 2012; Bestgen et al. 2016). One study compared three materials, namely RAP, RCA, and CB, and observed that RAP has higher M_R than RCA and CB (Mohammadinia et al. 2015).

2.2.7.3 Resilient Modulus of Treated Recycled Bases

Cement-treated RCA blends show higher M_R values than VA and increase RCA content up to 75% RCA (Behiry 2013). M_R of Cement treated RCA-RAP blends decreases with RAP addition at constant cement content (Mohammadinia et al. 2015), and there is a decrease in the M_R while replacing FRG with RCA. However, 90%RCA/10%FRG and RCA show higher M_R than other mixes (Behiry 2013). Mohammadinia et al. (2015) observed a decrease in the M_R of recycled materials with an increase in the cement content from 2 to 4% due to a reduction in ductility nature. Further, the M_R of the cement-treated materials increases with the curing period and is logarithmic (Mohammadinia et al. 2015). The M_R of cement-treated RAP blended materials is more than untreated; there is an increasing trend of M_R with the cement content and a decrease in the M_R with the addition of RAP into the blends (Taha et al. 2002). From past studies, it is clear that the increase or decrease in the M_R with the addition of the VA depends purely on the type of material used for blending. If the base material is superior to recycled aggregates, then there is a decrease in the stiffness with the further addition of the recycled aggregate.

Table 2.6 Effect of resilient modulus on cement treated recycled bases

References	Conclusions
Arshad (2020)	The M_R of the mixes increases with CC, curing time, and RAP content.
Beja et al. (2020)	Cement-treated C&D materials act as bound materials and are less dependent on the bulk stress. Improved stiffness is observed with stabilization and curing over the unstabilized layer.
Romeo et al. (2019)	Despite VA having a higher stiffness than RAP, no significant difference is observed in terms of performance between RAP and VA.
Fedrigo et al. (2018)	A significant decrease in stiffness is found with RAP and is influenced by compaction effort. Using the Indirect Tensile Fatigue Test, the M_R is overestimated apart from the flexural beam and triaxial tests, consistent with back-calculated values.
Puppala et al. (2012)	RCA material met the specifications at 4% CC. At 6% of CC, all the RAP and RCA combinations satisfied the specifications.
Arulrajah et al. (2015)	The combination of 90% RCA and 10% FRG has higher M_R values, and there is a decline in M_R and an increase in permanent strains with the further addition of FRG.
Mohammadinia et al. (2015)	There is an increase in M_R with the deviatoric and confining stresses and curing period. RAP has higher stiffness values, followed by RCA and CB.
Behiry (2013)	There is a significant increase in M_R values with RCA content up to 75% and then decreases at 100% RCA.
Melese et al. (2020)	Cement-treated quarry fines show higher stiffness than untreated QF and RAP materials at high confining pressures and deviatoric stresses.
Puppala et al. (2011)	Cement-treated RAP bases show higher stiffness than untreated RAP bases, and the confining pressure does not influence CTB at high CC.

On the other hand, if recycled material is superior to the base material, there is an increase in strength with the further addition of the recycled material. Further, there is increased stiffness with the confining pressure and deviatoric stress in untreated and cement-treated base materials. The confining pressures do not influence the base materials (Puppala et al. 2011). So, the indirect tensile fatigue tests are optional to determine the M_R of cement-treated materials. Some of the M_R studies on recycled materials are summarised in Table 2.6.

2.2.7.4 Influence of Elastic Modulus and Secant Modulus on Cement Treated Recycled Bases

Several laboratory and field studies were conducted to determine the elastic modulus of the cement-treated recycled bases. Some studies were identified directly from the specimens; others were determined from the back-calculation using Falling Weight Deflectometer (FWD) and other instruments. Secant modulus is generally used to define the material's stiffness in the inelastic region of the stress-strain diagram. The studies show that the elastic modulus of the cement-treated recycled aggregates or road base materials increases with the curing period and cement content. Further, the cement content is the most governing factor for developing modulus of elasticity (Guthrie et al. 2007b; Lim and Zollinger 2003; Faysal et al. 2016; Miller et al. 2006). However, the increase in stiffness is a problem in cement-treated recycled, leading to early cracking as the material becomes brittle when too much cement is added. So, a significant amount of cement should be added in the case of cement-treated recycled bases.

Recycled aggregates have a more elastic modulus than the mixes made of coarse recycled aggregates (Arulrajah et al. 2015). Further, there is a decrease in the modulus with an increase in the RAP content (Yuan et al. 2011; Faysal et al. 2016). Cement-fiber treated RAP exhibited a higher modulus than cement-treated RAP bases (Hoyos et al. 2011). Miller et al. (2006) and Wilson and Guthrie (2011) observed a tremendous decrease in the modulus values after micro-cracking or along the wheel paths. It is noted that the modulus of elasticity varies from 5000 to 6500 MPa at 28 days for the Recycled concrete aggregate bases at 3-4% (Lim and Zollinger 2003; Arulrajah et al. 2015). Considerable variation in modulus values depends on the various factors, including fines content, cement, coarse and fine aggregate content, etc. Different studies proposed models to estimate the elastic modulus and secant modulus using parameters like density, compressive strength, and RAP content in the mix, as shown in equations 2.7 to 2.10.

Lim and Zollinger (2003),

$$E(t) = 4.38 \times w^{1.5} \times f_c(t)^{0.75} \tag{2.7}$$

ACI Model (Lim and Zollinger 2003),

$$E(t) = 33 \times w^{1.5} \times f_c(t)^{0.5} \tag{2.8}$$

Where $w_{(\text{pcf})}$ is the density of the mixture and $f_c(t)$ (psi) is the compressive strength at a particular time or curing period.

Faysal et al. (2016),

$$E_{25} = 9.06(\text{UCS}) + 2599 \tag{2.9}$$

The secant modulus is at 25% of the ultimate strength, and this model holds good for cement-treated RAP RCA blends with UCS as a known parameter.

Faysal et al. (2016),

$$E_{25}(RAP) = E_{25}(RCA) - 139.9(RAP\%) \tag{2.10}$$

The secant modulus of RAP can be calculated if the secant modulus of RCA is known when RAP and RCA are included in the stabilized base. Units are in psi.

2.2.7.5 Effect of Shear Modulus on Cement Treated Recycled Bases

Shear Modulus is one of the critical properties because shear failure eventually leads to the rutting of the pavement. The pavement's stabilization and thickness should be adequate to prevent shear failure under traffic loads (Wilson and Guthrie 2011). As the shear modulus is high, the chances of sliding/shear off the surfaces over each other are less. The shear failure may occur internally or at the interfaces of two layers. So, studies revealed an improvement in the shear modulus with an increase in the cement content of RAP bases (Hoyos et al. 2011).

2.2.8 Permanent Deformation Characteristics of CTB

Permanent deformation occurs when the material undergoes a plastic state or cannot regain its original position after several repeated vehicle passes or standard load applications. The load application in the laboratory tests depends on the actual traffic. This permanent deformation is restricted to the pavement to ensure safety. Permanent deformation takes place in all the pavement layers or maybe in some layers. So, to provide the benefits of recycled aggregates as base materials, several laboratory and field studies were carried out. The untreated recycled bases, blended RAP with base materials, show lower permanent deformation than RAP bases alone. Lower plastic strains were observed for untreated RCA bases compared with the blending of other aggregates (Haider et al. 2014; Bennert et al. 2000). The amount of permanent strain increases with the RAP content and decreases with the cement content (Arshad 2020).

From the earlier research results of the blending of RCA and VA, it is observed that blending may not help to decrease the permanent deformation (Haider et al. 2014; Bestgen et al. 2016). It depends on the type of material blended and the interlocking properties with the base material. Cement stabilization is considered to be one of the techniques which decrease permanent deformation. Due to the increase in stiffness of the material with stabilization, there will be a

decrease in elastic and plastic deformation. Further, minor plastic strains or deformations were observed for cement-treated recycled bases compared with untreated and conventional bases (Behiry 2013; Soares et al. 2013; Beja et al. 2020). When cement-treated recycled aggregates mixtures are used as sub-base, the deformation is reduced by half compared with VA bases (Agrela et al. 2012). Cement-treated bases with other stabilizers like emulsified asphalt have lower rutting than individual stabilizers (Mallick et al. 2002).

Similarly, Arulrajah et al. (2015) conducted an RLT test on the combination of RCA and FRG with 3% cement content and assessed permanent and resilient strains. The combination of FRG and RCA in the ratio of 10: 90 exhibits lower permanent strains compared with others. Furthermore, 70RCA/30FRG exhibits higher permanent deformations compared with others. The deformation increases with the increase in FRG content in the mix. It is because of the presence of fewer friction surfaces on FRG, which prevents better bonding with stabilization. Romeo et al. (2019) compared the permanent deformation of RAP with VA. From the results, treated RAP has an increasing rate of permanent deformation than VA.

2.2.9 Durability, Hydraulic Conductivity, Shrinkage and Thermal Characteristics

Durability represents the long-lasting nature of any material. It can be expressed in dielectric value using the Tube Suction Test (TST), wet-dry cycles, and freeze-thaw cycles. The selection of each process depends on the climatic conditions of the base at which it was used. With the increase in wet and dry cycles, there is a loss of material and strength. The wet condition represents the rainy season, and the dry state means summer. One wet and dry condition is generally represented as one year. Typically, 14 cycles that represent 14 years are considered for the evaluation. In the case of cold regions, freeze-thaw cycles are used instead of wet-dry cycles. Dielectric values are indicators of the durability of the materials. Materials with a dielectric value of less than 10 are considered more durable (Guthrie et al. 2007b). There is a decrease in the dielectric values with the RAP and cement content in the mix (Guthrie et al. 2007b).

Bestgen et al. (2016) observed concerns with the durability of untreated RCA bases, and some others proved that RCA materials are durable in terms of the effluent pH and the metal concentrations. On the other hand, Miller et al. (2006) revealed that the durability of the cement-treated RAP blends was achieved at 6-8% of cement content. There are negligible volumetric changes, and maximum retained strengths were observed after 14 wet and dry cycles for the treated RAP bases (Puppala et al. 2017). Other industrial waste like electric arc furnace slag mixes, when treated with cement, showed durability concerns when used alone because of the internal oxidation and loss of aggregates during wet and dry cycles. However, when blended with VA, it performed well (Autelitano and Giuliani 2016).

Fedrigo et al. (2018) proved that the mixes without RAP and higher cement content (5%) are more durable and recommended a 30% RAP mix as an optimum durable mix for all cement contents. These results are affirmed using 12 wet and dry cycles. The cement stabilized Quarry by-products bases are durable and well below the observed field, and laboratory results specified limitations than the fly ash treated bases (Qamhia et al. 2020). Similarly, other recycled materials like steel slag achieved a minor loss at 50% replacement (Liu et al. 2020).

Hydraulic conductivity represents the water movement through the material. This property is essential to deal with the bases. Because hydraulic conductivity leads to erosion of fine material and weakens the base, the ingress of water can be prevented by stabilizing with cement. Several studies proved that the stabilized bases have low hydraulic conductivity compared with untreated bases. Hoyos et al. (2008) observed a decrease in hydraulic conductivity with the increase in the cement dosage. Further, no significant changes were observed in the hydraulic conductivity with the inclusion of the fibers (Hoyos et al. 2008). In untreated RAP blends, the hydraulic conductivity decreases with the decrease in the RAP quantity in the mix (MacGregor et al. 1999).

Shrinkage is the term that indicates the dimensional changes in the CTB with the time as a result of hydration reaction. The initial cracks, mainly shrinkage, are formed after 3 days of construction of the base and lost in 30 days (Gao et al. 2020). This primarily occurs due to environmental conditions like temperature and relative humidity and is also influenced by the type of aggregates, CC, degree of compaction, moisture content, and so on (Xuan et al. 2016). There are mainly two types of shrinkage cracks where cracks occur during the drying process and temperature. There is an increase in the dry shrinkage and temperature shrinkage with an increase in CC and curing period (Fedrigo et al. 2018; Arshad 2020; Wang et al. 2020). Xuan et al. (2016) studied the shrinkage effects on the cement-treated mix granulate composed of RCA and RMA in different proportions. It is concluded that the cement content has a significant impact on the shrinkage and an increase in RMA content in the mixture decreases the shrinkage. The shrinkage values are lower at the high degree of compaction and lower CC.

Furthermore, fine recycled aggregates exhibit lower shrinkage values than the specimens made of coarse recycled aggregates (Xuan et al. 2016; Wang et al. 2020). Similarly, increased RCA content and early strength anti-cracking material utilization reduce dry shrinkage and reduces temperature shrinkage strains (Guo et al. 2020). The Coefficient of Thermal Expansion is a constant given to a particular material that indicates the temperature's rate of expansion or contraction. The higher the coefficient indicates more expansion with the same temperature relative to the low coefficient of thermal expansion materials. A study conducted by Xuan et al. (2016) on the cemented treated recycled bases demonstrates an increase in the CTE with the

increase in CC and degree of compaction. This is due to the increase in the hydration reactions and the decrease in the air voids with a higher degree of compaction in the mixture. Further, CTE decreases slightly with the increase in the moisture and RMA content.

2.2.10 Field Evaluation and Fatigue Characteristics of CTB

Field evaluation of cement-treated recycled bases is more essential than that of the laboratory investigation as field conditions are the actual conditions in which the bases undergo testing under realistic environmental, climatic, and vehicle loads. Several studies evaluated the cement-treated bases comprising natural aggregates and recycled aggregates using the International Roughness Index (IRI) and deflections over the surface of sub-base and subgrade. It is observed that the mean surface deflections of the cement-treated recycled mixes with 3% of cement are lower than that of the VA, and lower IRI values were observed compared with VA (Agrela et al. 2012). Beja et al. (2020) performed a field evaluation of stabilized and unstabilized C&D wastes as a sub-base using FWD. The results demonstrated a drastic reduction in the deflection values and improved M_R.

Fatigue tests quantify the damage caused inside the specimen due to the repeated loading, which simulates the vehicle loads. There are several types of fatigue tests. Some are flexural beam fatigue, indirect tensile fatigue, semi-circular bending fatigue, compression fatigue, etc. Although there are relations between stiffness and fatigue life of the materials, several factors apart from the stiffness will damage the specimens' under vehicle loading. So, fatigue tests can be more relevant to assess the material resistance to wear under various stress levels (10%-80%), frequencies (0.5-10Hz) and temperatures (-5ºC to 60ºC). The failure of the base material under fatigue can be accessed in different criteria. The criteria include the number of cycles where the reduction in the initial modulus to half or complete collapse of the specimen, or reaching 5% of the strain of the largest dimension of the specimen or calculating the slope of the fatigue curve after the crack initiation stage. Understanding the failure behavior of the recycled materials is necessary as they have already been utilized in some of the structures before, which leads to some deterioration. Several authors conducted fatigue studies on recycled materials in various combinations. When the cement-treated RCA/FRG combination is subjected to a fatigue test, the mixes with 90%RCA/10%FRG exhibit better performance than the other blends (Arulrajah et al. 2015). Some of the fatigue tests and their specific conclusions are summarized and presented in Table 2.7.

Table 2.7 Fatigue studies on different cement treated materials

References	Type of Mix	CP(days)	CC (%)	M_R (MPa)	Conclusions
Melese et al. (2020)	60%RAP/40%VA 80%RAP/20%VA	28.0	6.0	1162-4093	The type of hydraulic binder did not influence the fatigue life and the behavior of RAP as a quasi-brittle & visco-elastic properties
Mohammadinia et al. (2019)	100%RCA	7.0	4.0	3027 (v) 2110 (h)	Stabilized RCA shows anisotropic behavior in M_R, and vertical deformations are maximum at the top of the base compared with stabilized base subgrade interface.
Lv et al. (2019)	100%VA	7.0	4.5	15000	Curing periods significantly affected the cement-treated bases' fatigue life and recommended restricting the traffic and construction equipment for short-term curing.
		14		17000	
		28		16400	
		90		20907	
Fedrigo et al. (2019)	20%RAP,50%RAP, 70%RAP with laterite soils	28.0	2.04.0	862 to1714, 1777to3620 for 4%CC	Low fatigue life is observed for the mixtures with low cement contents. The fatigue life increases with the thickness of the wearing course and base layer.
Hou et al. (2019)	100%RCA	7.0	4/5	800/1100	The fatigue life increases with the increase in the RCA dosage in the mix, and the stiffness increases with the curing period and cement content.
		28		1100/1400	
		60		1200/1550	
		90		1300/1560	
Arulrajah et al. (2015)	100%RCA	28.0	3.0	9601.05	The fatigue life and modulus of the mix combination with 90% RCA and 10% FRG are more.
	90%RCA			22600.22	
	80%RCA			13375.62	
	70%RCA			14577.31	
de Paiva et al. (2017)	30%RAP, 50%RAP 70%RAP	90.0	3.0		There is a decrease in the fatigue life with the increase in the % of RAP. The type of asphalt binder impacts the fatigue life of the base.
López et al. (2018)	20%RAP 50%RAP 70%RAP	28.0	2.0/4.0	1963-2528 for 2% CC, 3867-6740 for 4% CC	The fatigue failure of the cement-treated materials is the same as that of the cement-treated conventional aggregates. Fatigue life depends on the mixture composition and thickness of the asphalt wearing course.
Guo et al. (2020)	100%RCA, 100%VA,75%RCA 50%RCA,25%RCA	7.0	3.5/4.5		The incorporation of early strength anti-cracking material improved the fatigue life and cement content. The recycled aggregate combinations show lower fatigue life than VA.

2.3 Emulsified Asphalt Treated Bases (EATB)

The recycling process came to light when there was an increase in the cost of asphalt and petroleum products during the 19th century. It was considered the most appropriate for maintenance emulsified-Asphalt mixes composed of asphalt, water, Emulsified Asphalt (EA), additives, and aggregates. EA rejuvenates the old bitumen surrounded by the Reclaimed Asphalt Pavement (RAP) and makes a solid structural bond with new and old aggregates (Kumar et al. 2008). EA applications in pavement began in the early 20th century, and more than 8 million tons of EA were produced around the world (Asphalt Emulsion Technology 2006). The recycled aggregates can be reutilized with an optimum EA with or without using conventional aggregates from sustainable points of view. Despite these benefits, a few drawbacks like long curing periods, low early strength, and more air voids are reported (Taherkhani et al. 2016). Several design techniques, curing processes, and additives were introduced to overcome these problems.

Further, EATB helps rectify the deteriorated pavements' rutting, cracking, and slope (Nazarian and Yuan 2012). Based on the traffic and environmental conditions, there are several procedures involved in the design of EATB. Some researchers adopted the Marshall Method of mix design in which the % of air voids, stability, and flow values are considered the parameters (Joni and Hashim 2018; Thanaya et al. 2014; Choudhary 2012; Modarres et al. 2011). Some other researchers adopted the modulus method of mix design, where the modulus values are considered to select the OEAC.

Several EAs exist, such as slow setting; medium setting and rapid setting emulsified asphalt. Generally, the rapid setting EAs are preferred for surface treatments, seal coats, and surface courses. In contrast, the slow setting EAs construct the base layers or prime-coating over the granular layers. Further, the type of EA (cationic or anionic) is chosen based on the surface charge on the aggregate particles. After selecting the suitable type of EA, it is necessary to achieve the required strength of the mixes.

2.3.1 Different Stages of Setting of Emulsified Asphalts

The setting of EA is divided into two important stages. In the first stage, the water is separated from the EA, while the 2nd stage involves the loss of maximum moisture for better binding of asphalt with aggregates. There is a contact of asphalt emulsion droplet size ranging from 1-10 μm (Miljković and Radenberg 2014; Boucard et al. 2015; Ronald and Luis 2016) with the surface of the aggregates and cement; the pH values rise due to the adsorption of free emulsifier. The rise in pH values leads to flocculation that will gather the destabilized particles in one place. Then the coagulation takes place, which means the liquid phase slowly changes to a solid phase

where the escape of moisture takes place slowly during this process, and asphalt adsorbs onto the surface of the aggregates (Asphalt Emulsion Technology 2006).

2.3.2 Constituents of Emulsified Asphalt Treated Bases

EATB consists of aggregates of different sizes, additives, emulsified asphalt, air, and water (Nazarian and Yuan 2012). EA comprises water, asphalt, emulsifier, or rejuvenating agents like C60B5REC REJUV (Flores et al. 2019). Majority of the studies utilized RAP, VA, RCA, and Steel slag in different compositions as aggregates with encouraging results. Water includes pre-wetting water, naturally in the aggregates, and water present in the EAs. Initially, aggregates are treated with pre-wetting water, which makes the natural spreading of the EA on the aggregate surface. This pre-wetting water helps prevent the absorption of extra moisture present in the EA by the aggregates. Additives raise the pH, thereby increasing the adsorption of the asphalt emulsion onto the surface of the aggregates. These additives help evaporate the moisture present in the treated base and make the base stiffer with time. Moreover, there is an increase in air voids with curing as the escaped moisture leaves more air voids. EATB has more air voids than Hot Mix Asphalt (HMA) (Li and Liu 2014).

2.3.3 Role of Additives in EATB

Additives are necessary to develop early strength and accelerate the curing process. In other words, if the EA alone does not provide adequate strength and durability to the base, dual stabilization using cement and EA is preferred (Nazarian and Yuan 2012). Additives like fly ash, cement, lime, Ground Granulated Blast-furnace Slag (GGBS), etc., are recommended in EATB. These additives can be used alone or in a combination of two; the majority recommended cement in the range of 1-3% due to its availability in the markets. However, other additives are also encouraged based on their availability. The amount of additives is optimized based on the laboratory experience. Likewise, silica fume up to 3% is recommended for improved mechanical properties (Joni and Hashim 2018). Kumar et al. (2008) observed that adding 2% cement or lime effectively improved all the performance parameters compared with other additives or combinations. Ellis et al. (2004) compared the HMA and EATB with cement and GGBS as additives. There is a continuous increase in the stiffness of the mixes with GGBS (as additive) even after 120 days of curing and crossing the HMA. Figure 2.7 shows the effectiveness of different additives. To treat the mixes as EATB, agencies suggest that the ratio of residual Asphalt (A) to the Cement (C) (A/C) is 2: 1 and 3: 1 (Asphalt Academy 2009; ARRA 2018). The mechanical properties of the mixtures change from cement-dominated to asphalt-dominated when the A/C ratio changes from 1 to 2 (Miljković et al. 2019). This increases the flexible nature of the bases.

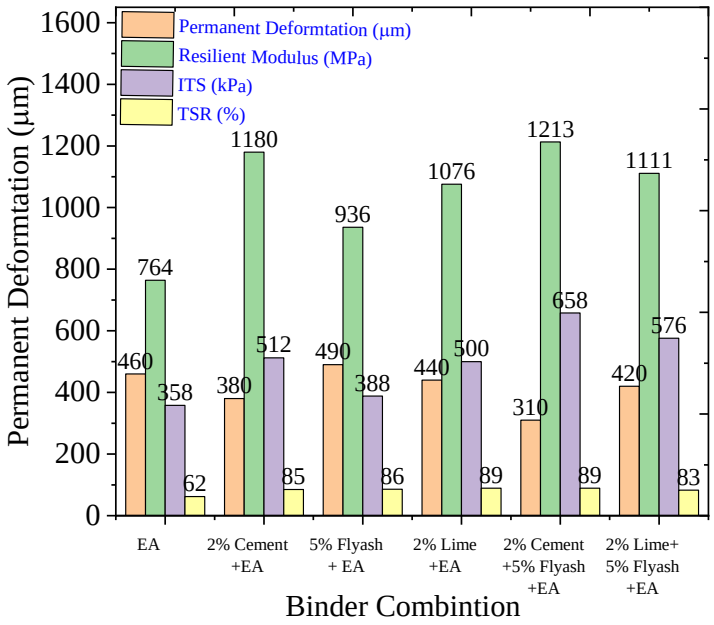

Figure 2.7 Effectiveness of different additives in terms of performance parameters

The presence of cement in the EATB acts as a secondary binder and improves the mechanical properties (Taherkhani et al. 2016; Nazarian and Yuan 2012; Yan et al. 2017; Hodgkinson and Visser 2004; Flores et al. 2019; Oruc et al. 2007; Du 2014; Xiao et al. 2018; Needham 2000; Li et al. 2019; Gao et al. 2016; Fang et al. 2016; Shanbara et al. 2018). Further, there is a significant increase in strength and stiffness of the EATB mixes when additives are incorporated (Thanaya et al. 2014; Modarres et al. 2011; Yan et al. 2017; Sangiorgi et al. 2017; Moghadam and Mollashahi 2017; Baghini et al. 2017). Higher cohesion and low ravelling were observed at higher cement contents (Yan et al. 2017). However, more than 2.5% of cement content leads to fatigue cracks (Bessa et al. 2016). Besides, EATBs with 1% cement and without cement exhibited low stiffness and high permanent deformation with temperatures. An increase in the cement content leads to decreased temperature susceptibility, water susceptibility, and additives highly recommended in cold countries for early strength development (Yan et al. 2017; Asphalt Academy 2009; ARRA 2018; Oruc et al. 2007; Swaroopa et al. 2015; Gurney 2013). Even though Asphalt Academy (2009) suggested maximum additive content as 1% for cement and 1.5% for lime. Studies showed better results at cement content, more than 1%. Xiao et al. (2019) observed that maximum strength was obtained at 3% cement content at constant EA content. However, high amounts of cement are not recommended as it is left unhydrated inside the specimen (Saadoon et al. 2018). So, cement content less than or equal to 1% might not always be applicable as it differs from the EA source and aggregates. Brittle nature increases with the increase in additives; also, the visco-elastic behavior increases with EA content. These parameters must be considered while designing the EATB (Asphalt Academy 2009).

The type of cement used in the mix design also influences strength development. A study by Kavussi and Modarres (2010) concluded that the initial strength development of Type I cement is 10-20% more than that of the Pozzolanic cement. However, for extended curing periods, the difference in strength for both the mixes is negligible. Rapid setting cement is more preferred than ordinary Portland cement as it produces more hydration products and makes the baseless permeable (Saadoon et al. 2018).

2.3.4 Mix Design of EATB

Various mix design methods exist worldwide depending on the curing period, additive contents, EA contents, compaction, maximum dry density, total fluid content, curing methods, temperature, etc. Many studies adopted design techniques that can best suit their environmental conditions. Flores et al. (2019) proposed a design methodology with 100% RAP based on the volumetric and mechanical properties. The properties include ITS, TSR, % air voids, stiffness modulus, rutting, and fatigue life. These properties are measured based on performance indices of 0 to 1 based on their performance. A global performance index is the average of all the individual performance indices for all the mixes. The mix that gives the highest international performance index is the final optimum mix design. Various mix design parameters are briefly discussed in the following sections.

2.3.5 Mix Design Parameters

Different studies consider mix design parameters like ITS, Marshall Stability, Air voids, Water absorption, Fatigue, and retained stability to optimize the EA content. However, most studies preferred ITS as the design parameter because of its reliability to the field conditions. One research proposed a two-tier method where UCS represents the rutting potential, and ITS represents the cracking potential (Nazarian and Yuan 2012). Some of the specification requirements of ITS to use as EATB are presented in Table 2.8. The ITS ranges are fixed based on the traffic plying on the road and the type of road.

Table 2.8 Permissible ITS values used in the design of EATB

Source or Author	**ITS (kPa)**		
Asphalt Academy (2009)	BSM 1	BSM 2	BSM 3
	>225	175-225	125-175
IRC 37 (2018)	>225 (India)		
Suda et al. (2017)	>300 (Czech)		
Sangiorgi et al. (2017)	>350 (Italy)		
Poland Specifications	500-1000 at seven days of curing 700-1600 at 28 days of curing		
Texas DOT (Tex-226-F)	345 min		

*BSM-Bitumen Stabilized Materials, 1, 2, 3 indicate the level of traffic.

2.3.6 Code of Practices for the Mix Design of EATB

There is no universally accepted design method for EATBs. However, the most preferred is the Asphalt Academy (2009) method, in which the design should meet the gradation and satisfy the strength requirements based on traffic. Several studies optimized the EA content at constant additive content, and then additive content is optimized (Xiao et al. 2018). Some of the design methods are presented in Table 2.9. Some of them varied curing techniques and compaction phenomena to get the desired strength of the base, and some suggested optimum moisture content as the basis for the variation of Total Fluid Content (TFC) in the mix. The TFC is the sum of EA content and pre-wetting water content that should be equal to the Optimum Moisture Content (OMC) (Asphalt Academy 2009).

Table 2.9 Various design methods used for EATB

Description	MS-19 (1979)	Asphalt Academy (2009)	IRC:SP:100 (2014)	IRC:37 (2012)
Design based on	DGB and IEAC	03 Traffic levels (L1, L2, and L3)	BM/SDBC&IEC	TFC-dry density OEAC-ITS.
Pre-water content	Coating test	1-2%	2-3%	-
Compaction	Marshall-50 Blows	Marshal, Vibratory for L-2 and L-3; 75 blows for L-1	Marshal-50 blows	75 blows
Curing	48 h at 60^{o}C	L-1 72 h at 40^{o}C L-2, 26h at 30^{o}C 48 h at 40^{o}C unsealed and sealed condition.	72 h at 40^{o}C	72 h at 40^{o}C
Design Parameters used	Hveem/Marshall	L-1, ITS; L-2, ITS, and TSR; ITS, TSR, ϕ, c, and retained cohesion	Marshall, density, and flow value	ITS

DGB: Dense graded bituminous; BM: Bituminous Macadam; SDMB: Semi Dense Bituminous Concrete; IEAC: Initial Emulsified Asphalt Content (IEAC).

2.3.7 Initial Emulsified Asphalt Content (IEAC) and Total Fluid Contents

Several codes of practices selected IEAC based on gradations, as shown in Table 2.10. The IEAC selection is influenced by the percentage of retained particles passing through the 4.75 mm sieve, the percentage of fines, the residual binder in the EA, etc. Nazarian and Yuan (2012) adopted a design methodology to calculate the maximum allowable EA content from the maximum total liquid content and minimum moisture content. Pre-wetting water is required to ensure better coating and workability of the EATB. There is no particular trend observed in

selecting the pre-wetting water from studies. However, guidelines recommended 1-2% of pre-wetting water and used equations (Dolzycki et al. 2017).

Table 2.10 Equations used by authors to calculate the required emulsified asphalt content for EATB

Author	Equation used
Choudhary et al. (2012) Arimilli et al. (2016) IRC SP-100 (2014)	$P=\left(0.05A+0.1B+0.5C\right)\times 0.7$ Here, *P* is the minimum residual bitumen required, *A* is the percentage of particles retaining on 4.75 mm, *B* is the percentage of particles passing 4.75 mm and retaining on 0.075 mm, and *C* is the percentage of particles passing 0.075mm sieve,
Illinois department of transportation Joni and Hashim (2018)	$E=\frac{0.00138AB+6.358\log C-4.655}{p}$ Here, *E* = initial emulsion content in percentage, *p*= percentage of bitumen in the emulsion
MS-19 (1979)	$E=\frac{\left[0.06B+0.01C\right]\times 100}{A}$

$W_{dod}=W_{opt}-W_{nat}-W_{em}-0.5\times B$

Here W_{dod} is added water, W_{opt} the optimum moisture content calculated from the Proctor method, natural moisture in the aggregate mixture, and bitumen in the bitumen emulsion (%).

The amount of pre-wetting water required depends on the ingredients such as the aggregates combination like recycled aggregate and VA, cement content, gradation, and other parameters. According to MS-19 (1979), the pre-wetting water is adopted based on the degree of coating of the EA, which should be more than 50% (MS-19 1979). Moreover, studies considered pre-wetting water on a trial basis where the mixed samples are visually observed. After mixing with the EA content, the too dry and too wet samples are discarded. Furthermore, samples with medium pre-wetting water are verified using the maximum bulk density (Flores et al. 2020). Some studies fixed the particular EA content and varied the pre-wetting water, and the pre-wetting water is considered at which the maximum strength is achieved. Graziani et al. (2018) observed that the water dosage and air voids content has little effect on the ITS of the mixes in the long run. A similar study by Nassar et al. (2016) observed decreased air voids content with increased water content. If the water content is more than required for lubrication and compaction purposes, it creates more air voids after the curing period. However, the minimum air voids and maximum strengths are not represented at the same water contents. The formation of the dense microstructure of Cement asphalt emulsion paste is the reason for the strength improvement at lower water contents (Nassar et al. 2016). The pre-wetting water ranges from 0.5 to 3.5% from various studies (Modarres et al. 2011; Oruc et al. 2007; Sangiorgi et al. 2017;

Swaroopa et al. 2015; Nassar et al. 2016; Chelelgo et al. 2019; Dong and Charmot 2019). Further, there is a need to study the influence of pre-wetting water on the performance of the bases.

TFC plays a significant role in the mix design of EATB. Because a minor change in the TFC affects the strength of EATB drastically. Before compaction, the moisture content is a concern in the field as it impacts compaction drastically (Nazarian and Yuan 2012). The fluid content at which the maximum strength or density is obtained will be taken as the TFC (Kumar et al. 2008). TFC includes pre-wetting water, water present naturally in the aggregates and EA. Generally, it ranges between 50 to 80% of OMC according to the sand equivalency value of the given material (Al-Mishhadani and Al-Baid 2014). Nazarian and Yuan (2012) proposed a new method to calculate the TFC based on the density and percentage of saturation. Other researchers used ITS and bulk density to optimize the TFC (Kumar et al. 2008; Arimilli et al. 2016; Al-Mishhadani and Al-Baid 2014). The required amount of water varies with RAP percentage and additives. As per Power's theory, 23 g of water chemically bonded when 100g of cement undergoes a reaction (Jensen and Hansen 2001). The requirement of fluid content is more for VA compared with RAP mixes (Arimilli et al. 2016). This is due to the more absorption capacity of the VA than RAP.

2.3.8 Cement Water Emulsion Interactions of EATB

Reaction among cement, water, and EA are necessary to understand its impacts on strength, stiffness, and long-term performance. Table 2.11 shows some research studies on the interactions between cement water and asphalt emulsion.

Table 2.11 Summary of research works on cement water and asphalt emulsion interactions

Study	Recommendations
Ouyang et al. (2019)	The addition of super-plasticizers and wetting agents significantly improved the strength and reduced the Cement asphalt Emulsion (CAE) air void contents at lower water contents. The strength of CAE mixes depends on the air voids content, microstructure of CBE, interface between CBE paste and aggregates
Xiao et al. (2019)	An increase in cement content leads to a decrease in the viscosity of the cement emulsified asphalt mixtures that reduce the workability, resulting in poor compaction and higher percentages of air voids that directly degrade the strength of the mix.
Du (2014)	Cement emulsified asphalt mixes adopt the characteristics of both cement and asphalt, and the reaction mechanism is similar to that of the cement water mixes, where the hydration process is delayed in cement asphalt mixes. The Optimum water content is influenced by cement and emulsified asphalt contents that impact ITS.

Li and Wang (2014)	The compressive strength and elastic modulus degraded with emulsified asphalt content increase the mix's ductility. However, emulsified asphalt content in the mix improves the impact and crack resistance.
Garcia et al. (2013)	The addition of cement helps to evaporate the water by hydration process that hardens the composite of cold asphalt mixes. Cold mixes without the addition of the cement exhibit lower stability than HMA even after long curing periods
Oruc et al. (2007)	The mechanical properties like resilient modulus, temperature susceptibility, water damage, creep, and permanent deformations are improved with cement to the cold mixes equivalent to the HMA.

2.3.9 Criteria Selected for Fixing Optimum Emulsified Asphalt Content

Fixing OEAC is the final stage in the mix design of EATB. This step is essential because EA content significantly impacts the strength. OEAC is the EA required to achieve the desired strength or modulus (Nazarian and Yuan 2012). After the addition of sufficient pre-wetting water, the sample is mixed thoroughly for sufficient time. This will allow the uniform mixing and coating of the EA onto the aggregate surface (Nottingham et al. 2011). Then, constant EA is added to the mixture and tested for maximum strength. This step follows the determination of the OEAC by changing from IEAC. The EA content at which the maximum strength, modulus, or other criteria is achieved will be considered the OEAC. Variation of different parameters with the EA content is presented in the Table. 2.12. Generally, the amount of EA required for RAP is less than that of the VA mixes. It is observed that there is a participation of the old binder beside the virgin binder that helps to increase the resistance to moisture damage and improves deformation characteristics (Nottingham et al. 2011). However, some researchers questioned the possibility of rejuvenating the aged binder at ambient temperatures (Graziani et al. 2018).

Table 2.12 Variation of mechanical properties with different parameters

Parameter	**RAP content**	**PWWC**	**TFC**	**EAC**	**Curing time**	**Temperatures**	**CC**	**RM**	**CT**
ITS	Increases	Increases and then decreases	Increases and then decreases	Increases and then decreases	Increases with curing time	Decreases with increase in Temperature	Increases	Increases with a decrease in RM	Increase with an increase in curing CT
M_R/ ITSM	-	-	Increases and then decreases	Increases and then decreases	Increases	Decreases with Temperature	Increases with cement	-	Higher modulus at higher CT
Permanent deformation	-	-		Increases	-	-	Decreases	-	Low at high CT
Void volume	-	-	Decreases and then increase	Decreases and then increases	-	-	Decrease	-	Increases with CT
Durability	Increases	-		Increases and then decreases	-	-	Increases	-	-
Specific Gravity/density	-	Increases & decreases	Increases & decreases	Increases and then decreases	-	-	Increases	-	-
Compressive Strength	-	-	-	Increases and then decreases	Increases	-	-	-	-
TS	-	-	-	-	-	-	Decreases	-	-
FS	-	-	-	Decreases	-	-		-	-

ITSM-Indirect Tensile Stiffness Modulus, FS-Flexural Strength, EAC-Emulsified Asphalt Content, CC-Cement Content, RM-Residual moisture, CT-Curing Temperatures, TS-Temperature Sensitivity, PWWC-Pre-Wetting Water Content, TFC-Total Fluid Content

2.3.10 Mixing, Compaction and Curing of EATB

Compaction is one of the critical parameters that impact the mechanical properties of the EATB. Before compaction, aggregates and additives are mixed thoroughly to form a uniform mixture. Then pre-wetting water is added to the mixture and mixed for 1-2 minutes, followed by the addition of the required emulsified asphalt and mixing for 1-2 minutes until breaking down of emulsified asphalt. Usually, higher compaction energy is necessary for the EATB as the material is not heated up like HMA and due to the nature of the included materials. Several compaction methods are available, including Marshall Method of Compaction (MMC) with different blow applications, Gyratory compaction with a variation of gyrations, and Vertical Vibration Compaction Method (VVCM), and vibratory roller compaction in case of field. The application of the compaction method depends on the type of gradation, field conditions representation, temperature conditions, traffic, etc. The majority adopted gyratory compaction from the review, similar to the field compaction followed by MMC with a different number of blows, as shown in Figure 2.8.

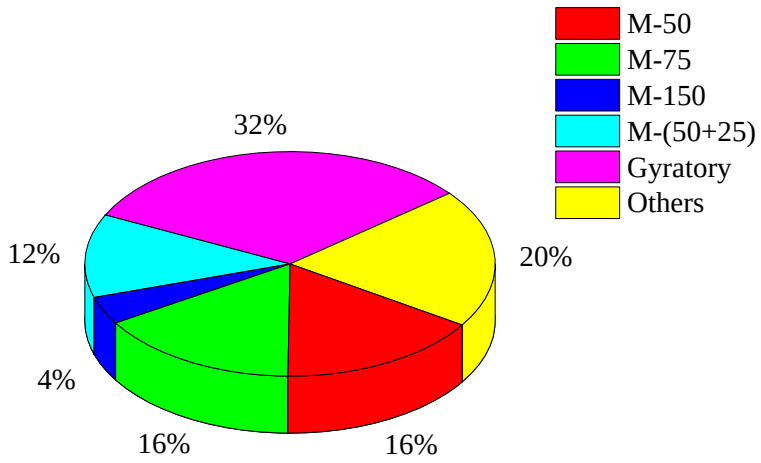

Figure 2.8 Different Compaction techniques adopted for laboratory evaluation of EATB

Kumar et al. (2008) showed that the MMC with 115 blows represents the same density as the field. However, recommended vibratory or gyratory compaction as a high level of MMC leads to aggregate degradation. Jiang et al. (2019) proved that VVCM is advantageous over MMC with improved mechanical properties with less moisture and EA contents. Other studies confirmed that samples compacted with a gyratory compactor performed better than MMC and proctor compaction (Nazarian and Yuan 2012; Joni and Hashim 2018). Studies recommended more substantial compaction for Cold mixes to achieve maximum stiffness (Thanaya 2007). Thicker bases typically need more compaction energy, and gyratory compaction can achieve field compaction (Flores et al. 2020). Therefore, the compaction energy is proportional to the thickness of the base. EATBs are generally prepared at ambient temperatures in the mixing and compaction temperatures, which is one of its main advantages. Nottingham et al. (2011) showed

that the cold mixes compacted at 32℃ temperature performed better fatigue. Further, high shear mixers achieved homogeneous mixtures and higher strength properties than concrete mixers and hand mixing (Nazarian and Yuan 2012).

The curing of EATB is crucial as insufficient curing leads to low-performance characteristics. Additives are generally added to accelerate curing, which is already discussed in the additive section. It helps to gain strength early, and early age strength is directly proportional to the long-term performance characteristics of the EATB (Yan et al. 2017). Moreover, fully cured specimens exhibit low permanent deformations than early tested specimens (Nottingham et al. 2011). Curing conditions, temperature, and time affect the strength and stiffness of the base (Cardone et al. 2018; Monney et al. 2007). The amount of curing depends on the climate, mix composition, humidity, and permeability of EATB. The curing process involves evaporating the water present in the EATB and stiffening the base. As the presence of water is inversely proportional to the strength and rigidity of the EATB, proper curing is required to evaporate the amount of water (Graziani et al. 2018; García et al. 2013). Several laboratory curing procedures were adopted worldwide, presented in Figure 2.9. Among them, 72 hours curing at 60°C are mostly preferred, followed by 72 hours curing at 40°C and followed by the rest. Generally, it is impossible to cure the samples as much time exists in the field. In such a case, the equivalent accelerated curing temperatures should be determined.

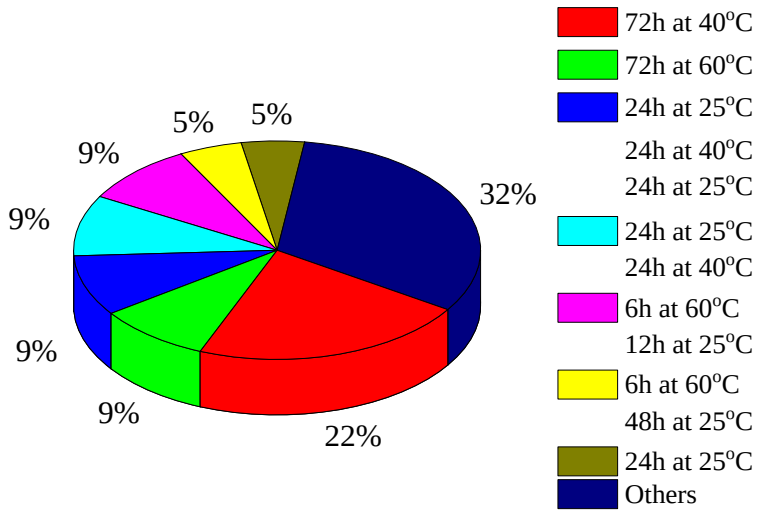

Figure 2.9 Curing techniques adopted for EATB around the world

Kumar et al. (2008) showed that the 48 hours of curing 60°C represents the field curing for 28 days. Besides, the 3-day curing period 40°C represents the field curing for 30 days (Arimilli et al. 2016). Samples cured in the range of 35−40℃ temperature achieved more than 80% of the 28 days strength in the first 3 days of curing (Graziani et al. 2018). The curing rate is more in the case of higher temperatures than in lower ones (Thompson and Carpenter, 2009). Mignini

et al. (2018) revealed that unsealed samples exhibit higher strength and modulus than sealed samples. This represents that sufficient curing occurs when the base is opened to the environment rather than covered immediately with a surface or binder course.

Further, Saadoon et al. (2018) concluded that the curing time depends on the thickness of the base. As the base thickness increases, the curing time will increase proportionally. Flores et al. (2019) sealed the entire sample except the top surface using plastic bags, representing the exposure of the base in the field. The degree of curing adopted by different authors varies. Some researchers do not thoroughly explain the theory behind adopting particular temperatures and the curing time. In some studies, the curing is continued until the weight is constant. This is one of the criteria for terminating the curing period. Some studies used fixed curing whether the constant weight was achieved or not. However, the curing procedure depends entirely on the local environment and field conditions. From the studies, it is recommended that curing can be done for 28 days is sufficient time is there for testing as in the field, keeping it in the local environmental exposure. If time did not permit curing for long periods, any curing methods could be adopted, ensuring the field curing for a particular number of days.

2.3.11 EATB with Recycled Aggregates Other than RAP

Several studies are performed nationally and internationally with different aggregates like RCA, VA, copper slag, and different percentages with different additives. Copper slag and cement are proved to be adequate for VA and additive in terms of improved mechanical characteristics. There is degradation in the mix properties when replaced with RCA and withstands within the specification limits and environmental regulations (Behnood et al. 2015). Ge et al. (2015) used VA, RCA (28%, 70%) blends with 2% cement as additives. Resulted mixes achieved suitable mechanical properties as a flexible base with cost savings of 34%. Mixes with Construction and Demolition Waste (CDW) have more stiffness and increased length of curing (Gómez-Meijide et al. 2016).

Further, the sensitivity toward temperature is less for CDW mixes than for VA mixes (Gómez-Meijide et al. 2015). Incorporating steel slag into RAP mixes improved the mechanical properties, and steel slag is more compatible with the anionic type of EA, where high strength is achieved (Ameri and Behnood 2012). A combination of RAP, masonry, and CDW with Ground Granulated Blast-furnace Slag (GGBS) as an additive in EATB is studied. From the observations, GGBS improved the mechanical properties of the mix for long curing periods and humid environments; EA improved the ductility and usable life (Ellis et al. 2004).

2.3.12 Performance Characteristics of EATB

Different studies considered the performance parameters like ITS, TSR, M_R, Marshall Stability, Rutting, Fatigue and Creep. The variation of performance indicators with the components of the EATB as explained in Table 2.12.

2.3.12.1 Indirect Tensile Strength of EATB

ITS is considered the performance and the design parameter in the preparation of EATB. It is essential to assess the tensile strength as the pavements failed mainly in bottom-up cracking. The respective authorities determine ITS values based on the field performance at different traffic levels, as shown in Table 2. Several factors influence the mix's ITS, including aggregate gradation, cement content, EA content, curing period, curing temperatures, residual moisture, pre-wetting water, TFC, recycled aggregate content, testing temperatures, etc.

Aggregate gradation influences the ITS of EATB. Kumar et al. (2008) showed that the modified gradation showed higher ITS than the direct utilization of the milled material. Xu et al. (2017) evaluated the influence of aggregate gradation on ITS by converting gradation into a suitable measurement, namely Fractal dimension and fineness modulus. Fractal dimension is generally related to the surface irregularities of aggregates. Mix with optimum fractal dimension, and good fineness modulus values achieved maximum ITS values. Further, excess sand or fines lead to the ITS decline, whereas UCS improved with the sand fines (Nazarian and Yuan 2012).

Similarly, Deng et al. (2019) studied the properties of the RAP incorporated EATB at different sizes of aggregate and mineral filler contents. The study obtained maximum ITS values at 3% mineral filler, 20% machine-made sand, and 10-30% coarse aggregates (9.5-19 mm). Zhu et al. (2019) evaluated the EATB with three different gradations close to the upper limit, close to intermediate gradation, and lower gradation. The gradation with more fine aggregates (Close to upper gradation limits) has improved mechanical properties and requires more EA than the remaining gradations (Zhu et al. 2019).

2.3.12.2 Tensile Strength Ratio (TSR)

TSR is one of the durability parameters considered by most researchers. The addition of cement and limestone fillers into the EATB increases resistance to moisture damage (Oruc et al. 2007; Nottingham et al. 2011). Furthermore, RAP mixes exhibited better durability than NA mixes, and the TSR increases with an increase in RAP content in the blend (Nottingham et al. 2011; Cardone et al. 2018). An increase in maximum aggregate sizes worsens the durability of the mix (Moghadam and Mollashahi 2017). The type and amount of additives play a significant role in making more durable mixes. Cement is considered an effective additive that makes the mix moisture resistant, and

rice husk ash have problems with high water absorption resulting in the stripping of asphalt from the aggregates (Behnood et al. 2015).

According to Spanish technical specifications, the TSR limit is 70%. Asphalt Academy (2009) states that it is 50% where the allowable value is well below the surface and binder course (Flores et al. 2019; Asphalt Academy 2009). Further, the Optimum Emulsified Asphalt Content (OEAC) is essential as the durability increases with asphalt content reaching the maximum and then decreasing (Li et al. 2019).

2.3.12.3 Rutting Behavior of EATB

Rutting is considered to be one of the premature failures in the EATB. Different parameters influence the rutting characteristics. An increase in maximum aggregate size improves the rutting resistance of the EATB even at high air voids (Moghadam and Mollashahi 2017). The increase in aggregate size in a well-graded mix provides better interlocking between the aggregates and prevents deformation. EATB without cement content exhibited premature failure compared with the cement-modified mixes (Oruc et al. 2007). As already discussed, the presence of the cement accelerates the curing process by evaporating the available water by hydration reaction. A decrease in the rutting with the cement content is observed in the previous investigations (Flores et al. 2019; Oruc et al. 2007; Du 2014; Needham 2000; Li et al. 2019; Flores et al. 2020; Dong and Charmot 2019; Thanaya 2007).

Further, the permanent deformation increases with the EA content (Li et al. 2019; Dong and Charmot 2019). This implies more ductility nature adopted by the bases with the increase in the EA. However, the optimum amount of EA is required, which increases the usable life of the EATB (Ellis et al. 2004). The curing temperature well influences the curing process of the bases. Usually, the EATB in cold regions has a delay in the curing compared with the tropical environment. The study revealed that lower permanent deformation is observed at higher curing temperatures (Nassar et al. 2016a).

2.3.12.4 Indirect Tensile stiffness Modulus (ITSM) and Resilient Modulus (M_R)

The ITSM and M_R are two important stiffness parameters. ITSM is used frequently to determine the fatigue life cycles, and M_R is used to characterize the base material used in the pavement design. In fatigue testing, the initial stiffness in terms of ITSM is calculated in the first 100 cycles of the test, and the test is terminated when the ITSM reaches half of its initial value. It is revealed that the stiffness increases with TFC reaches a maximum and then decreases (Nassar et al. 2016b). The same scenario is repeated in EA content, where the stiffness increases first to reach maximum and then decreases (Xiao et al. 2019). So, it is usual practice to determine the Optimum TFC and EAC to prevent this problem. Besides, the ITSM depends on relative

humidity, where the samples with less relative humidity exhibited a higher modulus (Nassar et al. 2016b). Further, the stiffness of the base increases with the curing period, cement content, and curing temperature (Taherkhani et al. 2016; Modarres et al. 2011; Flores et al. 2019; Oruc et al. 2007; Needham 2000; Shanbara et al. 2018; Kavussi and Modarres 2010; Flores et al. 2020; Mignini et al. 2018; Thanaya et al. 2009; Grilli et al. 2019; Nassar et al. 2016a; Barbod and Shalaby 2014; Nassar et al. 2016b). In case of higher temperatures, the stiffness decreases (Taherkhani et al. 2016; Li and Liu 2014; Oruc et al. 2007; Shanbara et al. 2018; Kavussi and Modarres 2010; Nassar et al. 2016b; Nottingham et al. 2011; Yan et al. 2010; Budge and Wilde 2008; Li and Liu 2010). As asphalt is a visco-elastic material sensitive to temperature changes, little variation in temperature impacts the modulus. The increase in temperature proportionally increases the permanent strains.

2.3.12.5 Marshall Stability and Percentage of Air Voids in EATB

Marshall Stability is one of the design parameters adopted by many researchers where the EA content at which maximum stability value is obtained is considered OEAC (Joni and Hashim 2018; Thanaya et al. 2014; Kavussi and Modarres 2010; Pi et al. 2019). Besides, the percentage of air void is adopted as a design parameter. According to the specifications of Poland and China, the required percentage of air voids are 8-15% and 9-14% (Dolzycki et al. 2017; Pi et al. 2019). Generally, the design of HMA considers the percentage of air voids as one of the critical parameters. However, little or no importance is given to the mixes prepared with EATB.

The higher percentage of air voids in EATB is due to water evaporation during the curing period and leaves behind pores (Nottingham et al. 2011). The air voids content impacts the strength and stiffness of the bases. A decline in stiffness is observed with an increase in the air voids (Nottingham et al. 2011). Besides, the percentage of air voids depends on the design parameters like TFC, OEAC, cement content, curing time, curing temperature, etc. There is a continuous decrease with EA content in air voids, and others observed a decrease in air voids first and then increases (Flores et al. 2019; Li et al. 2019; Nassar et al. 2016; Pi et al. 2019). The percentage of air voids starts increasing after reaching the required amount of water needed for compaction from these observations. Further, a decrease in air voids with the cement content as voids filled the added cement (Flores et al. 2019; Du 2014; Needham 2000; Li et al. 2019). The percentage of air voids increases with the curing temperatures, where more water evaporates with the increased temperature and left the voids in the base (Gandi et al. 2019).

2.3.12.6 Field Evaluation of EATB

Performance evaluation of any field material is much more essential than a laboratory. Unexpected climate changes, weather conditions, traffic loads, and temperatures lead to the premature failure of the base layer. The behavior of the base layer will be evaluated at frequent

intervals to determine the stiffness, deformation, and other measurements. For this purpose, destructive and non-destructive instruments are used. Several researchers evaluated the field performance of the EATB alone or combined with laboratory evaluation to predict the correlations between field and laboratory. Budge and Wilde (2008) evaluated EATB made of gravel using a Dynamic Cone Penetrometer. It is found that there is an increase in the stiffness of the base with the increase in the curing period. Another field investigation revealed that the stiffness of the EATB increased with the curing period up to 3-5 years and later decreased due to the traffic-related damages (Godenzoni et al. 2018). Field evaluation of the EATB without additives shows a decline in the modulus values than that of the subgrade and recommended using additives like cement (Gurney 2013).

The period of opening to traffic after the construction of EATB depends on several factors that include ambient temperatures, humidity, etc. The field study recommends opening the base to traffic or construction vehicles after achieving the minimum required strength or stiffness (Nazarian and Yuan 2012; Gurney 2013). Quick and Guthrie (2011) recommended curing for at least 2 weeks before opening to traffic to prevent premature failure. The surface layer on top of EATB can be placed only after completing the base (Gurney 2013).

2.3.12.7 Fatigue Characteristics of EATB

Asphalt pavements mainly fail in rutting and cracking. Every pavement is designed to withstand fatigue cracks. The behavior of the EATB is expected to be the same as that of the asphalt mixes. A study revealed that recycled bases with the same void ratio show better fatigue life than HMA (Miro et al. 2004). The composition of EATB completely differs from the HMA mixes. The inclusion of cement as an additive along with emulsified asphalt and the curing process may vary the properties of the EATB from HMA. This unique composition, design characteristics of the EATB, and advantages of the EATB over conventional bases made researchers study the fatigue characteristics at different stress levels, temperatures, curing periods, cement contents, types of cement, and curing temperatures.

Generally, the fatigue characteristics of EATB are evaluated using stress-controlled and strain-controlled methods. Stress-controlled methods involve the measurement of strain at the individual stress level. At the same time, corresponding stress is applied to induce fixed strain in the case of strain-controlled analysis. In the stress-controlled method, increased stiffness led to increased fatigue life, and increased stiffness led to decreased fatigue life in the strain-controlled process (Tayebali et al. 1992). The fatigue cycles or the failure criteria of the given base material and test conditions vary worldwide. Individual specifications differed based on the traffic, climatic conditions, and base layer thickness. Further, studies used flexural beam

fatigue, Indirect Tensile (IDT) Fatigue Test, and Semi-Circular Bending (SCB) Fatigue Test for the analysis. Some of the fatigue studies are included in Table 2.13.

Table 2.13 Fatigue characteristics of EATB highlighted by the authors

Author, year	**Country**	**Conclusions/Recommendations**
Pi et al. (2019)	China	The fatigue life of dry samples with low emulsified asphalt is more at low-stress levels, whereas the scenario is reverse at high-stress levels. Cold mixes are not recommended in the bending tension fatigue zone because of their poor fatigue performance compared with HMA.
Chelelgo et al. (2019)	Kenya	Curing time and temperatures significantly influence the fatigue life of Cold mixes. Loss of flexibility is observed at long curing periods that achieve maximum asphalt stiffness, resulting in low fatigue.
Jiang et al. (2019)	China	Improvement in the Fatigue life is observed for the mixes prepared using Vertical Vibration Compaction Method compared with the Modified Marshall Compaction Method.
Flores et al. (2019)	Spain	Cement is considered a critical factor for the increase in fatigue life, and the maximum number of fatigue life is obtained at 2% cement content-4% Emulsified asphalt content.
Cheng et al. (2018)	China	Both HMA and Cold mix base have similar fatigue characteristics, and mixtures subjected to traffic loads previously have less fatigue life. Suggested stiffness modulus over ITS for fatigue evaluation of the mixtures.
Buczynski & Iwanski (2016)	Poland	Specimens with foamed bitumen binder exhibit higher fatigue resistance and exceeds the acceptable strain levels at high-stress levels of 500 kPa compared with emulsified asphalt mixes.
Gao et al. (2016)	China	1.5% of cement improved the fatigue performance at the same stress level. Both SCB and IDT fatigue tests exhibited the same outcome with a deviation in the results, and cold mixes have large tensile strains and poor fatigue performance compared with HMA at the failure point.
Taherkhani et al. (2016)	Iran	There is an increase in fatigue life with the cement content. (up to 3%). Moreover, loss of sensitivity towards fatigue life is observed with an increase in the cement content.
Arimilli et al. (2016)	India	Mixes containing 50% and 60% RAP exhibit increased stiffness and fatigue life more than 4.5 times than VA mixes.
Kavussi and Modarres (2010)	Iran	Specimens with higher cement contents performed well at lower strains, less than 200 micro strains, and higher strains. Sudden failure is observed at higher cement contents and lower temperatures. There is also a decrease in the slope of the fatigue curve with the increase in cement content.
Yan et al. (2010)	China	Three-stage failure in emulsified asphalt and two-stage failure in foamed asphalt mixes is observed. More fatigue life is observed at higher stress levels for emulsified asphalt mixes than for foamed asphalt mixes.

2.4 Summary of Literature Review

Utilization of EA in the stabilization of recycled materials and deteriorated pavements as bases, binder courses, and the surface course is a part of the conservation of natural sources. It consumes less energy and provides a safe working environment without heat application. More research is carried out to pronounce the advantages of EATB in long-term mechanical and performance characteristics. A detailed review is carried out on the EATB to understand the new technologies in the design and utilization of the recycled materials as a pavement base, and the following conclusions are drawn:

- From the studies, additives improved the mechanical properties of the base, and cement is considered an additive by a majority and used in the range of 1-3 percent. Beyond this range is not suggested as it is not usable, and it may fall well below the acceptable A/C ratio (treated as a cement-treated base), which should be more than 1. Moreover, it is not economical to use higher cement contents besides EA. It will increase the cost of construction.
- Short-term curing in the laboratory with field curing is well correlated between 25-60 degrees Celsius. This range depends on the climatic conditions like temperature and humidity of the existed base layer in various countries. Apart from climatic conditions, long curing periods are recommended for thicker bases. A three-day laboratory curing develops more than 80% of the strength or stiffness developed in field curing for 30 days. So, testing the samples after 3 days of laboratory accelerated curing is preferred.
- There is an improvement in fatigue life with the addition of cement. However, optimization of additive is required. Temperature, stress state, induced strains, additive content, material composition, curing period, and dry or wet conditions influence the fatigue life of the base.
- The performance of the EATB is not always the same as that of the HMA. Mix design, materials, curing, and compaction, to make the difference.
- Maximum dry density, Marshall Stability, and ITS are considered primary performance indicators of the EATB. Resilient Modulus, Rutting, and fatigue are regarded as secondary performance indicators.
- The difference in the additional water at the design time is alleviated at more extended curing periods and exhibits the same strength. However, the minimum required water for workability, compaction, and better coating should be added.
- EA rejuvenates the aged binder present in RAP. RAP mixes require a minimum binder compared with VA and C&D mixes that absorb more asphalt. Moreover, the binder content depends on the gradation. A higher percentage of lower-sized aggregates consumes more asphalt due to higher surface area. The Source of RAP might not significantly affect the

performance of the cold mixes, whereas RAP content or depth of recycling substantially affects the properties. The addition of a small percentage of mineral filler or VA in the range of 10-30 % is preferred to fill the gaps of the missed aggregates due to recycling as it may change the gradation during recycling.

- VVCM is the most advanced and simulates the field compaction characteristics compared with other compaction methods.

The detailed literature review shows several studies on cement-treated and untreated recycled aggregate bases and sub-base courses. The majority of the studies recommended that recycled aggregates be a viable alternative for base material that is environmentally sustainable. Further suggested stabilizing and blending the recycled aggregates with base materials will obtain a sound base/ sub-base for the pavements. The following are the specific conclusions that are drawn from the review.

- The UCS value of the recycled aggregate mixes depends on the type of material, percentage of recycled aggregate, curing period, compaction effort, and cement used in the combination. Some recycled materials addition shows a decline in the mechanical properties; others did not show any trend in their addition, and others show improvement in the properties up to some percentages of addition
- Cement by-products like fly ash and cement kiln dust can be replaced with cement by optimizing carefully to achieve better mechanical properties.
- Higher cement contents are required to achieve the acceptable UCS values for 100% RAP materials. The addition of VA or base materials provides proper interlocking for recycled mixes. Fiber inclusion has no significant difference in strength and other properties, and further research is recommended in this area.
- Less quantity of recycled plastic (<5%) and glass (<10%) materials are preferred in the stabilized road bases. Pre-treatment is required for industrial waste materials to avoid leachate problems. Higher water absorption is observed in RCA or RMA mixes, and RCA bases serve better when the moisture content is less than OMC. The rate of gain in strength for stabilized RCA is more than that of RAP and VA due to self-cementing properties.
- The flexural strength of cement-treated bases increases with the curing period and decreases with the inclusion of recycled aggregate content. The flexural strength ranges between 10-20% of the UCS. RCA alone shows higher flexural strengths than mixing with other recycled aggregates.
- RCA bases have higher M_R than other aggregates, exhibiting anisotropic behavior. Further, the stiffness value is observed at higher cement dosages. Some recycled materials improve M_R, and the other studies showed a decline. The secant modulus, shear modulus, and

dynamic modulus value increase with cement dosage. The combination of cement with asphalt emulsion is more resistant to rutting than cement stabilization and other stabilizers and combinations.

- The permanent deformation decreases with cement and is influenced by the recycled aggregate type and content. Cement stabilized bases show higher modulus indicating high stiffness represents susceptibility to cracking.
- The recycled aggregate content influences the fatigue life of cement-treated recycled bases, type of the recycled aggregate, cement content, curing period, applied stress levels, and sometimes temperatures (if RAP is used).

2.5 Gaps in the Literature Review

- Limited studies were found on the fatigue performance of EATB using RAP, RCA and other recycled aggregates in different combinations.
- Influence of the residual binder on the performance of the EATB to be evaluated
- Limited studies were observed on the Permanent deformation characteristics of EATB regarding binder content and recycled aggregate content.
- Limited studies compared the fatigue characteristics of recycled aggregate with conventional aggregates.
- No specific Indian codes are available for Emulsified asphalt treated bases.

2.6 Scope of the Present work

The scope of the study includes the characterization of recycled aggregates (RAP and RCA) along with VA and comparison with the MoRTH, 2013 specifications. Determination of the physical characteristics of the binders that include emulsified asphalt and cement as per IS 8887:2018 and IS 12269: 2003. Blending the aggregates into the respective gradation specified by the MoRTH, 2013 specifications for CTB. Blending the aggregates for EATB as per Asphalt Academy Technical Guidelines, 2009 ideal gradation. Determination of the Optimum Moisture Content and Maximum Dry Density for CTB using Modified Proctor method of compaction and Optimum Emulsified Asphalt Content for EATB according to the Asphalt Academy Technical Guidelines, 2009. Determination of the Unconfined Compressive strength for CTB at 7 and 28 days of curing period and comparison with the specification limits. Determination of the Indirect Tensile Strength properties of the CTB at 7 and 28 days of curing periods. Evaluation of the density and dynamics of moisture loss characteristics of the EATB. Determination of the rutting characteristics using Dynamic Creep Rutting apparatus at different temperatures 25℃ and 40℃. Determination of the influence of temperature on M_R of EATB. Evaluation of the moisture damage characteristics of the EATB using Indirect Tensile Strength

Ratio. Investigation of the fatigue characteristics (three stress levels were considered) of the CTB and EATB concerning the different stabilization levels and the recycled aggregate contents using the Indirect Tensile Fatigue Testing apparatus.

CHAPTER 3

RESEARCH METHODOLOGY

3.1 General

The previous chapter reviewed various research works on cement-treated and emulsified asphalt-treated bases. This chapter presents the material, research methodology, mix design, and testing procedures adopted in the current study. The study aims to evaluate the performance of cement and emulsified asphalt treated bases using various parameters. To assess the performance of stabilized bases, preliminary studies were conducted on the materials used in this study according to the Ministry of Road Transport & Highways (MoRTH), 2013 specifications. A typical overall research methodology is shown in Fig. 3.1.

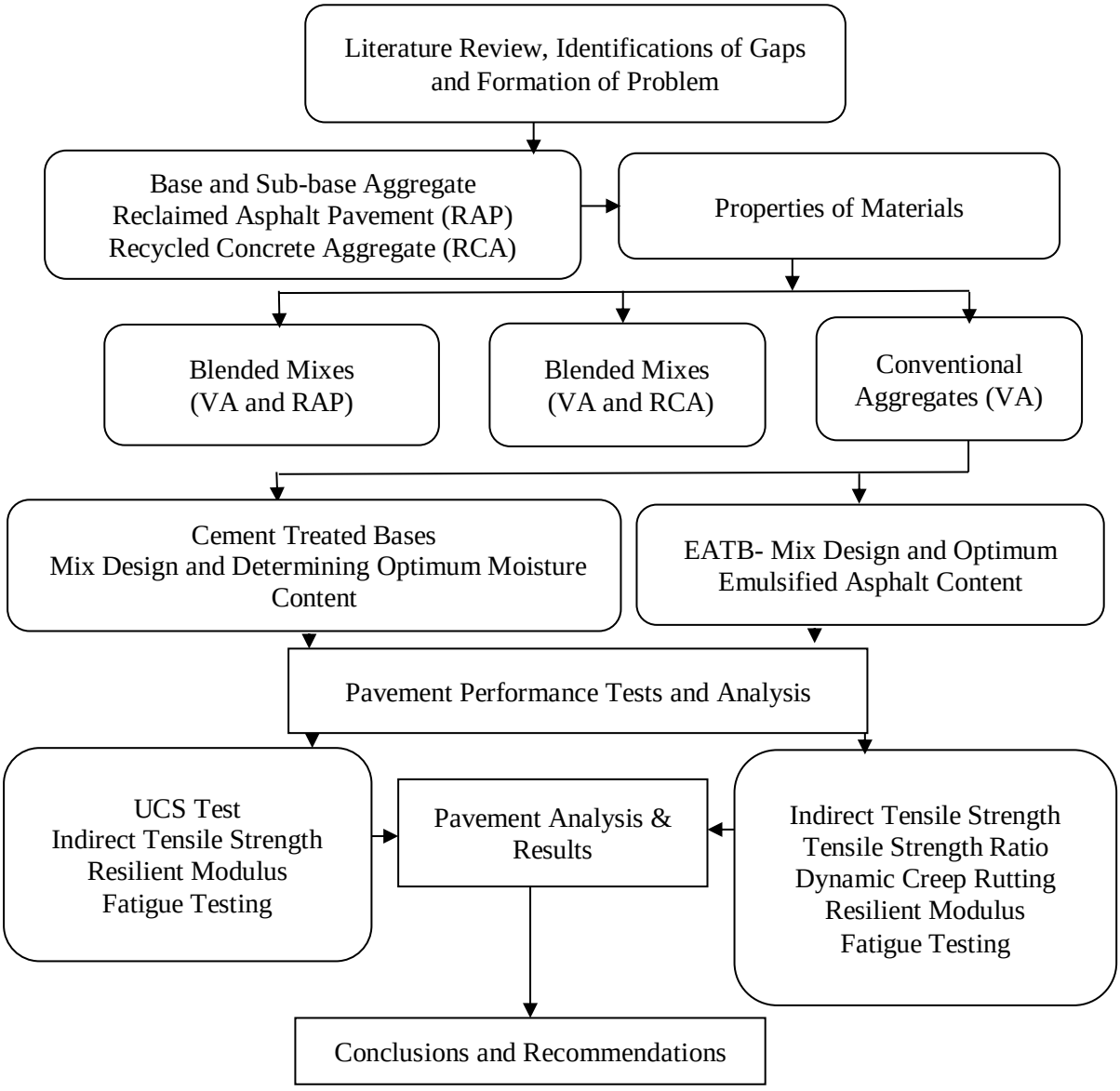

Figure 3.1 Adopted Research Approach

Initially, a thorough literature review is carried out nationally and internationally on the utilization of recycled aggregates in the cement stabilized and emulsified asphalt stabilized bases to identify the possible gaps. Upon identification of the gaps, respective objectives were framed. For Cement treated bases, the studies considered the following parameters, as shown in Figure 3.2. Most of the studies used UCS, followed by M_R, durability and the remaining parameters following the list. Similarly, the share of the different recycled materials in the literature is shown in Figure 3.3. Here, RAP is utilized by most of the studies and followed by RCA in the pavement bases. So, the researchers preferred the recycled deteriorated pavement with a stable base over the other recycled materials. It is an easy process and also saves transportation costs.

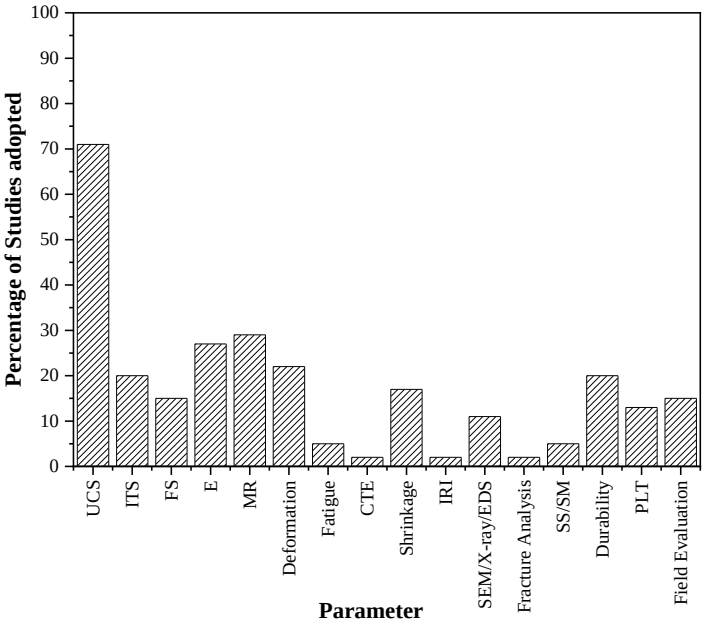

Note: FS-Flexural Strength, SS-Shear Strain, SM-Shear Modulus, PLT- Permeability and Leaching Tests, CTE – Coefficient of Thermal Expansion, SEM – Scanning Electron Microscope, EDS- Energy-dispersive X-ray Spectroscopy,

Figure 3.2 Parameters that are used in the CTB studies

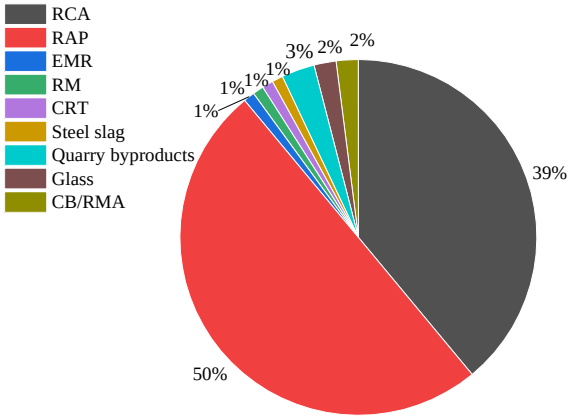

Figure 3.3 Percentage of studies that adopted different Recycled aggregates in CTB

Note: EMR-Electrolyte Manganese Residue, RM- Red Mud, RMA-Recycled Masonry Aggregate, CRT-Cathode Ray Tubes

Similarly, for EATB, the parameters like ITS, Modulus/ Stiffness, Fatigue life, dry density, UCS/ Compressive strength, durability, Marshall stability, air voids/Porosity, Cohesion, Raveling, high-temperature stability, low temperature cracking resistance test, Rutting test/deflection, fracture energy, X-ray microtomography/X-ray diffraction, Flexural strength, SEM, Dynamic Cone Penetrometer (DCP), Hydraulic conductivity, water loss, cracking test index, semicircular bending are adopted. The percentage of studies adopted by different parameters is shown in Figure 3.4. Most researchers adopted modulus, follows ITS, fatigue life, UCS/Compressive strength, rutting or deflection. And the recycled aggregates used in the studies are shown in Figure 3.5. The majority used RAP in the recycling process, followed by the VA, RAP+VA, C & C&D.

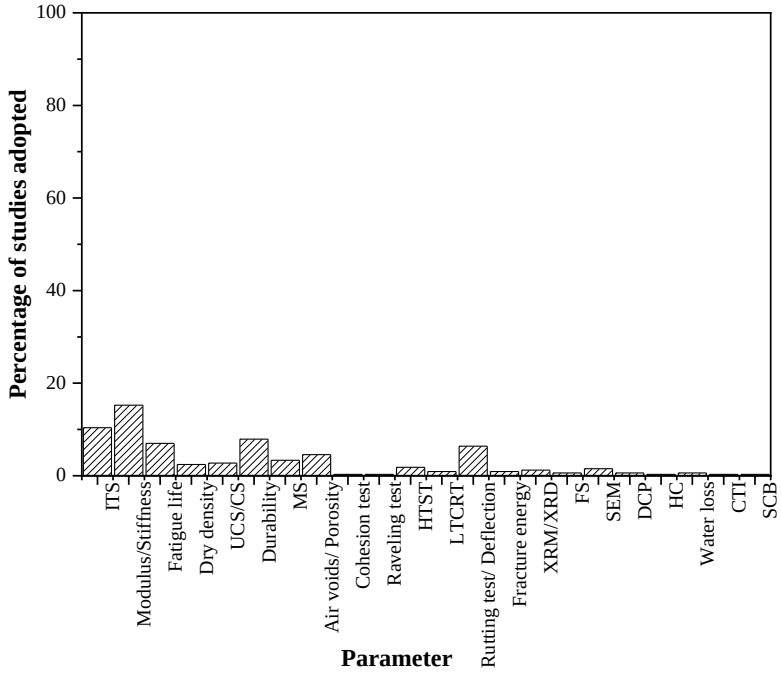

Note: CS-Compressive Strength, MS-Marshall Stability, HTST-High Temperature Stability Test, LTCRT- Low-Temperature Cracking Resistance Test, XRMX-Ray Microtomography, XRD-X-ray Diffraction, FS-Flexural Strength, HC-Hydraulic Conductivity, CTI-Cracking Test Index, SCBSemi-Circular Bending

Figure 3.4 Parameters that are used in the EATB studies

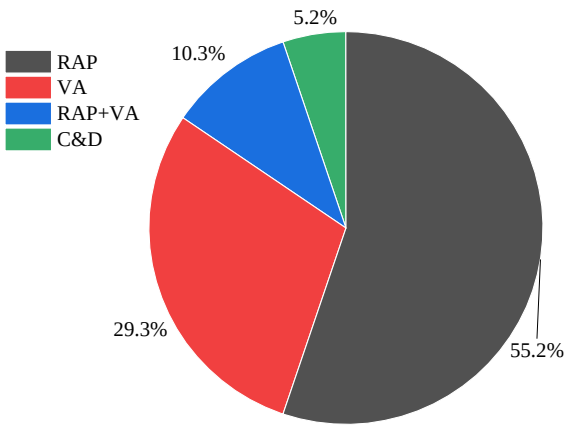

Figure 3.5 Percentage of studies that adopted different Recycled aggregates/ VA/ together in EATB

3.2 Materials and Testing

The following are the materials used in the study; Reclaimed Asphalt Pavement (RAP), Virgin Aggregate (VA), Recycled Concrete Aggregate (RCA), Cationic Slow Setting asphalt emulsion (CSS-2), Ordinary Portland Cement (OPC). The recycled aggregates are collected from the locally demolished concrete waste, and the RAP is reclaimed from Mulugu to Khammam road, which was laid 5 years ago, shown in Figure 3.6. The natural aggregates are collected from the nearby quarry. The OPC and emulsified asphalt are taken from the local suppliers.

Figure 3.6 Location of the RAP material collected

3.2.1 Aggregates

The aggregates are evaluated for engineering properties to confirm their suitability as a base material. The properties of various aggregates RCA and RAP are obtained after processing. The percentage of asphalt in the RAP is extracted using the centrifugal extraction method. RCA aggregates are crushed to a suitable gradation, washed, and dried. After sieve analysis, properties including flakiness and elongation index, abrasion value, aggregate impact value, and water absorption were carried out on RCA, VA, and bitumen free RAP aggregates and compared with MoRTH, 2013 specifications which are tabulated in Table 3.1.

Table 3.1 Physical Properties of aggregates for unbound or bound base layer as per MoRTH, 2013

Property	**MoRTH, 2014 Specifications**	**Method**
Combined flakiness and Elongation index (%)	35.0	IS 2386 Part I
Abrasion Value (%)	40.0	IS 2386 Part IV
Aggregate Impact Value (%)	30.0	IS 2386 Part IV
Water absorption (%)	2.0	IS 2386 Part III

3.2.1.1 Blending of Aggregates

The aggregate gradation curves for RAP, RCA and VA are determined and blended to a suitable gradation to satisfy the specification requirements. For EATB, the Asphalt Academy Technical Guidelines-2 ideal case is adopted, and the aggregates are blended in such a way to fall within the upper and lower limits of the specification as shown in Table 3.2.

Table 3.2 Gradation requirements of EATB

Sieve Size (mm)	Percentage Passing	
	Ideal	Less suitable
50	100	-
37.5	87-100	-
26.5	77-100	100
19.5	66-99	99-100
13.2	67-87	87-100
9.6	49-74	74-100
6.7	40-62	62-100
4.75	35-56	56-95
2.36	25-42	42-78
1.18	18-33	33-65
0.6	12-27	27-54
0.425	10-24	24-50
0.3	8-21	21-43
0.15	3-16	16-30
0.075	2-9	9-20

For CTB, the blending of the aggregates is according to the MoRTH, 2013 specifications as shown in the Table. 3.3. The blending of aggregates is required to fall within the upper and lower limits of the specifications.

Table 3.3 Gradation requirements of CTB

IS sieve size	Percentage Passing
53	100
37.5	95-100
19	45-100
9.5	35-100
4.75	25-100
0.6	8-65
0.3	5-40
0.075	0-10

3.2.2 Cement

Ordinary Portland Cement of Grade 53 is selected as a stabilizer and evaluated for the basic properties like fineness, normal consistency, initial setting time, final setting time, and specific gravity according to IS 12269: 2003 specifications. Cement is used as a stabilizer for CTB and as an active filler for EATB.

3.2.3 Cationic Slow Setting Asphalt Emulsion (CSS-2)

Tests on Emulsified asphalt were performed as prescribed by IS 8887: 2018 and IS 3117: 2004 to characterize the material and verify the suitability for EATB. The summary of the test method and specifications are presented in Table 3.4.

Table 3.4 Summary of tests on Cationic slow-setting asphalt emulsion

Characteristics	Specifications, IS 8887: 2018	Test Method
Residue on 0.6 mm IS Sieve, % by mass, Max	0.05	IS 8887: 2018
Viscosity, Seconds (At 25°C)	30-150	IS 3117: 2004
Storage stability, %, Max	2	IS 8887: 2018
Particle charge	Positive	IS 8887: 2018
Mixing stability (cement), %, Max	2	IS 8887: 2018
Residue by evaporation, (%)	60 (min)	IS 8887: 2018
Penetration 25°C/ 100g/5, sec	60-120	IS 1208: 1978
Ductility, 25°C/ 100g/5, sec	50	IS 8887: 2018
Solubility, % by mass, min	98	IS 1216: 1978

3.3 Mix Design of CTB

The mix design of CTB is carried out by determining the OMC at which the MDD is achieved. The compaction is carried out using the Modified Proctor testing procedure as per the AASHTO T180 protocol. The mould dimensions were 102 mm in diameter by 127 mm in height. The hammer weight was 4.4 kg, and it had a free-fall distance of 457 mm. As a mould correction, all the particle sizes greater than 19 mm were replaced with the same amount of particles less than 19 mm from the mix. Samples are casted at obtained OMC to evaluate for various performance characteristics. The experimental sample test matrix for CTB is shown in Table 3.5. Each test is conducted three times to represent the repeatability of the results.

Table 3.5 Experimental sample test matrix for CTB

Mix Composition	Mix Design (No. of Samples)	UCS		ITS		M_R		Fatigue
		7 Days	28 Days	7 Days	28 Days	7 Days	28 Days	
RAP, RCA, VA, 25RAP, 50RAP, 75RAP, 25RCA, 50RCA, 75RCA @ 2, 4, 6% Cement	54	81	81	81	81	81	81	162

3.4 Mix Design of EATB

There is no universally accepted mix design to determine Optimum Emulsified Asphalt Content (OEAC). Some studies used ITS as design criteria, others recommended UCS and Marshall Stability to determine the OEAC. The present study considered ITS as the criteria to determine

the OEAC. The mix design of EATB involves optimizing pre-wetting water and emulsified asphalt in the mix. The pre-wetting water is added to the aggregate and cement (additive) mixture. The emulsified asphalt content is varied at an interval of 0.5% by weight of the dry aggregate and tested for the ITS properties after curing for 72 hours at 40°C. The Initial Emulsified Asphalt Content (IEAC) is determined based on the equation given in IRC: SP: 100-2014, based on the mixes' final gradation.

$$IEAC\ (\%) = 0.05A + 0.1B + 0.5C \qquad (3.1)$$

Here, *A* is the percentage weight of sieved material retained on a 2.36 mm sieve, *B* is the percentage weight of sieved material passing through a 2.36mm sieve and retained on a 0.09 mm sieve, and *C* is the percentage weight of material passing through a 0.09 mm sieve.

The trial emulsified asphalt content (TEAC) was determined by using the following equation (3.2)

$$TEAC(\%) = IEAC - \frac{P_{b,RAP} \times (RAP - content)}{P_{b,Emulsion}} \qquad (3.2)$$

IEAC, as calculated from equation (3.1), Pb, RAP, is the Bitumen content in RAP material (%), *RAP content* is the RAP content in the blended mix (%), $P_{b,\,Emulsion}$ is the residue by evaporation in emulsified asphalt (%).

Step-1

Step-2

Step-3

Step-4

Step-5 Step-6 Step-7

Figure 3.7 Steps involved in the mix design of EATB

Initially, the aggregates were thoroughly mixed with the additive to form a homogeneous mixture as shown in Figure 3.7. step-1. In step-2, the pre-wetting water is added to the aggregate additive mixture and mixed for 1-2 minutes to confirm proper coating around the aggregate

surface. Then, the required quantity of emulsified asphalt is added and mixed thoroughly, shown in step-3. Then the mixture is allowed for 1-2 minutes to break the asphalt emulsion and compacted using the Marshall Method of compaction by applying 75 blows as shown in Step-4. The compacted specimens were cured for 72 hours at 40℃ a temperature in a temperature-controlled hot air oven in step-5. The cured samples were shown in step-6, which are tested for ITS value after 24 hours of the curing period as shown in step-7. Each test is conducted 3 times to represent the repeatability except the fatigue testing, where the test is carried out 2 times at each stress level. A typical experimental sample test matrix is shown in Table 3.6.

Table 3.6 Experimental sample test matrix for EATB

Mix	**Mix design**	**TSR 27°C**		**Rutting**		**M_R**		**Fatigue 27°C**
		Dry	**Wet**	**27°C**	**40°C**	**27°C**	**40°C**	
25RAP, 50RAP, 75RAP, 25RCA, 50RCA @L, O, H of EAC	45	45	45	30	30	45	45	90

3.5 Laboratory performance tests

Laboratory performance tests, including UCS, ITS, M_R, TSR, and fatigue, were performed according to the specifications discussed in the following sections.

3.5.1 Unconfined Compressive Strength (UCS)

The importance of UCS is already discussed in the literature section. UCS samples were casted at OMC according to ASTM D 1632 specifications. The dimensions of the cylindrical mould are selected so that the ratio of height to diameter should be equal to 2. So, the specimen dimensions considered are 101.6 mm in diameter and 200 mm in height. Samples were cured in closed plastic bags to prevent the escape of moisture. The maximum load taken by each specimen divided by the cross-sectional area gives the compressive strength. Typical testing of the sample for UCS is shown in Figure 3.8.

Figure 3.8. Testing of sample for UCS

3.5.2 Indirect Tensile Strength (ITS)

It is an important parameter used to optimize the mix design of asphalt emulsion aggregate mixes. To test ITS, samples were compacted at each emulsified asphalt content and then cured for 72 hours at $40℃$. The cured samples were kept idle for one day at room temperature and tested for ITS as per ASTM D6931 at a loading rate of 50.8 mm per minute. The ITS was determined by using the following equation (3.3).

$$S_T = \frac{2000P}{\pi Dt} \qquad (3.3)$$

Where S_T is the ITS in N/mm^2, D is the specimen diameter in mm, t is the thickness of the specimen in mm, and P is the ultimate failure load in kN.

For Cement treated specimens, the samples are compacted at the required MDD with dimensions of the internal diameter of 101.60 mm and 63.5 ± 2.5 mm in height and then extracted after 24 hours, followed by curing for seven and 28 days. Then the samples are tested for ITS as per ASTM D6931 at a loading rate of 50.8 mm per minute. This test is performed for CTB and EATB specimens at respective curing periods.

3.5.3 Tensile Strength Ratio (TSR)

The Tensile Strength Ratio is the ratio of strength of the conditioned samples to the unconditioned samples. This test represents the durability of the specimens. This test is performed for EATB samples in which the samples are conditioned in water for 24 hours at $25 \pm 2℃$ temperature, as shown in Figure 3.9. This test is performed according to Asphalt Academy Technical Guidelines -2, 2009, in which the required TSR should be 50% and above.

Figure 3.9 Conditioning of samples underwater

3.5.4 Density and Moisture loss of EATB

The dynamics of moisture loss are essential in understanding the early strength properties of the cold mixes. The percentage of moisture loss is calculated by measuring the weights of the specimens at 24, 48, and 72 hours after the compaction. The difference in weight of the sample at respective time intervals gives the moisture loss in percentage, which is determined by using the following equation (3). The percentage of moisture loss is used to observe the curing rate of the cold mixes.

$$\%Moisture\,loss = \frac{W_{initial} - W_{final}}{W_{initial}} \times 100 \qquad (3.4)$$

Where $W_{initial}$ is the initial weight of the sample and

W_{final} is the final weight of the sample.

Before determining the dry density of the specimens, the bulk density is calculated for the initial weight and corresponding volume. Then, the dry density is calculated using the following equation (4).

$$Dry\,density = \frac{Bulk\,Density}{1 + Total\,Fluid\,Content} \times 100 \qquad (3.5)$$

3.5.5 Resilient Modulus (M_R)

The importance of the Resilient modulus test is discussed in the literature review chapter. The samples were prepared according to ASTM D 1632 and ASTM D 6926 using a cylindrical

metal specimen with an internal diameter of 101.60 mm and 63.5 ± 2.5 mm in height. The repeated load, indirect tension test determines the M_R of the mixtures according to the ASTM D 7369 by applying compressive loads with a waveform. The equipment can maintain the temperature from ambient to $60°C$, and the testing frequency can be variable from 1 Hz to 5Hz. The loading and unloading cycles can be varied depending on the requirement, and the loading can be varied from 50 kg to 5000 kg.

In contrast, the test is performed at $27°C$ for CTB samples and at two different temperatures for EATB which are at $27°C$ and $40°C$. A repeated load is applied at the rate of 1 Hz frequency in which 0.1 seconds of the loading period and 0.9 seconds of the rest period. Repeated load is applied to about 10-20% of the failure load during ITS testing as per the specifications. A typical M_R and load-deformation pulse diagram is shown in the Fig. 3.10. The Poisson's ratio for the calculation of M_R is taken as 0.25 and calculated using equation (3.6). The modulus values are also calculated using the empirical equation from UCS. The empirical equation from IRC 37: 2018 is shown in equation (3.7).

$$M_R = \frac{P(\mu + 0.27)}{\Delta H \times t} \qquad (3.6)$$

Here μ is the Poisson's ratio and ΔH the horizontal resilient deformation.

$$E = 1000 \times UCS \qquad (3.7)$$

Here, E is the modulus value in MPa, and UCS values are at 28 days curing period in MPa.

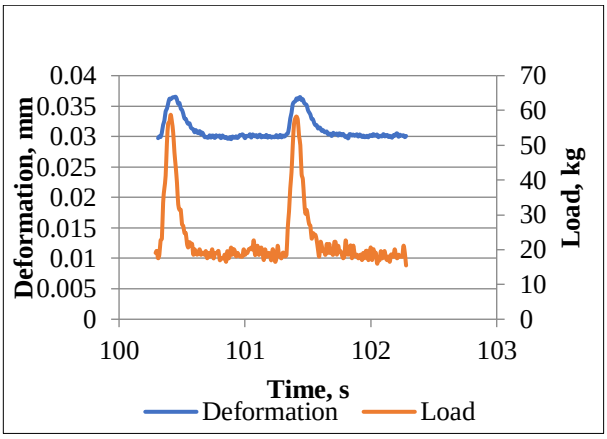

(a) Load-deformation pulse diagram

(b) Setup to measure deformation

Figure 3.10 Typical data acquisition and setup of fatigue testing machine

3.5.6 Dynamic Creep Rutting Test on EATB

A dynamic creep rutting test was performed on the EATB to determine the rutting potential. The test was conducted at a temperature of $25 \pm 2°C$ and $40°C$. The dynamic loading was applied during the 0.1 seconds loading period and 0.9 seconds rest period, representing a 1 Hz frequency. The applied loading created stress of 150 ±5kPa, and deformation was measured

using a Linear Variable Deformation Transducer (LVDT) with an accuracy of 0.0001 mm. It could be noted from previous studies that there is no consensus in choosing the stress levels that ranges between 69 kPa to 1000 kPa. The temperature conditions ranged from ambient to 60°C, and a majority of the studies have adopted 0.1 seconds as the loading period and 0.9 seconds as the rest period. The test termination is either in 3600 cycles or the collapse of the sample due to tertiary flow. A typical test setup is shown in Fig. 3.11.

Figure 3.11 Dynamic creep rutting test apparatus

3.5.7 Indirect Tensile Fatigue Testing

The importance of fatigue testing is discussed in the literature review chapter. The indirect Tensile fatigue test is simple to use where cores from the in-situ pavement sections and the laboratory samples can be tested. It is easy to extract cylindrical cores rather than beam types. The repeated load is applied on diametrical plane in which the complete collapse of the sample is considered the failure criteria, and the number of cycles was noted. The fatigue testing is performed at a 1 Hz frequency in which loading is applied at 0.1 seconds and 0.9 seconds rest periods. The repeated loading is applied in such a way to simulate the field conditions. Three stress levels were considered to draw the fatigue lines for different combinations. A typical view of the fatigue test setup is shown in Figure 3.12.

(a)

(b)

(c)

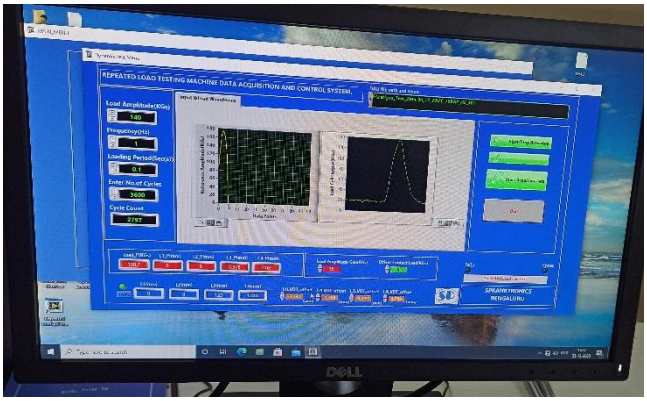

(d)

Figure 3.12 Fatigue testing machine (a) Controller (b) Hydraulic chamber (c) Loading frame (d) Data acquisition.

Fatigue testing is done using the repeated load testing machine at various stress levels for EATB. CTBs were tested at ambient temperature at different stress levels. The stress ratios selected were 0.4, 0.6 and 0.7 for EATB and 0.6, 0.7, and 0.8 for CTB based on the previous research (Pi et al. 2019, Jiang et al. 2019, Cheng et al. 2018, Lv et al. 2019, Hou et al. 2017). The vertical deformation and the number of cycles required to complete the breakdown of the sample are measured. The stresses and strains are calculated from the applied loads using the following equations.

$$\varepsilon_t = (1+3\mu)\frac{\sigma}{M_R} \qquad (3.8)$$

The Poisson's ratio is 0.35 for EATB and 0.25 for CTB, M_R which is the Resilient Modulus, σ is the applied stress, and ε_t is the tensile strain.

3.6 Summary

This chapter presents a detailed research methodology and the adopted specifications and experimental procedures. A detailed flow chart of the flow of the research is shown at the start of the chapter, following the details about the aggregates collection, processing and the basic physical properties determination specifications and limitations were presented. This follows the mix design procedures for the CTB (OMC and MDD), and EATB (OEAC) preparation is presented briefly. After the performance tests, including UCS, ITS, Density, moisture loss, TSR, Dynamic creep rutting, MR and fatigue characteristics were presented with specifications and apparatus figures.

CHAPTER 4

LABORATORY INVESTIGATION OF CTB

4.1 General

The previous chapter presents a detailed research methodology to accomplish the objectives and laboratory performance tests and specifications. In this chapter, a laboratory performance evaluation of the CTB is carried and the results are presented along with the specifications limitations. This chapter includes engineering properties of aggregates, gradation requirements, mix design, and laboratory performance tests. The laboratory performance tests include UCS, ITS, M_R, and fatigue evaluation.

4.2 Engineering Properties of the Aggregates

The following are the aggregates used in the study; Reclaimed Asphalt Pavement (RAP), Virgin Aggregate (VA), and Recycled Concrete Aggregate (RCA).

4.2.1 Aggregates

Virgin aggregates are collected from the local quarry, RCA is collected from and around the city, then processed manually and crushed using a jaw crusher to obtain the required gradation. They are washed thoroughly to avoid any form of loose particles. The processing of RCA is shown in Figure 4.1.

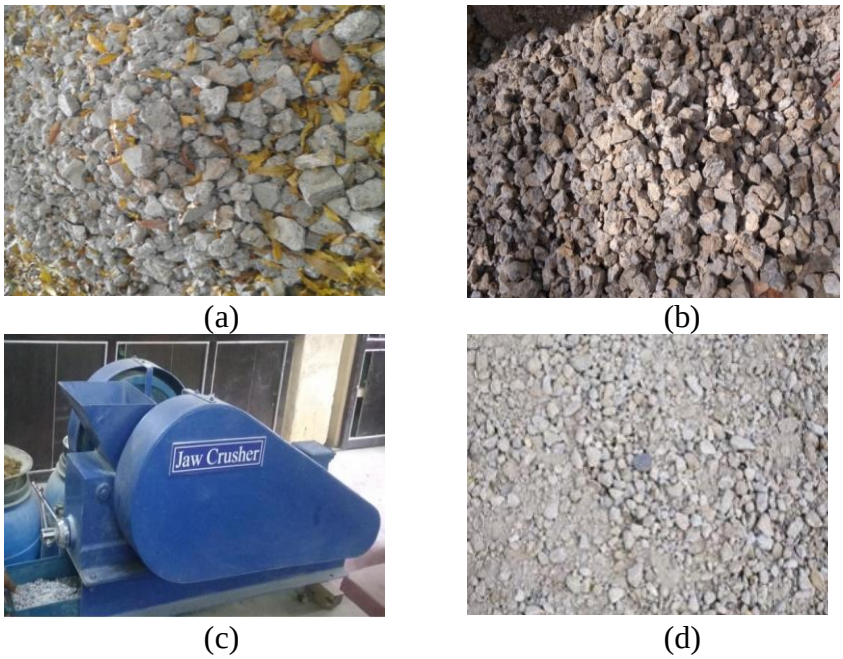

(a) (b) (c) (d)

Figure 4.1. (a) The first stage of manual crushing of RCA in the range of 50-100 mm size, (b) Screening and crushing of RCA into the size range of 30-40 mm, (c) Final Crushing using Jaw crusher in two stages, (d) Final product of RCA after processing

RCA is processed in three stages to eliminate the presence of any foreign matter and provide

homogeneous material. In the first stage, the demolished RCA is crushed into the size range of 50-100 mm, and any visible clayey and metal substances are removed. The RCA is further crushed into 30-40 mm in the second stage to feed easily into the Jaw crusher. At this stage, further screening is done to remove loose particles and dust. After, the processed RCA is fed into the jaw crusher in two stages to eliminate flaky and elongated particles, followed by washing and drying. The recycled concrete from crushing is subjected to physical characterization using MoRTH, 2013 specifications.

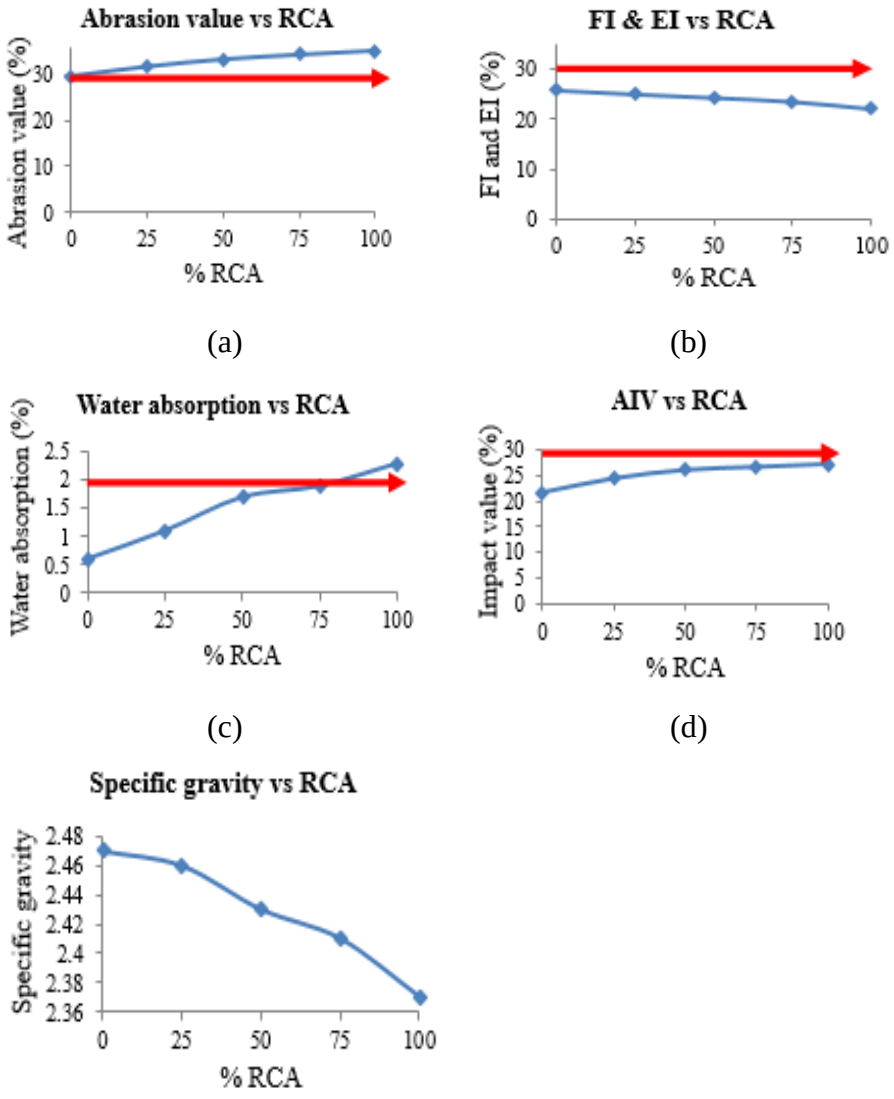

Figure 4.2 Variation of physical properties with RCA content in the blends.

The properties of the RCA and VA blends were studied to understand their variation with the RCA percentage, as shown in Figure. 4.2. The Percentage of RCA in the blend is shown on the *x*-axis, and the corresponding property is shown on the *y*-axis. The red line represents the limitation of the specification. It is evident that there is a significant increase in abrasion, water absorption, aggregate impact value, and a decrease in specific gravity is observed with the

addition of RCA. Further, there is a decrease in the blends' Flakiness and Elongation Index (FI & EI) with the increase in RCA share in the mix. RCA was found inferior to VA in Los Angeles abrasion and water absorption. Depending on the quality of RCA, the adhered mortar loss depends on the strength of RCA. During the testing process, this adhered mortar might be subjected to abrasion. Further, the water absorption rate increased with the addition of RCA, as observed from the previous studies (Guo et al. 2020; Mohammadinia et al. 2015; Lim and Zollinger 2003).

The collected material is processed, and the percentage of asphalt from the RAP after centrifugal extraction using n-Propyl Bromide is determined, which is 4.47%. After sieve analysis, the engineering properties, including FI & EI, abrasion value, aggregate impact value, and water absorption, were carried out on RCA, VA and asphalt free RAP aggregates and compared with MoRTH 2013 are tabulated in Table 4.1.

Table 4.1 Properties of RAP, RCA and VA

Property	**VA**	**RAP**	**RCA**	**MoRTH, 2014 Specifications**
Combined FI & EI (%)	25.73	47.66	22.17	35.0
Abrasion value (%)	29.59	30.12	35.16	40.0
Aggregate Impact Value (%)	21.55	19.17	27.12	30.0
Water absorption (%)	0.6	-	2.3	2.0
Asphalt Content (%)	NA	4.47	NA	-

The strength and stiffness of compacted cement-treated RAP mixes are mainly determined by the gradation of the mix and the cement hydration rather than the properties and shape of aggregates (Yuan et al. 2011). From the properties, water absorption of RCA is high compared with VA and RAP has high flakiness and elongation index and does not satisfy the specifications. Further, the higher water absorption of RCA is due to the mortar surrounding the aggregates. The FI & EI of RAP is more than the specified limits due to the breaking of aggregates along the fracture surface while crushing. These fracture surfaces are formed during the service of the aggregates or maybe during reclamation. So, the RAP material is considered an alternative material, although the combined FI & EI of RAP did not satisfy the specifications.

4.3 Properties of Cement

The ordinary Portland cement of grade 53 is selected as a stabilizer and evaluated for the basic properties in Table 4.2.

Table 4.2 Physical properties of cement

Test	Result	Specifications (IS 12269: 2013)
Fineness (%)	95.0	-
Normal consistency	35.0	-
Initial setting time (minutes)	68.0	30.0
Final setting time (minutes)	435.0	600
Specific gravity	3.20	

4.3.1 Gradation of RAP and RCA

The gradation curves for the RAP-VA blends and RCA-VA blends are presented in Figure 4.3. The gradation chart shows that all the combinations within the specifications lower and upper limits and almost follow the mid-gradation.

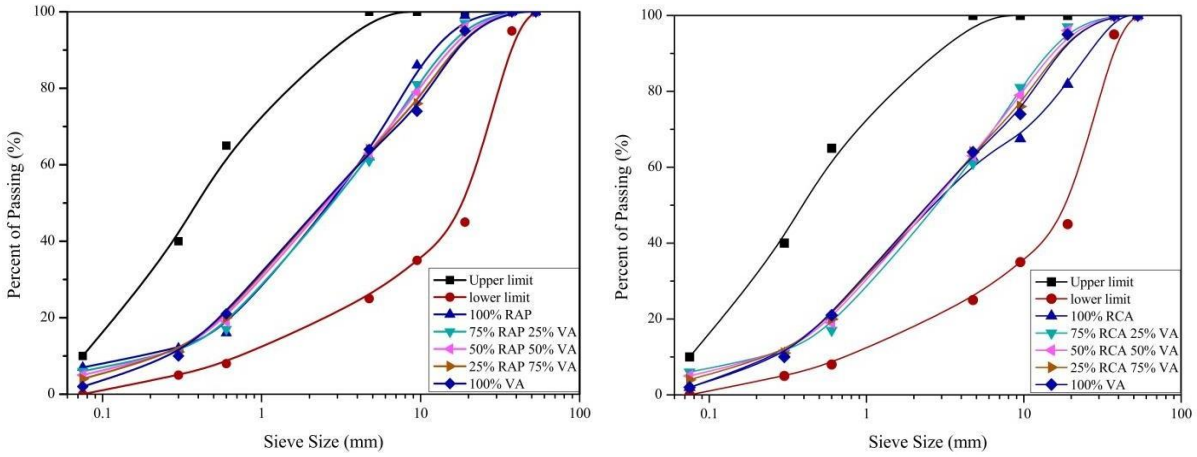

(a) RAP-VA blends (b) RCA-VA blends

Figure 4.3 Gradation charts for CTB

4.4 Design of Cement Treated Bases

The mix design of CTB involves the determination of compaction characteristics which are OMC and MDD. The Modified Proctor's test was conducted to determine OMC and MDD as IS: 2720 (part 8-1985). The compaction test is performed on all the mixes prepared with different proportions of RAP and RCA blends. Each test is repeated three times to consider the repeatability of the results. The OMC and MDD obtained for different blending mixes are shown in Table 4.3 and 4.4. Relatively less water content is required at higher percentages of RAP due to less water absorption of RAP because of asphalt coating. MDD is low at 100% RAP and increases with VA content due to the low specific gravity of the RAP aggregates, and also, it is observed that MDD increases with the cement content. This increase is due to the higher specific gravity of the cement compared with aggregates.

On the other hand, the RCA blends do not show any trend due to non-homogeneity properties. Further, the gradations of RCA-VA blends are not the same and might not be required to follow some trends. The nonhomogeneity represents that some samples get more mortar surrounded

by the aggregates and others surrounded by less mortar. More mortar presence leads to high water absorption, which increases the OMC. The same is verified by conducting a water absorption test on two samples of the same gradation with the mortar presence. This variation of mortar percentage in the sample causes significant variations in the OMC and MDD at high percentages of RCA in the mix (100%RCA and 75% RCA). These results agree with the previous study stating that the determination of the OMC and MDD for C&D waste mixtures is slightly tricky due to the differences in the constituent materials due to breakage during the compaction process (Leite 2007). The MDD values of RAP and RCA blends range between 1.93 to 2.23 g/cc and 1.97 to 2.25 g/cc.

Table 4.3. Optimum Moisture Content and Maximum Dry Density Results for RAP Blends

% of Cement	100% RAP		75% RAP		50% RAP		25% RAP	
	OMC (%)	MDD (g/cc)	OMC (%)	MDD (g/cc)	OMC (%)	MDD (g/cc)	OMC (%)	MDD (g/cc)
0	7.06	1.93	7.44	2.03	7.61	2.13	7.16	2.20
2	7.13	2.08	7.52	2.08	7.72	2.14	7.38	2.22
4	7.24	2.11	7.64	2.10	7.89	2.15	7.67	2.22
6	7.45	2.21	7.88	2.11	7.95	2.16	8.09	2.23

Table 4.4. Optimum Moisture Content and Maximum Dry Density Results for RCA Blends

% of Cement	100% RCA		75% RCA		50% RCA		25% RCA	
	OMC (%)	MDD (g/cc)	OMC (%)	MDD (g/cc)	OMC (%)	MDD (g/cc)	OMC (%)	MDD (g/cc)
0	9.7	2.14	9.2	2.13	12.3	2.02	9.44	2.13
2	8.2	2.1	10.2	1.98	7.93	2.16	10.06	2.2
4	11.1	2.06	9.2	2.01	9.28	2.17	9.44	2.22
6	9.5	2.09	11.5	1.97	10.92	2.2	10.35	2.25

4.5 Performance Evaluation of CTB

After determining the compaction characteristics, laboratory performance tests were carried out on the samples. This includes UCS, ITS, M_R, and Fatigue evaluation.

4.5.1 Unconfined Compressive Strength (UCS) of CTB

UCS test is performed on the specimens of dimensions 100 mm diameter and 200 mm height. A typical testing and tested specimens are shown in Figure 4.4. The results of UCS for 7 days of the curing period are shown in Figures 4.5 and 4.6. From Figure 4.5, the strength increases with the VA and cement content. It gets reduced as RAP content increases because RAP content increases the surface area coated with asphalt in a specimen, forming a weaker bond with the other aggregates, requiring a higher quantity of the stabilizing agent.

On the other hand, from Figure 4.5, 50% RCA shows higher strength irrespective of the cement content due to RCA's better interlocking with the VA, which increases the strength. At 6% cement content, all the mixes exhibit higher strengths. The results are compared with the low-volume road standards for cement-treated bases of local transportation authorities. As per the design standards for 7 days of curing period, RAP/RCA blends with 25% RAP and 6% cement content have UCS of 3.4 MPa /3.19 MPa and 50% RCA with 6% cement with UCS of 3.37 MPa satisfied the Ministry of Rural Development (MoRD) specification value, i.e., 2.76 MPa and didn't satisfy MoRTH specifications, i.e., 5 MPa. So, 25% RAP/RCA-75%VA and 50% RCA and 50%VA with 6% cement content can be used in low volume roads as they acquired the required strength properties. However, most of the mixes satisfied the requirements as a sub-base (1.7 MPa) at 6% cement content except treated RAP.

a) UCS Testing b) Tested Samples

Figure 4.4 A typical Unconfined Compressive Strength testing

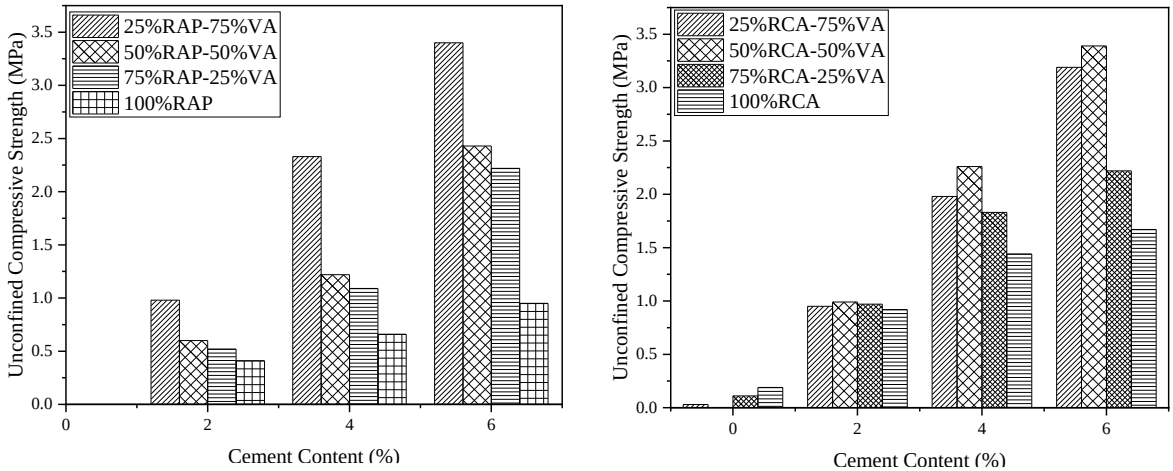

(a) RAP-VA blends (b) RCA-VA blends

Figure 4.5 Unconfined Compressive Strength at 7 days of curing period

From Figure 4.6, compared with RAP blends, RCA blends show more strength. This is due to a strong bond between RCA, VA, and cement. 100% RCA blends show almost double strength compared with 100% RAP blends. The mortar, coated with the RCA aggregates, contributes to developing strength in agreement with the previous studies (Gabr and Cameron 2012; Poon et al. 2006). RAP blended mixes have a weaker bond than RCA due to the existing asphalt coating.

Attempts were made to perform the UCS for the RAP blended mixes without stabilization, but they are fragile and collapsed while removed from the split mould. This represents the weak bonding between the untreated RAP and RAP and VA blends.

On the other hand, all the untreated RCA blends withstand after removing the split mould. This represents the mortar present in the RCA helps in bonding in the RCA blends, representing the RCA's self-cementing property in an agreement with the previous studies carried (Gabr and Cameron 2012; Poon et al. 2006). The strength development of mixes depends on the mix proportion, cement content, and the residual cement present in the existing RCA. In contrast, the asphalt coating of RAP did not contribute to strength development. A linear relationship is observed between different blends' UCS and cement content. The higher RAP presence slows down the strength gain rate, as observed in Figure 4.6. Of these, 25% RAP-75% VA blends show a rapid gain in strength rate. RCA blends have a similar trend in all cases except the 50% RCA - 50% VA blend, which has a higher rate of strength gain. This effect is due to the mortar's presence and better inter-locking between two aggregates and the cement content.

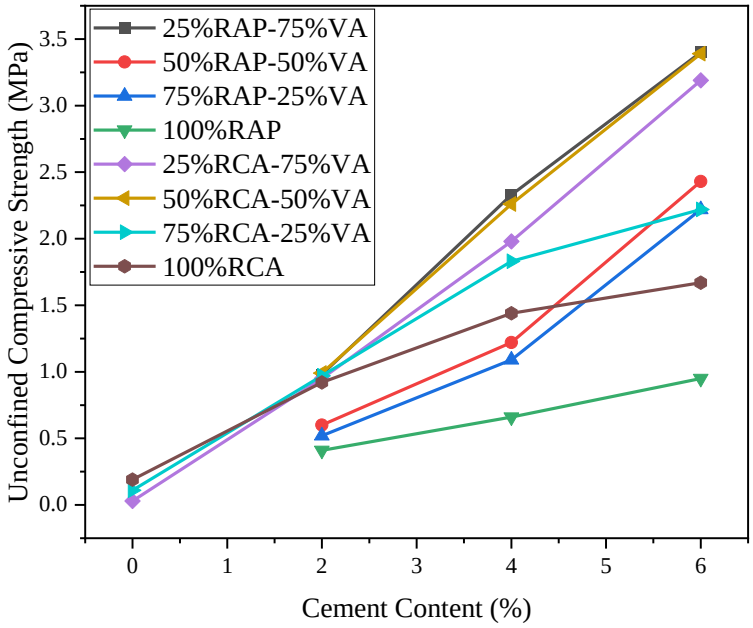

Figure 4.6 Unconfined Compressive Strengths at varying cement percentages

The UCS of various RAP and RCA combinations with VA are tested at 28 days of the curing period to determine the rate of gain in strength. Figures 4.7 and 4.8 show a significant increase in strength with the curing period and cement content. However, there is a decline in the strength with the increase in RAP content in the mix because of an increase in the asphalt coating surface area in the combination. Further, the 50RCA combination has more strength compared to the remaining combinations. After 28 days of curing, 25RAP, 50RAP and VA have nearly UCS of 5 MPa. Similarly, all the RCA combinations have a UCS value near 5 MPa at 28 days of the

curing period, which is the requirement for the base layers for high-volume roads. However, the UCS values of the recycled blends are comparatively equivalent to that of the VA mixes.

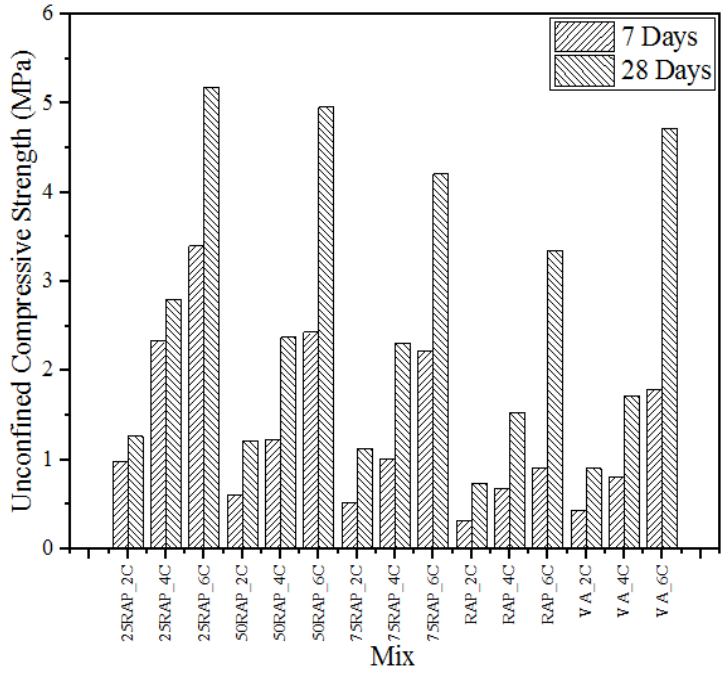

Figure 4.7 Unconfined Compressive Strengths of RAP - VA blends at various curing periods

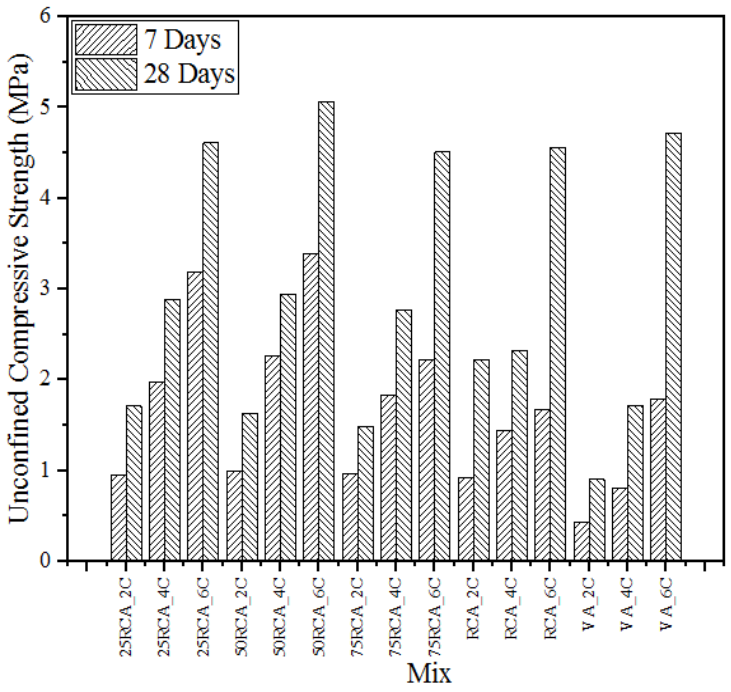

Figure 4.8 Unconfined Compressive Strengths of RCA - VA blends at various curing periods

4.5.2 Indirect Tensile Strength Properties of CTB

Indirect tensile strength is an essential property in pavement analysis. Generally, the tensile strain at the bottom of the bituminous layer is considered for analysis, representing the cement-treated Base's top. Higher the ITS value means the Base is more resistant to tensile stresses. Typical testing is shown in Figure 4.9. The test is carried out on RAP and RCA blends at

different cement contents after curing for 7 days to determine the tensile strength characteristics. The results of the ITS test are shown in Figures 4.10 and 4.11.

a) ITS Testing b) Sample breaking at failure load

Figure 4.9. Typical testing for Indirect Tensile Strength

Figure 4.10 shows that an increase in RAP content led to lower ITS values due to weak bonding between the RAP and conventional aggregates as RAP is coated with asphalt, whereas cement content improves the ITS values. Mix with 25% RAP and 50% RCA with 6% cement content has higher ITS among the different mixes. From Fig. 4.11, RCA blends show more strength compared with RAP blends. 50% RCA blends followed by 25% RCA blends show higher strength than the remaining blends. This is due to proper interlocking between RCA and VA in addition to RCA's self-cementing behaviour.

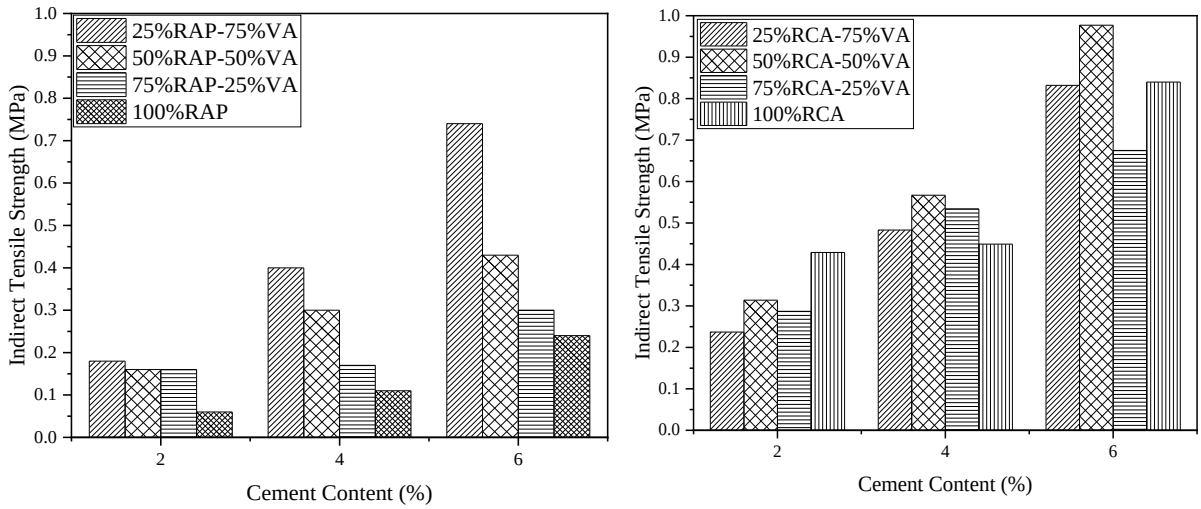

(a) RAP-VA blends (b) RCA-VA blends

Figure 4.10 Indirect Tensile strengths at 7 days of curing period

In contrast, the RAP blended mixes have a weak bond than RCA due to the existing asphalt coating. A similar trend as UCS is observed in the case of ITS, in which the rate of gain in

strength depends on the material proportions. On average, the ITS value is 0.2 times that of the UCS value of RAP treated bases and 0.32 times that of UCS value in the case of RCA treated bases for a 7-day curing period.

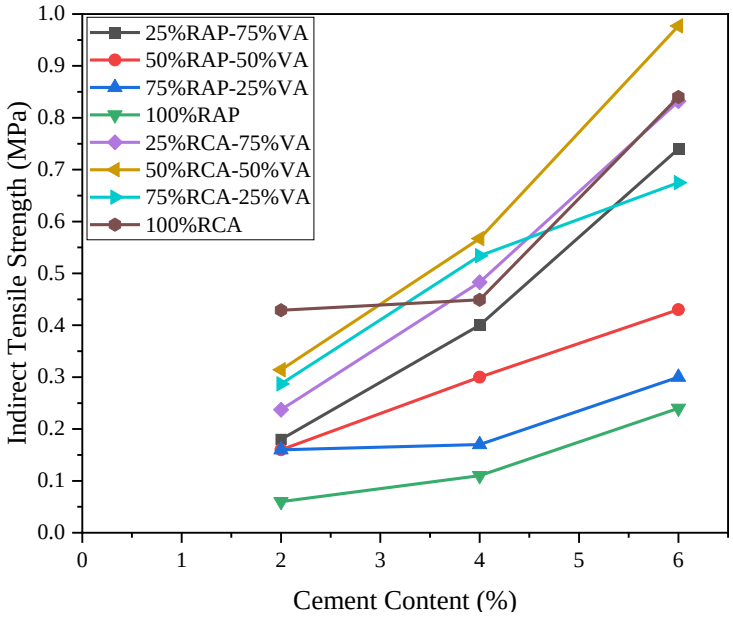

Figure 4.11 Indirect Tensile strengths at varying cement percentages

The ITS is calculated at different curing periods, namely 7, 28, 90, and 140 days as shown in Figure 4.12. The strength rapidly increases during the 28 days of the curing period and remains constant thereafter. The strength at 28 days of curing is nearly 80% of the strength compared with the strength at 140 days. This trend is observed in all the mixtures independent of the RCA content present in the mix. Logarithmic models are best fitted for the variation of ITS with the curing period, as shown in equation (4.1).

$$ITS = a \ln x - b \qquad (4.1)$$

Here, a, b are the coefficients, and x is the curing period in days.

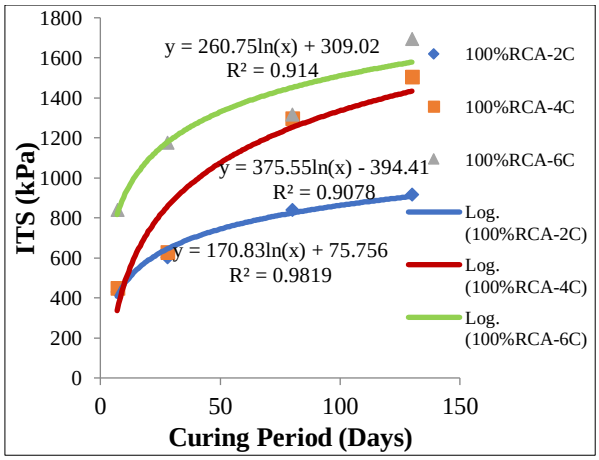

(a) 100%RCA

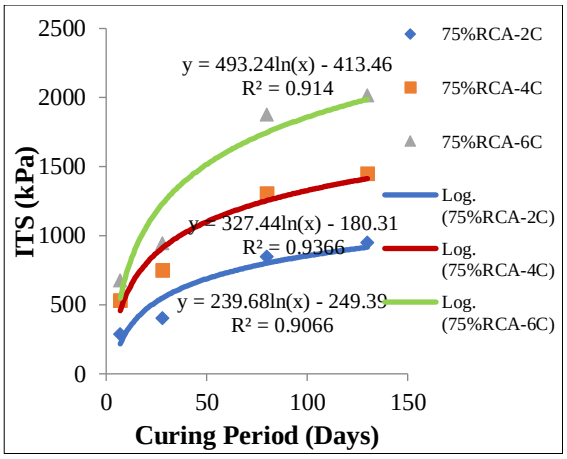

(b) 75%RCA

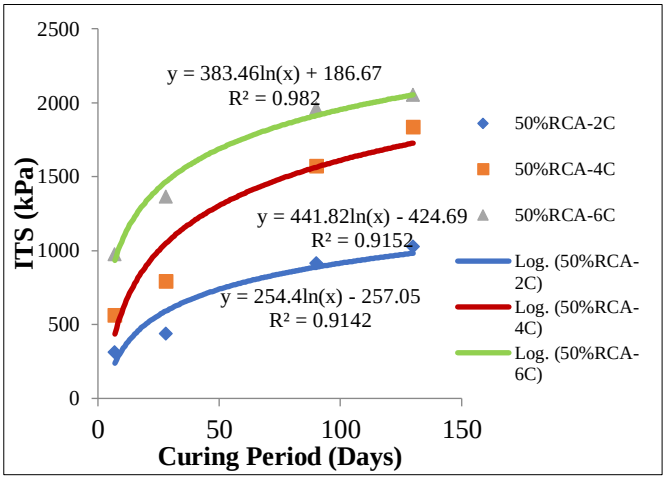

(c) 50%RCA

Figure 4.12 Variation of the ITS with the curing period

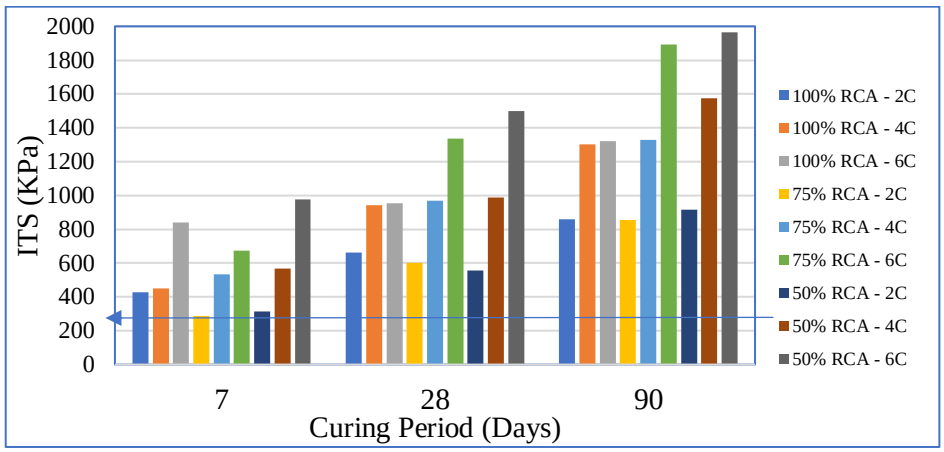

Figure 4.13 Variation of ITS with Cement content, RCA and Curing Period

From Figure 4.13, the ITS is significantly improved with the curing period and cement content. Further, a decrease in the strength with the addition of RCA content is observed in all cement contents. The higher the ITS strength, the more resistance to the tensile stresses.

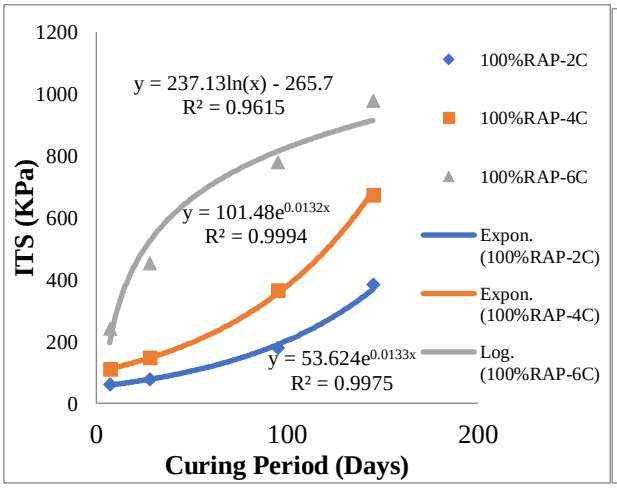

(a) 100%RAP

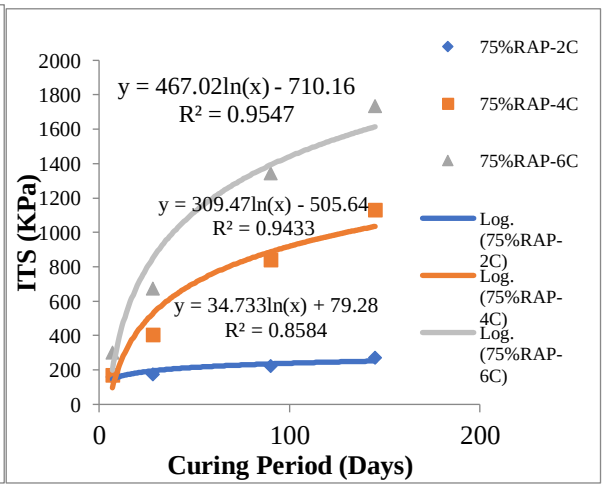

(b) 75%RAP

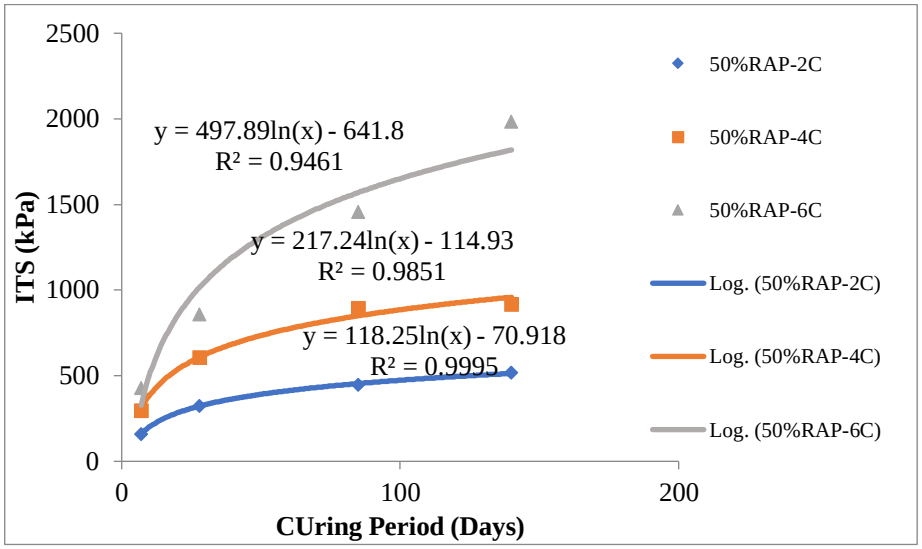

(c) 50% RAP

Figure 4.14 Variation of the ITS with the cement content for RAP blends

From Figure 4.14, it is clear that Logarithmic curves are best fitted for ITS variation even for the RAP-VA blends except for 100% RAP with 2%CC and 4%CC. But some of the RAP mixes show an exponential increase in strength. Figure 4.15 shows the graphical presentation of the ITS comparison of RAP-VA blends.

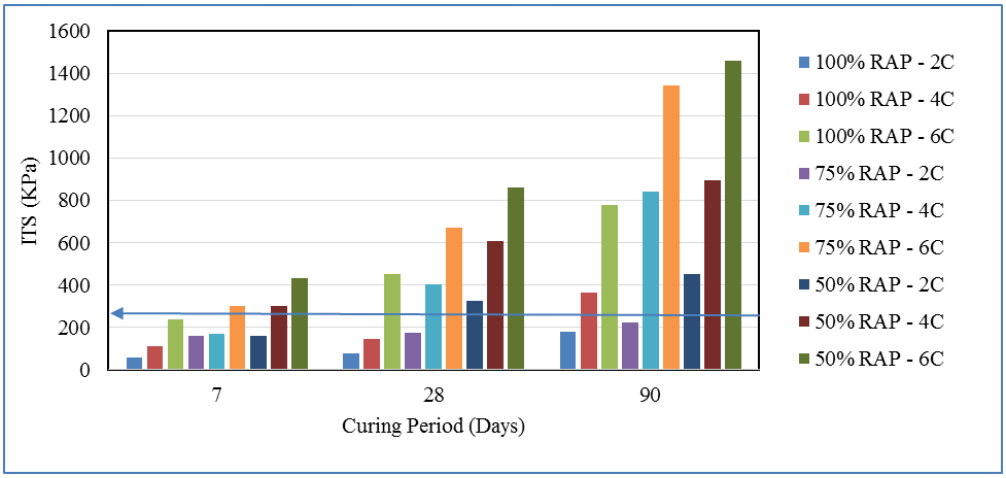

Figure 4.15 Variation of ITS with Cement content, RAP, and Curing Period

From observations, it is evident that the mixes' strength increases with an increase in cement content curing period, and decreases with RAP content in the mix. Multi-linear regression models are developed based on ITS results, as shown in equations 4.2 and 4.3. Three significant distinct variables were considered in the model after checking for their correlation, such as curing period, cement content, and % of VA replaced with RCA or % of VA replaced with RAP. The obtained Adj-R^2value of the model is 0.87 for RCA mixes and 0.79 for RAP mixes.

$$ITS_{RCA} = 7.547 \times CP + 181.527 \times CC - 1.867 \times RCA - 0.605 \quad (4.2)$$

$$ITS_{RAP} = 5.236 \times CP + 171.940 \times CC - 7.836 \times RAP + 125.79 \quad (4.3)$$

4.5.3 Resilient Modulus Characteristics of CTB

The Resilient Modulus is calculated using an Indirect Tensile Resilient Modulus Test setup where cylindrical samples of diameter 100 mm and thickness of around 65 ± 2 mm were used to calculate the M_R. The test is carried out according to the ASTM D 7369.

Sample calculation of M_R for 100% RCA with a sample thickness of 66 mm on one plane using equation 3.4 is shown below. The applied repeated load is 157.258 kg taken from the failure load (10-20%), the Poisson's ratio (μ) is assumed as 0.25 for cement-treated bases. Out of the total 150 cycles, the first 100 cycles are used for conditioning the sample, and any 5 cycles from the last 50 cycles are considered for the analysis. There are two LVDTs on either side of the specimens to measure the horizontal deformation. The measured resilient deformations from the two LVDTs were added up to get the total resilient deformation ΔH. The resilient deformation from one LVDT is shown in Figure 4.16, equal to 0.0111 (0.0279-0.0168). Similarly, from the other LVDT, the resilient deformation is 0.0295.

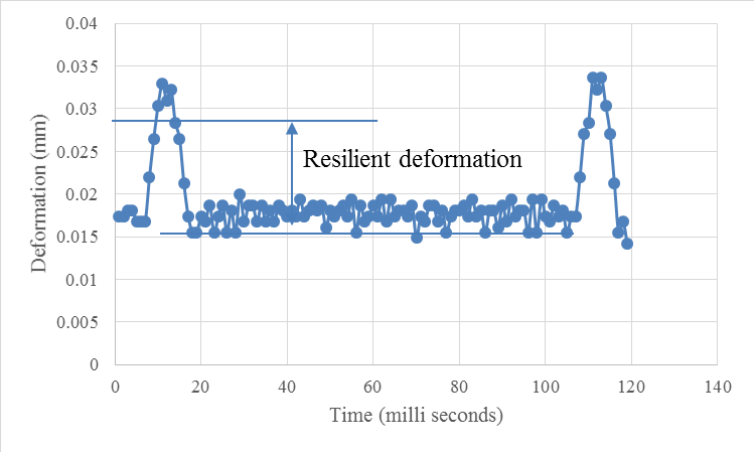

Figure 4.16 Typical deformation pulse diagram

Calculate the M_R using equation 3.4 as follows:

$$M_R = \frac{P(\mu + 0.27)}{\Delta H \times t}$$

$$= \frac{157.258 \times 9.81(0.25 + 0.27)}{(0.0111 + 0.0295) \times 66}$$

$$= 299.37 \text{ MPa}$$

Average of the last five cycles M_R are taken. The average is taken as the final MR value for the corresponding mix type. Likewise, there are two planes in a perpendicular direction for each sample with a repeatability of 3. Total 6 M_R values are calculated.

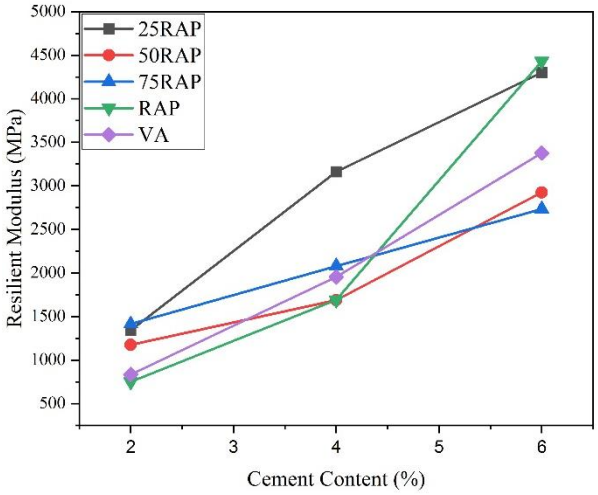

a) Variation of M_R with Cement Content

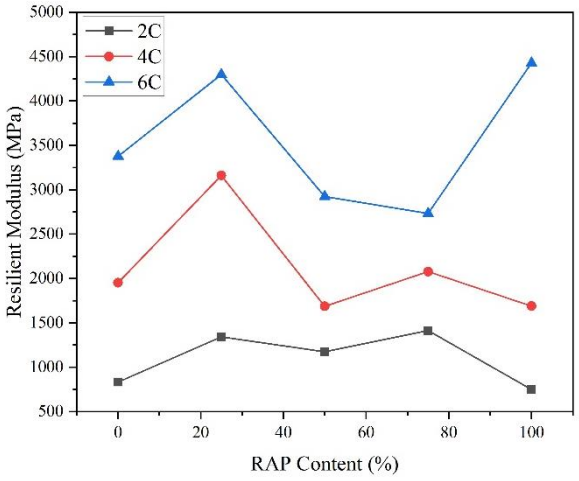

b) Variation of M_R with RAP Content

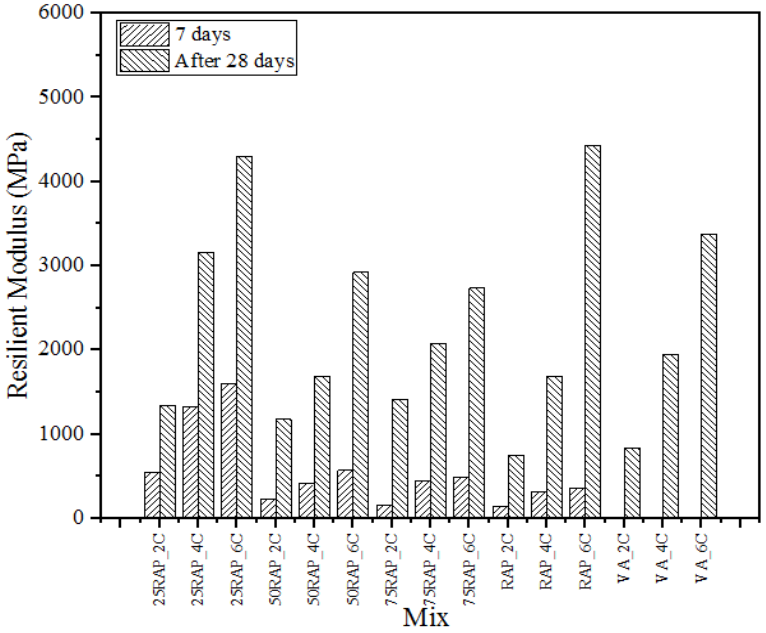

c) M_R results at various curing periods

Figure 4.17. Resilient Modulus of RAP-VA mixes

The experimental results of different mixes are shown in Figures 4.17 and 4.18. There is a noticeable increase in the modulus values with the curing period. Further, there is a decline in the M_R with the inclusion of the RAP content upto in the mix at 2% and 4% cement contents as shown in Figure 4.17 b. However, at 6% cement content, 100%RAP shows highest strength . At the same time, 100% RCA alone exhibits highest M_R because of the self cementing properties of the RCA. The modulus values from the Indirect Tensile resilient modulus test are higher than the plate load test, compression modulus testing, and RLT testing (Behiry 2013; Hou et al. 2019; Yan et al. 2020; Arulrajah et al. 2015). Further, the M_R testing from the Indirect Tensile mode is more straightforward and measures the stiffness of the cylindrical cores obtained from the field. Additionally, it is challenging to extract beam cores from the field.

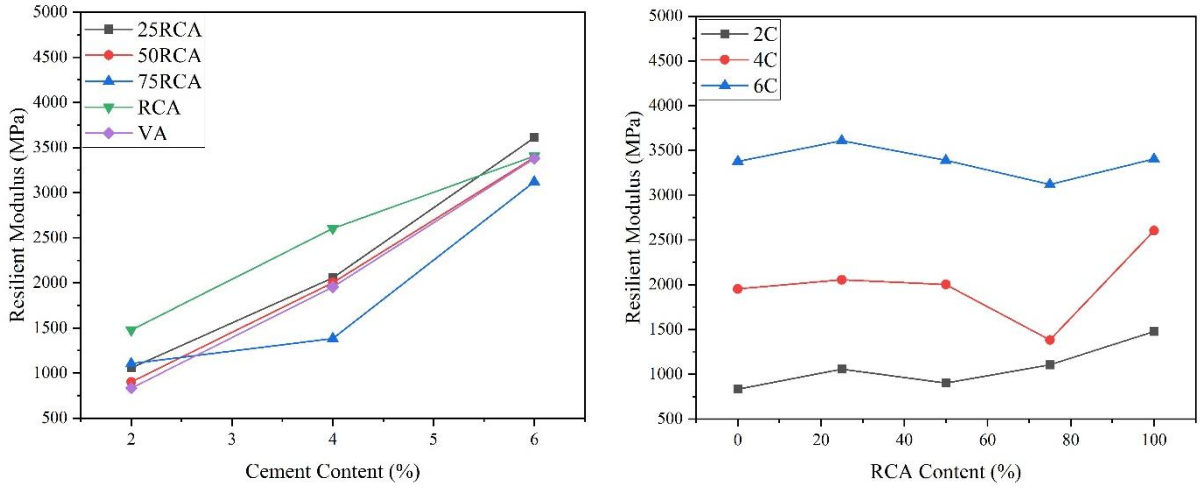

a) Variation of M_R with Cement Content b) Variation of M_R with RCA Content

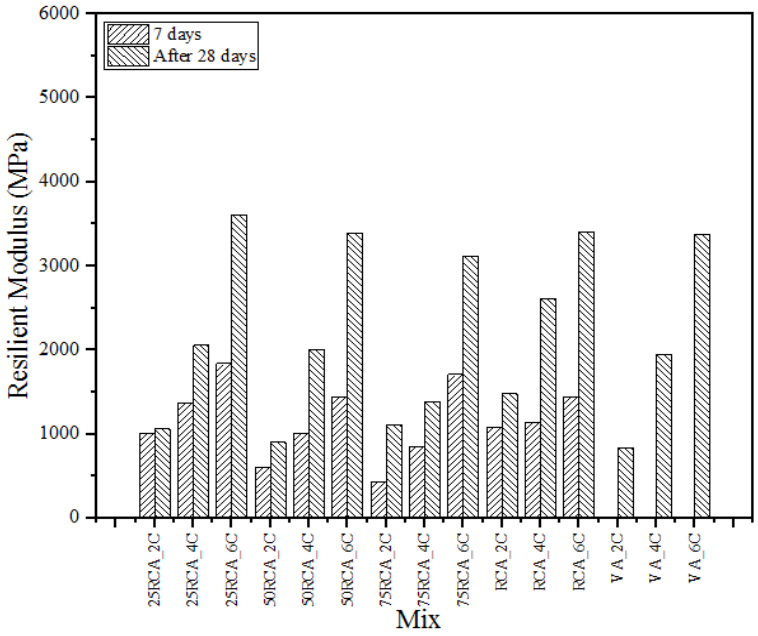

a) M_R results at various curing periods

Figure 4.18. Resilient Modulus of RCA-VA mixes

The modulus values at 6% cement content are around 3500 MPa from the laboratory testing. According to the specification limitations, the recommended modulus value is 5000 MPa after 28 days of curing (IRC 37, 2018). However, the M_R values with respect to the recycled aggregate combinations are comparatively equal or more than that of the VA. Nevertheless, the obtained values did not reach the specified limits. The test method and techniques might differ in the modulus values.

In contrast, the modulus values from the empirical equations are close to 5000 MPa. A linear relationship is established between UCS and M_R from the obtained results of various blends, as shown in Figures 4.19 and 4.20. It is found that the two parameters are well correlated, and the following equation is established.

$$M_R = 658.17UCS \pm 105.27 \quad (4.4)$$

$$M_R = 736.71UCS \pm 2.20 \quad (4.5)$$

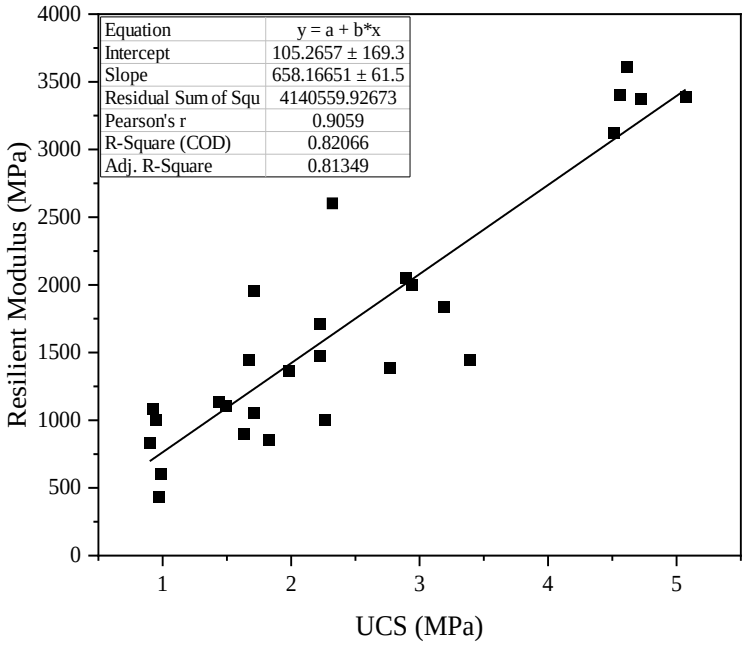

Figure 4.19. Relation between Resilient Modulus and UCS for RCA blends

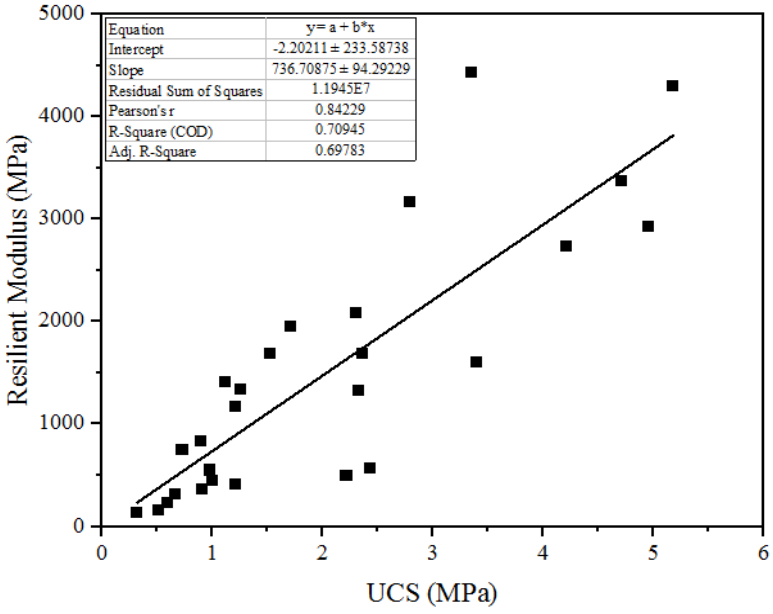

Figure 4.20. Relation between Resilient Modulus and UCS for RAP blends

4.5.4 Fatigue Evaluation of CTB

Fatigue evaluation is carried out on the CTB at three different stress levels to determine the fatigue life of the different recycled aggregate combinations and to observe the sensitivity towards different stabilization levels. For fatigue evaluation, each sample is subjected to a repeated load, and the fatigue life is considered when the complete failure of the sample takes place. A typical failure pattern in terms of the deformation of a specimen is shown in Figure

4.21. In the experimental study, the applied stress ratios are more than 0.55 because cemented specimens generally possess three fatigue curves for stress ratios less than 0.45 which has infinite fatigue life; for stress ratios between 0.45-0.55 and the stress ratios greater than 0.55, which have different fatigue equations.

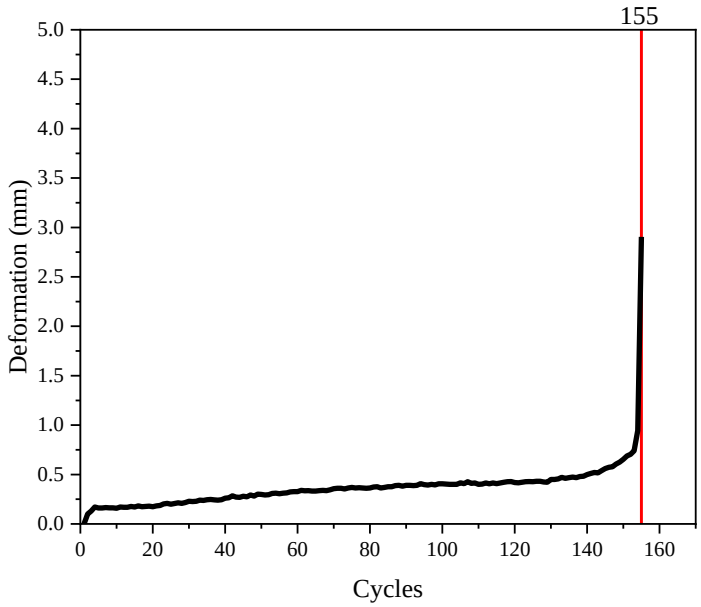

Figure 4.21 Typical failure of 25%RAP specimen at 85% stress level

From Figure 4.21, a repeated load is applied at a stress level of 85%, which is 85% of the failure load applied on a 25% RAP specimen stabilized with 4% cement. Three regions were observed from the curve. Initially, the deformation is gradually increased, which is the primary region. It slows down and exhibits a straight line with some slope in the secondary region. Finally, the slope changes in the tertiary region, the deformation progresses faster, and the sample breaks. When the sample breaks, the number of cycles was noted as 155, which is the fatigue life of the specimen at the corresponding stress level. This can also be explained that the fracture in the specimens starts at the loading plane and grow slowly along the diametrical loading plane. It is the failure process where the specimen begins to decay physically and mechanically such that no longer it can bear the loads. This is due to the accumulation of the damage internally through micro-cracks developing into a large crack which is caused due to a series of load cycles that exceeds the acceptable limits.

All the samples were cured for 90 days before the commencement of the fatigue testing. From Figure. 4.22, on the *x*-axis, the stress ratio is represented, which is the ratio of the applied stress to the tensile strength; on the *y*-axis, the number of cycles to failure is presented. Figure 4.22 shows fatigue curves for RAP-VA combinations at 6% cement content. It is observed that the fatigue life decreases with the increase in stress ratio. Commonly, higher stress ratios have lower fatigue life. Further, the fatigue life of the 25RAP mix is higher compared with VA and

other mix combinations because of the better interlocking between the RAP and VA in the mix. In the case of RCA-VA mixes, a similar trend of 25RCA mix has higher fatigue life than the remaining mixes, shown in Figure 4.23. After 25RAP or 25RCA combinations, VA mixes performed better in fatigue life. The fatigue life of the RAP mix is significantly low compared with other mixes. And also, the fatigue life declines with the addition of the RAP into the bases, as in agreement with the previous studies done with flexural fatigue testing (de Paiva et al., 2017).

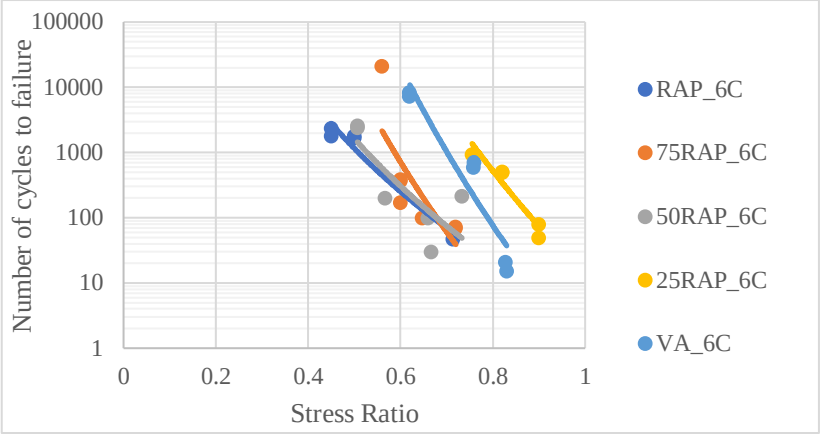

Figure 4.22 Fatigue life of RAP-VA mixes at 6% cement content

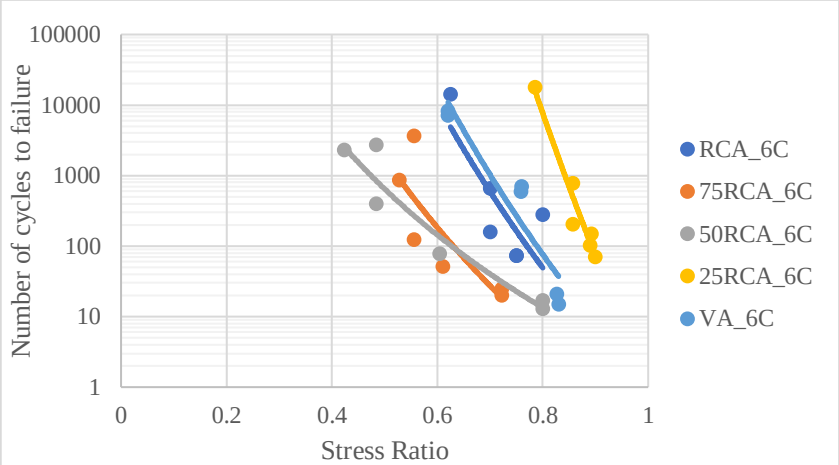

Figure 4.23 Fatigue life of RCA-VA mixes at 6% cement content

Similarly, fatigue characteristics were determined for all the combinations at different stabilization levels. From Figures 4.24 to 4.27, it is evident that the fatigue life increases with the increase in the cement content in the mix. The RAP content in the mix significantly increases the ductile nature. Further, the steepness of the curves represents the brittle nature.

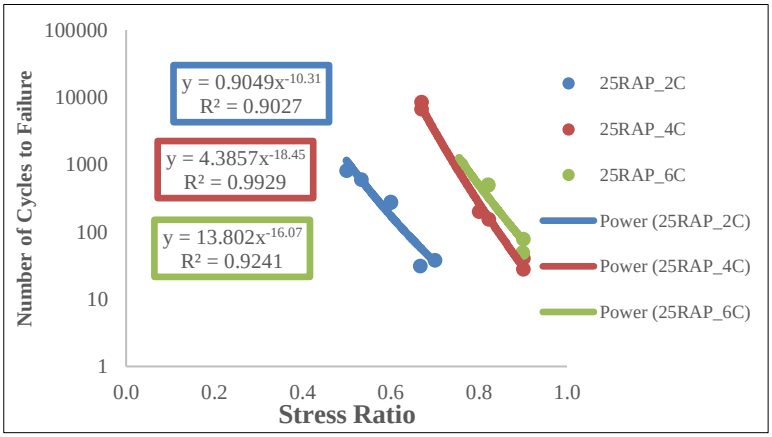

Figure 4.24 Fatigue life of 25RAP mix at various cement contents

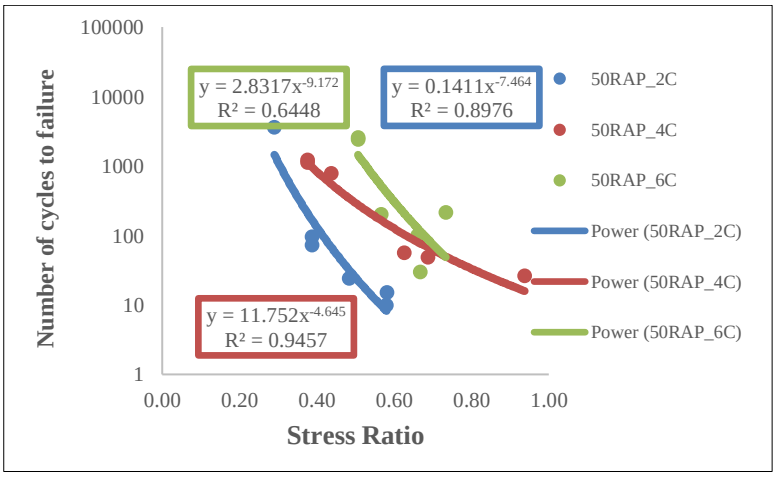

Figure 4.25 Fatigue life of 50RAP mix at various cement contents

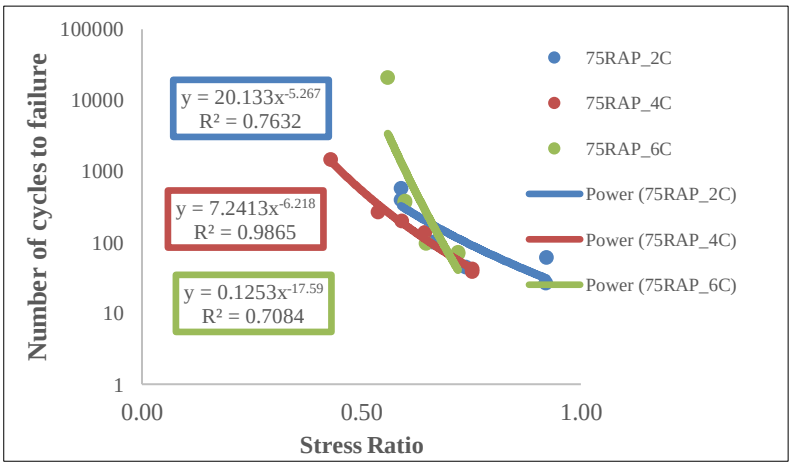

Figure 4.26 Fatigue life of 75RAP mix at various cement contents

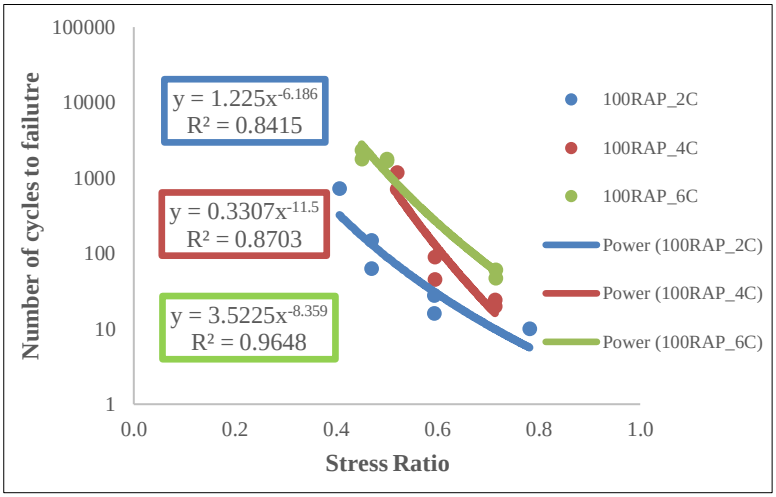

Figure 4.27 Fatigue life of RAP mix at various cement contents

Similarly, the fatigue curves were drawn for RCA-VA blends at various stabilization levels. Exponential relationship is well fitted between the stress ratio and the number of cycles to failure. Similarly, the studies were done by Fedrigo et al. 2018, Lv et al. 2019, Lv et al. 2018 used exponential relationships to relate the stress ratio and the fatigue life of cement-treated bases. From Figures 4.28 to 4.31, it is evident that the RCA content present in the mixes dominates the fatigue life rather than cement content at more than 50% of RCA in the mix. At 100% RCA at lower cement content (2%), the fatigue life is not well distinguished with respect to the stress levels because of the domination of heterogeneous nature at higher RCA content. However, these differences are eliminated at more than 2% of cement contents. Further, it was evident that the increase in cement content improved the fatigue life of the mixes.

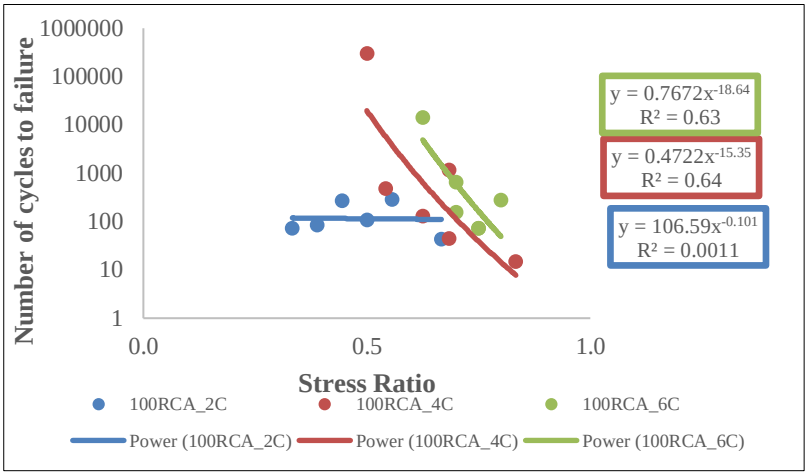

Figure 4.28 Fatigue life of RCA mix at various cement contents

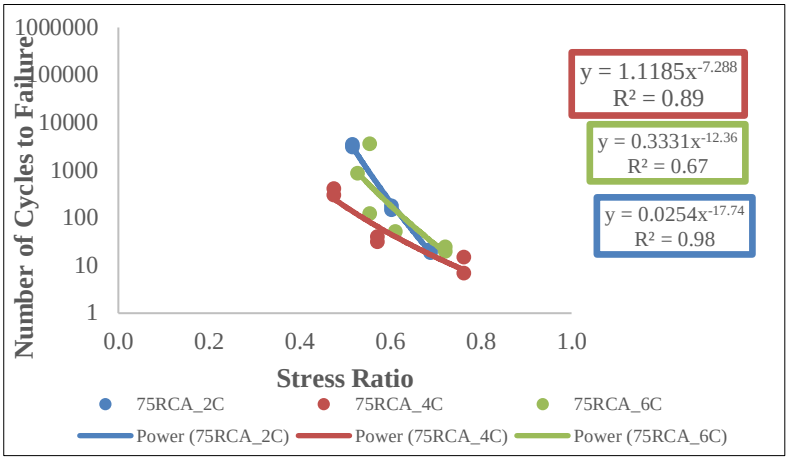

Figure 4.29 Fatigue life of 75RCA mix at various cement contents

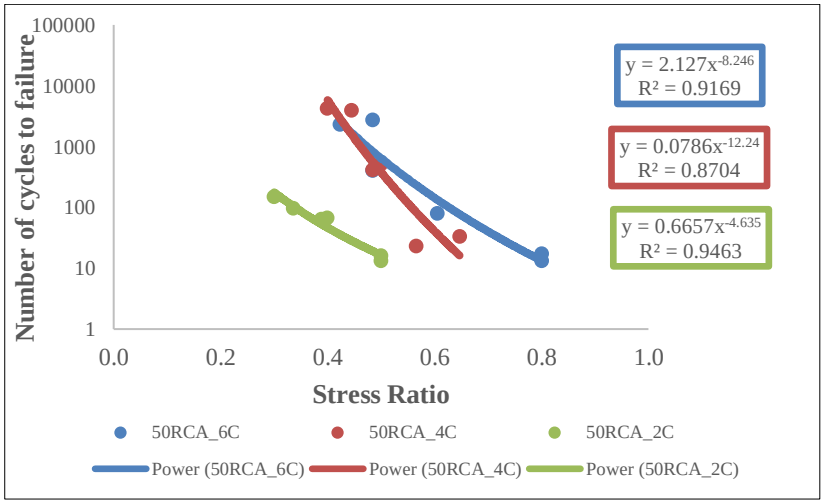

Figure 4.30 Fatigue life of 50RCA mix at various cement contents

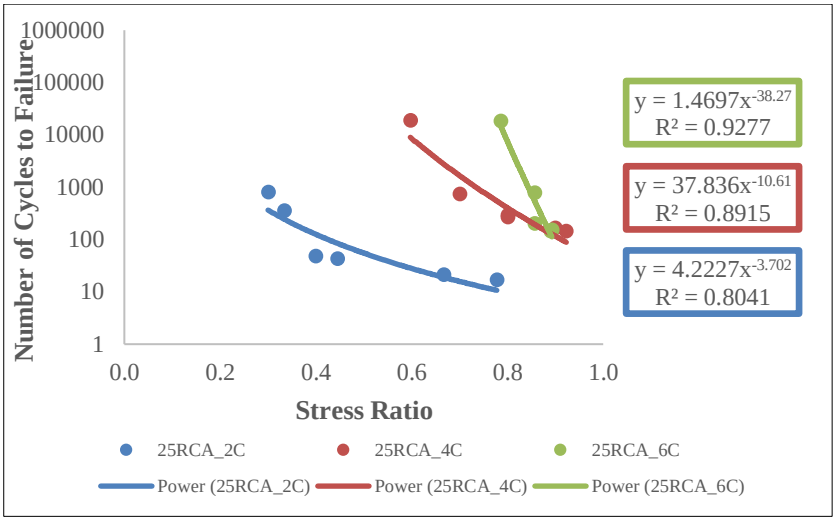

Figure 4.31 Fatigue life of 25RCA mix at various cement contents

4.6 Summary

The preliminary CTB mixes prepared with recycled aggregates (RAP & RCA) and VA combination reported the following trends and the overall performance of the CTBs with different combinations of recycled aggregates are shown in APPENDIX A.

- From physical characteristics, it is observed that RAP has higher combined flakiness and elongation index and the RCA has higher water absorption than the specification limits. The compaction characteristics show a decrease in the MDD and OMC with the addition of RAP content in the mix, whereas the MDD is increased with cement content. In the case of RCA mixes, no specific trend is observed in OMC and MDD.
- The UCS of the CTB decreases with the RAP content and increases with the cement content. In cases of CTB with RCA, at 50%RCA content has more strength than other combinations. Similar trends were observed in the case of ITS results.
- RAP and RCA bases require more than 6% of cement content or 28 days of curing periods to serve as pavement bases according to Indian specifications.
- The rate of gain in strength for stabilized RCA is more than that of RAP and VA due to self-cementing properties. The apparent increase in strength of bases is observed up to 90 days of the curing period.
- The 28day strength is 70 to 80% of the 140-days strength in VA-RCA bases and 50 to 60% of the 140-day strength in VA-RAP bases.
- The stiffness of the CTB is significantly increased with the curing period. However, the obtained values are typically less than the specification limitations.
- Differences in fatigue life are observed in RCA CTB mixes at lower stabilization levels. Higher fatigue life and brittleness are kept at higher cement contents and lower RAP contents. Ductile nature is increased with RAP content in the mix.

CHAPTER 5

LABORATORY INVESTIGATION OF EATB

5.1 General

In the previous chapter, a laboratory performance evaluation of CTB was carried out. In this chapter, the performance evaluation of the EATB is carried and the results are presented along with the specifications limitations. This chapter includes gradation requirements, mix design, and laboratory performance tests. The laboratory performance tests include ITS, Dynamic creep rutting, M_R, and fatigue evaluation.

5.2 Properties of Emulsified Asphalt

Cationic Slow Setting (CSS-2) emulsified asphalt is evaluated for the properties according to the IS 8887: 2018 specifications presented in Table 5.1.

Table 5.1 Properties of CSS-2

Test	Permissible Values	Obtained Result	Test Method
Residue on 0.6 mm IS Sieve, % by mass, Max	0.05	0.02	IS 8887: 2018
Viscosity (Say bolt furol viscometer), seconds, (at 25°C)	30-100	31.0	IS 3117: 2004
Storage stability (24 h), %, Max	2.0	0.62	IS 8887: 2018
Particle charge	Positive	Positive	IS 8887: 2018
Stability to mix with cement (% coagulation), Max	2.0	1.84	IS 1203: 1978
Residue by evaporation (%), Min	60.0	62.66	IS8887: 2018
Penetration 25°C/ 100g/ 5 sec	60-120	67.0	IS1208: 1978
Ductility,27 °C/cm, Min	50.0	60.0	IS8887: 2018

5.3 Gradation and Blending of RAP and RCA with Virgin Aggregates

Three different mixes were prepared using RAP which was partially replaced with VA in the ratio of 1:1, 1:3 and 3:1 (RAP-50, RAP-25, RAP-75) contents, representing the depth of milling or replacement. The gradation curves for different stacks of VA and RAP with the corresponding Nominal Maximum Aggregate Size (NMAS) and RAP blends are shown in Figure 5.1. All the mixes fall within the upper and lower limits of the Asphalt Academy 2009 specifications.

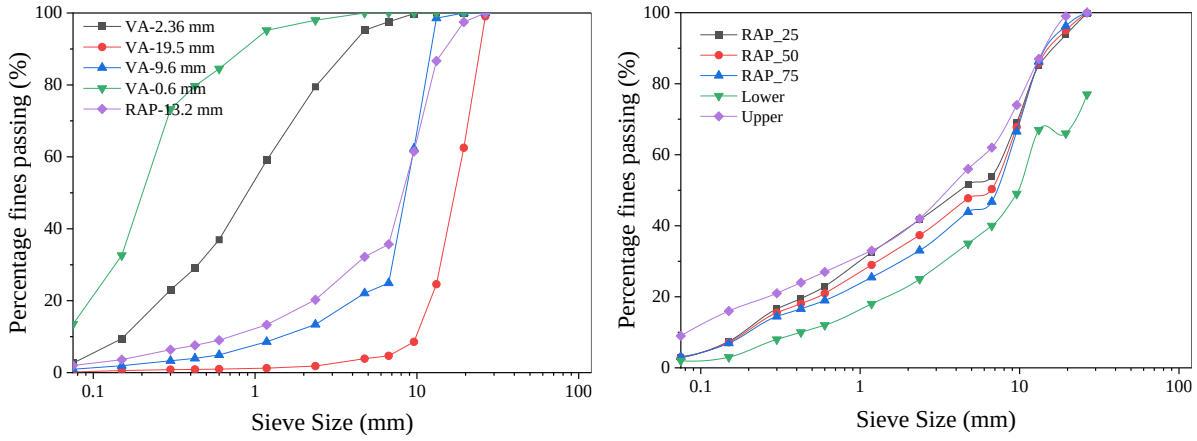

(a) Different Stacks of VA and RAP **(b)** Blended RAP mixes

Figure 5.1 Gradation curves of EATB RAP mixes with lower and upper limits of AA-2009

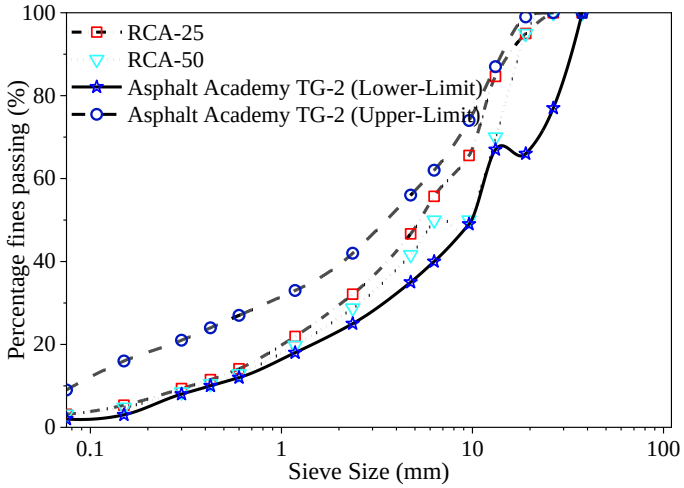

Figure 5.2 Comparison of RCA-VA blended curves with lower and upper limits of AA-2009

Similarly, RCA-VA combinations are blended up to 50% of the replacement of VA. The obtained blends fall within the specifications of Asphalt academy TG-2, as shown in Figure 5.2.

5.4 Mix Design of EATB

Three different mixes were prepared using RAP replaced with VA in the ratio of 1:1, 1:3, and 3:1, i.e., 50%, 25%, and 75% RAP (RAP-50, RAP-25, RAP-75) contents. Similarly, RCA is replaced with VA in the ratio of 1:1 and 1:3, i.e., 50% RCA and 25%RCA (RCA-25 and RCA-50), respectively. A homogeneous mixture was prepared with calculated quantities of dry aggregates and cement. Based on the previous research, around 2% cement is selected as an additive, which helps break the emulsified asphalt. Adding 1-2% of cement to the EATB mixes is useful in forming a homogeneous mixture (MS-19 1997). Next, the amount of pre-wetting water was selected based on the minimum degree of coating, i.e., 50% coating (MS-19 1997). Pre-wetting water was added to the mix, and the degree of the coating was observed visibly to confirm more than 50% coating of the asphalt emulsion (MS-19 1997). Around, 2.5%, 2.5%, and 1.5% of pre-wetting water content were obtained for 25%, 50%, and 75% of RAP mixes.

Next, specimens of size 100 mm diameter and 63 ± 2 mm height were prepared using the Marshall method of compaction with 75 blows on each side. The prepared samples were cured for 72 hours 40°C in a hot air oven, representing a field curing of 30 days (Asphalt Academy TG-2 2009). The specimens were demoulded after one day of curing as samples were weak initially after the preparation.

The preparation of specimens involved optimizing pre-wetting water and emulsified asphalt content in the mix. After mixing 2% cement with the aggregate mixture, the pre-wetting water is added to the mix. The emulsified asphalt content is varied at an interval of 0.5% weight of the dry aggregate and tested for the ITS properties. The IEAC is determined based on the equation given in IRC: SP: 100-2014, which depends on the mix final gradation from equation 3.1 and the TEAC is determined using equation 3.2.

The mix design of EATB involves the preparation of samples using the Marshall Method of compaction, followed by the determination of OEAC at which the mix achieves maximum strength (ITS). Samples were prepared for different Emulsified Asphalt contents in the range of 4.5% to 7% by dry weight of the aggregates at an interval of 0.5%. Three representative samples were prepared for each emulsified asphalt content to ensure the repeatability of the test results. Each sample was compacted and cured. After curing, the samples were allowed to cool to room temperature (25 ± 2°C) before testing for ITS. The variation of ITS with emulsified asphalt content for mixes with different RAP contents is shown in Figures 5.3, 5.4 and 5.5.

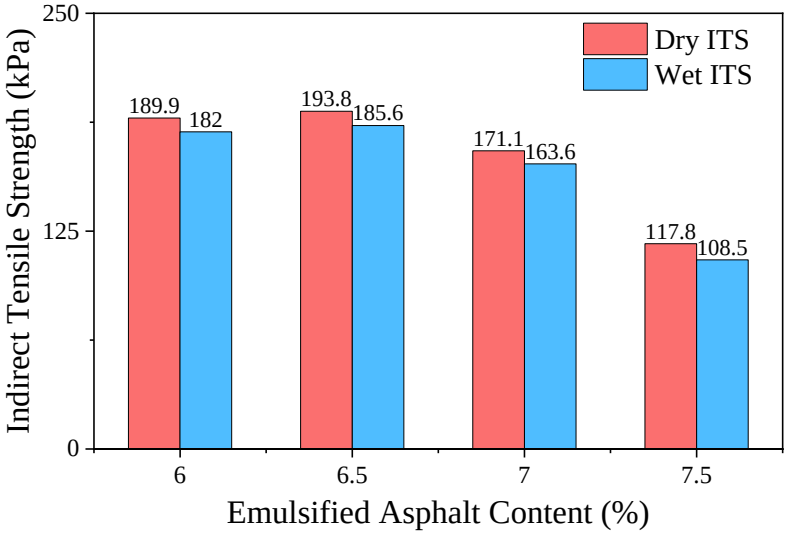

Figure 5.3 ITS results of EATB for RAP-25

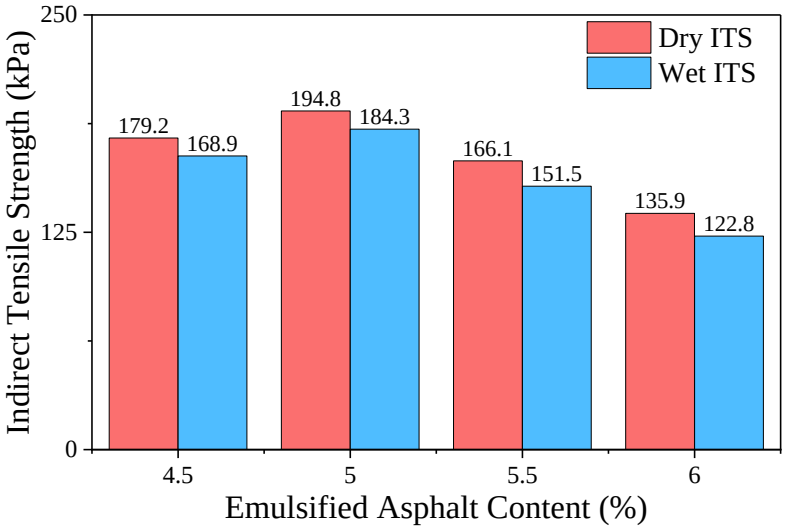

Figure 5.4 ITS results of EATB for RAP-50

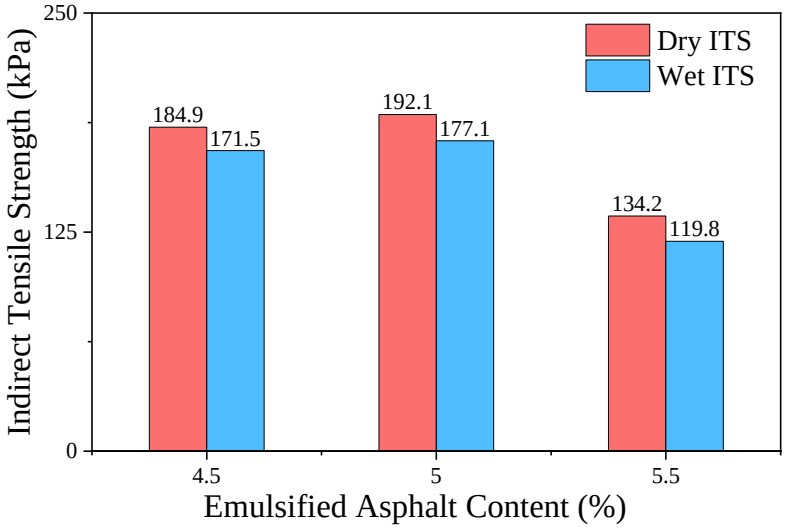

Figure 5.5 ITS results of EATB for RAP-75

From the observations of Figures 5.3, 5.4, and 5.5, it is evident that the obtained ITS values are less than 225 kPa for 100 mm diameter specimens. For a stabilized base layer, the dry ITS value should be greater than 225 kPa (IRC 37: 2018). This value is not achieved immediately after 3 days of accelerated curing, representing nearly 30 days of field curing. However, the base gained the required strength for 60 and 90 days long curing periods, as shown in Figure 5.6. The mix of 75RAP-H did not achieve the minimum ITS because of the higher amount of residual asphalt content.

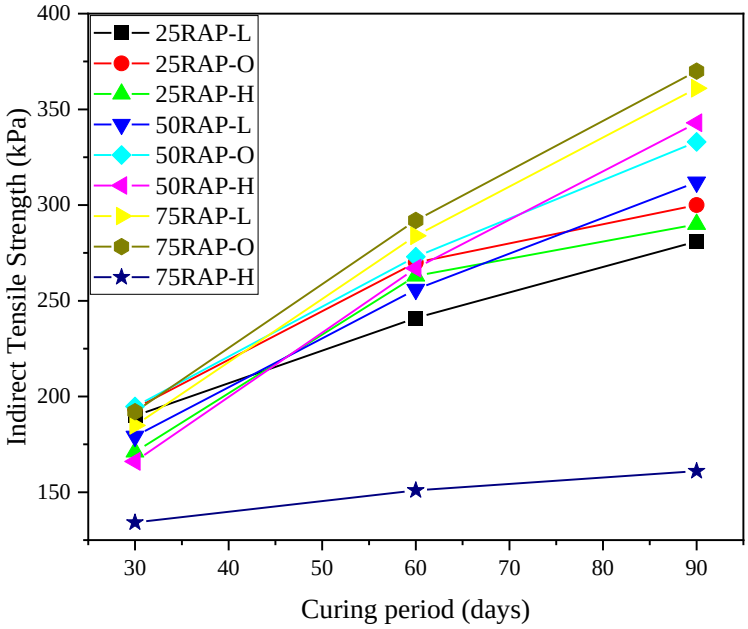

Figure 5.6 Variation of ITS of EATB with curing period

The maximum dry-ITS is achieved at 6.5%, 5%, and 5% of emulsified asphalt content for the RAP-25, RAP-50 and RAP-75 mix. The emulsified asphalt content corresponding to the maximum strength achieved is OEAC. The OEAC is different for different RAP contents because the asphalt absorption varies with the presence of VA. Further, RAP does not act simply as a normal aggregate, and there is a possibility of rejuvenating aged binder present in the RAP with asphalt emulsion. The variation in the maximum dry-ITS values corresponding to OEAC is shown in Figure 5.7. The variation in dry-ITS is significantly small compared to the variation in RAP content from 25% to 75% at the corresponding OEAC values. Maximum dry-ITS is achieved at 50%RAP content due to its good packing density compared with other mixes. The variation of Optimum Total Fluid Content (OTFC), OEAC, and Optimum Residual Binder Content (ORBC) with RAP content are depicted in Figure 5.8. It was observed that the required OTFC decreased as the RAP content increased from 25% to 75%. The OTFC values were 9%, 7.5%, and 6.5% for 25%, 50%, and 75% RAP mixes, respectively. The decrease in total fluid content with the increase in RAP content is due to the increase in the aggregate surface area of RAP. RAP aggregates have less water absorption due to asphalt coating; VA absorbs water and binder initially on its surface. The broken specimens were observed after the ITS test, as shown in Figure 5.9. It was evident that the failure of the sample was along with the bonding interface, and the samples were completely cured with no free moisture.

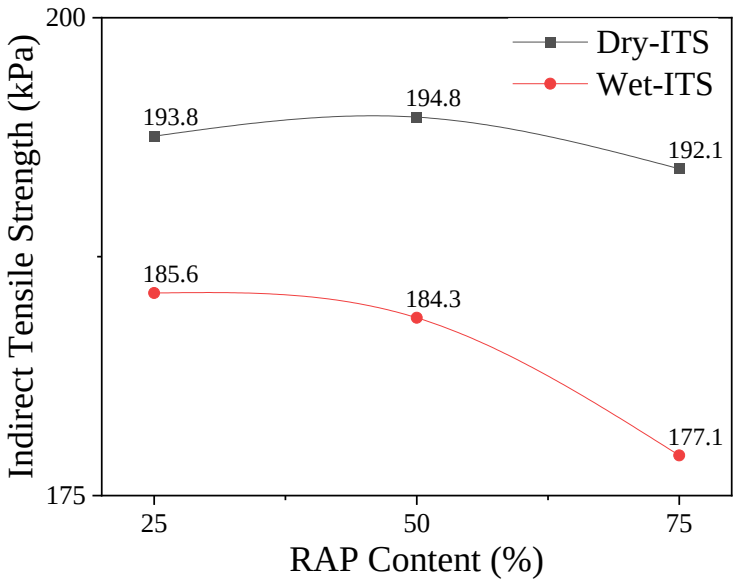

Figure 5.7 Variation of ITS with RAP content at OEAC

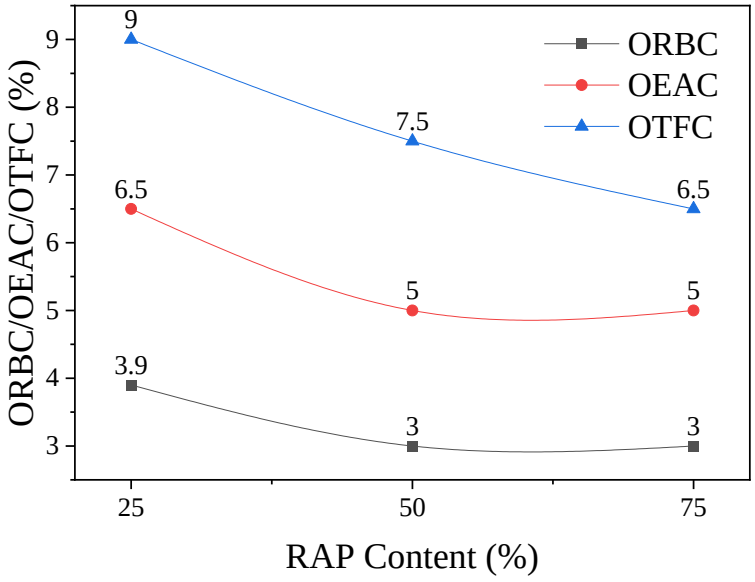

Figure 5.8 Variation of ORBC/OEAC/OTFC with RAP content

Figure 5.9 Failure patterns of RAP blends

In the case of RCA mixes, the failure pattern and the aggregate interface due to the breaking of RCA are commonly observed in Figure 5.10. It is important to note that even if the EATBs are prepared with the same amount of the pre-wetting water content and emulsified asphalt, the 25%RCA mixes possess greater ITS (203.1 kPa) as compared to that (168.4 kPa) of EATB with 50% RCA corresponding to the OEAC as shown in Figure 5.11 and 5.12. This is a commonly expected finding indicating that the EATBs with lower RCA content develop high tensile strength properties. The results showed that the values of dry-ITS lie in the range of 111.9 kPa and 203.2 kPa for EATBs with RCA, while the range is 72.4 kPa to 165.5 kPa for wet-ITS as shown in Figures 5.11 and 5.12.

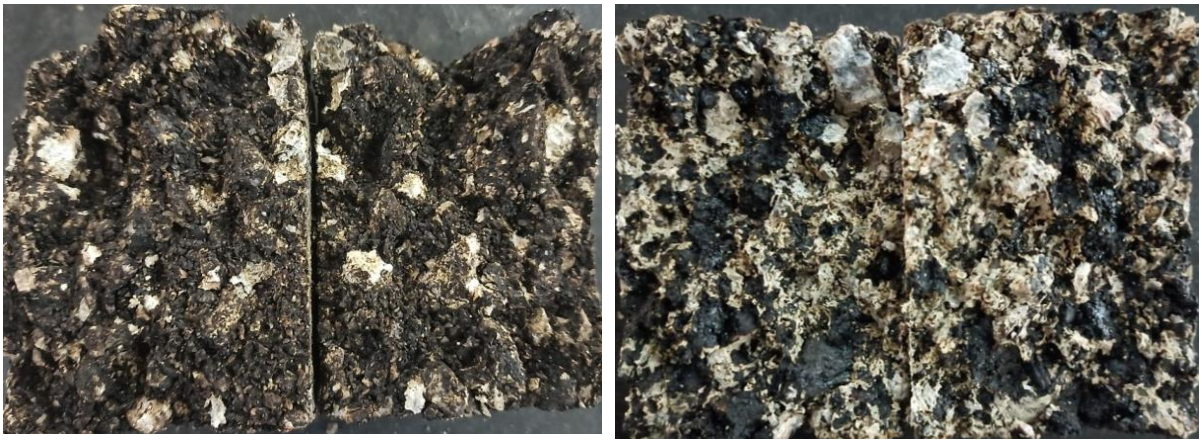

A **B**

Figure 5.10 Failure pattern of a) RCA-25 b) RCA-50

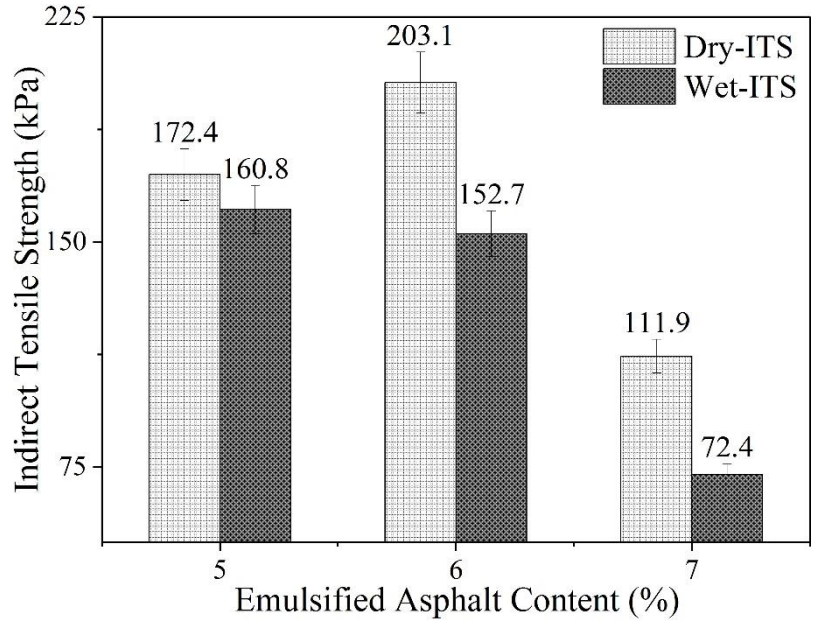

Figure 5.11 Dry and Wet ITS values of EATB with 25% RCA

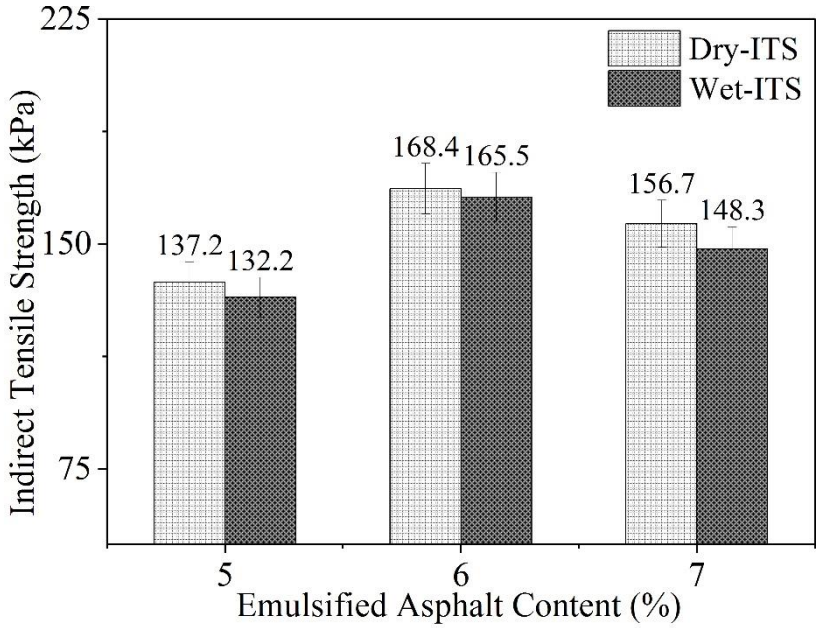

Figure 5.12 Dry and Wet ITS values of EATB with 50% RCA

5.5 Density and Water Loss Variation in EATB

To understand the early strength properties, it is necessary to determine the continuous moisture evaporation in EATB. To construct a layer over the base course with EATB, achieving a moisture content of around 1-2% is necessary. To achieve the required field moisture content, it is also necessary to monitor moisture loss dynamics. To understand the density variation with mix proportions and emulsified asphalt, each sampling density is measured after curing for 72 hours. The percentage of water loss was calculated by measuring the weight at regular intervals (0, 24, 48, and 72 h) during the three days of the curing period. The difference in weights of the

sample at respective time intervals will give the percentage of water loss, which is calculated using equation 5.1.

$$\%Water\ loss = \frac{W_{initial} - W_{final}}{W_{initial}} \times 100 \qquad (5.1)$$

Here, $W_{initial}$ the sample's initial weight after compaction W_{final} is the weight of the sample after curing.

The dry density of cold emulsified asphalt mixes depends on the emulsified asphalt, RAP content, the amount of natural aggregate, and their packing density within the mixes. The dry densities of the RAP-50 and RAP-25 mixes are more significant than that of the RAP-75, where good compaction is achieved, as shown in Figure 5.13.

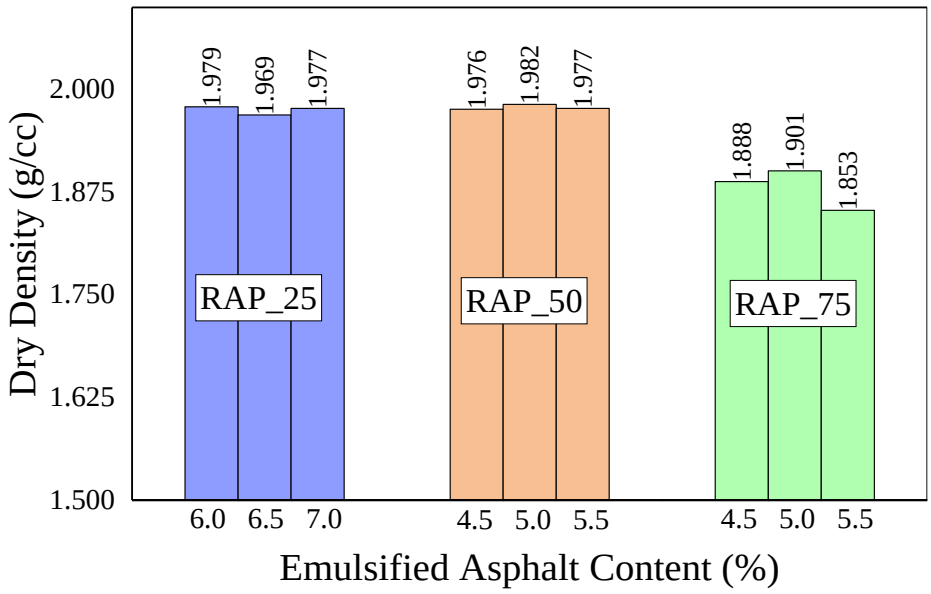

Figure 5.13 Variation of density with Emulsified Asphalt Content

The dynamics of moisture loss depend entirely on the composition of the aggregates, cement, water, and asphalt emulsion. In general, the curing rate is measured in terms of the percentage of water loss. The percentage of water loss considering the curing time for each sample is presented in Figure 5.14. The results indicate that the maximum curing rate was observed in the first 24 hours and gradually decreased later. The same trend is found in all the mixes. The reaction rate decreases with an increase in the percentage of RAP in the mixes.

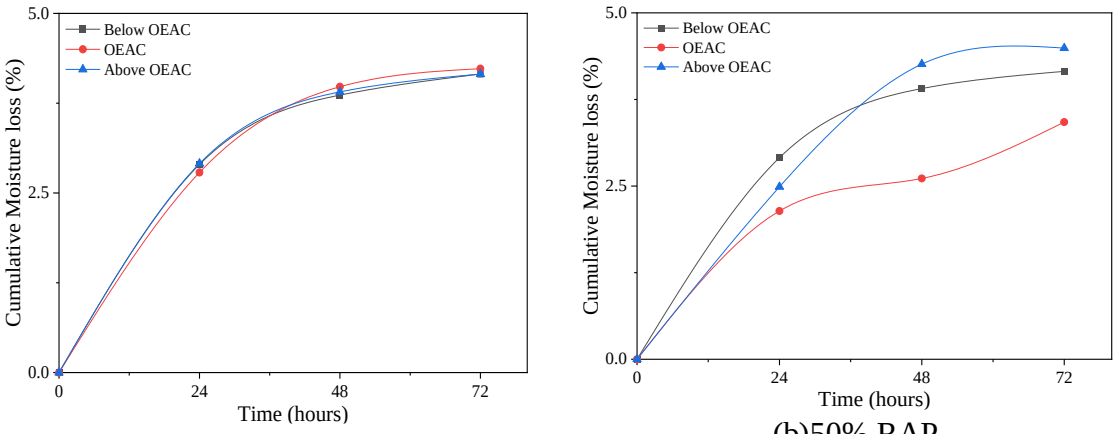

(a)25% RAP (b)50% RAP

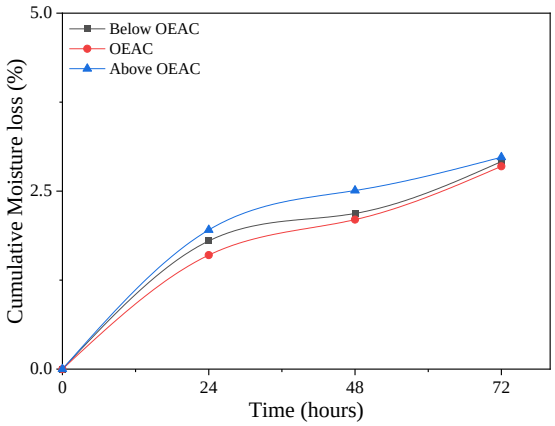

(c) 75% RAP

Figure 5.14 Percentage of water loss with time for different % RAP mixes

The results of dry densities and dynamics of water evaporation for RCA mixes are presented graphically in Figures 5.15 and 5.16.

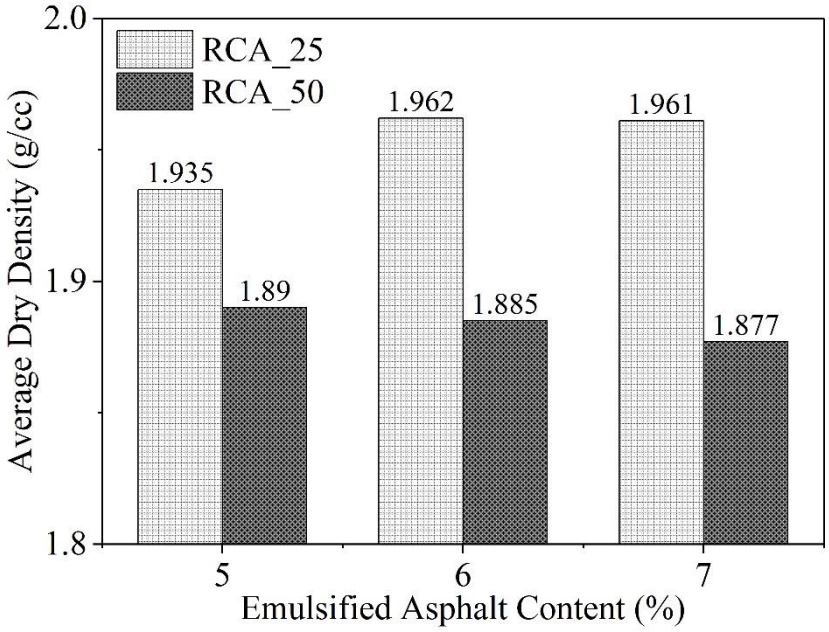

Figure 5.15 The dry densities of EATB with RCA

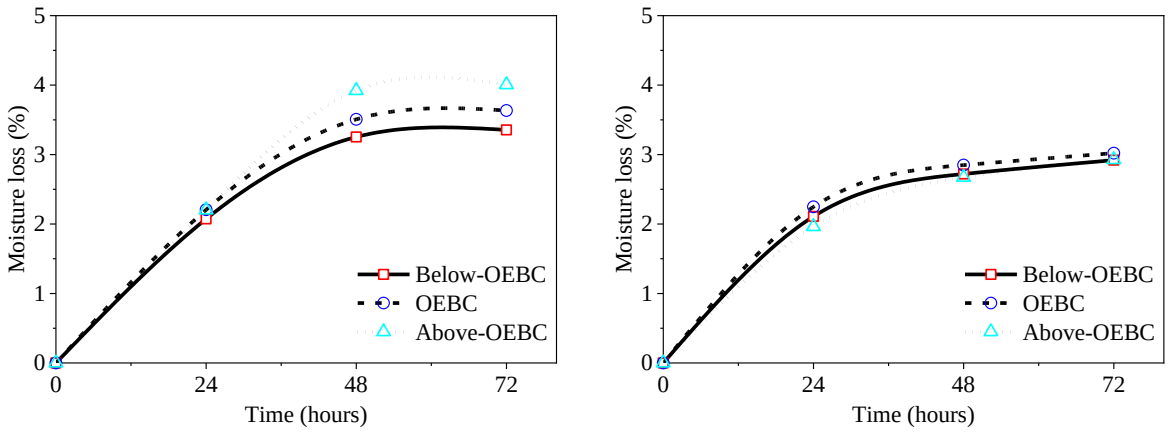

Figure 5.16 Dynamics of moisture loss for (a) 25% RCA (b) 50% RCA mixes

The observed results prove that the dry densities of EATBs with 25%RCA are more than EATBs blended by 50% RCA. For the EATBs with 50% RCA, the dry densities are reduced by 2.3, 3.9 and 4.3% for emulsified asphalt contents of 5, 6, and 7% of emulsified asphalt, as shown in Figure 5.15. It is found that the variation in dry density was observed due to the lower compactness of the mixes for corresponding gradations and RCA content. It is worth noting that the moisture loss in the mixes with 25% RCA is more, as observed from Figure 5.16, and it can be concluded that the higher the RCA content, the higher the water absorption and the lower will be the moisture loss.

5.6 Tensile Strength Ratio (TSR) of EATB

The tensile strength ratio is the ratio of the conditioned samples to the unconditioned samples ITS. TSR represents the percentage loss in strength when the material is subjected to prevailing field conditions. The samples were cured for 72 hours at 40°C conditioned by submerging in a water bath at room temperature for 24 hours (Asphalt Academy 2009). This represents the field conditions where the base is exposed to rain before placing a surface layer (Behnood et al. 2015). This property also embodies the durability of cold mixes. Both the conditioned and unconditioned samples were tested at ambient temperatures according to Asphalt Academy's guidelines 2009. Figure 5.17 shows that the TSR of all the mixes at the OEAC, below OEAC, and above OEAC exhibited a TSR of more than 80%, which is the permissible limit (IRC: SP 100: 2014). This indicates that the water did not affect the strength of the road base. Besides, the emulsified asphalt content did not significantly affect durability. Hence, when the emulsified asphalt content is less than or more than optimum, there is no significant influence on the TSR of the mixes. In this study, the emulsified asphalt contents considered are 0.5% below and above the optimum. Further, the RAP content in the blend does not influence the durability of the mixes.

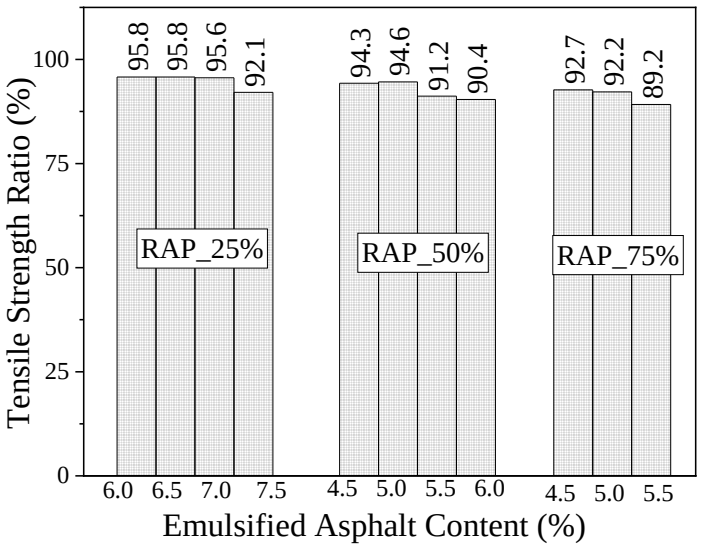

Figure 5.17 Tensile strength ratio of RAP mixes

From the laboratory results of RCA blends, all the specimens exhibited higher retained or TSR values, as shown in Figure 5.18, which exceeds 50% (Asphalt Academy TG-2, 2009). But, the 25% RCA mix did not satisfy the TSR value requirements of 80% as per IRC SP 100: 2014 specifications. Typically, lower TSR values are observed for EATBs with 25% RCA rather than 50% RCA. This investigation indicates that the retained tensile strength is sensitive to the RCA content and variation in the gradation. Hence, EATBs with RCA contents can be preferred as pavement bases (Asphalt Academy, 2009).

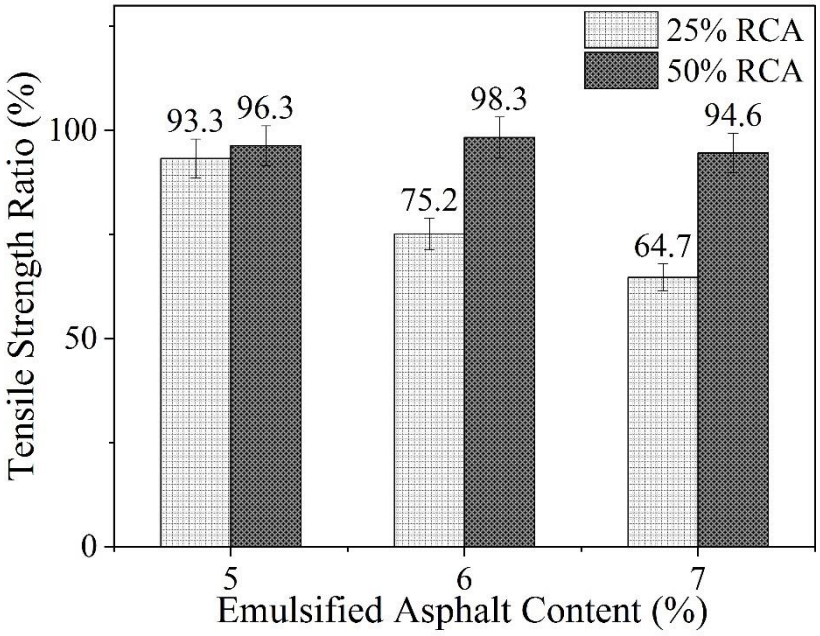

Figure 5.18 Tensile strength ratio of RCA mixes

5.7 Dynamic Creep Rutting Characteristics of EATB

The performance of all the samples under dynamic compressive loading for 3500 cycles was tested and is presented in Figure 5.19. In addition to the observed deformation, the

corresponding models of permanent deformations are depicted in the curves. The measured curves were smoothened using the Satitzsky-golay digital filter technique. This method of smoothing involves the least-squares fit of a small set of consecutive data points to a polynomial. It takes the calculated central point of the fitted polynomial curve as the new smoothed data point. The permanent deformation for different mixes is modelled in logarithmic and power-law curves. Models were developed for all the RAP blends to understand rutting behavior and validated, as shown in Figure 5.19.

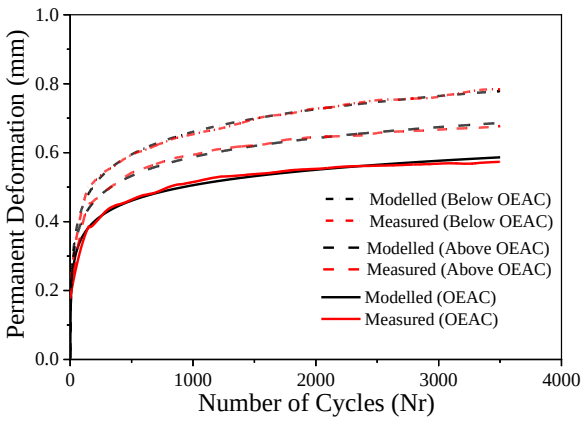

(a) Logarithmic model for RAP-25%

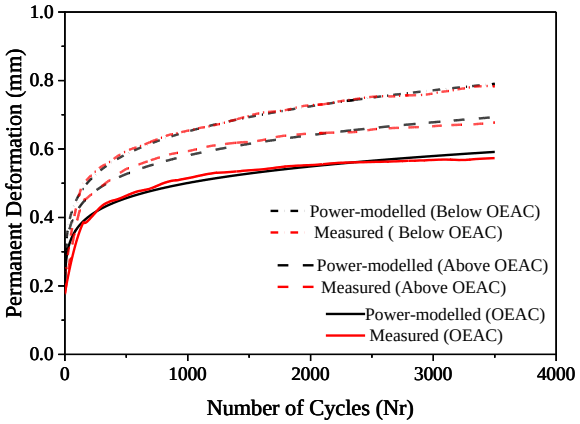

(d) Power-law model for RAP-25%

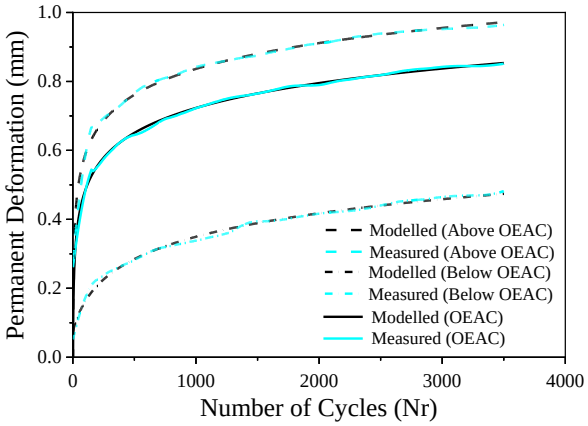

(b) Logarithmic model for RAP-50%

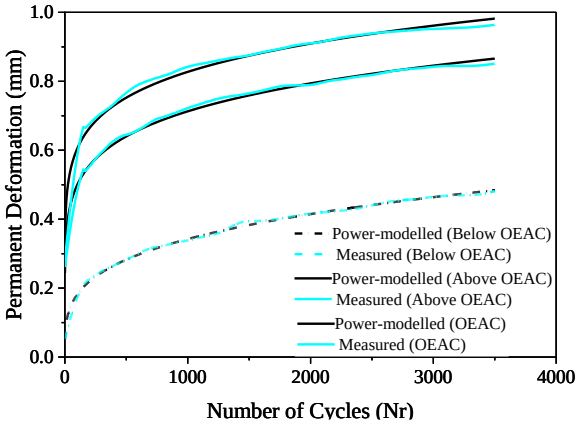

(e) Power-law model for RAP-50%

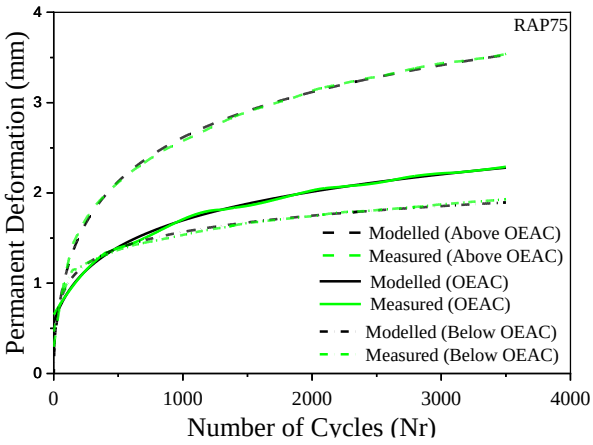

(c) Logarithmic model for RAP-75%

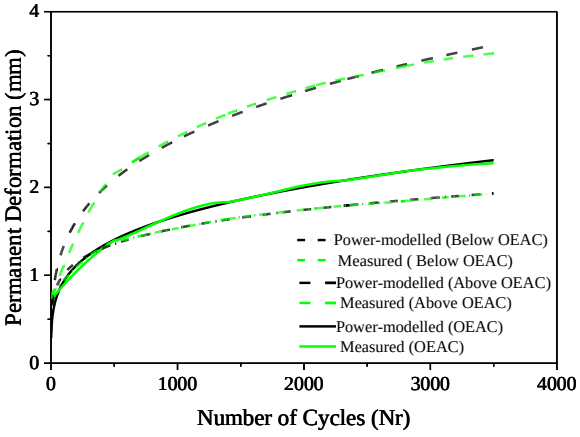

(f) Power-law model for RAP-75%

Figure 5.19 Permanent Deformation Curves for different Percentage of RAP

From the results, lower permanent deformations are observed at the OEAC, as shown in Figure 5.19. The observed permanent deformation curves for all the RAP mixes are compared at optimum, lower, and above optimum emulsified asphalt contents, as shown in Figure 5.20. It is demonstrated that the RAP-75 mixes show higher permanent deformation characteristics than RAP-25 and RAP-50. This indicates that the asphalt content present in RAP contributes to the permanent deformation characteristics of the mixes. The emulsified asphalt acts as not only a binder but also a rejuvenator. Hence, the contribution of aged asphalt towards higher permanent deformation characteristics is possible. The existing asphalt content present in the RAP-75 blend is greater than that of the remaining mixes, and there is a chance of higher binder content, which leads to more rut depth. This can also be because RAP-75 has 75% reclaimed material, which may not have the same angularity or may not provide the same shear strength due to the angle of internal friction. The RAP-25 mix contains 75% natural aggregates, whose particle shape contributes significantly to higher shear strength and enhanced rut resistance.

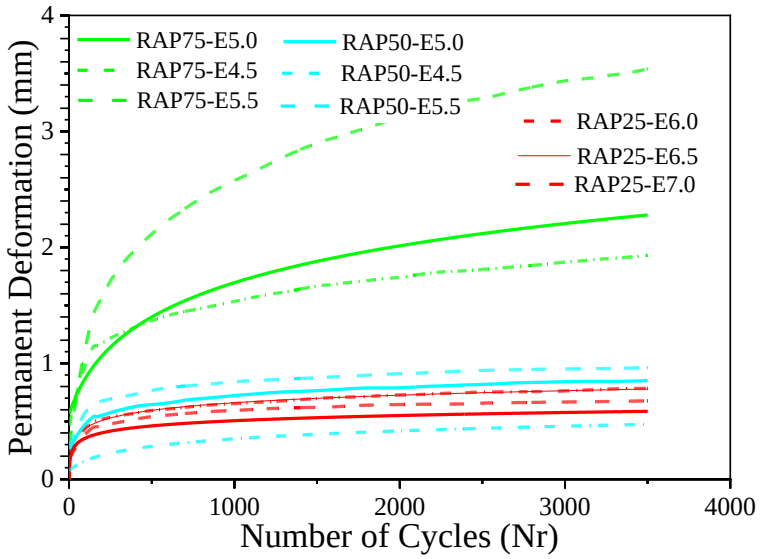

Figure 5.20 Comparison of permanent deformation curves of different RAP blends at optimum, below optimum, and above optimum emulsified asphalt contents

The effect of the Total Binder Content (TBC) of EATB on the resistance to permanent deformation at the end of the test is depicted as shown in Figure 5.21. The permanent deformation escalates with the RAP content and reaches a maximum at 75% RAP, and the observed lower and higher deformations are 0.48 mm and 3.54 mm, respectively. For the mixes with 50%RAP content, the significant observation is that the highest deformation is twice that of lower deformation. Mixes with 25% RAP content show the lowest deformation at the OEAC when compared with the lower and higher side of OEAC. It is also observed that the permanent deformation increases with the increase in TBC for mixes blended with RAP-50 and RAP-75. However, in the case of RAP-25 mixes, this trend does not appear.

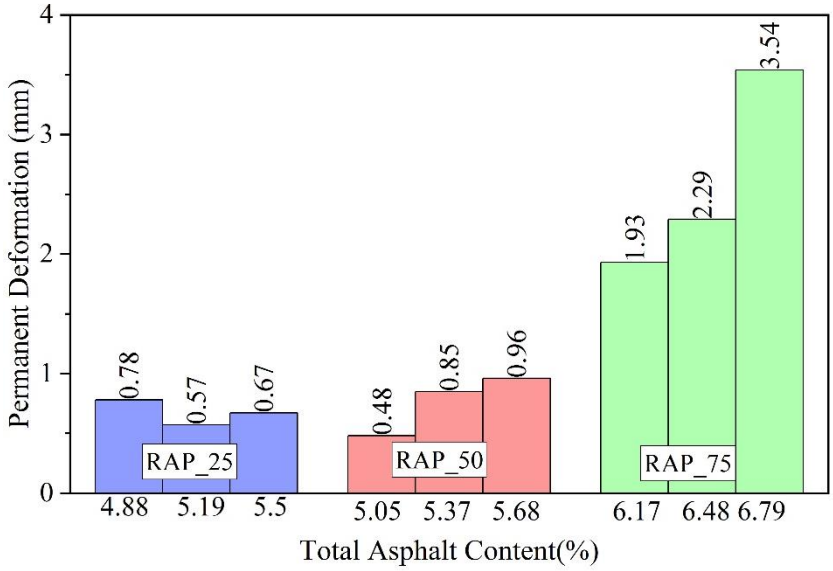

Figure 5.21 Effect of Total Asphalt Content on Permanent Deformation

Previously, a study developed a two-stage model for Styrene-Butadiene-Styrene (SBS) modified asphalt mixes (Ahari et al., 2013). The same method is tried for EATB combinations to predict permanent deformation characteristics. A logarithmic equation used to indicate the permanent deformation is shown in equation 5.2.

$$\Delta = a - b[\ln(N_r + c)] \qquad (5.2)$$

Where,

Δ is the permanent deformation or rutting in mm,

a, b, c are constants and are N_r the number of cycles.

A summary of all the models' statistical analysis is shown in APPENDIX B.. The standard error is negligible for each model, and the models are reliable, which indicates the best fit for defining the rutting potential of the RAP mixes. Further, the influence of the constant 'a' is negligible in all the mixes.

Like the logarithmic models, power equations were developed to calculate permanent deformation, as shown in equation (5.3).

$$\Delta = a \times N_r^{\,b} \qquad (5.3)$$

Where,

Δ is the permanent deformation or rutting in mm, a and b are constants, and

N_r is the number of cycles.

A summary of all the models' statistical analysis is shown in APPENDIX B. The standard error is negligible for each model, and the models are highly reliable, which indicates the best fit for defining the rutting potential of the RAP mixes. It is observed that the power-law equations

were best fitted to the permanent deformation curves, as observed in previous research works on HMA (Zhou et al. 2004, Ziari et al. 2016). The equation represents the deformations in the primary region of the creep deformation curve. If the curve stage moves to the secondary region, there is another slope parameter to determine the second region's strain slope, which is almost linear. When permanent deformation curves have primary and secondary regions, the equation will combine the power equation and straight-line equation. Only the primary region is analyzed where the logarithmic and power-law models are best fitted in the present study. This reveals that the emulsified asphalt mixes with 2% cement content behave like hot mix asphalts in permanent deformation.

The rutting behavior of EATBs consists of RCA is evaluated at various Emulsified Asphalt Contents (EAC) (below, above OEAC, and at OEAC). The permanent deformation increases with the increase in EAC for both the mixes (Figure 5.22). Further, greater resistance to permanent deformation is observed at 5% EAC (i.e., below OEAC). Hence, OEAC is determined based on ITS does not necessarily produce better resistance against the rutting.

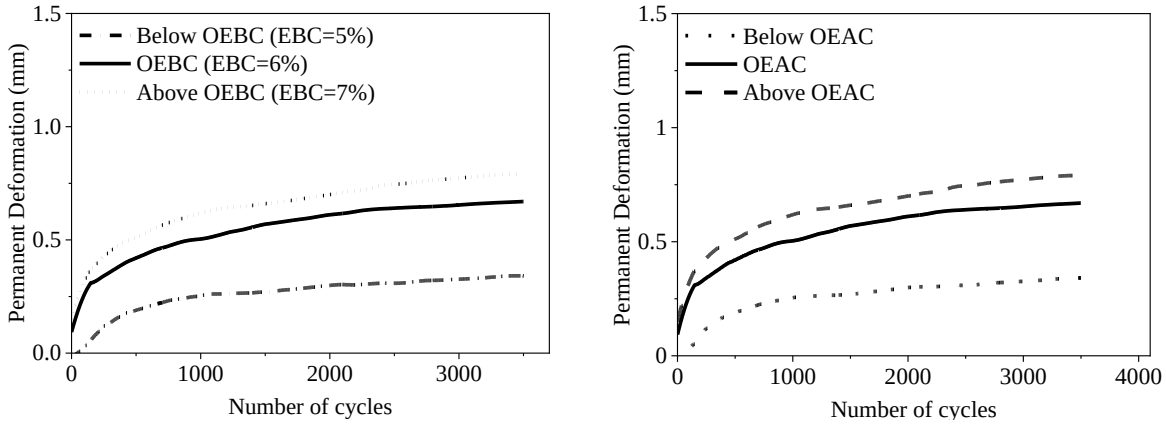

(a) RCA-25 (b) RCA-50

Figure 5.22 Permanent deformation of RCA mixes

Similarly, the permanent deformation characteristics of the RCA blends are determined using the Dynamic creep rutting test. From the results, 25RCA and 50RCA on the lower side of the optimum have lower permanent deformation than other mixes due to lower amounts of emulsified asphalt. The permanent deformation increases with the increase in emulsified asphalt content for both mixes. Further, greater resistance to permanent deformation is observed at 5% EAC (i.e., below OEAC).

Similarly, the test is carried out 40℃ to determine the temperature influence on the permanent deformation characteristics of the EATB. The test was carried out for 3500 cycles, and the accumulated strains were measured at all the cycles, which are presented in Figure 5.23.

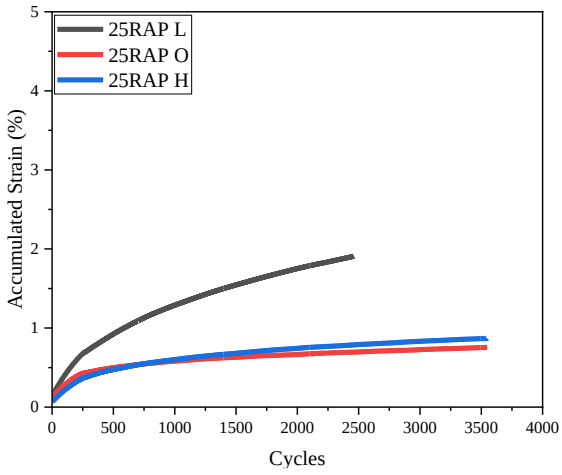

(a) RAP-25

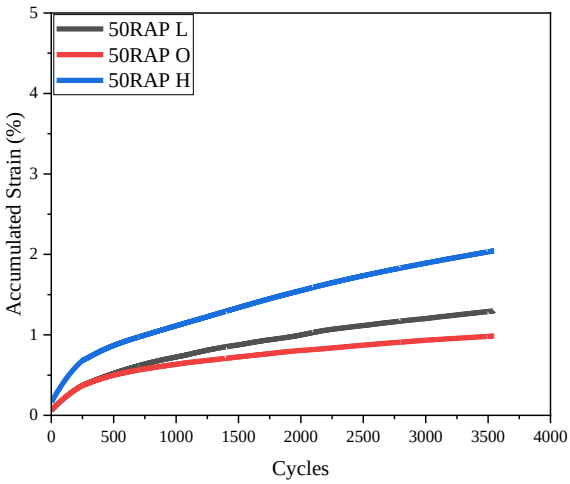

(b) RAP-50

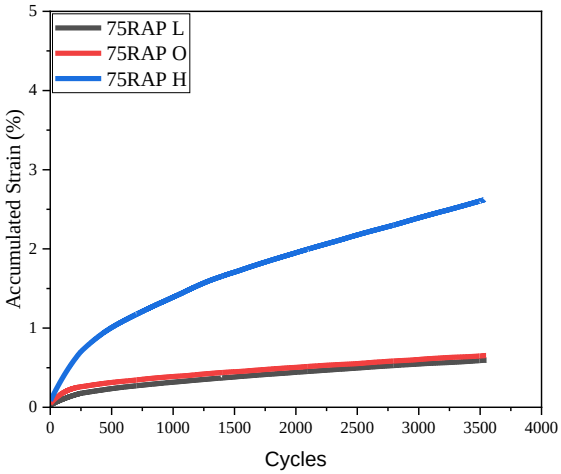

(c) RAP-75

Figure 5.23 Accumulated strains for RAP mixes at 40°C

From Figure 5.23, cycles are shown on the *x*-axis, and accumulated strain is shown on the *y*-axis. 25RAP L represents 25% RAP is present in the mix and prepared at the lower side of OEAC. Similarly, 50RAP O represents 50RAP present in the mixture, and the mix is compacted at OEAC, and 75RAP H represents 75RAP present in the mix and compacted at the higher side OEAC. Figure 5.23 (a) shows that 25RAP L has higher accumulated stains than the remaining mixes. This is due to less availability of the required amount of emulsified asphalt for proper coating at a higher temperature.

The rejuvenation of older asphalt of RAP may be possible due to the interaction between emulsified asphalt and RAP aggregates. Further, the availability of more residual asphalt from the RAP and emulsified asphalt, higher accumulated strains are exhibited by the 50RAP and 75RAP at the higher side of OEAC. On the other hand, 50RAP H and 75RAP H have higher accumulated strains.

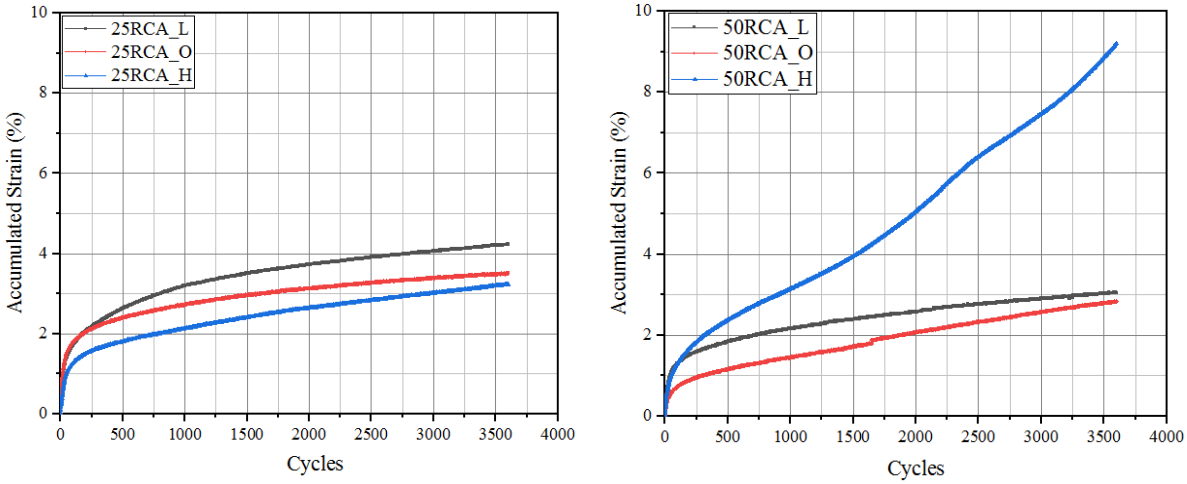

a) 25RCA (b) 50RCA

Figure 5.24 Accumulated strains for RCA mixes at 40°C

The aggregate combination, emulsified asphalt content, and temperatures significantly influence the accumulated strains of the RCA mixes, as shown in Figure 5.24. Similarly, 25RCA and 50RCA are evaluated under the Dynamic creep rutting test for 3500 cycles, and the accumulated strains are measured. From the results, 25RCA have higher accumulated strains at the lower side of OEAC. This is due to less availability of the required amount of emulsified asphalt for proper coating at a higher temperature. The 50RCA has higher strains at the higher side of OEAC and has lower accumulated strains at OEAC. This is expected to find that the RCA is generally sensitive to the present fluid and has higher accumulated strains.

5.8 Resilient Modulus Characteristics of EATB

The resilient modulus test is performed at 1Hz frequency by applying a repeated cyclic load. The Resilient Modulus results of the tested samples at a temperature 27°C are shown in Figures 5.25 and 5.26.

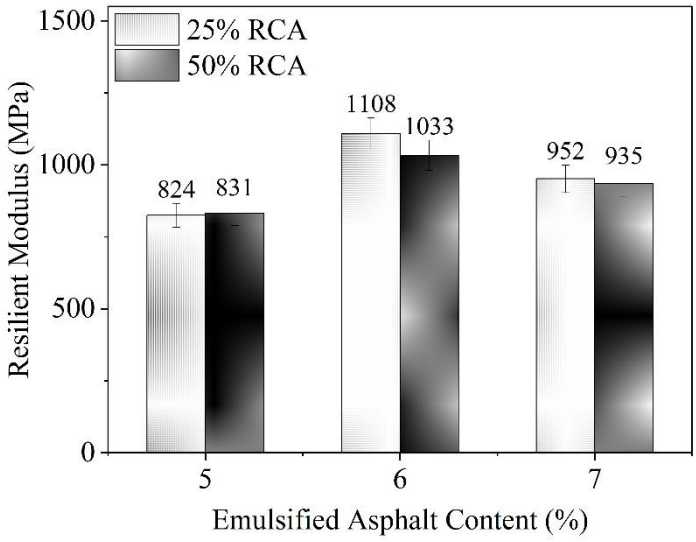

Figure 5.25 Resilient moduli of EATB with RCA at 27°C

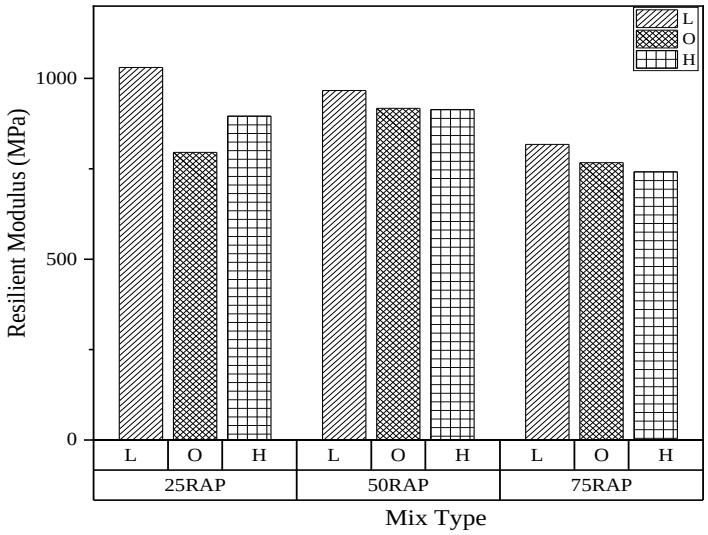

Figure 5.26 Resilient moduli of EATB with RAP at 27ºC

From the observations of M_R results in Figure 5.25, the maximum M_R is obtained at the OEAC which is similar to ITS results where the maximum ITS is observed at the OEAC. Further, the mixes with 25RCA have slightly more stiffness than the 50RCA. The increase in the recycled aggregate content influences the stiffness of the mixes.

From Figure 5.26, the stiffness decreases with the increase of RAP in the total mix. This indicates the recycled aggregate content in the mix effect the M_R of the mixes. Further, the RAP aggregate have a higher combined flaky and elongation index which significantly influenced the stiffness of the mixes.

However, all the mixe combinations achieved desirable stiffness properties recommended by IRC 37: 2018, around 800MPa. Further, no proper trend is observed with varying asphalt emulsion content in the 25RAP mix. For 50RAP mixes, there is a decline in the stiffness with the increased asphalt emulsion.

Figure 5.27 shows the stiffness of EATB with RAP mixes at a higher temperature i.e., 40°C. Here, the stiffness is relatively lower than the acceptable limits of 800 MPa to serve as a base (IRC 37: 2018). Relatively lower stiffness values were observed at 40°C temperatue independent of the asphalt emulsion content. So, the temperature rise can effect the performance of the emulsified asphalt treated base.

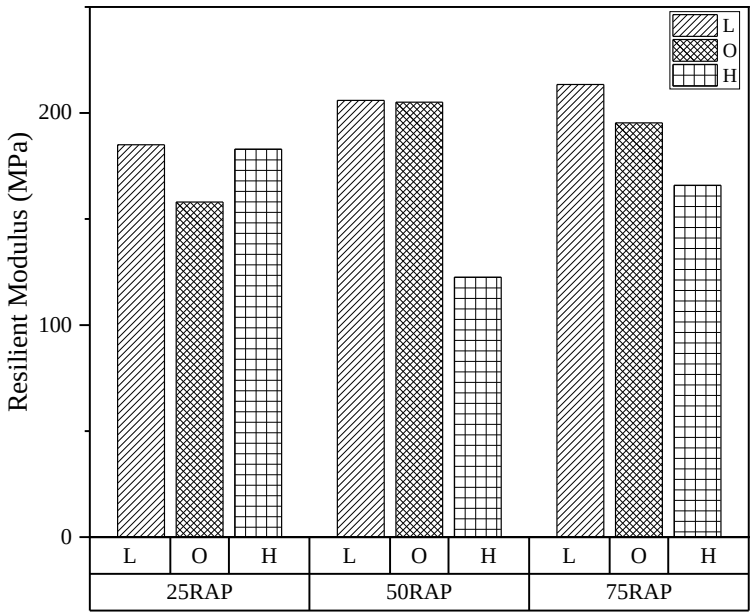

Figure 5.27 Resilient moduli of EATB with RAP at 40°C temperature

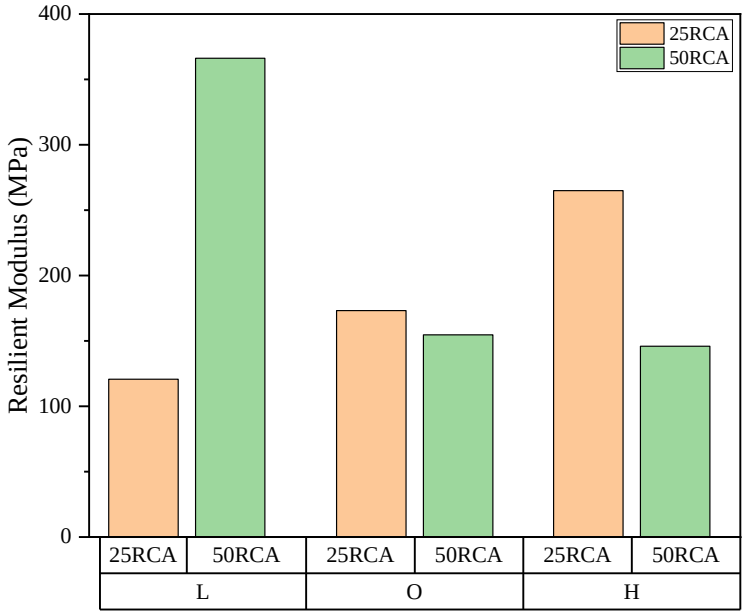

Figure 5.28 Resilient moduli of EATB with RCA at 40°C temperature

Figure 5.28 shows the M_R values of EATB mixes with RCA at 40°C. The stiffness values are typically lower at 40°C temperature and did not meet the specifications. The M_R values are increased gradually with the increase in the emulsified asphalt content for 25RCA mixes and decreases in the case of 50RCA. So, the performance of 25RCA is better at higher emulsified asphalt contents, while the 50RCA performed better at lower emulsified asphalt contents at higher temperatures.

5.9 Fatigue Characteristics of EATB

A stress-controlled indirect tensile fatigue testing machine determines the fatigue life of different EATB mixes (25RAP, 50RAP, 75RAP, 25RCA and 50RCA). Three different

emulsified asphalt contents were considered at OEAC, lower than OEAC and higher than OEAC. It is on either side of the OEAC. Appendix C shows the given fatigue data, including applied load, tensile stress, corresponding stiffness, tensile strain and fatigue life. The initial tensile strains are calculated using the tensile strength, Poisson's ratio, and the resilient modulus using equation 3.8. The M_R is taken as the average of 6 values (three samples with two planes perpendicular to each other) are taken. The tensile stress is calculated using equation 3.3, a function of applied load, the diameter of the specimen, and the thickness of the specimen. The graphical representations of variation of initial tensile strains concerning the number of cycles are shown in Figures 5.29 to 5.34. It is well known that the fatigue life decreases with an increase in the stress ratio. The same scenario is repeated in the mixes with RAP and RCA. From the observations, the fatigue life is influenced by the emulsified asphalt content, percentage of recycled aggregate content in the mix, and the stiffness of the mixture. More enormous tensile strains were observed for 75% RAP mixes than the remaining mixes.

A sample calculation of the tensile stress and tensile strain from the load application of 0.8 kN, stiffness of 895.91 MPa, having a thickness of the specimen 66 mm, the stress and strain are calculated as shown below.

$$\begin{aligned}\sigma &= \frac{2P}{\pi Dt} \\ &= \frac{2\times 0.785\times 1000}{\pi\times 100\times 66} \\ &= 0.0757\,\text{MPa} \\ &= 75.7\,\text{kPa}\end{aligned}$$

$$\begin{aligned}\varepsilon_t &= (1+3\mu)\frac{\sigma}{M_R} \\ &= (1+3\times 0.35)\times\frac{0.0757}{895.91} \\ &= 0.00017330 \\ &= 173.30\,\mu\varepsilon\end{aligned}$$

Similarly, all specimens' tensile stresses and tensile strains were calculated and presented in Appendix C.

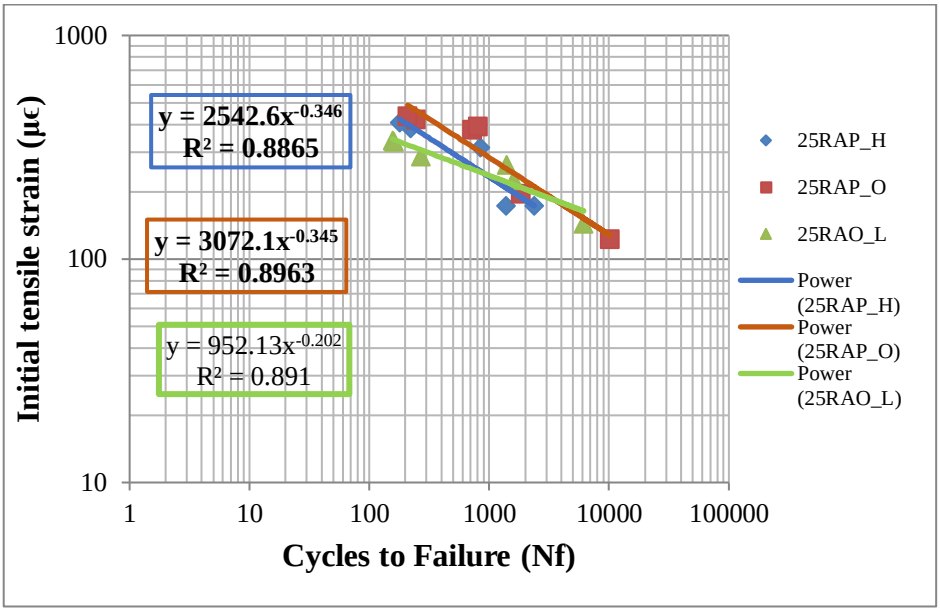

Figure 5.29 Fatigue performance of 25RAP mixes

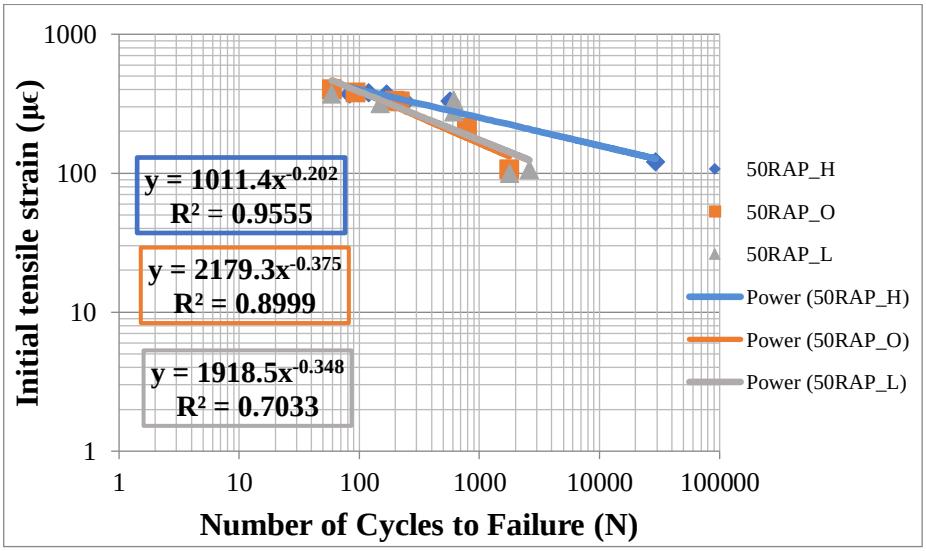

Figure 5.30 Fatigue performance of 50RAP mixes

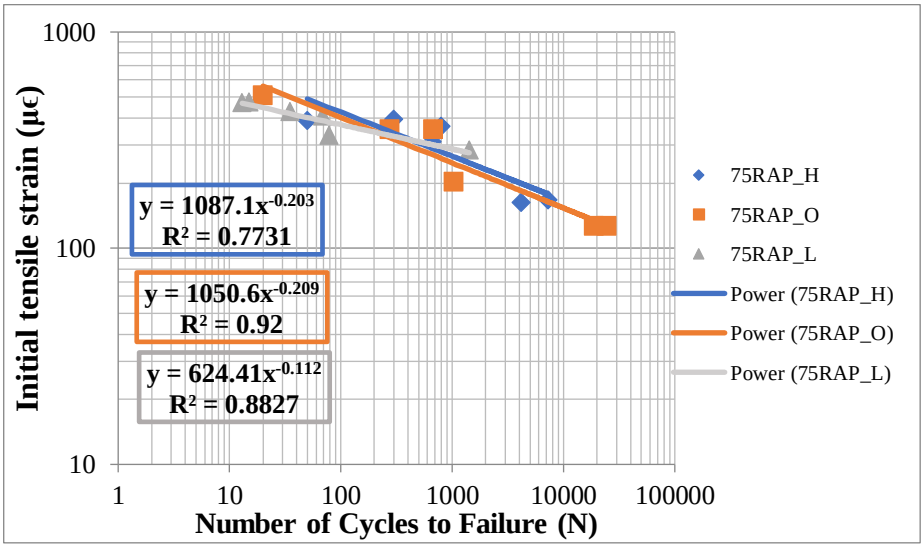

Figure 5.31 Fatigue performance of 75RAP mixes

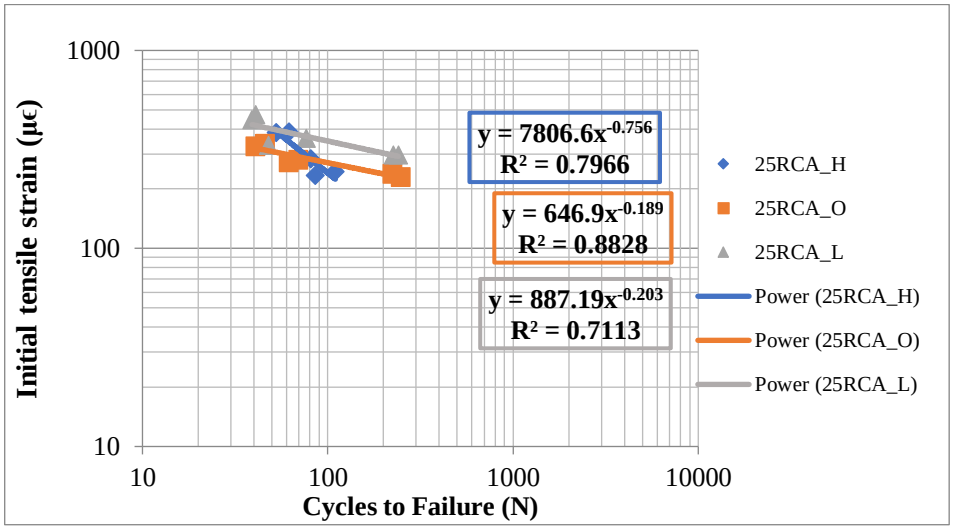

Figure 5.32 Fatigue performance of 25RCA mixes

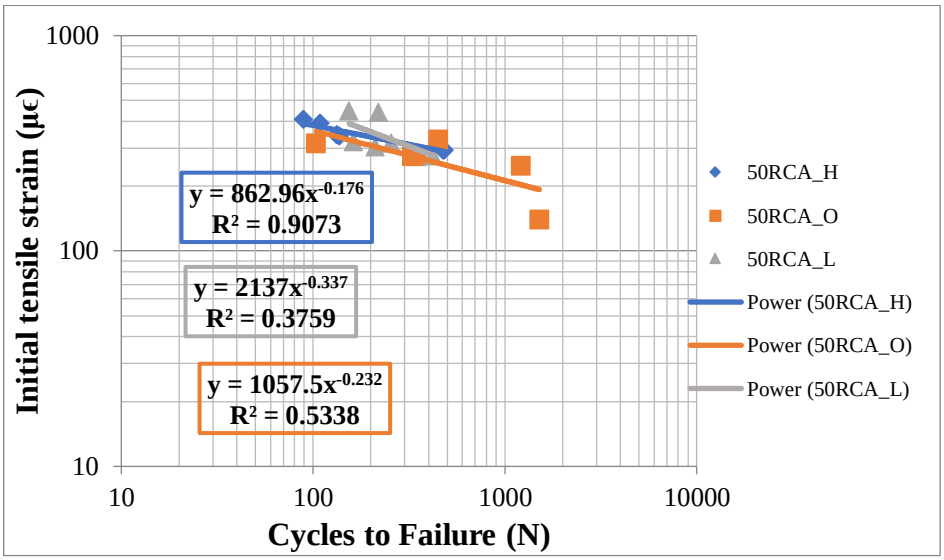

Figure 5.33 Fatigue performance of 50RCA mixes

From Figures 5.29 to 5.34, it is observed that the fatigue life changes with respect to the initial tensile strains. From the 25RAP mixes results in Figure 5.29, the optimum and higher side of OEAC has higher fatigue life at higher initial tensile strains. However, at lower initial tensile strains, the lower side of optimum gave high fatigue life.

From 50RAP mixes in Figure 5.30, at higher initial tensile strains, the optimum and lower side of OEAC have higher fatigue life. However, the higher optimum side gave higher fatigue life at lower initial tensile strains.

From Figure 5.31, for 75RAP mixes, optimum and higher side of optimum have more fatigue life at higher initial tensile strains. At lower tensile strains, the lower side of optimum has higher fatigue life.

From Figure 5.32, for 25RCA mixes, the higher side of OEAC has higher fatigue life at higher initial tensile strains. For 50RCA mixes in Figure 5.33, all the mixes follow the same fatigue

behavior. However, the sensitivity towards emulsified asphalt content is less for the RCA mixes than RAP combinations.

All the RAP mixes are compared at OEAC, as shown in Figure 5.34. At lower initial tensile strains, the superior order follows 75RAP, 25RAP and 50RAP and at higher initial tensile strains, 25RAP is followed by 50RAP and then 75RAP mixes. The 75RAP mix exhibited lower fatigue life at higher initial tensile strains due to higher stiffer asphalt, which does not allow higher tensile stresses. The trend is reversed at lower initial tensile strains that exhibited higher fatigue life. From the overall results, the fatigue life is influenced by the stress level, initial tensile strains, stiffness of the specimen, emulsified asphalt content, and the percentage of recycled aggregate in the combination.

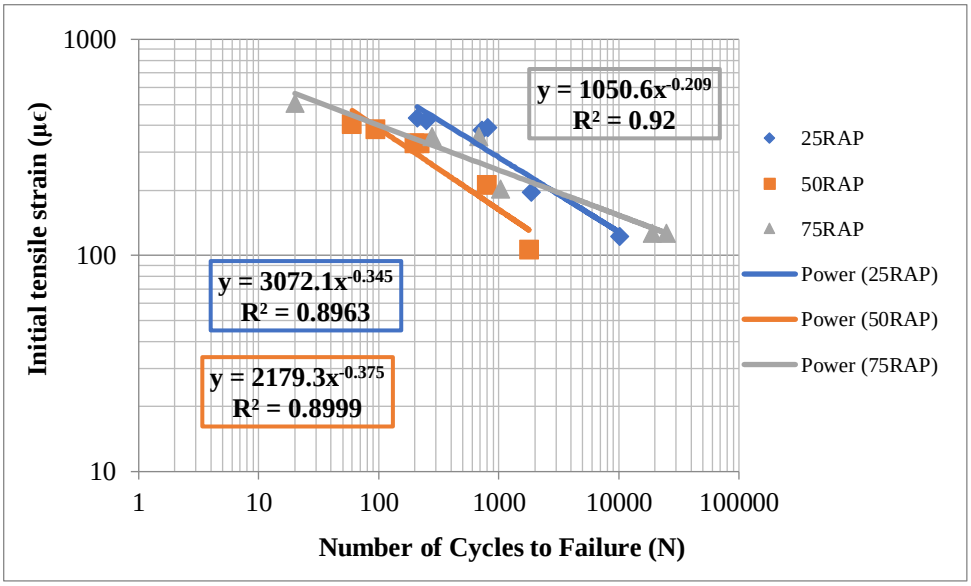

Figure 5.34 Fatigue performance of RAP mixes at OEAC

5.10 Summary

The preliminary analysis of EATB prepared with RAP and RCA exhibits the following trends. The overall characteristics of the EATB are shown in APPENDIX D.

- It is observed that the emulsified asphalt content required for the specimens with 75% RAP content is typically lower than that of the 25% RAP content mixes. The ITS obtained at OEAC is generally less than 225 kPa specified by the IRC 37:2018. However, the strength is satisfactory as per Asphalt Academy TG-2 guidelines. Further, the strength is achieved at longer curing periods greater than 60 days.
- The curing rate is high in the first 24 hours after the preparation of the bases and declines in later stages. The failure pattern of the EATB mixes prepared with RAP occurs along with the bonding interface and exhibited higher TSR values than the specification limits, which are considered durable.

- When subjected to the dynamic creep rutting test at ambient or higher temperatures, mixes with 75% RAP have more (3.54 mm) permanent deformation. The combined residual binder is present in the RAP, and emulsified asphalt influences the rutting characteristics of the EATB.
- Lower permanent deformations were observed for the mixes with lower emulsified asphalt contents than OEAC, and more permanent deformations are observed at higher emulsified asphalt contents than optimum for mixes made of 50% RAP and 75%RAP. However, lower permanent deformations were observed at the OEAC for RAP-25. Further, 50% RAP and 75% RAP mixes show similar permanent deformation characteristics.
- For larger initial tensile strains, 25 RAP mixes at the optimum and higher optimum side have higher fatigue life. However, the lower side of the optimum at lower strains gave high fatigue life.
- For 50 RAP mixes at higher initial tensile strains, the optimum and lower side has a higher fatigue life. However, the higher optimum side at lower strains gave high fatigue life.
- The optimum side has more fatigue life for 75 RAP mixes at higher tensile strains. At lower tensile strains, the more downside of optimum has high fatigue life.
- Based on the performance evaluation of the EATB, for better performance, the selction of multi-variant performance criteria of various parameters gives better results than the individual parameters. That means ITS may not be the criteria for selecting the OEAC of the mix, further consideration of performance parameters like rutting, fatigue, and durability is necessary for choosing the OEAC for better performance.
- In the case of EATB prepared with RCA, the dry-ITS, wet-ITS, and TSR values exceed the permissible values described in Asphalt Academy-2009 guidelines; the mixes with 25 and 50% RCA can be recommended as the emulsified asphalt stabilized layers.
- However, the TSR values of EATBs prepared using RCA are within the acceptable limits, the retained tensile strength is lower in the EATBs with 25% RCA rather than 50% RCA Hence, it implies that the gradation parameter like percentage of fines is also an essential factor in affecting the moisture sensitivity apart from the RCA content.
- For EATB mixes with RCA, 25RCA performs better at OEAC in rutting and fatigue. At the same time, 50RCA performed better at optimum and lower than OEAC in rutting and fatigue.

CHAPTER 6

PAVEMENT ANALYSIS AND DESIGN

6.1 General

In the previous chapter, a laboratory performance evaluation of EATB is carried out. In this chapter, pavement analysis and design are carried out using the obtained CTB and EATB. For pavement analysis, IITPAVE software (IRC 37:2018) calculates the stresses and strains at the critical locations. Further, the cross-sections are compared with the conventional pavement sections.

6.2 Pavement Analysis

For the design of flexible pavements, the Indian code of practice, IRC 37:2018, specified 6 cross-sections, as presented below in Figures 6.1 to 6.6.

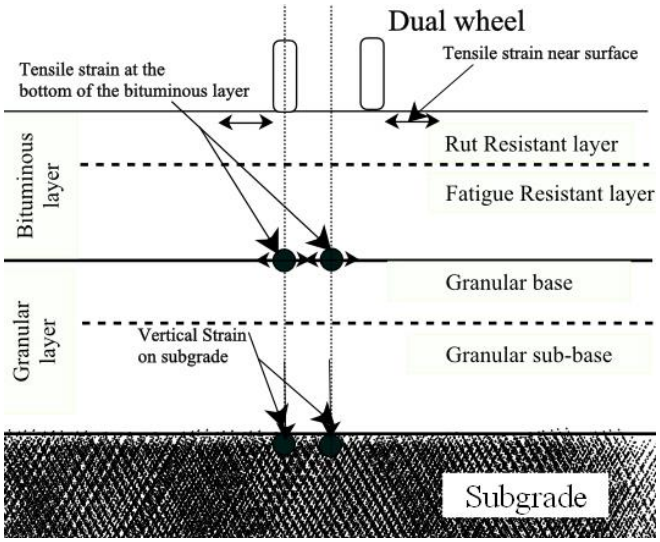

Figure 6.1 A Pavement Section with Bituminous Layer(s), Granular Base and GSB Showing the Locations of Critical Strains

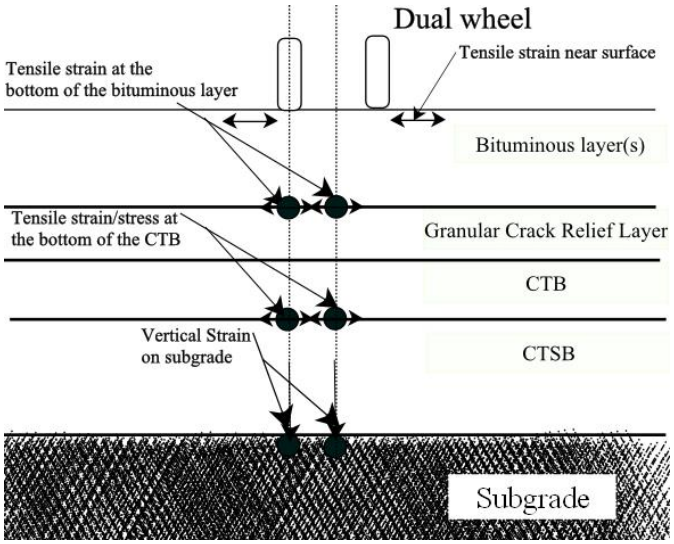

Figure 6.2 A Pavement Section with Bituminous Layer(s), Granular Crack Relief Layer, CTB, and CTSB Showing the Locations of Critical Strains/Stresses

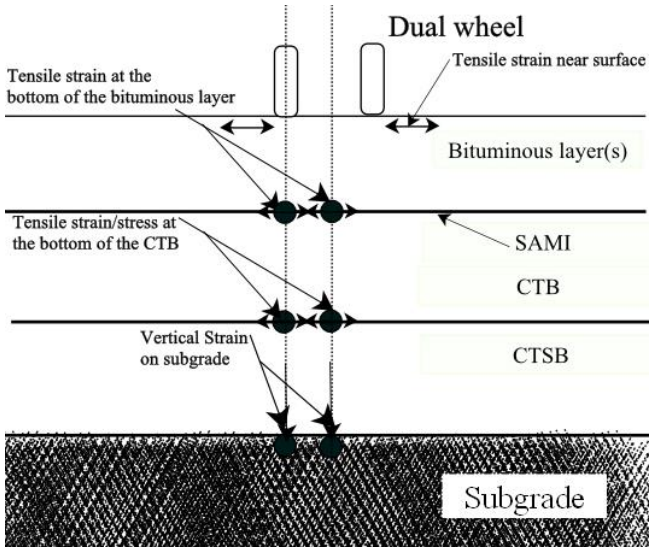

Figure 6.3 A Pavement Section with Bituminous Layer(s), SAMI Crack Relief Layer, CTB and CTSB Showing the Locations of Critical Strains/Stresses

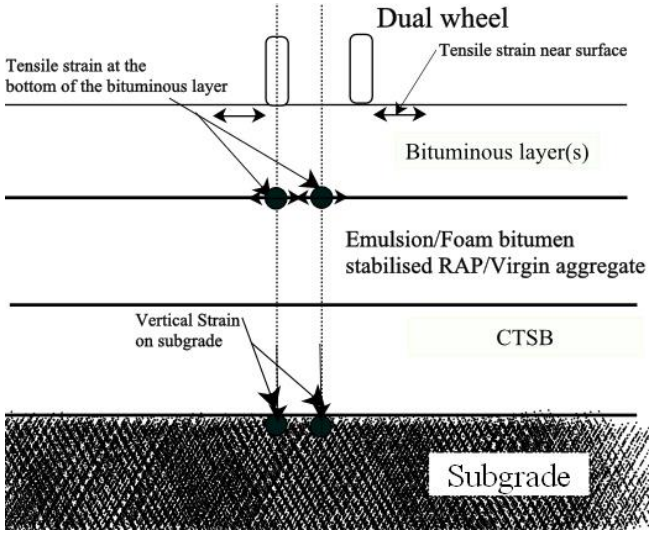

Figure 6.4 A Pavement Section with Bituminous Layer(s), Emulsion/Foam Bitumen Stabilised RAP/Virgin Aggregate Layer and CTSB Showing the Locations of Critical Strains

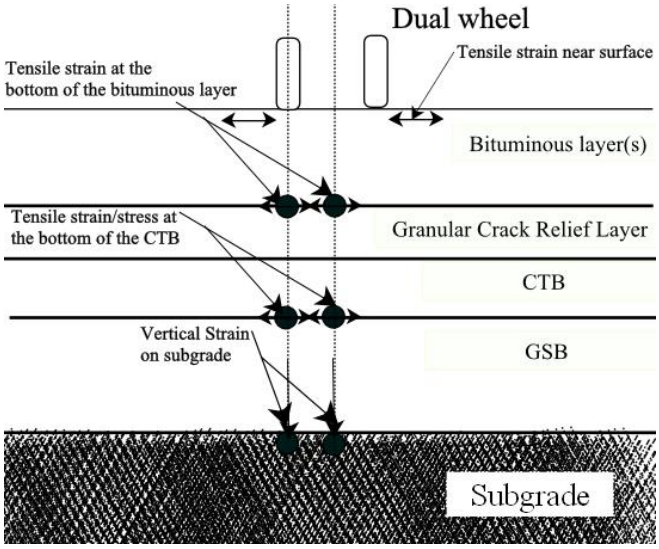

Figure 6.5 A Pavement Section with Bituminous Layer(s), Granular Crack Relief Layer, CTB and GSB Showing the Locations of Critical Strains/Stresses

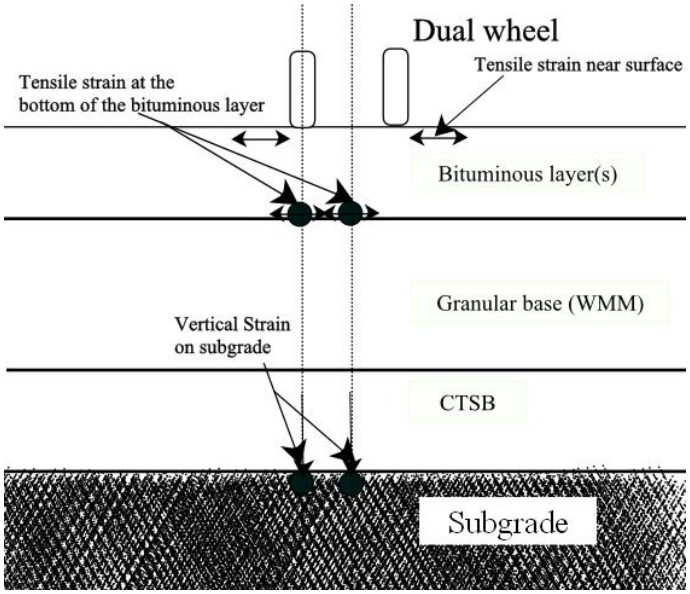

Figure 6.6 A Pavement Section with Bituminous Layer(s), Granular Base (WMM) and CTSB Showing the Locations of Critical Strains

The cross-sections include a bituminous layer, as common in all sections where the base layers change. The conventional base layers include Wet Mix Macadam (WMM) and GSB. The other sections have CTB and CTSB with granular crack relief and SAMI layers between the CTB and Bituminous layers. The fourth case is EATB and CTSB layers as base and subbase, shown in Figure 6.4. The fifth case is a CTB and GSB in which a stress-absorbing interface layer is provided between the bituminous layer and CTB. The sixth section is WMM as the base layer and CTSB as the subbase layer. The critical locations of the strains and stresses depend on the layers included in the pavement. The critical locations are horizontal tensile strains at the bottom of the bottom asphalt layer, tensile stresses at the bottom of the CTB, and the vertical compressive strains on top of the subgrade should be calculated under the centroid of the wheel and centroid of the dual wheel respectively. A typical cross-section of the flexible pavement with cement-treated bases and subbases and the critical stress or strain locations is shown in Figures 6.2 and 6.3.

In the present study, the base layers considered are CTB and EATB, and the subbase layer is CTSB. Further, the base layers are composed of different recycled aggregates proportions and stabilization levels. Pavement analysis is carried out using IIT PAVE software. In IIT PAVE, input values include the number of layers, elastic modulus values for different layers, Poisson's ratio for different layers, Wheel load, tire pressure, analysis points, locations of the analysis points, and wheelset be given. The output values include stress strains at the critical points in various directions at the specified points in the input data. Typical input and output of the IITPAVE are shown in APPENDIX E. The CBR value for the subgrade is taken as 5%, and the analysis is carried out for 30 msa. The elastic modulus and Poisson's ratio for subgrade are 62

MPa and 0.35. The elastic modulus and Poisson's subbase ratio are 600 MPa and 0.25. The obtained values from the test results are taken for the base course, and the Poisson's ratio is taken as 0.25. The elastic modulus and Poisson's crack relief layer ratio are 450 MPa and 0.35. The elastic modulus and Poisson's ratio of bituminous course are taken as 3000 MPa and 0.35. The analysis keeps the thicknesses of the subbase, bituminous course, and crack relief layer constant. The thickness of the stabilized recycled bases was compared with the conventional stabilized bases mentioned in the IRC 37: 2018, as shown in Figure 6.7.

The laboratory stiffness values are calculated using the Indirect Tensile resilient modulus testing machine. Five combinations with higher stiffness values, namely RAP-6C, 25RAP-6C, 50RCA-6C, 25RCA-6C, and RCA-6C, are considered. Their laboratory M_R values are 4431, 4300, 3389, 3609, and 3406 MPa. The recycled aggregate mixes are compared with the conventionally stabilized bases, with an M_R of 5000 MPa from IRC 37: 2018. Figure 6.7 shows that the recycled bases' overall thickness is slightly higher than the conventional stabilized material. However, the recycled aggregates incorporation into the bases saves a huge quantity of traditional material.

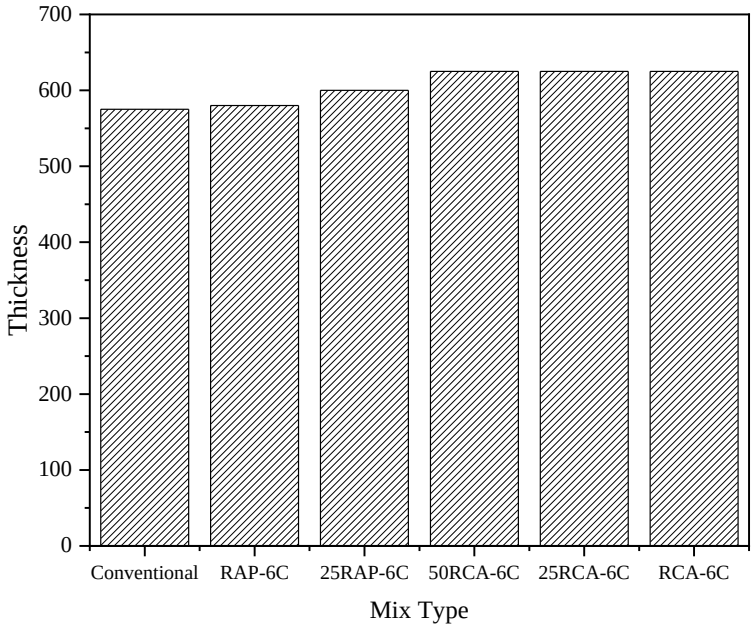

Figure 6.7 Thickness comparison of cement stabilized bases

6.3 Pavement Analysis of EATB

For a typical cross-section of pavement, the vertical compressive strains at the top of the subgrade and the horizontal tensile stresses at the bottom of the bituminous layers are considered for analysis. A typical cross-section of the flexible pavement with EATB and CTSB as base and subbase layers with the critical strain locations is shown in Figure 6.4. These strains are critical in determining the failure of the pavements in terms of rutting or fatigue failure. The prepared EATB using the recycled aggregate combination is incorporated in a typical pavement

section having surface course, binder course, EATB, and CTSB. The results obtained in the laboratory are used in the analysis of the strains at critical locations. The allowable vertical compressive strain at 90% reliability used for primary roads is calculated using equation 6.1 for subgrade rutting life from IRC 37 2018. The M_R value for the bituminous mix is considered 3000 with the mix parameters ($Va = 3, V_{be} = 11.5, M = 0.499, C = 3.16$). The allowable horizontal tensile strain is calculated from the following fatigue life equation 6.2. The strains are computed for a subgrade having a CBR of 5%; for CTSB, the M_R is 600 MPa, and the traffic considered is 30 million standard axles for the analysis.

$$N_R = 1.4100 \times 10^{-8} \left[1/\varepsilon_v \right]^{4.5337} \quad \ldots\ldots (6.1)$$

$$N_f = 0.5161 \times C \times 10^{-4} \left[1/\varepsilon_t \right]^{3.89} \times \left[1/M_{Rm} \right]^{0.854} \quad \ldots\ldots (6.2)$$

Here ε_v is the vertical compressive strain, ε_t horizontal tensile strain M_{Rm} is the Resilient modulus of the bituminous mix, C is the adjustment factor used to account for variation in the mix volumetric parameters.

Table 6.1Calculation of critical strains for a cross-section incorporating EATB

Mix type	Bitumen Emulsion rate	Resilient Modulus	ε_t	ε_{ta}	ε_v	ε_{v_a}
WMM		154	202.8	220	372.4	416.02
25RAP	L	1030	87.7	220	316.9	416.02
	O	795	93.8	220	417.9	416.02
	H	895	84.4	220	410.4	416.02
50RAP	L	966	78.5	220	405.7	416.02
	O	917	82.5	220	408.9	416.02
	H	913	82.8	220	409.2	416.02
75RAP	L	624	114	220	434.0	416.02
	O	574	121.2	220	439.8	416.02
	H	489	135.4	220	451.3	416.02
25RCA	L	824	90.9	220	415.6	416.02
	O	1108	68.2	220	397.4	416.02
	H	952	94.0	220	406.6	416.02
50RCA	L	831	90.2	220	415.1	416.02
	O	1033	87.5	220	401.6	416.02
	H	935	95.5	220	407.7	416.02

ε_t -Tensile strain at the bottom of the bitumen layer ε_{ta} is an allowable horizontal tensile strain in $\mu\varepsilon$ ε_v -Vertical compressive strain at the top of the subgrade $\mu\varepsilon$ and ε_{v_a} is the allowable vertical compressive strain from the formula.

To consider the safe design of the pavement, the vertical compressive strains at the top of the subgrade and the horizontal tensile strains at the bottom of the bottom bituminous layer should be within the allowable limits calculated from the equations. From Table 6.1, it is observed that the horizontal tensile strains are within the permissible limits. However, the vertical compressive strains at the top of the subgrade are satisfied if the M_R of the mixes is 800 MPa and above. The RAP replacement of RAP up to 50% fulfilled the requirements as a base layer at all emulsified asphalt contents, i.e., upper, lower, and OEAC. For 75RAP content, a little increase in the thickness of the base layer can satisfy the requirements. When the cross-section containing EATB and CTSB is compared with the conventional pavement with WMM and GSB as base and subbase layers, there is a reduction of the thickness of around 14%.

6.4 Summary

In this chapter, different pavement cross-sections considered by the IRC 37: 2018 were presented, along with the pavement cross-sections with the CTB and EATB layers and their critical locations of the strains. This follows the analysis of the pavement sections using IITPAVE software by incorporating the obtained modulus values for CTB and EATB of different recycled aggregate combinations. The investigation concluded a reduction in the thickness of the stabilized base layers compared with the conventional base layers in EATB. Further, the thickness of the stabilized conventional aggregates is almost equivalent to that of the stabilized recycled aggregate base layers and involves a considerable quantity of material savings.

CHAPTER 7

CONCLUSIONS AND SCOPE FOR FUTURE STUDY

7.1 General

The main objective of the present research work is to evaluate the laboratory performance of cement-treated and emulsified asphalt treated bases prepared using different combinations of recycled aggregates with conventional aggregates and at different stabilization levels. The recycled aggregates include Reclaimed Asphalt Pavement and Recycled Concrete Aggregates. The conclusions drawn from the present research are summarized in the following sections.

7.2 Conclusions of Cement Treated Bases

- The RAP content in the mix significantly influences the MDD, OMC, and strength properties. The RCA content does not follow any specific trend concerning the MDD, OMC and strength properties due to the heterogeneity nature of the RCA.
- RAP and RCA bases require more than 6% of cement content or 28 days of curing period to serve as pavement bases according to the Indian specifications.
- UCS values increase with the cement content curing period and decrease with the RAP content. The rate of gain in strength for stabilized RCA is more than that of RAP and VA due to self-cementing properties.
- There is an apparent increase in the strength of bases up to 90 days of the curing period. The 28-day strength is 70-80% of the 140 days strength in VA and RCA bases and 50-60% of the 140-day strength in VA-RAP bases. The Resilient Modulus of cement treated recycled aggregate bases exhibited the same as that of the cement-treated VA bases. However, the obtained values are significantly lower than modulus values using the flexural beam from other studies.
- The presence of RAP and RCA content significantly influences the cement-treated bases' fatigue life. The brittle nature increases with the cement content and decreases with the amount of RAP in the mix. Differences in fatigue life are observed at a higher percentage of RCA in the mixes. Mixes exhibited higher fatigue life at low-stress levels.
- Treated bases reduce the pavement's overall thickness and economize on conventional aggregates materials.

7.3 Conclusions of Emulsified Asphalt Treated Bases

- It is concluded that the optimum emulsified asphalt content required for the specimens with 75% RAP content is typically lower than that of the 25% RAP mixes. The ITS obtained at OEAC is generally less than 225 kPa specified by the IRC 37:2018. However, the strength

is satisfactory as per Asphalt Academy TG-2 guidelines. Further, the strength is achieved at longer curing periods greater than 60 days.

- The curing rate is high in the first 24 hours after the preparation of the bases and declines in later stages. The failure pattern of the EATB mixes prepared with RAP occurs along with the bonding interface and exhibited higher TSR values than the specification limits, which are considered durable. However, the failure pattern of EATB mixes prepared with RCA occurs along with the aggregate interface.
- The combined residual binder present in the RAP and emulsified asphalt influences the rutting characteristics of the EATB. When subjected to the dynamic creep rutting test at ambient or higher temperatures, mixes with 75% RAP have higher (3.54 mm) permanent deformation. The EATB at 2% cement content behaves like a hot asphalt mix.
- Lower permanent deformations were observed for the mixes with lower emulsified asphalt contents than OEAC, and more permanent deformations are observed at higher emulsified asphalt contents than OEAC for mixes made of 50% RAP and 75%RAP. However, lower permanent deformations were observed at the OEAC for RAP-25. Further, 50% RAP and 75% RAP mixes show similar permanent deformation characteristics.
- For larger initial tensile strains, 25 RAP mixes at the OEAC and higher side of OEAC have higher fatigue life. However, the lower side of the OEAC at lower strains gave high fatigue life.
- For 50 RAP mixes at higher initial tensile strains, OEAC and the lower side of OEAC have a higher fatigue life. However, the higher side of OEAC at lower strains gave high fatigue life.
- The optimum side has more fatigue life for 75 RAP mixes at higher tensile strains. At lower tensile strains, the more downside of optimum has high fatigue life.
- Based on the results obtained from the evaluation of the EATB, the selection of the EATB mixes with RAP is to be considered based on the multi-variant performance of parameters independent of the individual parameter.
- In the case of EATB prepared with RCA, the dry-ITS, wet-ITS, and TSR values are higher than the minimum required values described in Asphalt Academy-2009 guidelines. The mixes with 25 and 50% RCA can be recommended as the emulsified asphalt stabilized layers.
- The TSR values of EATB prepared using RCA are within the acceptable limits. The retained tensile strength is lower in the EATBs with 25% RCA than 50% RCA. Hence, it implies that the gradation parameter, like the percentage of fines, is also an essential factor in affecting the moisture sensitivity apart from the RCA content.

- For EATB mixes with RCA, 25RCA performs better at OEAC in rutting and fatigue. At the same time, 50RCA performed better at optimum and lower than OEAC in rutting and fatigue.

7.4 Recommendations

Based on the obtained UCS results, RAP and RCA bases require more than 6% cement content or 28 day curing period to serve as pavement bases and are recommended for sub-base applications at 2-4% cement contents according to Indian specifications.

For better performance of EATB in terms of durability, strength, stiffness, rutting and fatigue life, multivariate criteria are to be considered to adopt recycled aggregates.

7.5 Scope for Future Study

In the present study, laboratory performance evaluation is carried out on the stabilized RAP and RCA. The same can be validated using field performance studies and a relationship between field and laboratory studies in the long run. Further, microscopic analysis can be done on stabilized bases with RAP and RCA bases to understand the effectiveness of stabilization. Exploring more recycled materials like wastes from industries, glass manufacturing, plastics, electronics, and other solid wastes as pavement bases and sub-bases for sustainable construction and respective specifications can be developed.

References

American Association of State Highway and Transportation Officials. (2011). "Standard Method of Test for Moisture–Density Relations of Soils Using a 4.54-kg (10-lb) Rammer and a 457-mm (18-in.) Drop." T 180. AASHTO, Washington DC, USA, 2011.

American Society for Testing and Materials. (2012). "Standard test method for indirect tensile (IDT) strength of bituminous mixtures." D6931. ASTM International, West Conshohocken, PA, USA.

American Society for Testing and Materials. (2007). "Standard practice for making and curing soil-cement compression and flexure test specimens in the laboratory." ASTM, D. 1632. ASTM International, West Conshohocken, PA, USA.

American Society for Testing and Materials. (2016). D6926. "Standard practice for preparation of asphalt mixture specimens using Marshall apparatus." ASTM International, West Conshohocken, PA, USA.

American Society for Testing and Materials, D. (2009). 7369-09. "Standard test method for determining the resilient modulus of bituminous mixtures by indirect tension test." American Society for Testing and Materials.

Adaska, W. S., Luhr, D. R., and Conference, R. (2004). "control of reflective cracking in cement stabilized pavements ' Control of Reflective Cracking in Cement Stabilized Pavements ' ' Control of Reflective Cracking in Cement Stabilized Pavements ' 5th International RILEM Conference, Limoges, France, May ." *Prevention*, 2(May), 1–8.

Agrela, F., Cabrera, M., Galvín, A. P., Barbudo, A., and Ramirez, A. (2014). "Influence of the sulphate content of recycled aggregates on the properties of cement-treated granular materials using Sulphate-Resistant Portland Cement." *Construction and Building Materials*, Elsevier Ltd, 68, 127–134.

Agrela, F., Barbudo, A., Ramírez, A., Ayuso, J., Carvajal, M. D., Jiménez, J. R. (2012) Construction of road sections using mixed recycled aggregates treated with cement in Malaga, Spain. Resour Conserv Recycl 58:98–106.

Ahari, A. S., Forough, S. A., Khodaii, A., &Nejad, F. M. (2014). "Modeling the primary and secondary regions of creep curves for SBS-modified asphalt mixtures under dry and wet conditions." *Journal of materials in civil engineering*, Vol. 26(5), pp. 904-911.

Al-Mishhadani, S. A., and H.H.Al-Baid. (2014). "Some Properties of Emulsified Asphalt Paving Mixture at Iraqi Environmental Conditions." *Tikrit Journal of Engineering Science (TJES)*, (January), 21–1.

Alam, T. B., Abdelrahman, M., and Schram, S. A. (2010). "Laboratory characterization of

recycled asphalt pavement as a base layer." *International Journal of Pavement Engineering*, 11(2), 123–131.

Ameri, M., Behnood, A. (2012). "Laboratory studies to investigate the properties of CIR mixes containing steel slag as a substitute for virgin aggregates." *Constr. Build. Mater*. 26, 475–480. https://doi.org/10.1016/j.conbuildmat.2011.06.047

Arimilli, S., Jain, P. K., and Nagabhushana, M. N. (2016). "Optimization of Recycled Asphalt Pavement in Cold Emulsified Mixtures by Mechanistic Characterization." *Journal of Materials in Civil Engineering*, 28(2), 1–10.

Arshad, M. (2020). "Laboratory investigations on the mechanical properties of cement-treated RAP-natural aggregate blends used in base/subbase layers of pavements." *Construction and Building Materials*, Elsevier Ltd, 254, 119234.

Arulrajah, A., Disfani, M. M., Haghighi, H., Mohammadinia, A., and Horpibulsuk, S. (2015). "Modulus of rupture evaluation of cement stabilized recycled glass/recycled concrete aggregate blends." *Construction and Building Materials*, Elsevier Ltd, 84, 146–155.

Arulrajah, A., Piratheepan, J., Ali, M. M. Y., and Bo, M. W. (2012). "Geotechnical properties of recycled concrete aggregate in pavement sub-base applications." *Geotechnical Testing Journal*, 35(5), 1–9.

Arulrajah, A., Piratheepan, J., and Disfani, M. M. (2014b). "Reclaimed Asphalt Pavement and Recycled Concrete Aggregate Blends in Pavement Subbases: Laboratory and Field Evaluation." *Journal of Materials in Civil Engineering*, 26(2), 349–357.

ARRA (Asphalt Recycling and Reclaiming Association) (2018). "Recommended construction guidelines for cold in-place recycling (CIR) using Bituminous recycling agents," CR101, Glen Ellyn, IL: ARRA.

Asphalt Emulsion Technology (2006). Asph. Emuls. Technol. https://doi.org/10.17226/23246

Asphalt Academy, 2009. Technical Guideline: Bitumen Stabilised Materials.

Asphalt Institute and Asphalt Emulsion Manufacturers Association (MS-19) (1979). A basic asphalt emulsion manual. Department of Transportation, Federal Highway Administration.

Attia, M., and Abdelrahman, M. (2010). "Modeling the effect of moisture on resilient modulus of untreated reclaimed asphalt pavement." *Transportation Research Record*, 2(2167), 30–40.

Autelitano, F., and Giuliani, F. (2016). "Electric arc furnace slags in cement-treated materials for road construction: Mechanical and durability properties." *Construction and Building*

Materials, Elsevier Ltd, 113, 280–289.

Baghini, M. S., Ismail, A. Bin, Karim, M. R. Bin, Shokri, F., and Firoozi, A. A. (2017). "Effects on engineering properties of cement-treated road base with slow setting bitumen emulsion." *International Journal of Pavement Engineering*, Taylor & Francis, 18(3), 202–215.

Barbod, B., Shalaby, A. (2014). "Laboratory performance of asphalt emulsion treated base for cold regions applications." *In Proceedings of the 2014 Transportation Association of Canada (TAC) Conference*, Montreal, QC, Canada, 1-11.

Bazrafshan Moghadam, B., and Farhad Mollashahi, H. (2017). "Suggesting a simple design method for cold recycled asphalt mixes with asphalt emulsion." *Journal of Civil Engineering and Management*, 23(7), 966–976.

Beja, I. A., Motta, R., and Bernucci, L. B. (2020). "Application of recycled aggregates from construction and demolition waste with Portland cement and hydrated lime as pavement subbase in Brazil." *Construction and Building Materials*, Elsevier Ltd, 258, 119520.

Bennert, T., Papp, J., Maher, A., and Gucunski, N. (2000). "Utilization of construction and demolition debris under traffic-type loading in base and subbase applications." *Transportation Research Record*, 2(1714), 33–39.

Behnood, A., Modiri Gharehveran, M., Gozali Asl, F., Ameri, M. (2015). "Effects of copper slag and recycled concrete aggregate on the properties of CIR mixes with bitumen emulsion, rice husk ash, Portland cement and fly ash." *Constr. Build. Mater.* 96, 172–180.

Bessa, I. S., Almeida, L. R., Vasconcelos, K. L., and Bernucci, L. L. B. (2016). "Design of cold recycled mixes with asphalt emulsion and portland cement." *Canadian Journal of Civil Engineering*, 43(9), 773–782.

Bestgen, J. O., Hatipoglu, M., Cetin, B., and Aydilek, A. H. (2016). "Mechanical and Environmental Suitability of Recycled Concrete Aggregate as a Highway Base Material." *Journal of Materials in Civil Engineering*, 28(9), 04016067.

Boucard, L., Schmitt, V., Farcas, F., et al. (2015). "Bitumen emulsions formulation and destabilization process relationship: influence of salts addition." *Road Materials and Pavement Design*. 16, 330-348.

Budge, A. S., and Wilde, W. J. (2007). "Monitoring Curing of Emulsion-Stabilized Roadways Using the Dynamic Cone Penetrometer." *Soil and Material Inputs for Mechanistic-Empirical Pavement Design (GSP 169)*, 232, 7–7.

Budge, AS., Wilde, WJ. (2008). "A Modified Method for MR Testing to Evaluate Temperature Effects in Emulsion-Stabilized Gravel." I*n GeoCongress 2008: Characterization,*

Monitoring, and Modeling of GeoSystems. 12-19.

Buczyński, P., Iwański, M. (2017). "Fatigue Life Comparison of Recycled Cold Mixes with Foamed Bitumen and Bitumen Emulsion." *Procedia Eng*. 172, 135–142.

Cardoso, R., R. V. Silva, J. de Brito, and R. Dhir. 2016. "Use of recycled aggregates from construction and demolition waste in geotechnical applications: A literature review." Waste Manage. 49 (Mar): 131–145. https://doi.org/10.1016/j.wasman.2015.12.021.

Cardone, F., Virgili, A., and Graziani, A. (2018). "Evaluation of bonding between reclaimed asphalt aggregate and bitumen emulsion composites." *Construction and Building Materials*, Elsevier Ltd, 184, 565–574.

Castañeda López, M. A., Fedrigo, W., Kleinert, T. R., Matuella, M. F., Núñez, W. P., and Ceratti, J. A. P. (2018). "Flexural fatigue evaluation of cement-treated mixtures of reclaimed asphalt pavement and crushed aggregates." *Construction and Building Materials*, 158, 320–325.

CCANZ (2008). "Cement Stabilisation." *Cement & Concrete Association of New Zealand*, IB89.

Central Pollution Control Board (2017). "Guidelines on environmental management of construction & demolition (C&D) wastes, forests & climate change." *Government of India, Ministry of Environment*.

Chelelgo, K., Gariy, Z.C.A., Shitote, S.M. (2019). "Modeling of fatigue-strength development in cold-emulsion asphalt mixtures using maturity method." *Appl. Sci.* 9.

Cheng, H., Sun, L., Liu, L., and Li, H. (2018). "Fatigue characteristics of in-service cold recycling mixture with asphalt emulsion and HMA mixture." *Construction and Building Materials*, Elsevier Ltd, 192, 704–714.

Choudhary, R. (2012). "Use of Cold Mixes for Rural Road Construction." *Int. Conf. Emerg. Front. Technol*. 20–24.

Deng, C., Jiang, Y., Lin, H., et al. (2019). "Influence of gradations on the performance of emulsified asphalt cold recycled mixture produced using vertical vibration compaction method." *Road Materials and Pavement Design*. 1-21.

Dolzycki, B., Jaczewski, M., and Szydlowski, C. (2017). "The long-term properties of mineral-cement-emulsion mixtures." *Construction and Building Materials*, Elsevier Ltd, 156, 799–808.

Dong, W., Charmot, S. (2019). "Proposed Tests for Cold Recycling Balanced Mixture Design with Measured Impact of Varying Emulsion and Cement Contents." *J. Mater. Civ. Eng*.

31, 04018387. https://doi.org/10.1061/(ASCE)mt.1943-5533.0002611

Du, S. (2014). "Interaction mechanism of cement and asphalt emulsion in asphalt emulsion mixtures." *Mater. Struct. Constr.* 47, 1149–1159. https://doi.org/10.1617/s11527-013-0118-1

Ebrahim Abu El-Maaty Behiry, A. (2013). "Utilization of cement treated recycled concrete aggregates as base or subbase layer in Egypt." *Ain Shams Engineering Journal*, 4(4), 661–673.

El, S., Khay, E., Ph, D., El, S., Ben, E., Loulizi, A., Ph.D., Neji, J., and Ph, D. (2015). "Laboratory Investigation of Cement-Treated Reclaimed Asphalt Pavement Material." *Journal of Materials in Civil Engineering*, 27(6), 1–7.

Ellis, C., Zhao, B., Barnes, J., Jones, N. (2004). "Properties of GGBS-Bitumen Emulsion Systems with Recycled Aggregates." *Road Mater. Pavement Des.* 5, 373–383. https://doi.org/10.1080/14680629.2004.9689977

Faysal, M., Mahedi, M., Aramoon, A., Thian, B., Hossain, M. S., Khan, M. A., Khan, M. S. (2016). "Determination of the structural coefficient of different combinations of cement-treated/untreated recycled base materials." *Geotech Struct Eng Congress 2016*, 1198–1208.

Fang, X., Garcia-Hernandez, A., and Lura, P. (2016). "Overview on cold cement bitumen emulsion asphalt." *RILEM Technical Letters*, 1, 116.

Fedrigo, W., Núñez, W. P., Castañeda López, M. A., Kleinert, T. R., and Ceratti, J. A. P. (2018). "A study on the resilient modulus of cement-treated mixtures of RAP and aggregates using indirect tensile, triaxial and flexural tests." *Construction and Building Materials*, Elsevier Ltd, 171, 161–169.

Fedrigo, W., Núñez, W. P., Fernandes, D. P., Malabarba, L. M., Ceratti, J. A. P., and Brito, L. A. T. (2019). "Effects of RAP residual asphalt binder type, content and aging on the mechanical behaviour of cold recycled cement-treated mixtures." *Road Materials and Pavement Design*, 0629.

Gabr, A. R., and Cameron, D. A. (2012). "Properties of Recycled Concrete Aggregate for Unbound Pavement Construction." *Journal of Materials in Civil Engineering*, 24(6), 754–764.

Gandi, A., Cardenas, A., Sow, D., Carter, A., Perraton, D. (2019). "Study of the impact of the compaction and curing temperature on the behavior of cold bituminous recycled materials." *J. Traffic Transp. Eng*, 6, 349–358.

García, A., Lura, P., Partl, M.N., Jerjen, I. (2013). "Influence of cement content and environmental humidity on asphalt emulsion and cement composites performance." *Mater. Struct. Constr*. 46, 1275–1289. https://doi.org/10.1617/s11527-012-9971-6

Gao, J., Jin, P., Sheng, Y., and An, P. (2020). "A case study on crack propagation law of cement stabilized macadam base." *International Journal of Pavement Engineering*, 21(4), 516–523.

Gao, L., Ni, F., Ling, C., Yan, J. (2016). "Evaluation of fatigue behavior in cold recycled mixture using digital image correlation method." *Constr. Build. Mater*. 102, 393–402. https://doi.org/10.1016/j.conbuildmat.2015.11.014

Ge, Z., Li, H., Han, Z., Zhang, Q. (2015). "Properties of cold mix asphalt mixtures with reclaimed granular aggregate from crushed PCC pavement." Constr. Build. Mater. 77, 404–408.

Gómez-Meijide, B., Pérez, I., Pasandín, A.R. (2016). "Recycled construction and demolition waste in Cold Asphalt Mixtures: Evolutionary properties." J. Clean. Prod. 112, 588–598.

Gómez-Meijide, B., Pérez, I., Airey, G., Thom, N. (2015). "Stiffness of cold asphalt mixtures with recycled aggregates from construction and demolition waste." *Constr. Build. Mater*. 77, 168–178. https://doi.org/10.1016/j.conbuildmat.2014.12.045

Godenzoni, C., Graziani, A., Bocci, E., Bocci, M. (2018). "The evolution of the mechanical behavior of cold recycled mixtures stabilized with cement and bitumen: field and laboratory study." *Road Mater. Pavement Des*. 19, 856–877.

Graziani, A., Iafelice, C., Raschia, S., Perraton, D., Carter, A. (2018). "A procedure for characterizing the curing process of cold recycled bitumen emulsion mixtures." *Constr. Build. Mater*. 173, 754–762.

Grilli, A. (2019). "Field Behaviour of Cold-Recycled Asphalt Mixtures for Binder Field Behaviour of Cold-Recycled Asphalt Mixtures." (May).

Guo, Y., Yao, C., Shen, A., Chen, Q., Wei, Z., and Yang, X. (2020). "Feasibility of rapid-regeneration utilization in situ for waste cement-stabilized macadam." *Journal of Cleaner Production*, Elsevier Ltd, 263, 121452.

Guthrie, W., Cooley, D., and Eggett, D. (2007a). "Effects of Reclaimed Asphalt Pavement on Mechanical Properties of Base Materials." *Transportation Research Record*, 2005(1), 44–52.

Guthrie, W. S., Brown, A. V., and Eggett, D. L. (2007b). "Cement Stabilization of Aggregate

Base Material Blended with Reclaimed Asphalt Pavement." *Transportation Research Record*, 2026(1), 47–53.

Gurney, L. R. (2013). "Compositional and Structural Properties of Emulsion-Treated Base Material" : 7800 South in West Jordan, Utah.

Haider, I., Cetin, B., Kaya, Z., Hatipoglu, M., Cetin, A., and Ahmet, H. A. (2014). "Evaluation of the Mechanical Performance of Recycled Concrete Aggregates Used in Highway Base Layers." 3686–3694.

Halsted, G. E., Luhr, D. R., and Adaska, W. S. (2006). "Guide to Cement-Treated Base (CTB).

Hodgkinson, A., and Visser, A. T. (2004). "The role of fillers and cementitious binders when recycling with foamed bitumen or bitumen emulsion." *8th Conference on Asphalt Pavements for Southern Africa (CAPSA'04)*, (September), CD-ROM.

Hou, Y., Ji, X., and Su, X. (2019). "Mechanical properties and strength criteria of cement-stabilized recycled concrete aggregate." *International Journal of Pavement Engineering*, Taylor & Francis, 20(3), 339–348.

Hoyos, L. R., Puppala, A. J., and Ordonez, C. A. (2011). "Characterization of Cement-Fiber-Treated Reclaimed Asphalt Pavement Aggregates: Preliminary Investigation." *Journal of Materials in Civil Engineering*, 23(7), 977–989.

Hoyos LR, Ordoñez CA, Puppala AJ, Hossain MS (2008). "Engineering characterization of cement-fiber treated RAP aggregates." *In: GeoCongress 2008: characterization, monitoring, and modeling of GeoSystems*, pp 613–621.

https://www.cement.org/docs/default-source/th-paving-pdfs/ctbcement-treatedpuppala-base/cement-treated-base-pca-logo.pdf?sfvrsn=2. Accessed 17 Oct 2019

I.R.C (2018). "Guidelines for the design of flexible pavements (Fourth Revision)," IRC 37: 2018.

I.R.C (2012). "Guidelines for the design of flexible pavements (Fourth Revision)," IRC 37: 2012.

I. R. C (2014). "Use of Cold Mix Technology in Construction & Maintenance of Roads Using Bitumen Emulsion," IRC: SP-100: 2014.

IS 2386 (Part I, Part II, Part III and Part IV) (1963). "Tests on Aggregates." *Bureau of Indian Standards*, Manak Bhavan, New Delhi.

IS 2720 (Part VIII) (1983). "Methods of test for soils." *Bureau of Indian Standards*, Manak Bhavan, New Delhi.

IS12269, I. S. D. (2003). "Specification for 53 grade ordinary Portland cement." *Bureau of Indian Standards*, New Delhi.

IS 8887 (2018). "Bitumen Emulsion for Roads (Cationic type) Specification." *Indian Roads Congress*.

IS 3117. (2004). "Bitumen Emulsion for Roads and allied Applications (Anionic type)." *Bureau of Indian Standards*, Manak Bhavan, New Delhi.

IS 1208. (1978). "Indian standard methods for testing tar and bituminous materials (Determination of ductility)." *Bureau of Indian Standards*.

IS 1216. (1978). "Indian standard methods for testing tar and bituminous materials (Determination of Solubility in Carbon Disulphide Trichloroethylene)." *Bureau of Indian Standards*.

Jain, S., Singhal, S., and Jain, N. K. (2018). "Construction and demolition waste (C&DW) in India: generation rate and implications of C&DW recycling." *International Journal of Construction Management*, Taylor & Francis, 21(3), 261–270.

Jensen, O.M., Hansen, P.F. (2001). "Water Entrainment in Concrete: Techniques and Optimum Size of Inclusions." *Aalborg Dep. Mech. Eng.* , Aalborg Univ.

Jiang, Y., Lin, H., Han, Z., and Deng, C. (2019). "Fatigue Properties of Cold-Recycled Emulsified Asphalt Mixtures Fabricated by Different Compaction Methods." *Sustainability*, 11(12), 3483.

Jitsangiam, P., Nusit, K., Likitlersuang, S., and Kodikara, J. (2021). "Using damage evaluation to assess the fatigue behaviour of cement-treated base material from laboratory and full-scale performance tests." *Transportation Geotechnics*, Elsevier Ltd, 26, 100440.

Joni, H. H., and Hashim, M. S. (2018). "Evaluation silica fume addition on some properties of cold bitumen emulsion mixtures (CBEMs)." *IOP Conference Series: Materials Science and Engineering*, 433(1), 0–12.

Kavussi, A., Modarres, A. (2010). "Laboratory fatigue models for recycled mixes with bitumen emulsion and cement." *Constr. Build. Mater.* 24, 1920–1927. https://doi.org/10.1016/j.conbuildmat.2010.04.009

Kim, W., Labuz, J. F., and Dai, S. (2007). "Resilient modulus of base course containing recycled asphalt pavement." *Transportation Research Record*, (2005), 27–35.

Kishore Kumar, C., Amar Kumar, D.S.N.V., Amaranatha Reddy, M., Sudhakar Reddy, K. (2008). "Investigation of cold-in-place recycled mixes in India." *Int. J. Pavement Eng.* 9, 265–274.

Li, Y., and Wang, P. (2014). "Effect of emulsified asphalt content on mechanical property of

cement and emulsified asphalt mortar." *Applied Mechanics and Materials*, 587–589, 1132–1136.

Li, Y., Lyv, Y., Fan, L., Zhang, Y. (2019). "Effects of cement and emulsified asphalt on properties of mastics and 100% cold recycled asphalt mixtures." *Materials (Basel)*. 12. https://doi.org/10.3390/ma12050754

Lim, S., and Zollinger, D. G. (2003). "Estimation of the Compressive Strength and Modulus of Elasticity of Cement-Treated Aggregate Base Materials." *Transportation Research Record*, (1837), 30–38.

Liu, J., Yu, B., and Wang, Q. (2020). "Application of steel slag in cement-treated aggregate base course." *Journal of Cleaner Production*, Elsevier Ltd, 269, 121733.

Li, P., Liu, J. (2014). "Predictive model for nonlinear resilient modulus of emulsified asphalt treated base." *In Pavement Materials, Structures, and Performance*. 383-394.

Ministry of Road Transport and Highways (2013). "Specifications for road and bridgeworks." fifth revision, *Ministry of Road Transport and Highways*, New Delhi, India.

Ministry of Road Transport and Highways Annual report (2020-21), *Ministry of Road Transport and Highways*, New Delhi, India.

M. Arisha, A., Gabr, A. R., El-Badawy, S. M., and Shwally, S. A. (2018). "Performance Evaluation of Construction and Demolition Waste Materials for Pavement Construction in Egypt." *Journal of Materials in Civil Engineering*, 30(2), 04017270.

MacGregor, J. A. C., Highter, W. H., and DeGroot, D. J. (1999). "Structural numbers for reclaimed asphalt pavement base and subbase course mixes." *Transportation Research Record*, (1687), 22–28.

Mallick, R., Teto, M., Kandhal, P., Ray Brown, E., Bradbury, R., and Kearney, E. (2002). "Laboratory Study of Full-Depth Reclamation Mixes." *Transportation Research Record*, 1813(1), 103–110.

Marvila, M. T., Azevedo, A. R. G., and Monteiro, S. N. (2020). "Verification of the application potential of the mathematical models of lyse, abrams and Molinari in mortars based on cement and lime." *Journal of Materials Research and Technology*, Korea Institute of Oriental Medicine, 9(4), 7327–7334.

Melese, E., Baaj, H., and Tighe, S. (2020). "Fatigue behavior of reclaimed pavement materials treated with cementitious binders." *Construction and Building Materials*, Elsevier Ltd, 249, 118565.

Mignini, C., Cardone, F., and Graziani, A. (2018). "Experimental study of bitumen emulsion–cement mortars: mechanical behavior and relation to mixtures." *Materials and*

Structures/Materiaux et Constructions, Springer Netherlands, 51(6).

Miller, H. J., Guthrie, W. S., Kestler, M., Carbo, C. (2006). "Cement treatment of frost-susceptible New England base materials blended with reclaimed asphalt pavement." *In: Current practices in cold regions engineering*, pp 1–11.

Miljković, M., Radenberg, M. (2014). "Fracture behavior of bitumen emulsion mortar mixtures." *Constr. Build. Mater.* 62, 126–134.

Miro, R., Martinez, A., Cancela, A. (2004) "Case Study of In-Place Recycled Asphalt Pavement of the N–536 Highway in Spain." *In TRB 83th Annual Meeting*, Washington DC, USA.

Modarres, A., Nejad, F. M., Kavussi, A., Hassani, A., and Shabanzadeh, E. (2011). "A parametric study on the laboratory fatigue characteristics of recycled mixes." *Construction and Building Materials*, Elsevier Ltd, 25(4), 2085–2093.

Mohammadinia, A., Arulrajah, A., Sanjayan, J., Disfani, M. M., Bo, M. W., and Darmawan, S. (2015). "Laboratory Evaluation of the Use of Cement-Treated Construction and Demolition Materials in Pavement Base and Subbase Applications." *Journal of Materials in Civil Engineering*, 27(6), 04014186.

Monney, O. K., Khalid, H. A., and Artamendi, I. (2007). "Assessment of fracture properties of emulsified asphalt mixtures." *Road Materials and Pavement Design*, 8(1), 87–102.

Nassar, A. I., Thom, N. H., and Parry, T. (2016a). "Examining the effects of contributory factors on curing Cold Bitumen Emulsion Mixtures." *Functional Pavement Design - Proceedings of the 4th Chinese-European Workshop on Functional Pavement Design, CEW 2016*, (March 2018), 1037–1048.

Nassar, A. I., Thom, N., and Parry, T. (2016b). "Optimizing the mix design of cold bitumen emulsion mixtures using response surface methodology." *Construction and Building Materials*, 104(February), 216–229.

Nazarian, S., and Yuan, D. (2012). "Design and Constructability of Emulsion-Stabilized Bases for Full-Depth Reclamation."

Needham D, B.S.F. (2000). "A Study of Cement Modified Bitumen Emulsion Mixtures" Assoc. Asph. Paving Technol. 1–22.

Nottingham, T., and User, N. E. (2011). A study on the development of guidelines for the production of bitumen emulsion stabilized RAPs for roads in the tropics. Ph.D. thesis, University of Nottingham ."

Oruc, S., Celik, F., and Akpinar, M. V. (2007). "Effect of cement on emulsified asphalt mixtures." *Journal of Materials Engineering and Performance*, 16(5), 578–583.

Ouyang, J., Hu, L., Yang, W., Han, B. (2019). "Strength improvement additives for cement bitumen emulsion mixture." *Constr. Build. Mater.* 198, 456–464. https://doi.org/10.1016/j.conbuildmat.2018.11.280

de Paiva, C. E. L., de Oliveira, P. C. A., and de Franco Peixoto, C. (2017). "The influence of milling asphalt rates from wearing surface to the flexural strength applied to a recycled layer with Portland cement." *Construction and Building Materials*, Elsevier Ltd, 154, 1294–1300.

Pi, Y., Huang, Z., Pi, Y., et al. (2019). "Composition Design and Performance Evaluation of Emulsified Asphalt Cold Recycled Mixtures." *Materials*. 12(17), 2682.

Poon, C. S., Qiao, X. C., and Chan, D. (2006). "The cause and influence of self-cementing properties of fine recycled concrete aggregates on the properties of unbound sub-base." *Waste Management*, 26(10), 1166–1172.

Puppala, A. J., Hoyos, L. R., and Potturi, A. K. (2011). "Resilient Moduli Response of Moderately Cement-Treated Reclaimed Asphalt Pavement Aggregates." *Journal of Materials in Civil Engineering*, 23(7), 990–998.

Puppala, A. J., Pedarla, A., Chittoori, B., Ganne, V. K., and Nazarian, S. (2017). "Long-Term Durability Studies on Chemically Treated Reclaimed Asphalt Material as Base Layer for Pavements." 2500.

Puppala, A. J., Saride, S., and Williammee, R. (2012). "Sustainable Reuse of Limestone Quarry Fines and RAP in Pavement Base/Subbase Layers." *Journal of Materials in Civil Engineering*, 24(4), 418–429.

Qamhia, I. I. A., Tutumluer, E., Ozer, H., Boler, H., Shoup, H., and Stolba, A. J. (2020). "Durability Aspects of Chemically Stabilized Quarry By-Product Applications in Pavement Base and Subbase." *Transportation Research Record*, 2674(6), 339–350.

Quick, T., and Guthrie, W. (2011). "Early-Age Structural Properties of Base Material Treated with Asphalt Emulsion." *Transportation Research Record: Journal of the Transportation Research Board 2253, no.1*, 40–50.

Del Rey, I., Ayuso, J., Barbudo, A., Galvín, A. P., Agrela, F., and de Brito, J. (2016). "Feasibility study of cement-treated 0–8 mm recycled aggregates from construction and demolition waste as road base layer." *Road Materials and Pavement Design*, 17(3), 678–692.

Reddy, B. V., Kumar, H. H., Ullas, S. N., & Gourav, K. (2016). "Non-organic solid wastes–a potential resource for construction materials." *Current Science*, 1968-1976.

Romeo, E., Orazi, M., Orazi, U. S., Accardo, C., Noto, S., and Tebaldi, G. (2019). "Evaluation

of ‘long-term behavior under traffic’ of cement-treated mixture with RAP.” *Construction and Building Materials*, 208, 421–426.

Ronald, M., Luis, F.P. (2016). "Asphalt emulsions formulation: State-of-the-art and dependency of formulation on emulsions properties." *Constr. Build. Mater.* 123, 162–173. https://doi.org/10.1016/j.conbuildmat.2016.06.129

Flores, G., Gallego, J., Miranda, L., Marcobal, J.R. (2019). "Design methodology for in situ cold recycled mixtures with emulsion and 100% rap." *Constr. Build. Mater.* 216, 496–505.

Flores, G., Gallego, J., Miranda, L., Marcobal, J.R. (2020). "Cold asphalt mix with emulsion and 100% rap: Compaction energy and influence of emulsion and cement content." *Constr. Build. Mater*. 250, 118804. https://doi.org/10.1016/j.conbuildmat.2020.118804

Saadoon, T., Gómez-Meijide, B., Garcia, A. (2018). "Prediction of water evaporation and stability of cold asphalt mixtures containing different types of cement." *Constr. Build. Mater*. 186, 751–761.

Sangiorgi, C., Tataranni, P., Simone, A., Vignali, V., Lantieri, C., and Dondi, G. (2017). “A laboratory and field evaluation of Cold Recycled Mixture for base layer entirely made with Reclaimed Asphalt Pavement.” *Construction and Building Materials*, Elsevier Ltd, 138, 232–239.

Shanbara, H. K., Ruddock, F., Atherton, W., and Nassir, N. A. (2018). “Mechanical Properties of Ordinary Portland Cement Modified Cold Bitumen Emulsion Mixture.” *International Journal of Civil and Environmental Engineering*, 12(5), 576–581.

Soares, R., Haichert, R., Podborochynski, D., and Berthelot, C. (2013). “Modeling in situ performance of cement-stabilized granular base layers of urban roads.” *Transportation Research Record*, (2363), 88–95.

Spanish General Technical Specifications for Road Construction (PG3) (2004). Ministry of Development, Government of Spain.

Suda, J., Valentin, J., and Žák, J. (2017). “Cold bituminous emulsion mixtures - laboratory mix design, trial section job site and monitoring.” (June).

Suebsuk, J., Horpibulsuk, S., Suksan, A., Suksiripattanapong, C., Phoo-ngernkham, T., and Arulrajah, A. (2019). “Strength prediction of cement-stabilized reclaimed asphalt pavement and lateritic soil blends.” *International Journal of Pavement Engineering*, Taylor & Francis, 20(3), 332–338.

Swaroopa, S., Sravani, A., Jain, P. K. (2015). "Comparison of mechanistic characteristics of cold, mild warm and half warm mixes for bituminous road construction." *Indian J. Eng.*

Mater. Sci. 22, 85–92.

Tayebali, A. A., Rowe, G.M., Sousa, J.B. (1992). "Fatigue response of asphalt-aggregate mixtures." *Asphalt Paving Technology: Association of Asphalt Paving Technologists-Proceedings of the Technical Sessions*.

Tam, V. W. Y. (2008). "On the effectiveness in implementing a waste-management-plan method in construction. " *Waste Management*, 28, 1072-1080.

Taha, R. (2003). "Evaluation of Cement Kiln Dust – Stabilized Reclaimed Asphalt Pavement Aggregate systems in road bases." *Transportation Research Record*, 1819(1), 11–17.

Taha, R., Al-Harthy, A., Al-Shamsi, K., and Al-Zubeidi, M. (2002). "Cement Stabilization of Reclaimed Asphalt Pavement Aggregate for Road Bases and Subbases." *Journal of Materials in Civil Engineering*, 14(June), 239–245.

Taherkhani, H., Firoozei, F., Bolouri Bazaz, J. (2016). "Evaluation of the Mechanical Properties of the cement-treated Cold-in-Place Recycled Asphalt Mixtures." *Int. J. Transp. Eng.* 3.

Thanaya, I. N. A., Negara, I. N. W., and Suarjana, I. P. (2014). "Properties of Cold Asphalt Emulsion Mixtures (CAEMs) using materials from old road pavement milling." *Procedia Engineering*, Elsevier B.V., 95(Scescm), 479–488.

Thanaya, I. N. A. (2007). "Evaluating and Improving the Performance of Cold Asphalt Emulsion Mixes." *Civ. Eng. Dimens*. 9, 64–69.

Thanaya, I. N. A., Zoorob, S. E., and Forth, J. P. (2009). "A laboratory study on cold-mix, cold-lay emulsion mixtures." *Proceedings of the Institution of Civil Engineers: Transport*, 162(1), 47–55.

Thompson, M.R., Carpenter, S.H. (2009). Cold in-place recycling and full-depth recycling with asphalt products.

TIFAC (2001). Utilization of waste from the construction industry, technology, information, forecasting, and assessment council, New Delhi India

The Freedonia Group (2012) World construction aggregates

Wang, J., Wen, H., and Muhunthan, B. (2020). "Development of test methods to characterize the shrinkage properties of cementitious stabilized materials." *Transportation Geotechnics*, Elsevier, 25(January), 100405.

Wilson, B. T., and Guthrie, W. S. (2011). "Strength and Deformation Characteristics of Cement-Treated Reclaimed Pavement with a Chip Seal." *Transportation Research Record: Journal of the Transportation Research Board*, 2212(1), 100–109.

www.nhai.gov.in, Date of access: 23.11.2021.

www.materialflows.net, Dater of access: 25.10.2020

Xiao, F., Yao, S., Wang, J., Li, X., and Amirkhanian, S. (2018). “A literature review on cold recycling technology of asphalt pavement.” *Construction and Building Materials*, Elsevier Ltd, 180, 579–604.

Xiao, J., Jiang, W., Ye, W., Shan, J., Wang, Z. (2019). "Effect of cement and emulsified asphalt contents on the performance of cement-emulsified asphalt mixture."*Constr. Build. Mater.* 220, 577–586.

Xu, O., Wang, Z., Wang, R. (2017). "Effects of aggregate gradations and binder contents on engineering properties of cement emulsified asphalt mixtures." *Constr. Build. Mater.* 135, 632–640.

Xuan, D., Molenaar, A. A. A., and Houben, L. J. M. (2012). “Compressive and Indirect Tensile Strengths of Cement-Treated Mix Granulates with Recycled Masonry and Concrete Aggregates.” *Journal of Materials in Civil Engineering*, 24(5), 577–585.

Xuan, D. X., Molenaar, A. A. A., and Houben, L. J. M. (2016). “Deformation behavior of cement treated demolition waste with recycled masonry and concrete subjected to drying and temperature change.” *Cement and Concrete Composites*, Elsevier Ltd, 68, 27–34.

Yan, J., Cao, Y., Zhu, T., Cai, M., Cao, Z., Huang, W., and Dong, Q. (2010). “Copyright ASCE 2010 GeoShanghai 2010 International Conference Copyright ASCE 2010 GeoShanghai 2010 International Conference.” *In Paving Materials and Pavement Analysis (*, 1(I), 97–102.

Yan, J., Leng, Z., Li, F., Zhu, H., and Bao, S. (2017). “Early-age strength and long-term performance of asphalt emulsion cold recycled mixes with various cement contents.” *Construction and Building Materials*, Elsevier Ltd, 137, 153–159.

Yehia, S., Helal, K., Abusharkh, A., Zaher, A., and Istaitiyeh, H. (2015). “Strength and Durability Evaluation of Recycled Aggregate Concrete.” *International Journal of Concrete Structures and Materials*, Korea Concrete Institute, 9(2), 219–239.

You, L., Yue, Y., Yan, K., and Zhou, Y. (2020). “Characteristics of cement-stabilized macadam containing surface-treated recycled aggregates.” *Road Materials and Pavement Design*, Taylor & Francis, 0(0), 1–15.

Yuan, D., Nazarian, S., Hoyos, L. R., and Puppala, A. J. (2011). “Evaluation and Mix Design of Cement-Treated Base Materials with High Content of Reclaimed Asphalt Pavement.” *Transportation Research Record: Journal of the Transportation Research Board*, 2212(1), 110–119.

Zhang, Y., Liu, X., Xu, Y., Tang, B., Wang, Y., and Mukiza, E. (2019). “Preparation and

characterization of cement-treated road base material utilizing electrolytic manganese residue." *Journal of Cleaner Production*, Elsevier Ltd, 232, 980–992.

Zhou, F., Scullion, T., & Sun, L. (2004). "Verification and modeling of three-stage permanent deformation behavior of asphalt mixes." *Journal of Transportation Engineering*, Vol. 130(4), pp. 486-494.

Zhu, C., Zhang, H., Guo, H., Wu, C., Wei, C. (2019). "Effect of gradations on the final and long-term performance of asphalt emulsion cold recycled mixture." *J. Clean. Prod*. 217, 95–104.

Ziari, H., Nakhaei, M., Akbari Nasrekani, A., & Moniri, A. (2016). "Characterization of rutting resistance of EBS-modified asphalt mixtures." Petroleum Science and Technology, Vol. 34(13), pp. 1107-1112

APPENDIX A: PERFORMANCE EVALUATION OF CTB

Mix/ Property	OMC (%)	MDD (g/cc)	UCS_7D (MPa)	UCS_28D (MPa)	ITS_7D (MPa)	ITS_28D (MPa)	M_R_7D (MPa)	M_R_28D (MPa)	Fatigue Model, R^2
RAP_2C	7.13	2.08	0.321	0.73	0.06	0.084	138	749	$N_f = 1.225x^{-6.186}$, 0.84
RAP_4C	7.24	2.11	0.673	1.53	0.11	0.15	310	1689	$N_f = 1.4859x^{-9.014}$, 0.73
RAP_6C	7.45	2.21	0.91	3.35	0.24	0.34	363	4431	$N_f = 3.5225x^{-8.359}$, 0.96
RCA_2C	8.2	2.1	0.92	2.22	0.43	0.60	1081	1477	$N_f = 106.59x^{-0.101}$, 0.001
RCA_4C	11.1	2.06	1.44	2.32	0.45	0.63	1139	2603	$N_f = 0.4722x^{-15.35}$, 0.64
RCA_6C	9.5	2.09	1.67	4.56	0.84	1.18	1446	3406	$N_f = 0.7672x^{-18.64}$, 0.64
NA_2C	10.8	2.08	0.48	0.9	0.12	0.18	-	834	$N_f = 0.4789x^{-11.15}$, 0.93
NA_4C	11.26	2.12	0.81	1.71	0.19	0.30	-	1953	$N_f = 0.3817x^{-11.67}$, 0.85
NA_6C	12.14	2.29	1.79	4.72	0.43	0.75	-	3376	$N_f = 0.9832x^{-19.5}$, 0.98
25RAP_2C	7.38	2.22	0.98	1.26	0.18	0.25	549	1342	$N_f = 0.9049x^{-10.31}$, 0.90
25RAP_4C	7.67	2.22	2.33	2.8	0.4	0.56	1328	3162	$N_f = 4.3857x^{-18.45}$, 0.99
25RAP_6C	8.09	2.23	3.4	5.18	0.74	1.04	1598	4300	$N_f = 13.802x^{-16.07}$, 0.92
50RAP_2C	7.72	2.14	0.6	1.21	0.16	0.22	230	1174	$N_f = 0.1411x^{-7.464}$, 0.89
50RAP_4C	7.89	2.15	1.22	2.37	0.3	0.42	410	1688	$N_f = 11.752x^{-4.645}$, 0.95
50RAP_6C	7.95	2.16	2.43	4.96	0.43	0.60	571	2924	$N_f = 2.832x^{-9.172}$, 0.64
75RAP_2C	7.52	2.08	0.52	1.12	0.16	0.22	160	1414	$N_f = 20.133x^{-5.267}$, 0.76
75RAP_4C	7.64	2.10	1.01	2.31	0.17	0.24	448	2078	$N_f = 7.2413x^{-6.218}$, 0.98
75RAP_6C	7.88	2.11	2.22	4.21	0.30	0.42	491	2734	$N_f = 0.1253x^{-17.59}$, 0.71
25RCA_2C	10.06	2.2	0.95	1.71	0.24	0.33	1002	1058	$N_f = 4.2227x^{-3.702}$, 0.80
25RCA_4C	9.44	2.22	1.98	2.89	0.48	0.68	1366	2055	$N_f = 37.836x^{-10.61}$, 0.89
25RCA_6C	10.35	2.25	3.19	4.61	0.83	1.16	1837	3609	$N_f = 1.4697x^{-38.27}$, 0.93
50RCA_2C	7.93	2.16	0.99	1.63	0.31	0.44	600	901	$N_f = 0.6657x^{-4.635}$, 0.92
50RCA_4C	9.28	2.17	2.26	2.94	0.57	0.79	1004	2002	$N_f = 0.0786x^{-12.24}$, 0.87
50RCA_6C	10.92	2.2	3.39	5.07	0.98	1.37	1447	3389	$N_f = 2.127x^{-8.246}$, 0.92
75RCA_2C	10.2	1.98	0.97	1.49	0.29	0.40	434	1105	$N_f = 0.0254x^{-17.74}$, 0.99
75RCA_4C	9.2	2.01	1.83	2.77	0.53	0.75	854	1383	$N_f = 1.1185x^{-7.288}$, 0.89
75RCA_6C	11.5	1.97	2.22	4.51	0.68	0.95	1708	3120	$N_f = 0.3331x^{-12.36}$, 0.67

APPENDIX B: Modelling of Dynamic Creep Rutting Data

Table B1 Summary of logarithmic modeling data

25RAP		Value	SE	t-value	probability>|t|	Dependency	R^2 value
OEAC	a	0.05973	0.00126	47.377	0	0.982	0.98
	b	-0.06454	1.74E-04	-370.445	0	0.982	
	c	-0.81269	0.0294	-27.645	2.54E-152	0.055	
<OEAC	a	0.00737	7.98E-04	9.233	4.42E-20	0.983	0.99
	b	-0.09453	1.10E-04	-859.174	0	0.983	
	c	-0.34664	0.03877	-8.942	6.06E-19	0.123	
>OEAC	a	0.04233	0.00119	35.691	3.45E-238	0.982	0.99
	b	-0.0789	1.64E-04	-481.513	0	0.982	
	c	-0.75495	0.02919	-25.864	3.99E-135	0.063	

50RAP		Value	SE	t-value	probability>|t|	Dependency	R^2 value
OEAC	a	-0.00231	0.00114	-2.0312	0.04231	0.985	0.99
	b	-0.10494	1.56E-04	-672.969	0	0.985	
	c	0.5	0.09098	5.495	4.17E-08	0.213	
<OEAC	a	-0.22848	2.01E-03	-113.408	0.00E+00	0.985	0.97
	b	-0.08482	2.77E-04	-306.565	0	0.985	
	c	0.5	0.19973	2.503	1.24E-02	0.213	
>OEAC	a	0.08023	0.00173	46.509	0.00E+00	0.985	0.99
	b	-0.10936	2.37E-04	-461.628	0	0.985	
	c	0.5	0.13264	3.769	1.66E-04	0.213	

75RAP		Value	SE	t-value	probability>|t|	Dependency	R^2 value
OEAC	a	-1.78072	0.01197	-148.754	0	0.998	0.99
	b	-0.49563	1.52E-03	-326.304	0	0.997	
	c	112.80724	1.96092	57.527	0.00E+00	0.875	
<OEAC	a	-0.23449	3.57E-03	-65.633	0.00E+00	0.986	0.99
	b	-0.26084	4.90E-04	-532.827	0	0.986	
	c	1.10441	0.14279	7.734	1.35E-14	0.258	
>OEAC	a	-2.57575	0.00687	-375.113	0.00E+00	0.996	0.99
	b	-0.74692	8.97E-04	-832.261	0	0.996	
	c	42.55346	0.46929	90.675	0.00E+00	0.749	

APPENDIX B: Modelling of Dynamic Creep Rutting Data

Table B2 Summary of Power-law modeling data

25RAP		Value	SE	t-Value	Prob>|t|	Dependency	R^2 value
OEAC	a	0.1995	0.00101	196.9363	0	0.989	0.93
	b	0.1332	6.85E-04	194.4478	0	0.989	
<OEAC	a	0.2236	6.66E-04	336.0473	0	0.989	0.98
	b	0.1547	4.00E-04	386.5523	0	0.989	
>OEAC	a	0.2196	0.00107	204.735	0	0.989	0.95
	b	0.1408	6.58E-04	213.9372	0	0.989	

50RAP		Value	SE	t-Value	Prob>|t|	Dependency	R^2 value
OEAC	a	0.24	8.31E-04	293.8	0	0.989	0.97
	b	0.16	4.58E-04	339.1	0	0.989	
< OEAC	a	0.05	1.97E-04	257.6	0	0.993	0.99
	b	0.28	5.15E-04	537.1	0	0.993	
> OEAC	a	0.32	0.00132	243.9	0	0.989	0.95
	b	0.14	5.53E-04	247.4	0	0.989	

EAC		Value	SE	t-Value	Prob>|t|	Dependency	R^2 value
OEAC	a	0.28626	8.07E-04	354.569	0	0.993	0.99
	b	0.2559	3.75E-04	683.066	0	0.993	
< OEAC	a	0.43853	1.34E-03	327.996	0	0.990	0.98
	b	0.18168	4.09E-04	444.741	0	0.990	
> OEAC	a	0.36437	0.00157	231.385	0	0.992	0.99
	b	0.28134	5.73E-04	491.35	0	0.992	

APPENDIX C: Indirect Tensile Fatigue Test Data

Table C1 ITFT Data for EATB RAP mixes

25RAP	Load (kN)	Tensile Stress (kPa)	Stiffness (MPa)	Tensile Strain	Fatigue life
At the higher side of OEAC (H)	0.8	75.74	895.91	173.30	1375
	0.8	75.74	895.91	173.30	2377
	1.5	137.83	895.91	315.38	844
	1.7	167.57	895.91	383.42	220
	1.8	177.98	895.91	407.26	200
	1.8	177.98	895.91	407.26	180
At OEAC (O)	0.5	47.34	795.52	121.98	10192
	0.8	75.74	795.52	195.17	1854
	1.5	146.74	795.52	378.15	725
	1.5	151.33	795.52	389.96	810
	1.8	163.00	795.52	420.04	247
	1.8	167.87	795.52	432.58	209
At the lower side of OEAC (L)	0.8	75.74	1030.39	144.19	6149
	1.2	113.61	1030.39	226.03	1593
	1.4	132.54	1030.39	263.69	1401
	1.5	144.19	1030.39	286.88	268
	1.7	171.11	1030.39	340.43	156
	1.7	168.52	1030.39	335.27	160

50RAP	Load (kN)	Tensile Stress (kPa)	Stiffness (MPa)	Tensile Strain	Fatigue life
At the higher side of OEAC (H)	0.6	56.80	966	120.49	29371
	1.7	153.95	966	326.56	246
	1.7	156.21	966	331.36	571
	1.8	175.14	966	371.52	170
	1.9	174.59	966	370.34	83
	1.9	179.88	966	381.56	120
At OEAC (O)	0.5	47.4	917	105.79	1783
	1.0	94.67	917	211.59	798
	1.5	146.74	917	327.98	220
	1.5	147.32	917	329.27	200
	1.8	170.41	917	380.88	94
	1.9	179.88	917	402.04	60
At the lower side of OEAC (L)	0.5	47.34	914	106.19	2611
	0.5	44.39	914	99.58	1783
	1.3	123.07	914	276.09	615
	1.5	142.00	914	318.57	150
	1.5	149.58	914	335.56	620
	1.8	165.39	914	371.04	59

75RAP	Load (kN)	Tensile Stress (kPa)	Stiffness (MPa)	Tensile Strain	Fatigue life
At the higher side of OEAC (H)	0.6	58.81	742	162.48	4201
	0.6	60.59	742	167.41	7280
	1.3	112.82	742	311.71	662
	1.4	132.54	742	354.27	797
	1.5	143.06	742	395.27	300
	1.5	141.27	742	390.31	50
At OEAC (O)	0.5	47.34	767	126.52	19001
	0.5	47.34	767	126.52	24795
	0.8	75.74	767	202.44	1038
	1.4	132.54	767	354.27	682
	1.4	132.54	767	354.27	277
	2.0	189.35	767	506.09	20
At the lower side of OEAC (L)	1.2	113.61	817	284.91	1424
	1.4	132.54	817	332.39	79
	1.8	170.41	817	427.37	35
	1.8	163.00	817	408.79	69
	1.9	188.21	817	472.00	13
	2.0	189.35	817	474.85	15

APPENDIX C: Indirect Tensile Fatigue Test Data

Table C2 ITFT Data for EATB RCA mixes

25RCA	Load (kN)	Tensile Stress (kPa)	Stiffness (MPa)	Tensile Strain	Fatigue life	50RCA	Load (kN)	Tensile Stress (kPa)	Stiffness (MPa)	Tensile Strain	Fatigue life
At the higher side of OEAC (H)	1.9	179.60	824	446.82	39	At the higher side of OEAC (H)	1.84	180.66	831	445.68	154
	2.0	191.06	824	475.34	41		1.84	177.92	831	438.92	218
	1.4	133.74	824	332.74	48		1.37	128.59	831	317.24	255
	1.5	145.44	824	361.82	77		1.37	130.52	831	321.98	162
	1.3	119.41	824	297.09	241		1.37	123.17	831	303.84	211
	1.3	119.41	824	297.09	227		1.18	111.87	831	275.98	421
At OEAC (O)	1.9	182.58	1108	337.81	46	At OEAC (O)	1.78	158.36	1033	314.26	104
	1.9	176.85	1108	327.21	41		1.77	165.34	1033	328.12	451
	1.6	151.59	1108	280.47	70		1.52	138.31	1033	274.48	347
	1.6	146.97	1108	271.92	62		1.52	138.31	1033	274.48	330
	1.3	124.01	1108	229.44	250		1.27	124.93	1033	247.92	1211
	1.3	128.24	1108	237.26	224		0.78	70.38	1033	139.67	1515
At the lower side of OEAC (L)	2.0	181.05	952	389.87	62	At the lower side of OEAC (L)	1.96	178.46	935	391.29	109
	2.0	179.18	952	385.84	53		1.96	186.46	935	408.81	89
	1.5	132.49	952	285.30	81		1.72	156.16	935	342.38	137
	1.5	135.79	952	292.40	70		1.72	158.42	935	347.34	133
	1.2	108.63	952	233.92	86		1.47	133.85	935	293.47	483
	1.2	113.61	952	244.64	110		1.47	133.85	935	293.47	475

APPENDIX D: OVERALL CHARACTERISTICS OF EATB

Mix/Property	OEAC (%)	ITS (kPa)	TSR (%)	M_R (MPa)	M_R @40°C (MPa)	Fatigue equation
25RAP_L	6.0	190.0	95.8	1030	185	$\varepsilon = 952.13N^{-0.202}$, 0.89
25RAP_O	6.5	193.8	95.8	796	158	$\varepsilon = 3072.1N^{-0.345}$, 0.89
25RAP_H	7.0	171.1	95.6	896	183	$\varepsilon = 2542.6N^{-0.346}$, 0.88
50RAP_L	4.5	179.2	94.3	966	206	$\varepsilon = 1918.5N^{-0.348}$, 0.70
50RAP_O	5.0	194.8	94.6	917	205	$\varepsilon = 2179.3N^{-0.375}$, 0.89
50RAP_H	5.5	166.1	91.2	914	123	$\varepsilon = 1011.4N^{-0.202}$. 0.95
75RAP_L	4.5	184.9	92.7	624	213	$\varepsilon = 624.41N^{-0.112}$, 0.88
75RAP_O	5.0	192.1	92.2	574	195	$\varepsilon = 1050.6N^{-0.209}$, 0.92
75RAP_H	5.5	134.2	89.2	490	166	$\varepsilon = 1087.1N^{-0.203}$, 0.77
25RCA_L	5.0	172.4	93.3	824	121	$\varepsilon = 887.19N^{-0.203}$, 0.71
25RCA_O	6.0	203.1	75.2	1108	173	$\varepsilon = 646.9N^{-0.189}$, 0.88
25RCA_H	7.0	111.9	64.7	952	265	$\varepsilon = 7806.6N^{-0.756}$, 0.79
50RCA_L	5.0	137.2	96.3	831	366	$\varepsilon = 2137N^{-0.337}$, 0.37
50RCA_O	6.0	168.4	98.3	1033	155	$\varepsilon = 1057.5N^{-0.232}$, 0.53
50RCA_H	7.0	156.7	94.6	935	146	$\varepsilon = 862.96N^{-0.176}$, 0.90

APPENDIX E: Typical input and output data of IIT PAVE software

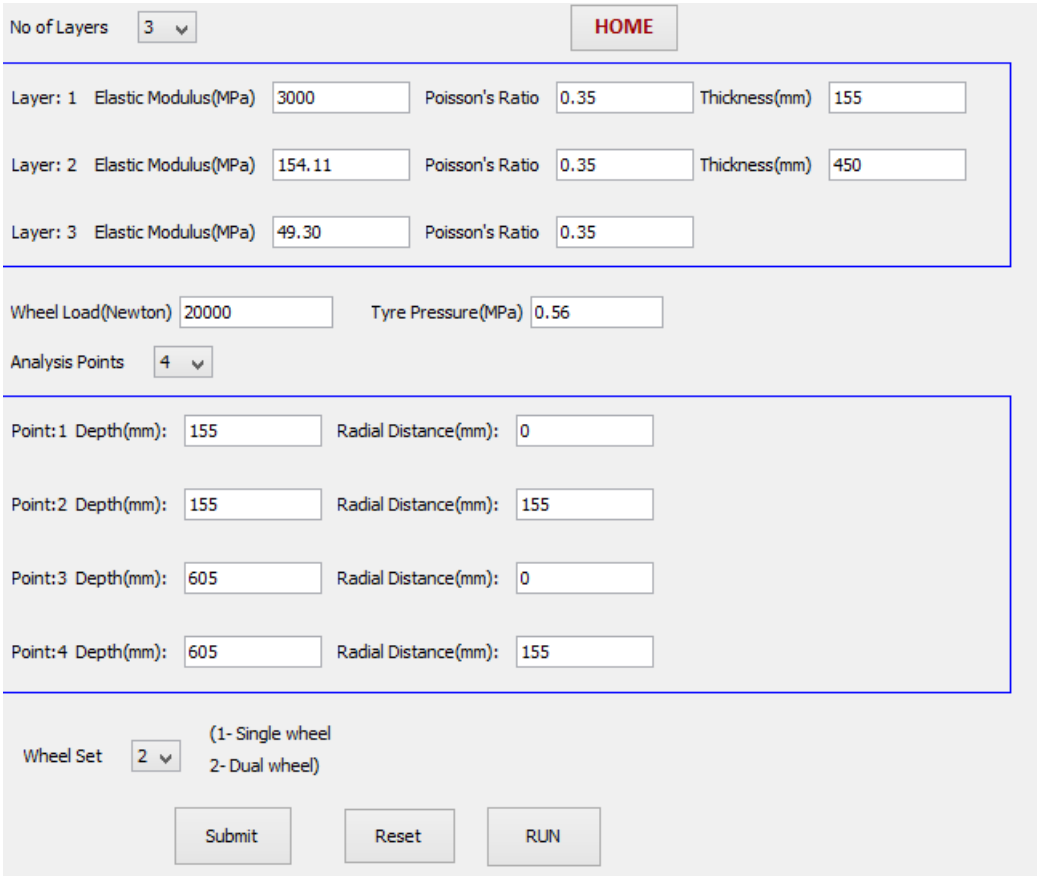

Figure E1 A typical Input data screen of IITPAVE software

```
No. of layers                3
E values (MPa)          3000.00  154.11   49.30
Mu values                  0.350.350.35
thicknesses (mm)         155.00  450.00
single wheel load (N) 20000.00
tyre pressure (MPa)        0.56
Dual  Wheel
  Z         R       SigmaZ       SigmaT      SigmaR      TaoRZ       DispZ       epZ         epT         epR
155.00     0.00-0.8436E-01 0.7937E+00 0.6430E+00-0.1261E-01 0.4930E+00-0.1957E-03 0.1994E-03 0.1316E-03
155.00L    0.00-0.8435E-01-0.2315E-02-0.1006E-01-0.1261E-01 0.4930E+00-0.5192E-03 0.1994E-03 0.1316E-03
155.00   155.00-0.7896E-01 0.7289E+00 0.4233E+00-0.3525E-01 0.5065E+00-0.1607E-03 0.2028E-03 0.6529E-04
155.00L 155.00-0.7896E-01-0.2888E-02-0.1858E-01-0.3524E-01 0.5065E+00-0.4636E-03 0.2028E-03 0.6529E-04
605.00     0.00-0.1668E-01 0.2322E-01 0.2087E-01-0.2422E-02 0.3648E+00-0.2083E-03 0.1412E-03 0.1205E-03
605.00L    0.00-0.1654E-01 0.1383E-02 0.6047E-03-0.2422E-02 0.3649E+00-0.3497E-03 0.1412E-03 0.1199E-03
605.00   155.00-0.1749E-01 0.2446E-01 0.2296E-01-0.3003E-02 0.3724E+00-0.2212E-03 0.1463E-03 0.1332E-03
605.00L 155.00-0.1749E-01 0.1421E-02 0.9429E-03-0.3003E-02 0.3724E+00-0.3715E-03 0.1463E-03 0.1332E-03
```

Figure E2 A typical output data screen of IITPAVE software

LIST OF PUBLICATIONS

Journal Publications from the Present Work

1. **Chakravarthi, S.,** Boyina, A., Singh, A.K., and Shankar, S. (2019). "Evaluation of cement-treated reclaimed asphalt pavement and recycled concrete pavement bases," *Int. J. Pavement Res. Technol.* 12(1) pp-581–588. https://doi.org/10.1007/s42947-019-0069-1.

2. **Chakravarthi, S.,** and Shankar, S. (2021). "Utilization of recycled aggregates in cement-treated bases: A state-of-the-art review," *Innov. Infrastructure. Solution*s 6(4), 1-22. https://doi.org/10.1007/s41062-021-00555-4.

3. **S. Chakravarthi,** G. Raj Kumar, S. Shankar, R. Vishnu. (2021). "Effect of Emulsified Asphalt Content on Creep Behavior and Mechanical Properties of Cold Recycled Emulsified Asphalt Mixes." *Journal of Rehabilitation in civil engineering*. https://doi.org/10.22075/jrce.2021.22513.1485.

4. **S. Chakravarthi,** G. Raj Kumar, S. Shankar (2022). "A review on design, evaluation, and performance of emulsified asphalt-treated bases using recycled aggregates." *Environ Sci Pollut Res*. https://doi.org/10.1007/s11356-022-20522-5.

Conference Publications from the present work

1. **S. Chakravarthi,** G. Raj Kumar, MD. Sameer, S. Shankar (2020) "Influence of fine aggregates on strength development of Emulsified Asphalt Treated Bases" Int. Conference on Construction Materials and Smart Structures for Sustainable Development (ICCMSSSD), Hyderabad ISBN:978-93-8935-488-1.

2. Daniel, M., **Chakravarthi S.,** and Shankar S. (2020)." Influence of recycled aggregate and curing period on cement-treated bases." Conference on Transportation Planning and Implementation Methodologies for Developing Countries, IIT Bombay, December 2020.

3. **S. Chakravarthi,** M. Devendra Vara Prasad, S. Shankar (2021) "Performance evaluation of cement treated recycled concrete aggregate bases" 8th International Conference on Transportation Systems Engineering & Management (CTSEM 2021), August 2021. (Accepted for Publication).

BIODATA

Name: Sarella Chakravarthi

Date of Birth: 20-07-1993

ACADEMICS:

Course	School/college	Board/University	Year
Ph.D	National Institute of Technology, **Warangal**	National Institute of Technology, Warangal	2017-2022
M. Tech (Transportation Engineering)	National Institute of Technology, **Warangal**	National Institute of Technology, Warangal	2015-2017
B.Tech (CIVIL)	Gayatri Vidya Parishad College of Engineering **(Visakhapatnam)**	Jawaharlal Nehru Technological University	2010-2014
Intermediate (MPC)	Gayatri junior college (**East Godavari)**	State Board of Intermediate Education	2008-2010
10th Class	A.F.D.T High School **(East Godavari)**	Board of Secondary Education	2007-2008

Course Work during Ph.D

S. No	Course Name
1.	Pavement Deterioration Modeling
2.	Mechanistic and Empirical Pavement Design for Flexible Pavements
3.	Advanced Pavement Materials
4.	English for Scientific Communication
5.	Fracture Mechanics

Contact Address:

D. No. 4-221/4,
Salipeta,
Malikipuram (Mandal),
East Godavari district,
Andhra Pradesh,
Pincode: 533253,
Phone Number: +91- 9493398864
Email Id: chakravarthi.sarella@yahoo.com
chakravarthi.sarella@gmail.com
chakravarthi.sarella@student.nitw.ac.in